

UNCLASSIFIED

AD NUMBER
AD461804
NEW LIMITATION CHANGE
TO Approved for public release, distribution unlimited
FROM Distribution authorized to U.S. Gov't. agencies and their contractors; Administrative/Operational Use; 1961. Other requests shall be referred to U.S. Naval Air Turbine Test Station, Trenton, NJ .
AUTHORITY
USNMC ltr, 8 Jan 1968

THIS PAGE IS UNCLASSIFIED

UNCLASSIFIED

AD 461804

DEFENSE DOCUMENTATION CENTER

FOR

SCIENTIFIC AND TECHNICAL INFORMATION

CAMERON STATION ALEXANDRIA, VIRGINIA



UNCLASSIFIED

Best Available Copy

NOTICE: When government or other drawings, specifications or other data are used for any purpose other than in connection with a definitely related government procurement operation, the U. S. Government thereby incurs no responsibility, nor any obligation whatsoever; and the fact that the Government may have formulated, furnished, or in any way supplied the said drawings, specifications, or other data is not to be regarded by implication or otherwise as in any manner licensing the holder or any other person or corporation, or conveying any rights or permission to manufacture, use or sell any patented invention that may in any way be related thereto.

461804

CONFERENCE ON ENVIRONMENTAL  
EFFECTS ON AIRCRAFT PROPULSION

A Compilation of the Papers Presented

U. S. Naval Air Turbine Test Station  
Trenton, ~~New Jersey~~ N. J.

June 22 and 23, 1961

**Best  
Available  
Copy**

TABLE OF CONTENTS

	Page
INTRODUCTION . . . . .	v
LIST OF CONFEREES. . . . .	vi

TECHNICAL PAPERS PRESENTED

1. Producing Weather for Turbojet Engine Testing by W. Walter and F. Schanne. . . . .	1
2. Some Problems Encountered in Establishing a Small Engine Icing Facility at the AEL, NAMC; by S. Hill and J. Thorpe . . . . .	14
3. The Photoelectric Raindrop-size Spectrometer; by D. Nelson Dingle. . . . .	25
4. Measuring Techniques Under Water and Icing Conditions; . . . by S. Kossayian . . . . .	44
5. A Comparison Between the Rotating Multicylinder Method and The Oil Slide Method. . . by . . . V. Cirrito . . . . .	58
6. National Severe Storms Project - Objectives and Operations; . . . by C.F. Van Thullenar . . .	67
7. Severe Weather Flight Testing of Jet Fighter Airplanes and Engines; . . . by LCDR D. Skalla.	78
8. Foreign Object Ingestion in Turbine Engines. by E. I. Briggs; . . . . .	87

## INTRODUCTION

This compilation contains copies of the technical papers presented at the Conference on Environmental Effects on Aircraft Propulsion. The conference was held on June 22 and 23, 1961 at Trenton, New Jersey. A list of the conferees, who are members of industry, universities and the governmental services is included.

## LIST OF CONFEREES

The following were registered at the NATTS Conference on Environmental Effects on Aircraft Propulsion, Trenton, N.J., 22 and 23 June 1961:

AGNELLO, J.	NATTS, Aeronautical Turbine Laboratory
BABINGTON, R.	NATTS, Aeronautical Turbine Laboratory
BLISNUK, B.	NATF, Lakehurst
BIANCHINI, G.	Allison Division, General Motors Corp.
BATHIN, C.	Lycoming Aircraft
BINCKLEY, E.	WADC
BORDEN, N.	Pratt and Whitney
BORIS, P.	FAA, Atlantic City
BRIGGS, E., Jr.	FAA, Washington, D. C.
BRUNDA, D.	NATTS, Aeronautical Turbine Laboratory
BULLION, J.	NAMC, Aeronautical Engine Laboratory
BUTTON, R.	General Electric
CARLSON, C.	Pratt and Whitney
CARLSON, G.	Woodward Governor Company
CHAPPELL, M.	National Research Council, Canada
CIRRITO, V.	NATTS, Aeronautical Turbine Laboratory
CONNORS, H.	Lycoming Aircraft
CRISTMAN, V.	NATF, Lakehurst
DANIEL, R.	General Electric
DANIELS, R.	Goodyear
DAVIDS, I.	NATTS, Aeronautical Turbine Laboratory
DINGLE, Prof.	University of Michigan
DINSMORE, D.	AIRL
DOUGALL, L.	Vapor Heating Company
DOW, M.	United Airlines
DUPLACE, A.	General Electric
DUNTON, W.	Curtiss Wright
GIANGRANDE, G.	FAA, New York
GIBBARD, G.	National Research Council, Canada
GRIFFIN, D.	Curtiss Wright
HAHN, T., LTJG	NATTS, Aeronautical Turbine Laboratory
HILL, S.	NAMC, Aeronautical Engine Laboratory
HOLLAND, A.	Mayor of Trenton
HOYER, M.	NATTS, Aeronautical Turbine Laboratory
JONES, F., CDR	BuWeps
KOSSAYIAN, S.	NATTS, Aeronautical Turbine Laboratory
KUSH, A.	NATTS, Aeronautical Turbine Laboratory
LEESON, P.	Woodward Governor Company
LICHTMAN, G.	NATTS, Aeronautical Turbine Laboratory
LIFF, B.	Kaman Aircraft

MALLIEN, T.	McDonnell Aircraft
MARCY, J.	FAA, Atlantic City
MARLIN, E.	AiResearch
MASI, F.	NAMC, Aeronautical Engine Laboratory
MAZZARELLA, D.	Science Associates
MC CLELLAND, C.	NAMC, Aeronautical Engine Laboratory
MC DERMOTT, J.	Goodyear
MC GEE, J.	NATTS, Aeronautical Turbine Laboratory
MC GUIRE, J.	Weather Bureau, N.Y.
MEE, T.	Cornell Laboratory, Buffalo, N.Y.
MENDRALA, J.	NATTS, Aeronautical Turbine Laboratory
MILLAR, D.	FAA, Atlantic City
MILLER, C.	BuWeps
MILLER, R.	BuWeps
MORROW, J.	N. American Aviation, Inc.
MURPHY, ADM.	NARDAC, Johnsville, Pennsylvania
PORTER, W.	Climatic Laboratory, Eglin A.F.B.
ROSS, S.	FAA, N.Y.
RUSSELL, R.	FAA, Atlantic City
RUST, H.	Douglas Aircraft
SANWALD, G.	NAMC, Aeronautical Engine Laboratory
SALERNO, P.	Vapor Heating Company
SCHANNE, F.	NATTS, Aeronautical Turbine Laboratory
SCICCHITANO, E.	Grumman Aircraft
SHAFFER, R.	BuWeps
SHACKFORD, CDR	NAMC, Aeronautical Engine Laboratory
SHEFRIN, J.	Curtiss Wright
SHOHET, H.	Sikorsky Aircraft
SKALLA, LCDR	NATC, Patuxent River, Maryland
SIMPSON, G.	NATTS, Aeronautical Turbine Laboratory
SLIVKA, W.	NATTS, Aeronautical Turbine Laboratory
SMITH, E.	NATTS, Aeronautical Turbine Laboratory
SOMMERS, J.	FAA, Atlantic City
STAWSKI, E.	NATTS, Aeronautical Turbine Laboratory
STIRGWOLT, T.	General Electric
SUTTON, C.	Grumman Aircraft
THOMPSON, J.	NAEC, Atlantic City
THORP, J.	NAMC, Aeronautical Engine Laboratory
TILTON, L.	NATTS, Aeronautical Turbine Laboratory
TONGE, W.	B. F. Goodrich
UNTIED, J.	Lycoming Aircraft
UTTERBACK, J.	Chance Vought
VAN GELDER, F.	NATTS, Aeronautical Turbine Laboratory
VAN THULLENAR, C.	NSSP, U. S. Department of Commerce
WALTER, W.	NATTS, Aeronautical Turbine Laboratory
WARWICK, W.	NATTS, Aeronautical Turbine Laboratory
WEINER, F.	N. American Aviation, Inc.

WHITELEY, G.  
WHITMORE, Q., CDR  
WITTMANN, N. CAPT  
WOESSNER, W.

Weather Bureau, Trenton, N.J.  
NATTS, Aeronautical Turbine Laboratory  
NATTS, Aeronautical Turbine Laboratory  
NATTS, Aeronautical Turbine Laboratory

## PRODUCING WEATHER FOR TURBOJET ENGINE TESTING

by

F. A. Schanne and W. F. Walter, Jr.  
U. S. NAVAL AIR TURBINE TEST STATION  
Aeronautical Turbine Laboratory  
Trenton, New Jersey

Because of the wide scope of this subject, "Producing Weather for Turbojet Engine Testing", I have subdivided the subject into the answers to three questions; Why?, What?, and How?. First, Why simulate weather conditions in a test Cell? Second, What weather conditions should be simulated? and Third, How do we simulate these weather conditions in the test cell?

The first division, Why simulate weather conditions in a test cell?

The aircraft industry has, from its inception, recognized the adverse effects that weather conditions can impose upon aircraft performance. The Navy has experienced difficulty with turbojet powered all-weather aircraft. The cause of many of these aircraft failures has been directly traceable to the effects of water ingestion and icing on the engine. In addition to these actual aircraft failures, there are two other less catastrophic effects, the first of a mechanical nature, and secondly, the effect on engine performance. The mechanical effects are compressor rub caused by differential thermal expansion between the compressor and compressor case due to water ingestion, and compressor blade damage caused by the ingestion of large pieces of ice which can form in the inlet duct, on the bulletnose and inlet struts during icing conditions. These conditions result in the shortening of engine life, if not in complete engine failure.

As far as the second effect, that is engine performance, almost every parameter associated with the engine operating characteristics is effected by water ingestion and icing: Engine thrust, Fuel flow, Airflow, Compressor discharge pressure and temperature, Compressor surge characteristics, etc. The effect of weather conditions on all of these parameters is of the utmost importance prior to flight test. Comprehensive details of the effects of weather on engine performance will be presented in papers given later in this session.

Why simulate weather conditions in a test cell? The atmosphere does not provide the desired test condition on any kind of a predictable schedule or degree of severity. In a test cell we can subject the engine to progressively increasingly severe weather conditions which can be accurately controlled and measured. In addition, all

the test facilities are available for measurement of engine performance during these weather tests. In the test cell, then, we can produce any desired weather condition when we want it without the expense and hazards of flight test and with far greater accuracy. The Naval Air Turbine Test Station was ideally suitable for this type of work since it already possessed all of the necessary ingredients, large air handling capacity, air tempering capabilities ranging from  $-65^{\circ}$  to  $+190^{\circ}$ F, large altitude test cells, the necessary supplementary utilities such as water, steam and compressed air, excellent altitude capability, and a complement of scientific personnel experienced in engine performance, instrumentation, and test installation design.

Figure 1 shows schematically the layout of the entire laboratory. At the extreme left is electrical sub-station A where (25,000 KVA) incoming 132,000 V is broken down to 13,200 V for driving the 6,500 HP ram blow motors. The ram blowers are housed in the blower wing and are capable of putting out 400 lbs/sec. airflow at 30 PSIA.

The header system and heating and cooling rigs between the blower and test wing provide for flexibility in laboratory operation, and supply combustion air to each test cell with a temperature range from  $-65^{\circ}$  to  $+190^{\circ}$ F. The 3E test cell, now under construction, which is the last cell at the bottom, will have a high air temperature capability of  $1200^{\circ}$ F. This cell will have about twice the capability of the two altitude chambers pictured just above it, which are presently in operation. The next two cells above are sea level cells and, as the name implies, are capable of all types of sea level engine testing. The cell at the top, which is called the general purpose cell, was originally built for testing turboprop engines with propeller attached. It is 33 feet square and 190 feet long, including the sound treatment for secondary air at each end. This cell has altitude capabilities and was used for installation of the F3H fuselage with the J71 engine, which will be discussed later. The four cells with altitude capabilities are tied into exhaust gas coolers which reduce the exhaust gas temperature to a maximum of  $175^{\circ}$ F.

Altitude conditions up to 90,000 feet are obtained by manifolding the exhaust gas coolers to a three stage system of exhausters in combination with engine exhaust gas ejectors in the cells.

The sub-station B supplies power to the fourteen exhauster motor drives. The pump houses circulate the water cooled in the cooling tower, and the water treatment plant provides makeup water from the Delaware River for the station water system.

The second major division of this discussion, What weather conditions should we simulate?, is a rather controversial subject, but strides are continually being made to obtain more knowledge about the conditions which are encountered in the atmosphere. I am speaking here in terms of degree or range of magnitude of weather conditions.

These conditions are broken down into three general categories: liquid water, supercooled water which causes icing conditions, and ice particles.

Liquid water has been measured in amounts as great as  $52 \text{ gm/M}^3$ . This is the equivalent of one inch of rain in one minute. In this area of the country, if it rained one inch in twenty-four hours, it would be considered a lot of rain. Actually, a realistic figure of 10 to  $12 \text{ gm/M}^3$  is considered a heavy rain with the possibility of  $20 \text{ gm/M}^3$  existing as an extremely heavy rainfall rate.

Supercooled water, by definition, only exists below the freezing point. Water drops have been known to exist at temperatures of  $-40^\circ\text{F}$  and below.

The ice particles or crystals, with the exception of hail stones, are generally so fine that they follow the airstream and do not impinge on aircraft surfaces. They do not constitute a serious icing problem. No facilities are presently available for this type of test, but several are under consideration. Most of the engine manufacturers have conducted extensive tests of this condition.

The third consideration is How to simulate weather conditions in the test cell.

In order to maintain liquid water in an airstream during water ingestion tests, it is necessary to establish 100 percent humidity prior to water injection. If water is injected in air which is not saturated, some or all of the water injected will evaporate. Even though all injected water is carefully measured before injection, the actual amount of liquid water entering the engine would be questionable if evaporation took place. This problem, coupled with temperature instability due to evaporation, makes it mandatory that the air be 100 percent saturated prior to water injection.

To accomplish saturation of the combustion air, it was decided to inject steam into the airstream. Because steam does not have to be evaporated by the air, it does not cause a temperature drop. This decision was also tempered by the fact that our steam plant could provide 35,000 lbs. of steam per hour, beyond its normal load requirements.

On a cold winter day when there is almost no moisture in the air, the full steam flow capacity is required to saturate for a high airflow hot day test. To give an idea of the magnitude of the water required to saturate the airstream, converting the steam flow to gpm of water; it takes about 60 gpm to raise 200 lbs. of air per second from 80 to 100 percent relative humidity.

The humidity system design consists of a network of steam lines feeding each test cell as far upstream of the water ingestion station as possible, modulating remotely controlled valves and humidity indication systems for each test cell. The operation of the system requires careful coordination with the combustion air temperature control system because of the effect of steam injection on the air temperatures.

When the desired degree of saturation has been established by the humidity control system, the combustion air is ready for water ingestion testing. The problem of what quality of water is required then arises. Initial tests at Trenton were conducted using plant cooling water which contained zinc chromate to prolong the life of the heat exchangers and piping system. It was found that this zinc chromate and other impurities were deposited on the compressor blades since this water evaporates in the compressor from the heat of compression. Since these early tests, we have used steam condensate from the steam plant. This has proven to be entirely satisfactory except that it heavily taxes the steam plant condensate makeup system. The water ingestion supply system which we plan to permanently install will use boiler feed water which has been treated by demineralizers.

In spite of our efforts to obtain water as free of contamination as possible, it is recognized that rain water is not perfectly pure. However, the purity is high, and it is felt that the water used is a good substitute.

This system will distribute conditioned and tempered water under pressure to each test cell in quantities from less than 1 gpm to 175 gpm. A 7,000 gallon tank is used to store enough conditioned water for one day's operation. This permits use of a low capacity purification system to makeup during off hours. This tank is plastic coated and plastic pipe, and fittings are used to prevent contamination of the water.

A system of three pumps is used to meet the requirements for the wide flow range. Steam heat exchangers located adjacent to each cell provide water temperature control. There is a school of thought that contends that the process of producing supercooled water is better accomplished when the water is cooled rapidly from an elevated temperature. This reasoning, plus the fact that high water temperature helps prevent freezing at the water spray nozzles, forms the justification for the heat exchangers.

The pressure control system for the water supply consists of a series of modulating, pneumatic, remote controlled valves and, a series of remote controlled on-off type solenoid valves. The modulating valves are used to preset required water flow rates prior to a test run, and the solenoid valves are used to give this preset flow rate instantaneously during the test. This arrangement is used for steady state running. For transient test a universal control valve is tied into the system. This control valve receives an input control signal from some engine parameter such as engine speed. The valve then controls the rate of flow as a function of the engine parameter.

In order to meet the requirement for both water ingestion and icing conditions, two systems of ingestion are used. The water ingestion arrangement is a system of uncomplicated water nozzles in the periphery of the engine inlet duct and a donut shaped pipe with a series of holes which is mounted inside the duct. The primary function of this arrangement is to provide an even water distribution at the engine inlet under a wide range of water flows. This system is mounted only a few feet in front of the engine inlet. No attempt is made to control drop size with this water ingestion system.

The objective of the icing system is to produce a homogeneous fog of the consistency and drop size required by the test. This spray arrangement is located in the large 12 foot diameter inlet pipe to reduce as much as possible the effect of air velocity on drop size and distribution. The location of this system varies somewhat from cell to cell, but is kept in the range of 28 feet from the engine inlet.

The heart of the icing rig is the concentric air-water nozzles which produce fog of varying droplet sizes depending on the combination of water and air pressure supplied to the nozzle. These nozzles have a relatively low flow rate and, since the water pressure is an important factor in the droplet size produced, it cannot be varied to change flow. Because of the low nozzle flow rate, it has been necessary to install as many as 100 nozzles to meet maximum test conditions. Intermediate and low flow rates are accomplished by a system of remotely controlled solenoid valves which divide the system into small banks of nozzles with as few as six nozzles in a bank. The nozzles are mounted in a series of air foil shaped spray bars installed in the 12 foot diameter inlet pipe.

The air supply for these icing nozzles is drawn from the 100 psi shop air system. The pressure of the air is modulated with remote controlled pressure regulators and heated through heat exchangers.

The warm air supplied to the nozzles gives added protection against nozzle freeze up. In addition to the dual piping for the air and water in the spray bars, a steam line is also inserted to prevent freezing of the water in the bars.

Figure 2 is a simplified drawing of the engine in the test cell showing the location of the water sprays and icing rig in the inlet pipe. At the extreme left is the T.V. camera which is used to monitor the condition of the engine during test. Photos of the T.V. monitor provide for a permanent record of these conditions. Conditioned combustion air enters the inlet pipe at the left, flows over the T.V. camera around the spray bars, where it picks up the icing fog, down the large inlet pipe and into the bellmouth and engine inlet duct. In this inlet duct are the two drop size measuring stations at sections A and B, and the water ingestion station. The engine is shown mounted in a typical thrust stand which is suspended from flexures for measuring thrust.

This then completes the general description of our facilities. Consideration will now be given to some of the usage that the facility has been put to, and what possibilities exist for future usage.

In solving the problem with the F3H aircraft, we found it expedient to install an aircraft fuselage in 3W, our general purpose test cell.

Figure 3 shows the F3H fuselage mounted on the test stand in 3W prior to making the combustion air connection. A special nose cone with a water supply was installed to simulate rain flowing over the frontal area. The extensive taping of the skin joints was necessary to prevent leakage into the air frame.

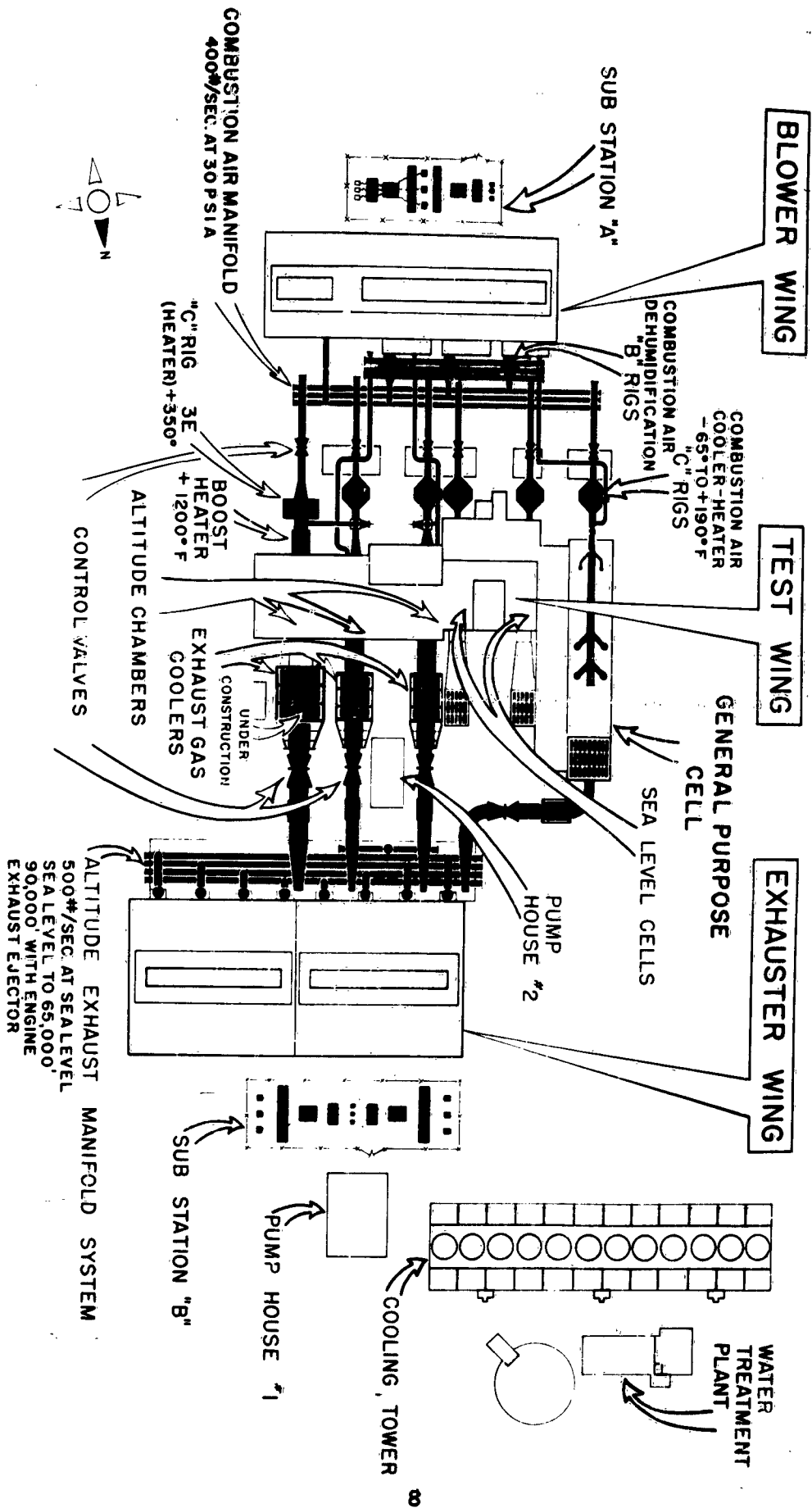
Figure 4 shows the inlet air pipe adaptor or glove section that makes the connection to the air frame. This glove section was designed to simulate actual air velocities over the inlet portion of the air frame.

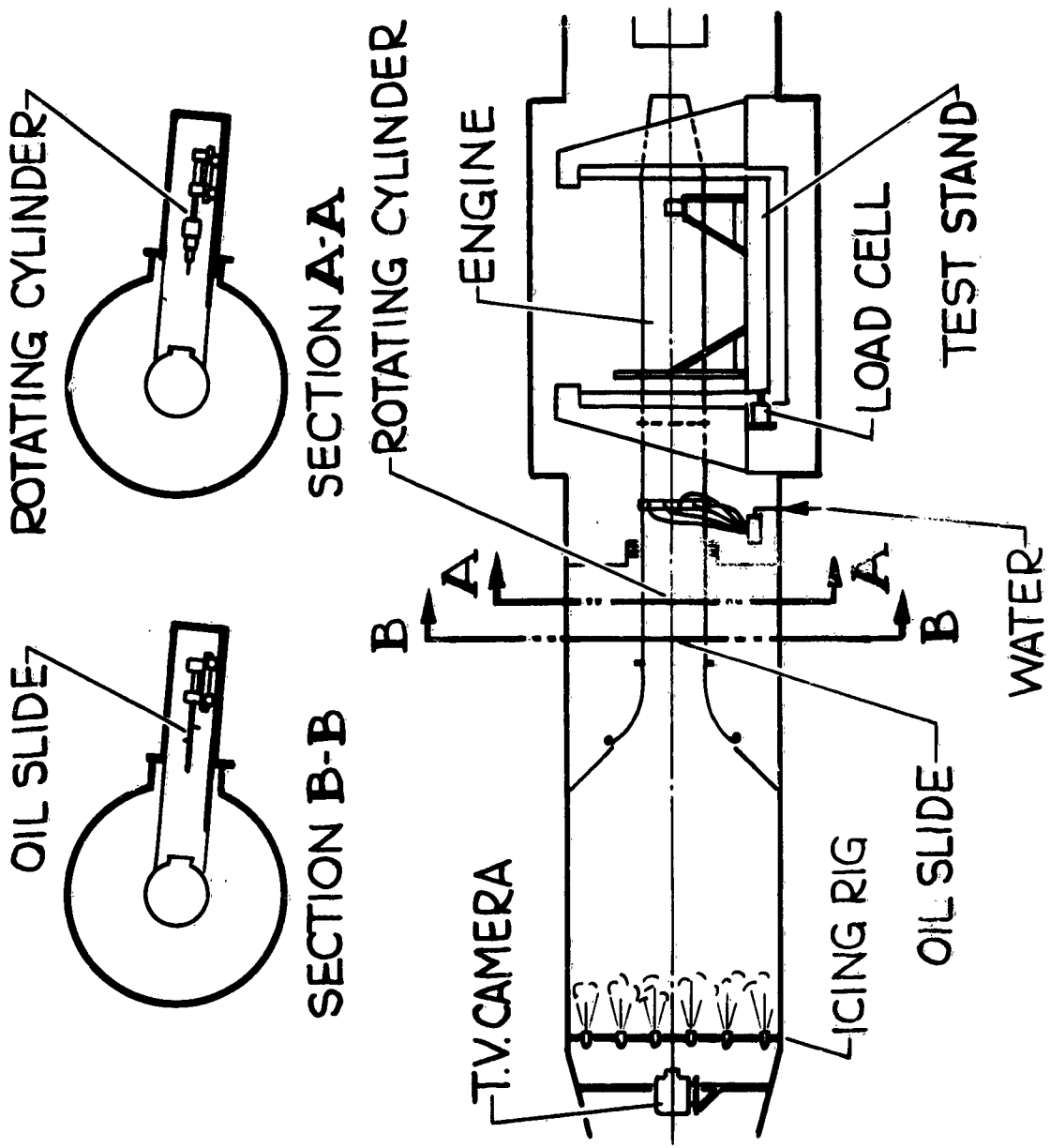
Figure 5 depicts a schematic of the fuselage and the engine installed in the cell with combustion air and exhaust pipe connections. The air flows from the left into the glove section over the fuselage and into the air intakes. The water introduced at the nose cone simulates the rain that impinges on the frontal area and runs into the air intakes, and the sprays at the air intake simulates the water carried directly by the air. The test results obtained from this installation will be covered in papers presented later in this session.

Figure 6 shows the operating envelope for the J79 engine superimposed on the plant facilities capabilities. Flight mach number is plotted against altitude. The plant pressure limit is shown along the bottom of the envelope and is not a significant limitation. The 1.8 mach number limitation is based on present inlet air temperature of 190° and present exhaust capacity. The two shaded areas show that NATTS is capable of icing and water test over the entire engine envelope. Inlet air temperature dictates whether icing or water ingestion conditions will take place. The overlapping region between icing and water ingestion is in the temperature range of 32° to 23°F.

# AERONAUTICAL TURBINE LABORATORY

FIGURE 1

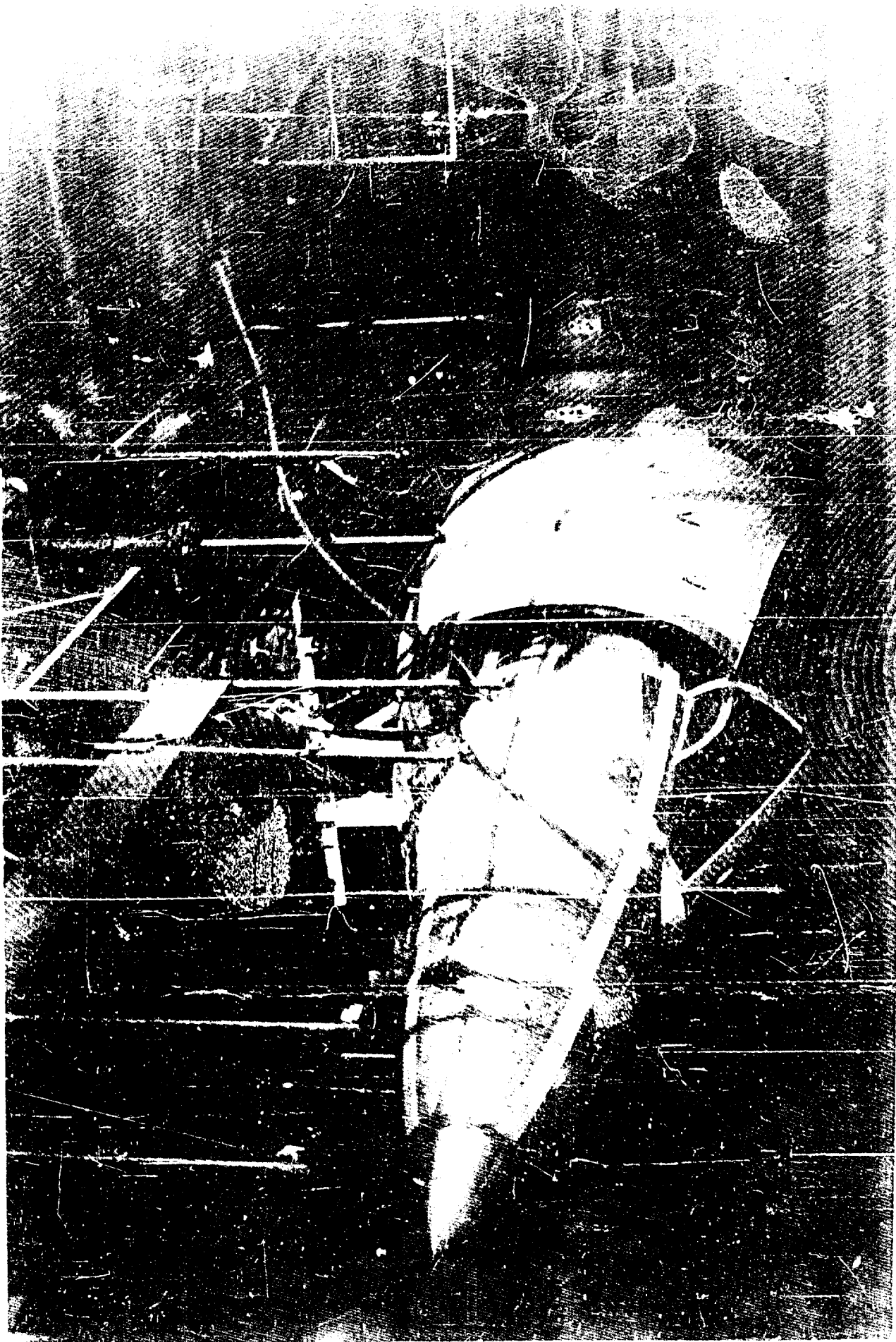


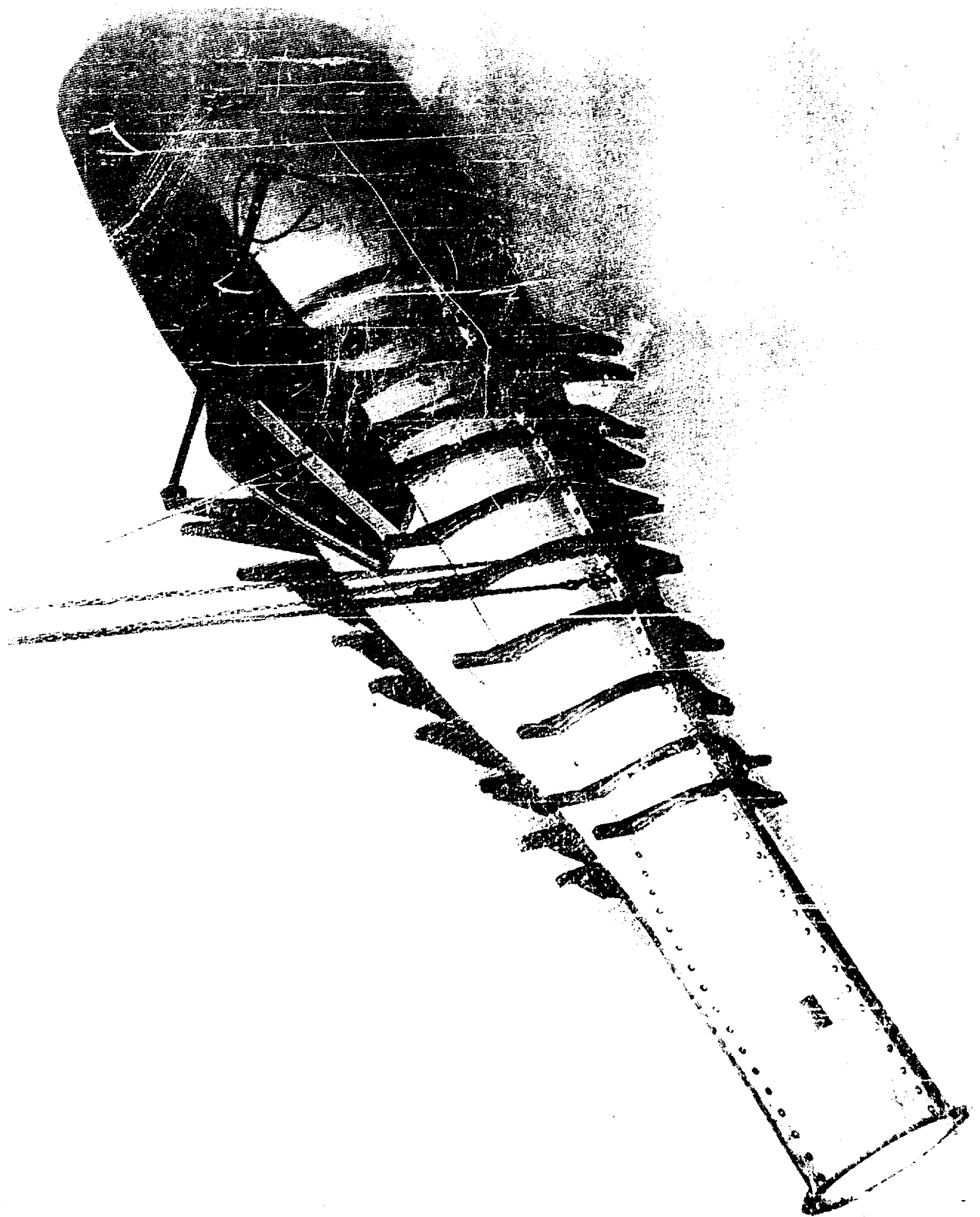


TEST CELL WITH WATER AND ICING RIGS

FIGURE 2

F3H BUZZBLADE MOUNTED ON THE TEST STAND IN 3V





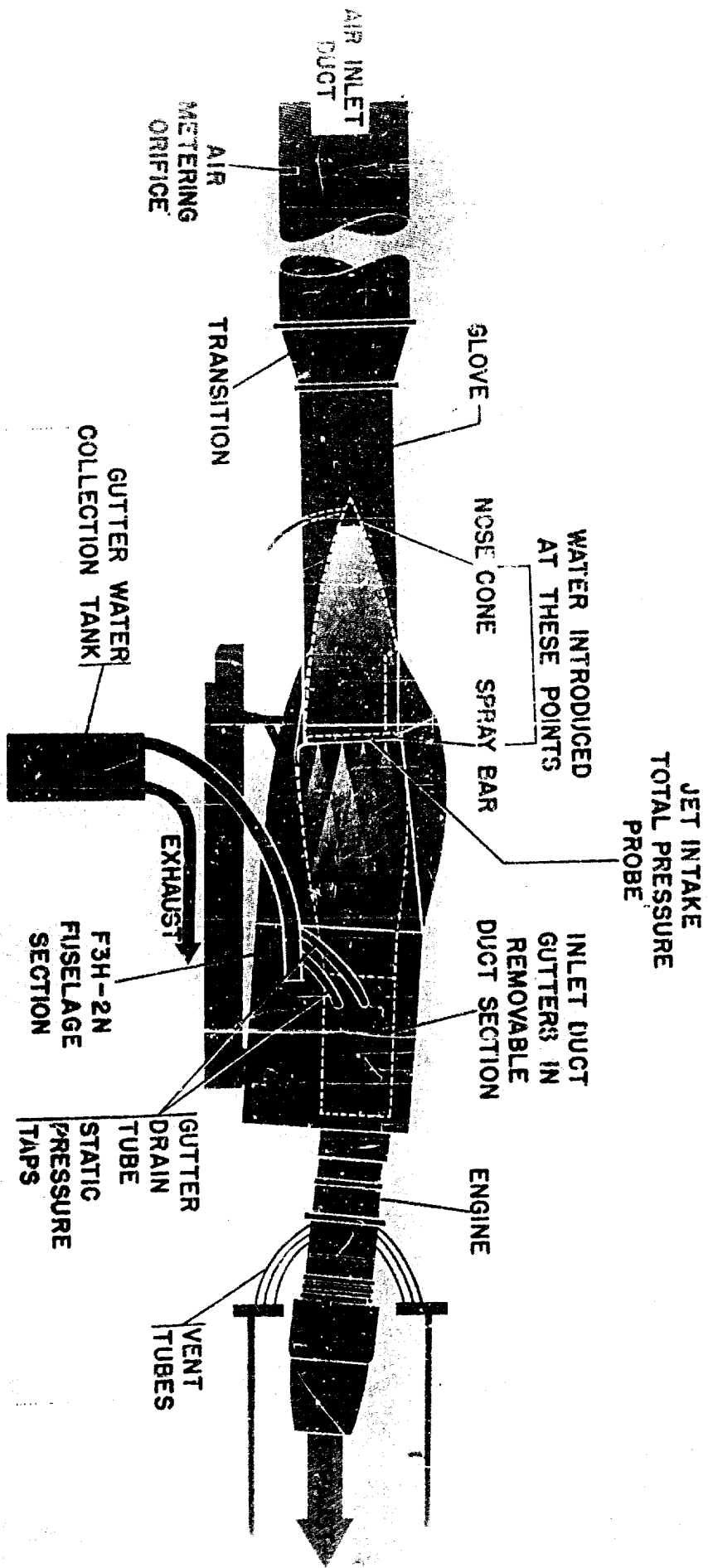


FIGURE 5: TEST INSTALLATION SCHEMATIC

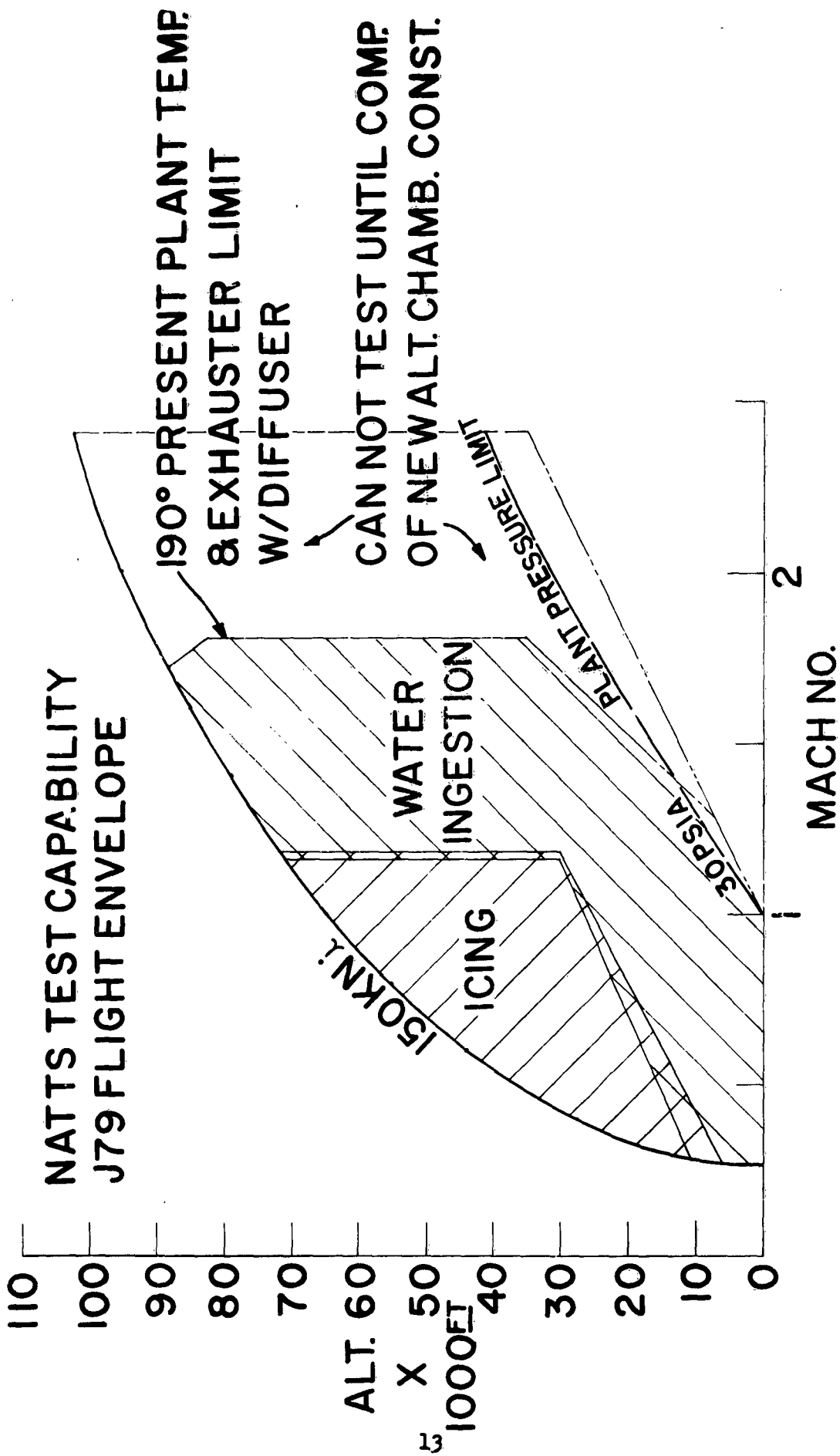


FIGURE 6

## SOME PROBLEMS ENCOUNTERED IN ESTABLISHING A SMALL ENGINE ICING FACILITY AT THE AEL, NAMC

By: S. C. Hill and J. A. Thorp  
Acting Branch Heads, Engines Division, AEL

It is well known that gas turbine engines are liable to cause serious damage or failure when operating under icing conditions. These conditions exist where ambient air temperature range from  $-10^{\circ}\text{F}$  to  $+30^{\circ}\text{F}$  and a fog of super-cooled water droplets is present. Test flights have shown that severe icing conditions exist when the liquid water content ranges beyond  $1/2 \text{ gram/m}^3$  and mean liquid water droplet sizes are from 10 to 30 microns in diameter. Under the warmer ambient conditions rapid-growing mushrooming ice formations occur on the engine inlet, restricting the required engine air supply and causing compressor stall and excessive exhaust gas temperatures. Under colder icing conditions, hard rime ice forms which may break off and cause compressor failure.

A word of explanation on icing test techniques may be in order for those that may not be familiar with the procedures. Liquid water content, mean droplet sizes, and drop size distribution have been generally determined by "rotating multi-cylinders" when standard pre-cooled aluminum cylinders, ranging in diameter from  $1/8$  inch to 3 inches are placed on a single rotating shaft in the inlet air stream at right angles to the air flow, for a carefully measured period of time. The cylinders are then removed and the ice accretion on each, carefully weighed. Since small droplets lack the momentum of larger droplets, they tend to travel around the larger cylinders rather than to strike and freeze as the larger drops will do. It may be seen, therefore, that the rotating cylinders offer a method of determining not only the liquid water content but the mean droplet sizes and drop size distribution. In addition, mean droplet sizes and drop size distribution can be verified by the "oil slide method". A small cup (perhaps 5 mm in diameter) of heavy oil is exposed briefly to the fog of the air stream and the sample is quickly photographed through a microscope. The mean droplet diameter is then determined by means of statistical analysis.

Early investigations of icing problems of gas turbine engines were conducted under natural icing conditions with turbo-jet engines. Small turbo-shaft engines were not con-

sidered important from the standpoint of national defense. AEL personnel conducted icing investigations under Project Summit on Mt. Washington, N. H., in the late 40's and early 50's, using both natural and artificial icing conditions. Icing test techniques were firmly laid out for large engines. In recent years, icing facilities were planned for even larger gas turbine engines, but under controlled laboratory conditions.

Allison and NATTS established laboratory icing facilities for gas turbine power plants. However, small turbo-shaft engines were coming into use and AEL was assigned the building of a small engine icing facility. Visits to other activities were made and available literature was studied. Design and construction of a facility capable of testing turbo-shaft engines in the range of 2,000-4,000 bhp was initiated. However, in March of 1961, the task of testing a 270-hp turbo-shaft engine on a maximum priority basis, was assigned, and work for the "larger" engines was deferred. Because of the urgency of the job, it was decided to incorporate as many proved features in the design as possible. Certain exceptions had to be taken and these will be pointed out as we go along.

The Bureau of Naval Weapons had stipulated that the AEL tests were to be run with complete engines and the effects of ice accretion, ice prevention, or ice removal on the output shaft horsepower noted. This meant that some power-absorbing device must be used. Our experience in this field led to the selection of a water brake for this function and, to date, its performance has been entirely satisfactory.

Briefly, this small turbo-shaft engine incorporates a centrifugal compressor, and an inlet diameter of 5 inches and has a maximum air flow of 5 pounds per second. Heretofore, to the best of our knowledge, the ducting to engines undergoing icing tests was approximately the same size as the engine inlet. As previously mentioned, we did not have time to develop new icing intensity measuring techniques and, since all previous endeavors in this field seemed to establish the "rotating cylinders" as the basic icing intensity measuring tool, it was decided that a 24-inch inlet duct would be necessary to accommodate the standard rotating cylinders which are 17 inches long. A 5-pound per second air flow in a 24-inch duct results in an air velocity of approximately 15 miles per hour, which appeared to be low for good rotating cylinder results.

Since altitude tests were not required, the engine inlet was placed just close enough to the exit of the 24-inch diameter duct to permit a few inches of "blow by space" around the engine inlet circumference. It remained to provide a method of supplying a uniformly distributed fog from spray nozzles of the desired size and number, to correlate these droplet sizes, numbers, and distribution and to determine the effect of such a controlled icing environment on the test engine.

Plate 1 is a sketch of the facility as it now exists. Air, near saturation conditions, is provided by the laboratory refrigeration system to the plenum of the conditioned-air inlet. Test temperatures are run at either  $-4^{\circ}\text{F}$  or  $+23^{\circ}\text{F}$  in accordance with the test specification. Extending from the plenum, the 24-inch diameter ducting carries the conditioned inlet air to the fog inducing spray section. The water preparation equipment supplying this section may be seen in detail on plate 3. One advantage present in a small engine test facility is the relatively low noise level (a maximum of 110 decibels, and this only in an unvisited area) which permits personnel with ordinary ear protection to perform their duties on the site. Thus, the water and compressed-air control system may be located close to the test engine.

The test engine is at the extreme end of the 24-inch ducting. Just aft of the engine and coupled to it is the water brake used to absorb the output power of the engine.

Telescopic observations from the rear viewing port were made during icing runs. A ten-power telescope enables a close-up study of the engine inlet ice formations to be made with considerably greater clarity than with television. The rear observation port was also used to check spray nozzle operation, uneven or turbulent fog patterns, freeze out, etc. It was originally planned to install the television camera at this position and use the camera's zoomar lens for close-up views. Telephoto lens photographs from this location show excellent detail.

The location of the television camera as installed in icing inlet duct is shown. The television receiver was located in the upper deck engine control room where any dangerous engine inlet icing condition, as well as rotating

cylinder exposures and ice accretion, and oil drop sampling exposures, were observed by means of the zoomar lens adjustment.

The spray control bench where an operator sets up the required water flows, water pressures, air pressures and temperatures, and checks on uniform nozzle operation during a test run is shown lower right on the sketch.

The gap between the engine and 24-inch duct is readily discernible. This distance of approximately 1 foot was found to be optimum for our test purposes, and we also believe that this arrangement may be a more accurate simulation of actual operating conditions since the cold wet air is impinging on the entire frontal area of the engine and flowing over the compressor case. Another advantage of the gap was that photographs of the icing formations could be made through the gap.

Plate 2 shows the individual nozzle holder developed at AEL specifically for these icing tests. It was decided that the usual spray bars containing many nozzles would not suffice for these tests since the low total water flows required could only be attained by strict control of individual nozzles. Several agencies have developed satisfactory nozzles; however, this nozzle is a modified NACA design of our own manufacture and copied from that used at Allison during their icing tests at Indianapolis. The nozzle calibration runs showed that the slightest leak between the air and water chambers resulted in severe distortion of the spray pattern and abnormally large water droplets. It was also found that any minute solid contaminant in the water would distort the spray pattern, necessitating the use of distilled water in this rig. Analysis of the final water spray patterns achieved showed that the largest droplets were only 25 microns in diameter when the mean droplet size was 15 microns and only 32 when the mean droplet size was 25, and no freeze-out was noted. This absence of freeze-out is explained in "Modern Icing Technology" by Myron Tribus where it is shown that water droplets of this magnitude will not freeze spontaneously at temperatures above  $-18^{\circ}\text{F}$ .

The configuration of the spray nozzles in the 24-in. duct is shown on plate 3. Since the design water flow of the NACA atomizing spray nozzle is 10 pounds per hour per nozzle and these icing tests required 30 to 60 pounds per hour water flow with excess blow-by air flow, the ring of six nozzles was designed

to provide the proper total water flow by using either all six nozzles or three alternate nozzles as required. A ten-inch diameter ring was selected to provide uniform central distribution and minimize freezing-out on the duct wall. Before installation of the test engine, a 1/2-inch mesh wire screen was placed on the exit flange of the 24-inch duct and observations were made of ice distribution under the various conditions anticipated in engine tests to insure satisfactory distribution.

In spite of the effort to keep impurities out of the spray nozzles, preliminary tests were interrupted frequently by nozzle clogging. As it was shown finally, these impurities were introduced chiefly through the compressed-air system when, following a test run, compressed air was used to purge the nozzle water tubes. Improved filtration of the compressed-air system was adopted and the trouble alleviated.

Two sets of rotating cylinders were used. The larger is the conventional design using 6 cm long cylinders, while the smaller set consists of cylinders that are 3 cm in length. The shafts were equipped with quick disconnects so that the same power shaft can be utilized for several cylinder runs during a single icing run. The cylinder assemblies were chilled in an insulated cold box which, when in use, contains dry ice and a desiccant. Our procedure was to couple the chilled cylinder assemblies to the power shaft and insert them into the 24 in. duct as quickly as possible. After exposure, the cylinders were placed immediately in glass jars, with screw-on lids and equipped with special gaskets of non-hygroscopic material.

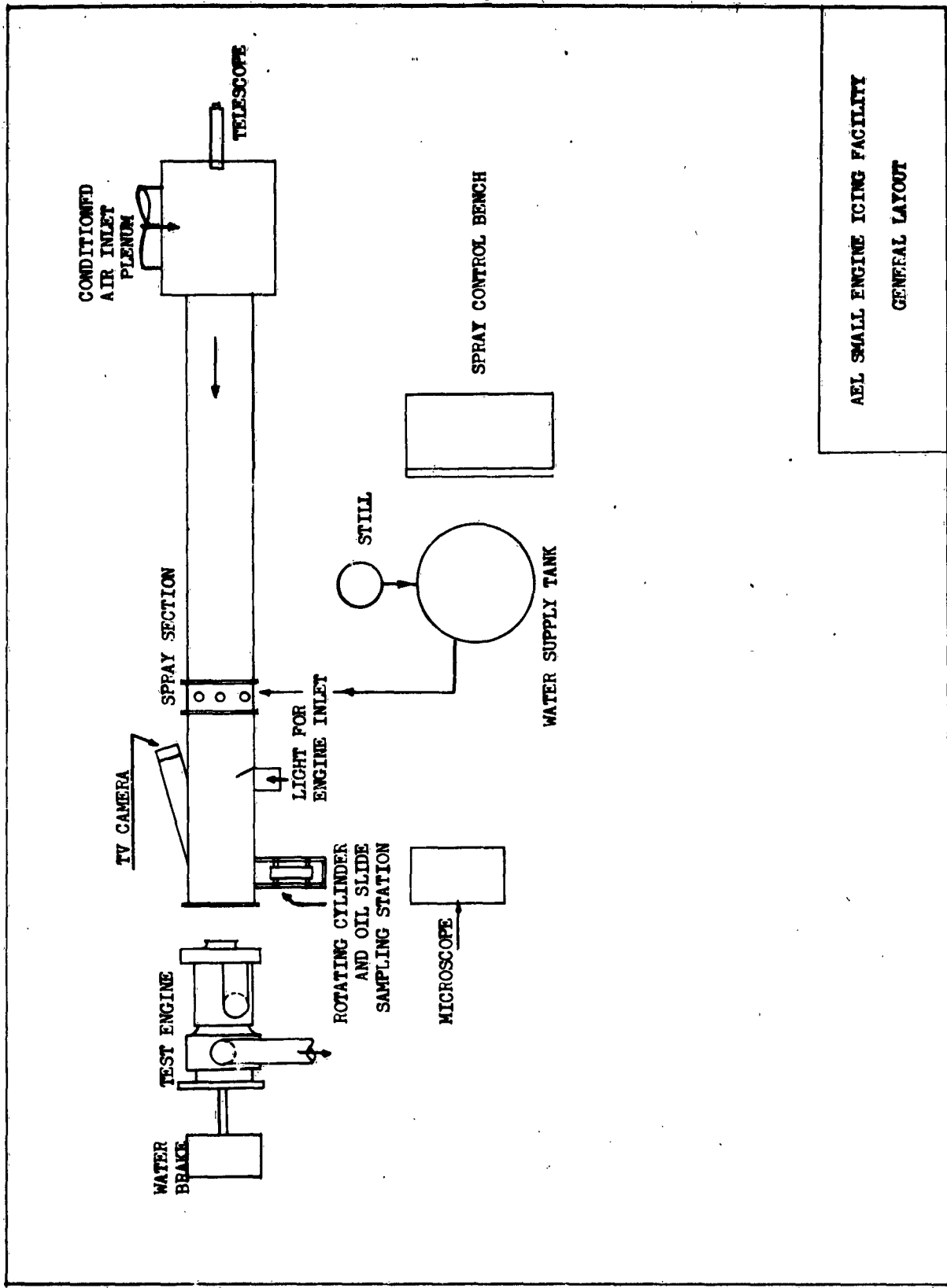
The small cylinder assembly was designed to approximate more closely the inlet diameter of the engine under test. Preliminary analysis of these readings have not been as successful as those results determined by using the standard cylinders. However, these discrepancies are under investigation.

The average time that the chilled cylinders were exposed to the ambient test-area conditions was determined and a corresponding experimentally-determined correction, depending upon the absolute humidity, was applied to the differential weight of the cylinders. Plate 4 shows the magnitude of the correction. It was found that the median droplet size thus determined from the cylinders correlated within 10% compared with the droplet size as determined by photomicrography. Satisfactory correlation with the calculated liquid water contents (within 25%) was also

obtained providing the inlet air was at or near a saturated condition.

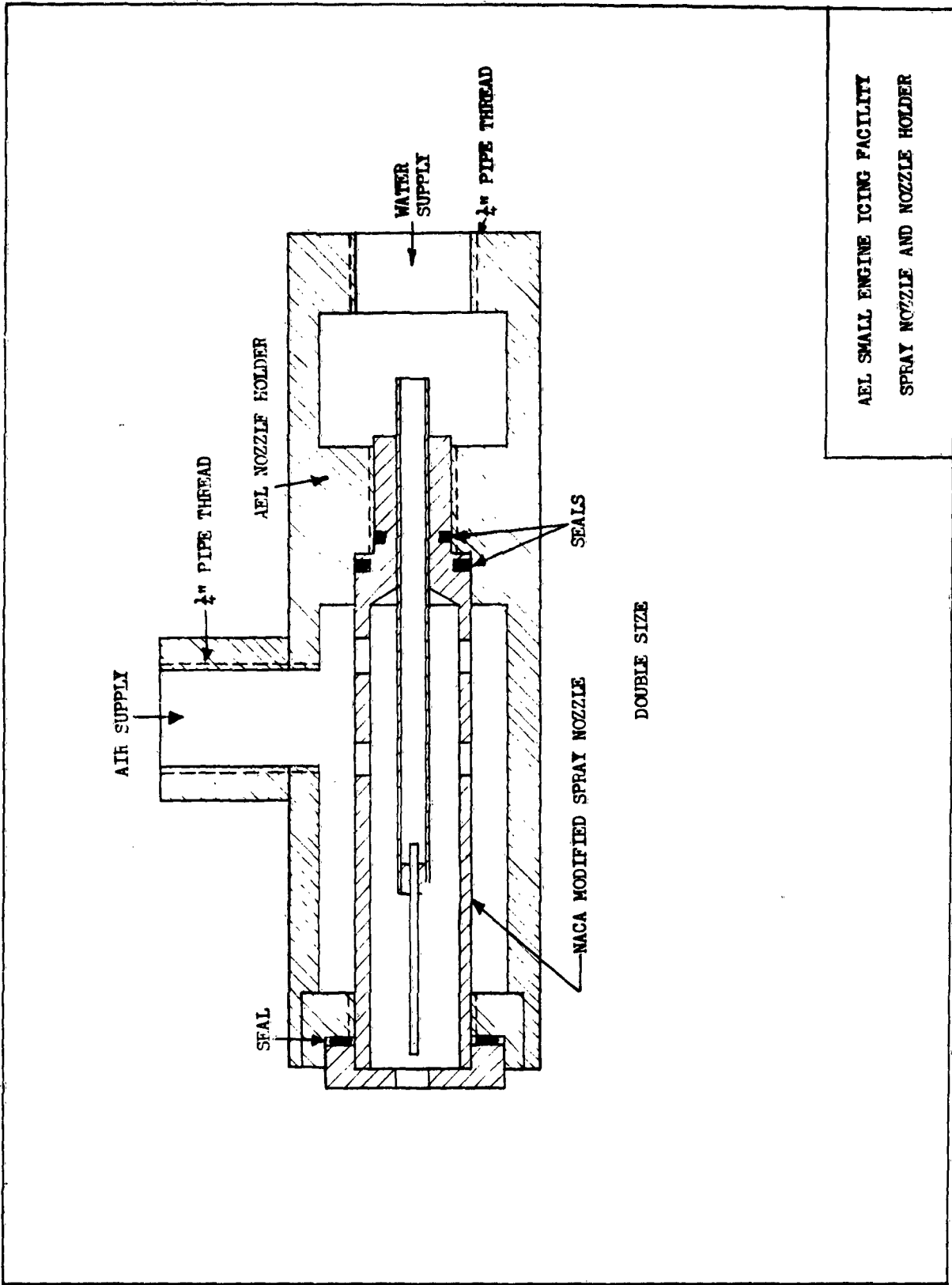
The importance of photographing the sampling oil slide promptly is disclosed on plate 5. Rapid evaporation and coalescence of the sampled droplets change the results as time elapses between taking and photographing the sample. Further, it was found that the total volume of entrapped water decreased to approximately 25% of the original volume in this same interval of time.

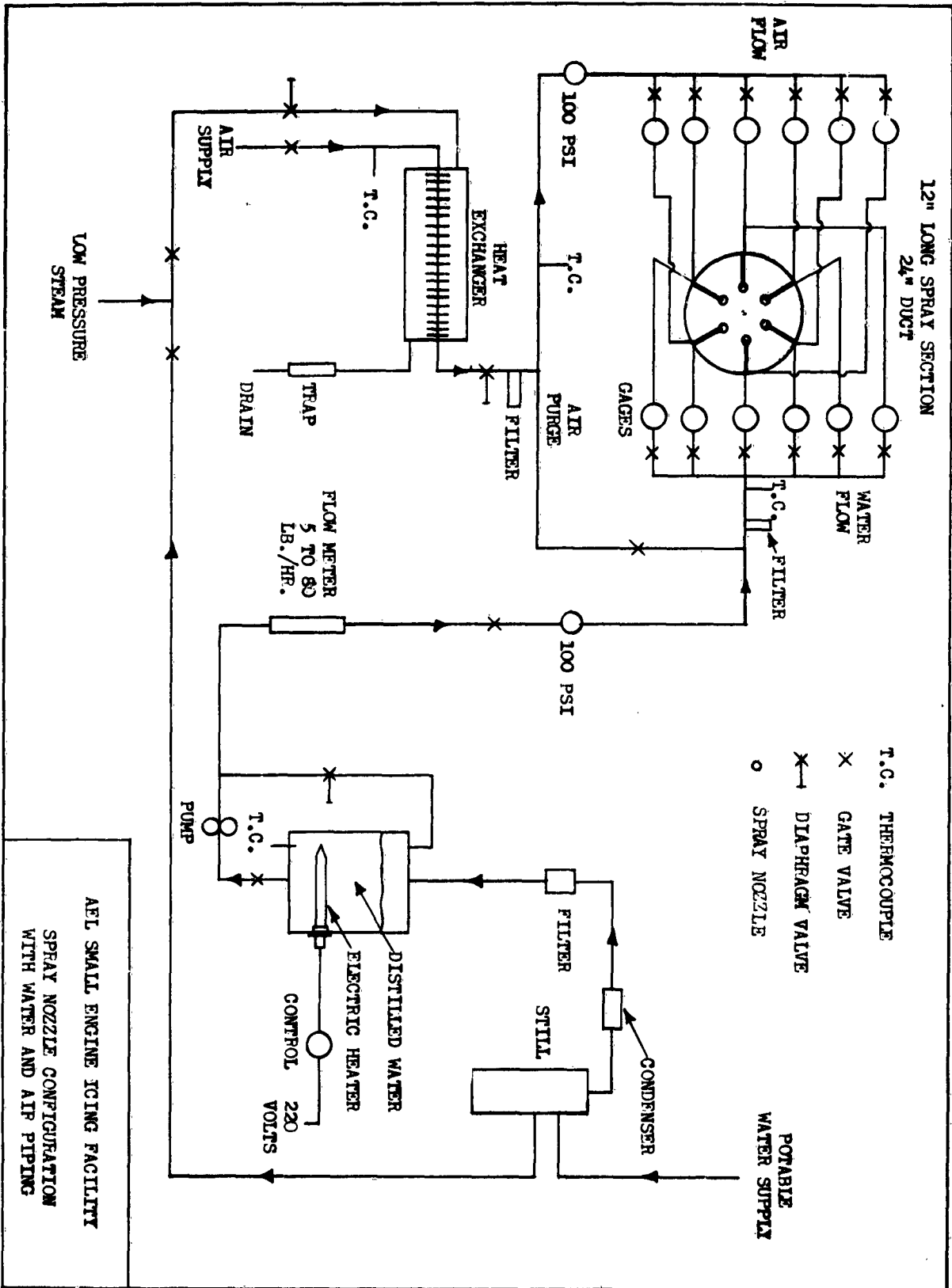
A description of our small engine icing facility has been presented and some of the problems in making it operational have been discussed. Although limited in quantity, the results of our tests have been gratifying, especially when it is considered that only a few months were available for the development of the facility and conducting of the tests. The largest single problem that we encountered was that of supplying liquid water droplets of the proper size, concentration, and distribution to the test area. We would like to acknowledge the technical advice of NATTS and Allison Division of General Motors.



AEL SMALL ENGINE ICING FACILITY  
GENERAL LAYOUT

PLATE #1





ANALYST MOISTURE  
PICK UP ON  
ROTATING CYLINDERS

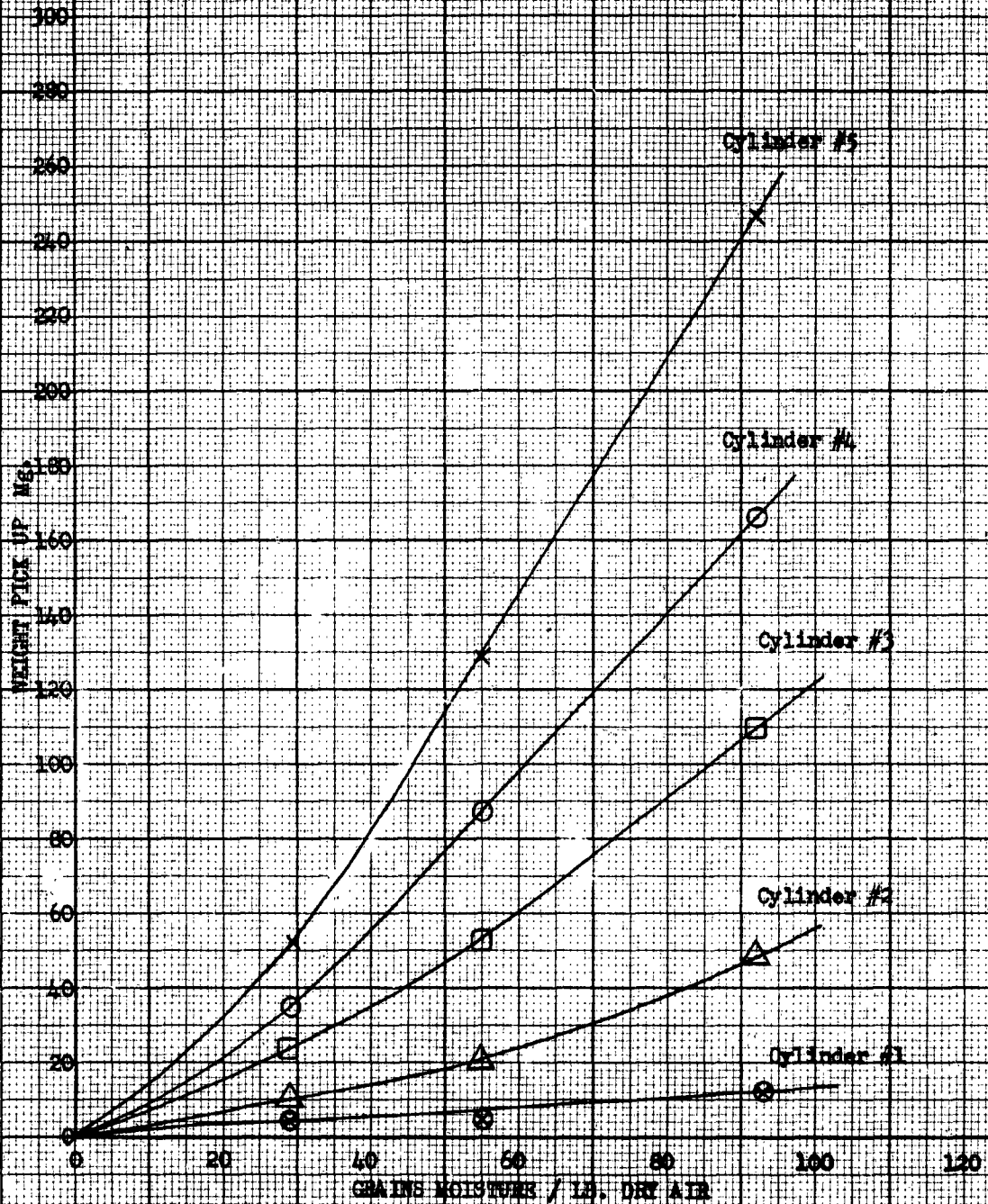
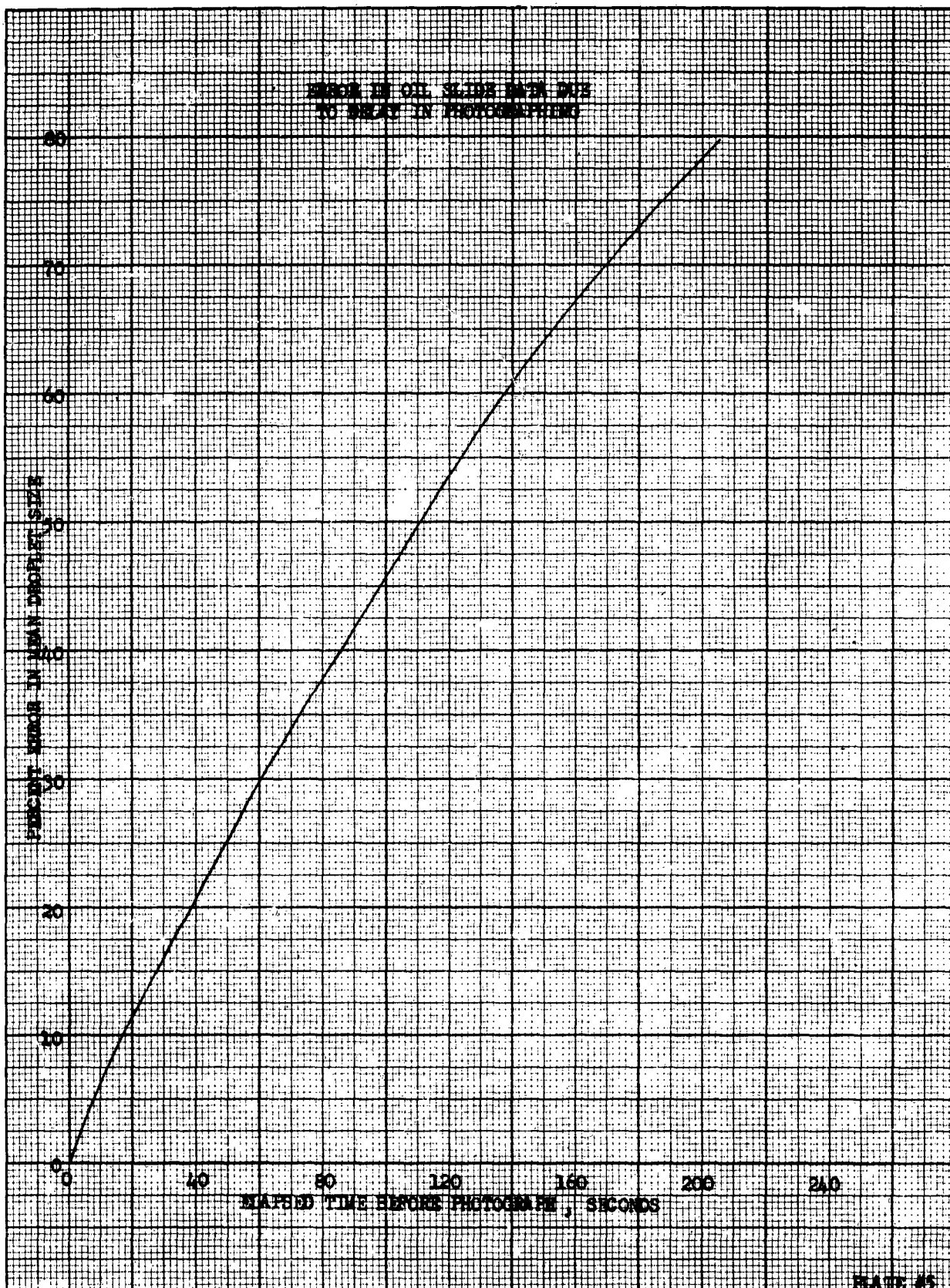


PLATE #4



## THE PHOTOELECTRIC RAINDROP-SIZE SPECTROMETER

By: A. Nelson Dingle  
Associate Professor of Meteorology  
Department of Engineering Mechanics  
The University of Michigan

### ABSTRACT

The measurement and counting of raindrops is accomplished simultaneously by means of a photoelectric device using forward-scattered light from an optically-defined sensitive field. The present device is designed to serve as a ground-based instrument, hence to obtain an adequate sample, the sensitive field is made to scan the rain field by means of mechanical rotation about a vertical axis. A sampling rate of  $0.54 \text{ m}^3 \text{ min}^{-1}$  is obtained in the present instrument.

Considerable interesting detail of the structure of rain in space and time is revealed in records acquired with this instrument.

### INTRODUCTION

Until the last decade or so the information available on rain, by virtue of nearly a century of weather observation, was confined to that obtainable by the use of a bucket and a measuring stick. For purposes such as that of this conference, and also purely for the sake of knowledge, this kind of rain information is simply inadequate. Particularly is this so as it applies to that part of physical meteorology that is concerned with precipitation physics.

It has been recognized for some time that detailed knowledge about raindrop sizes should form a basis for, and a limitation upon, any complete theory about the formation of rain and about the effects of rain wherever it is encountered. The first recorded attempts to study rain in this way antedate the present century (Lowe, 1892; Wiesner, 1895), and many others have followed. The present instrument represents an effort to use electronic techniques so as to obtain the desired details about raindrop numbers and sizes with good fidelity without excessive labor. This device is designed for operation at a ground-level station. The principles used in its design should prove useful for the development of an airborne raindrop-size spectrometer.

## THE RAINDROP-SIZE SPECTROMETER

The basic instrument is an optical photometer which is arranged to respond to forward-scattered light. This arrangement is quite important because it makes possible the definition of the sample to be observed without the use of physical obstructions and because by this means precise observation from a distance can be accomplished. Obviously in the observation of drop-size spectra of natural rains, the results can be seriously distorted by the presence of splatter drops in the sample space.

### The Sensitive Field and the Scattering Angle

The optical definition of a "sensitive field" is, at first thought, a relatively straightforward problem. The solution, briefly stated, is to project a beam of light from a light source unit, and to view a portion of the beam using a photometer unit with optics directed at an angle to the projected beam. With this arrangement, light scattered from the beam toward the photometer by particles in the sensitive region provides the information desired.

To achieve the maximum photometric signal for a given source intensity, it is clear from light scattering theory (Mie, 1908) that forward-scattered light may be used to a considerable advantage over 90°-scattered light. It is important, however, that signals generated by equal drops in all parts of the sensitive field be equal within small limits of error. Consideration of the optical geometry of the photometer objective lens in relation to the sensitive field (figure 1) shows that both the forward-scattering angle and the light-gathering power of the lens change from place to place within the sensitive field

These variations fortunately oppose one another, and thus tend to dictate the most functional scattering angle,  $\theta_A$ . The variation of the intensity of light scattered by "very large" water drops has been tabulated (Van de Hulst, 1957) for selected scattering angles,  $\theta$ . In this case "very large" means that the circumference of the drop must be more than 30 times the wave length of the light used. The values for the gain,  $G_\theta$ , of intensity in the direction  $\theta$ , from a spherical raindrop relative to that from an isotropic scatterer are given in table 1. The values at 35° and 45° are graphically interpolated from figure 2, hence they are set in parentheses.

TABLE 1: Computation of  $R_{\theta}/40^{\circ}$

$\theta^{\circ}$	$G_{\theta}$	$\left[ \frac{\sin \theta}{\sin 40^{\circ}} \right]^2$	$R_{\theta}/40^{\circ}$
15	11.38	0.162	1.84
20	8.70	0.284	2.47
25	6.41	0.434	2.78
30	4.67	0.605	2.82
(35)	(3.37)	0.798	(2.69)
40	2.36	1.000	2.36
(45)	(1.66)	1.210	(2.01)
50	1.13	1.425	1.61

The light-gathering power of the photometer objective lens may be assumed to follow the inverse square law in the present case. It is clear that the distance from the sensitive field to this lens is a function of the angle  $\theta$  (figure 1). Combining the inverse square effect with the effect of the scattering angle upon intensity, and using  $40^{\circ}$  as the reference angle for the inverse square effect, the values of

$$R_{\theta}/40^{\circ} = G_{\theta} \left[ \frac{\sin \theta}{\sin 40^{\circ}} \right]^2$$

were computed and plotted against the scattering angle (figure 2) to obtain a graphical solution for the best value of  $\theta_A$  for the present purpose. This turns out to be  $28.8^{\circ}$  for  $\Delta\theta = 5^{\circ}$ , and under these circumstances, the predicted signal variation attributable to the incomplete compensation between these two effects (scattering angle and inverse square) is  $+2.2\%$  which corresponds to a variation of  $+1.1\%$  in the estimated diameter of a particular spherical raindrop in different parts of the sensitive field.

#### The Light Source and the Beam

To achieve the sensitivity desired of the instrument, it is essential to use as intense a source as possible. The Sylvania type C-100-P concentrated arc lamp is rated at 100 watts. Its entire light output comes from a refractory source of about 1.5 mm diameter. It thus supplies good light intensity and approaches the point

source requirement. An anastigmatic lens of 78 mm focal length is used to produce a parallel beam from this source; however, the finite size of the source and other practical optic limitations combine to give a beam that is neither perfectly collimated nor perfectly uniform. These imperfections represent compromises accepted in the interest of obtaining maximum light intensity. The beam is shaped to a rectangular cross section of 4.0 x 0.5 cm by means of a slit. Under these conditions, the intensity of the center of the beam is reduced relative to the portions about 1.5 cm removed from the optic axis. The resulting variation in the incident light intensity available across the beam is about  $\pm 4\%$ . Along the beam, the intensity is very nearly constant.

### Optics of the Photometer

The optics of the photometer serve two functions, (1) they select a segment of the light beam so as to define the sensitive field, and (2) they image the objective lens of the photometer in a constant position upon the cathode of the photocell. The first function is served by means of a field stop (figure 3) placed in the plane into which the photometer objective lens focuses the central plane of the sensitive field. The present design selects a rectangular section of the beam measuring 10.0 x 3.5 cm. These dimensions together with the beam thickness of 0.5 cm define a sensitive field of 17.5 cm<sup>3</sup>.

The second function is served by an "eyepiece" combination of two lenses (figure 3). Thus the light scattered from drops in the beam but outside the sensitive field is entirely blocked by the field stop, and that from drops in the sensitive field is uniformly distributed over the image of the objective lens which is projected upon the photocell cathode. It is important that this be a constant area because of variations of the photo-response of different portions of the cathode surface.

### The Rain Sample

In view of the fact that raindrops fall with various terminal speeds, which become quite small for small raindrops, it is not satisfactory to use the fall speeds of the drops as the means of bringing the rain sample into the sensitive field. Neither is it feasible, because of evaporation effects and mechanical distortions, to accelerate the drops by means of an air stream, etc. To obtain the required motion, the sensitive field in the

present instrument is caused to sweep out a continuous horizontal path by means of rotation about a vertical axis.

The arrangement for doing this in the present instrument is shown in figure 4. The midpoint of the sensitive field is about 30 cm from the axis of rotation, and the beam is so oriented as to make an angle of about  $26^\circ$  with a radial line. The present rotational speed of  $1.76 \text{ rev. sec}^{-1}$  thus enables the instrument to scan a volume of  $9.33 \times 10^3 \text{ cm}^3 \text{ sec}^{-1}$  whereas the sensitive volume at any instant is  $17.5 \text{ cm}^3$ . Obviously, it is essential in this device that the instrument "see" only one drop at a time, hence the sensitive field must be held small relative to the volume of free air which, on the average, contains one raindrop. In the present case, coincidences occur, but their occurrence is infrequent (see Results, below), and the consequent distortion of the size spectra is very small.

#### The Control of Extraneous Light

It is basically necessary to provide a uniform background of minimum luminosity against which the photometer may view drops incident in the sensitive field. This requirement is approached by the provision of a light trap which is most readily described by means of a diagram (figure 5). The light trap is "doughnut-shaped" in horizontal projection, and its surfaces are so arranged as to return the least amount of reflected light to the photometer and to produce no more than a minimum disturbance of the natural wind field. The cross section (figure 5) shows the physical relationships that are of most concern. To minimize the turbulence in the central opening, the "doughnut" is set on legs, allowing free passage of the wind both above and below the light trap.

In addition to the direct optical background of the sensitive field, scattered light from the sky and reflected light from the ground may be sources of varying illumination that can reach the photocell. To control these, an extended visor is used on the photometer unit.

The spectral sensitivity of the 922 photocell (the choice of which is explained below) is shown in figure 6 which also shows the spectral distribution of energy from the light source. Because both of these curves reach their maxima in the deep red to infrared, the effect of uncontrolled natural lighting of the sensitive field may be

reduced by the use of a red-infrared filter. The Corning No. 2403 filter transmittance curve (figure 6) indicates its suitability for this purpose.

The use of these control measures makes daytime use of the instrument possible without serious loss of fidelity.

### The Photometer

The light pulse generated when the sampling field intercepts a raindrop is converted into an electrical pulse by the electronic portion of the photometer (figure 7). A 922 vacuum phototube serves as the transducer in this unit. To transform the phototube signal impedance of 10 megohms down to less than 700 ohms, a direct-coupled cathode-follower stage is used as shown. This impedance step-down is necessary to prevent pulse-shape distortion caused by the stray capacitance-to-ground which is present in the signal transmission system. Operating bias for the phototube is supplied by the 30-v silicon junction Zener regulator diode, D1. This part of the electronic system is enclosed immediately behind the phototube in the photometer housing.

The photometer, as the sensing element, determines the signal-to-noise ratio of the spectrometer. The load-resistor,  $R_1$ , is critical in determining both the noise level and the sensitivity of the photometer. By choosing  $R_1$  so as to obtain the most functional compromise between these characteristics, the optimum design is achieved. In the present case, the thermal noise in  $R_1$  has a root-mean-square value of

$$E = 26.4 \mu\text{v.}$$

Since this noise level has a Gaussian distribution, peaks of four times this magnitude are to be expected only rarely (less than 0.01% probability of occurrence). The value of about  $100\mu\text{v}$  therefore fixes the lower limit on drop size measurements. The equivalent drop size is 0.18 mm diameter.

Two additional sources of spurious signals are present in electronic systems of this type. The first, called shot-noise, is attributable to the random velocity distribution of the electrons in the vacuum tube, and, in the present case, is not a significant factor. The second is the microphonic effect due to minute relative movements

of the elements in the cathode-follower. This effect is produced by mechanical vibration or shock. Because in the present instance, a mechanical rotation is introduced, the photometer is subject to these effects. Comprehensive study of tube characteristics as regards the microphonic effect led to the determination that the military specification Raytheon CK6533WA premium subminiature triode would have to be used for the photometer circuit. The combined thermal and microphonic noise output under operating conditions using this type of tube is limited to 125  $\mu$ v (equivalent to a drop of 0.20 mm diameter).

Criteria for the selection of the 922 phototube involve spectral response, linearity, temperature stability of photometric response, and aging characteristics. As shown above, its spectral characteristics (S1) are useful in the elimination of much of the uncontrolled daytime illumination by the use of an optical filter. Its linearity and photometric stability in the anticipated operating range of temperatures are well below other error-introducing effects. In use, it has been necessary to replace the phototube only after a year and a half of use (about 200 hours' operation).

#### The Pulse Amplifiers and Limiter

Consideration of the dynamic range required of the system shows the necessity for special measures to handle the signals without loss of fidelity. Calibration experiments using uniform drops of various independently determined sizes give the following relation between the pulse amplitude, E, in millivolts, at the photometer output, and the drop diameter, D, in mm:

$$E = 3.09 D^2.$$

It is difficult to obtain an exact evaluation of the error, but this equation appears to hold within  $\pm 10\%$  on E or  $\pm 5\%$  on D.

Taking 0.25mv as a minimum useful pulse (twice the level of the combined thermal and microphonic noise), and assuming that the largest discriminated drop will be 6 mm in diameter, hence the maximum measurable pulse must be 112 mv, the amplitude ratio is found to be 450 to 1.

To record this range of pulse amplitudes effectively so that the entire spectrum of drop sizes may be reasonably determined, two amplification stages are used with a

pulse limiter between them. This circuit is shown in figure 8. The first amplifier operates upon all pulses with a gain of 270. Its output is transmitted (1) to a readout device which serves to record the amplitudes of all pulses at this point, and (2) to the pulse limiter which transmits small pulses intact, but limits large pulses to a maximum of 5 v. The output of the limiter then feeds the second amplifier which operates at a gain of 15.5, and serves to boost the smallest useful pulses to a level of 0.87 v. The output of the second amplifier then feeds a second readout device which records the smaller pulses intact (i.e., all those less than 5 v at the output of the limiter).

The performance of this system is indicated in table 2. The arrows indicate the signal level ranges selected for useful data accumulation. Obviously the pulse-amplitude recording allows for adequate overlap because the first amplifier is capable of handling more than the required 6 to 1 ratio of pulse amplitudes.

TABLE 2: Performance of the Amplifier-Limiter System

Drop Dia. $\mu$	Photometer Output Peak mv	1st Amp. Output Peak v	Limiter Output Peak v	2nd Amp. Output Peak v
6000	111	30	5.0	77
2450	18.5	5.0	5.0	77
260	0.21	0.056	0.056	0.87

Except for one RC network at the second amplifier input, the circuit is DC-coupled throughout. This is done to minimize the effect of pulse-overshoot which always occurs in AC-coupled amplifiers. When pulse-overshoot is present, and two drops follow each other closely in time, the second pulse is superimposed upon the decaying pulse-overshoot waveform generated by the first pulse. The resulting error in the absolute magnitude of the second pulse is a function of the

percentage overshoot, its associated decay rate, and the time between pulses. When data are to be analyzed by measuring pulse deflection on oscillograph records, the reader can correct for overshoot error, but when pulse-height discriminators are used, correction is not feasible in a system required, as in the present case, to handle a random time distribution of randomly sized pulses.

Feedback is used in the first amplifier to enhance the DC gain stability and to reduce the variation in DC output level which occurs whenever the background illumination changes during operation. The feedback loop from the output of the first amplifier to the right-hand section of  $V_{10}$  has a time constant of 1 sec. This effectively prevents pulse degeneration although it reduces the DC gain by a factor of 60.

#### Data Recording and Processing

The output of the amplifiers may be recorded in any of a number of different forms. Because of the research nature of the work to date, it is desirable to have a record of the original form of the data. The size and the time of observation of each drop should therefore be recorded with the necessary resolution. Although this can be done so as to present the data on punched cards or tape, a much lower first cost for equipment is incurred by the use of a less completely automated system. The present practice is to use a recording oscillograph (two channels plus a reference tract) together with technician labor to translate the record to digital form.

#### CALIBRATION

An integral part of the development of such an instrument as this is its calibration and the design of routine procedures for making frequent checks on the calibration during field use of the instrument. Laboratory studies have served to evaluate the proportionality between the photometer response and the surface area of the drop viewed (see above, p. 31). Thenceforward it has been necessary only to determine the pulse amplitude corresponding to a drop of known size to specify the entire scale of drop sizes in terms of pulse amplitudes.

To do this it was necessary to devise the means for generating uniformly sized drops of sizes well-distributed over the range of drop sizes encountered in rain. Methods of generating uniformly sized drops have been presented by Magarvey and Taylor (1958), and Walton and Prewett (1949). Experiments were also conducted to determine the utility of glass beads as facsimile water drops for calibration purposes in the field. Special problems are encountered because of the rotary motion of the unit, and to date, the best calibrations have been obtained using a hypodermic tip to form drops under a constant hydrostatic head.

Independent measurements of the intensity of the beam in the sensitive region, and of the response of the photocell to constant flashes of light in various parts of the field have been made. These constitute useful tests, but are less satisfactory for calibration than the drop-dripping technique. The problem is still under study and improved techniques are being developed.

## RESULTS

A number of interesting results have been obtained in the early observations made with the spectrometer. For details, the reader is referred to references 7 and 8, and to forthcoming papers from this laboratory.

Briefly summarized, the maximum 1-min rainfall intensity observed has been  $79 \text{ mm hr}^{-1}$ . In such rains, it is found that the number density of drops 1 mm in diameter and larger is about  $1000 \text{ m}^{-3}$ . This supports the design assumption discussed above (p. ) that a volume of  $17.5 \text{ cm}^3$  will contain two or more drops only very rarely. Whereas nominal agreement with the Marshall-Palmer raindrop-size distribution function (ref. 9) is found when large samples are assembled, there appear to be significant variations among short-period samples, up to a few minutes in length, that may prove helpful in the interpretation of radar echoes and in analysis of the rain-forming processes.

## REFERENCES

1. Lowe, E. J., 1892: Raindrops. *Quart. J. r. Meteor. Soc.*, 18, pp. 242-245.
2. Wiesner, J., 1895: Beiträge zur Kenntniss des tropischen Regens. Akademie d. Wissenschaften, Vienna, Math.-Naturw. Klasse, Sitzungsberichte, 104, pp. 1397-1434.
3. Mie, G., 1908: Beiträge zur Optik trüber Medien. *Annalen der Physik*, 25, pp. 377-445.
4. Van de Hulst, H. C., 1957: Light Scattering by Small Particles. John Wiley and Sons, New York, Chap. 12 and 13.
5. Magarvey, R. H., and B. W. Taylor, 1958: Apparatus for the production of large water drops. *Rev. of Sci. Inst.*, 27, pp. 944.
6. Walton, W. H., and W. C. Prewett, 1949: The production of sprays and mists of uniform drop size by means of spinning disc type sprayers. *Proc. of the Physical Soc.*, 62, Part 6, pp. 341-350.
7. Dingle, A. N., 1960: The microstructure of rain in a summer shower. *Proc. Eighth Weather Radar Conference*, San Francisco.
8. Hardy, K. R., and A. N. Dingle, 1960: Raindrop-size distributions in a cold frontal shower. *Proc. Eighth Weather Radar Conference*, San Francisco.
9. Marshall, J. S., and W. McK. Palmer, 1948: The distribution of raindrops with size. *J. Meteor.*, 5, pp. 165-168.

# Optical Geometry of the Sensitive Field

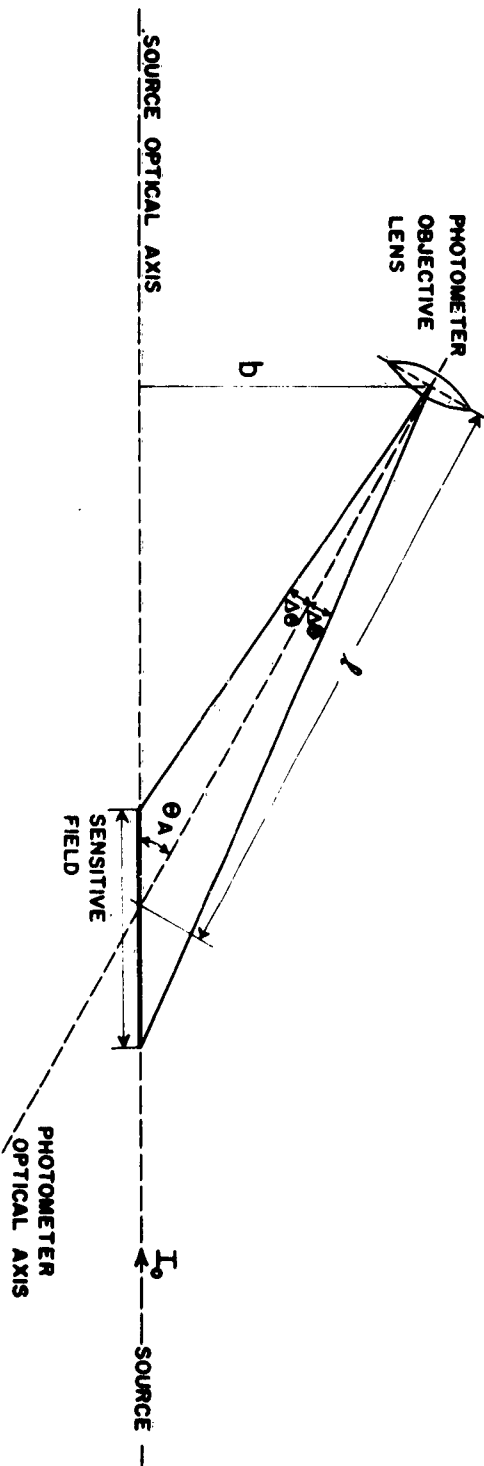


Figure 1. Optical geometry of the sensitive field.

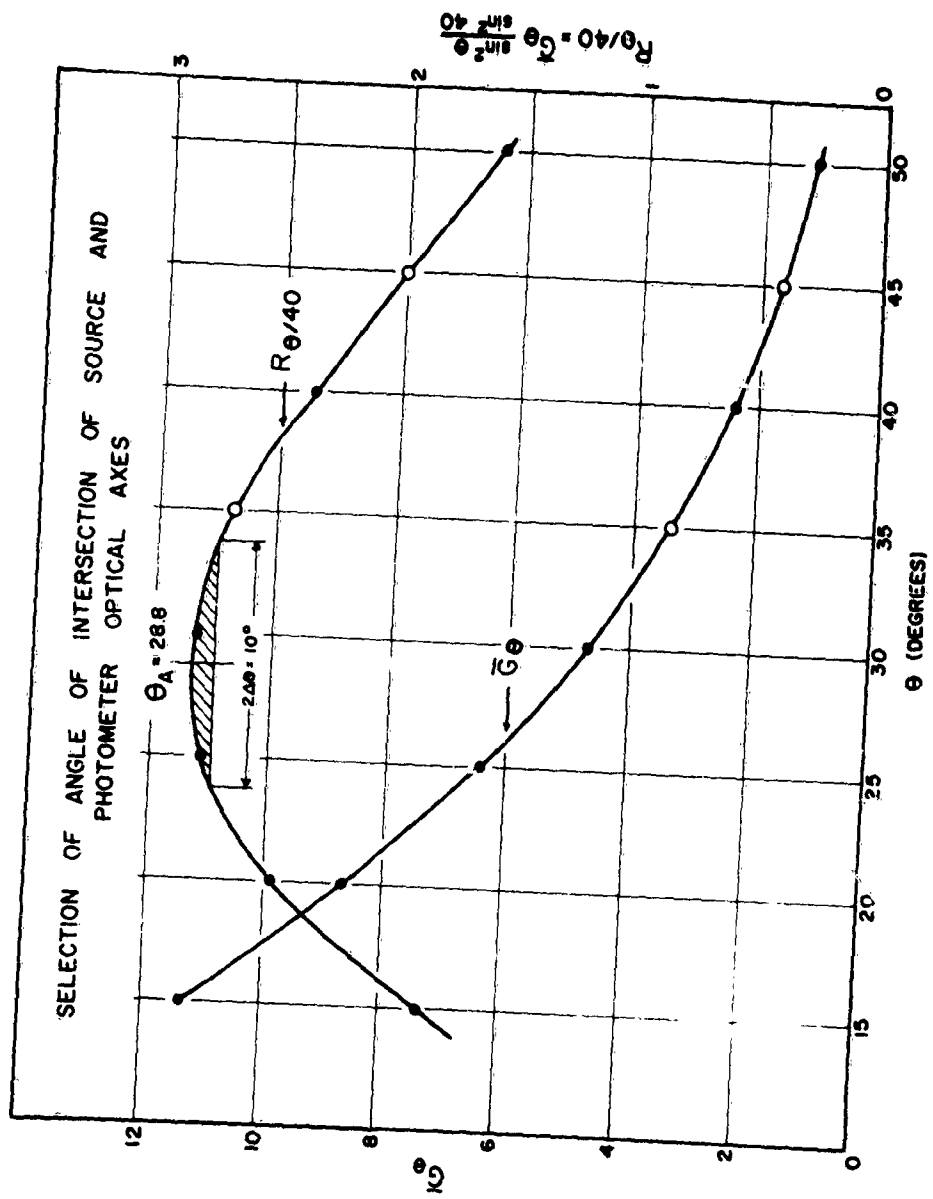
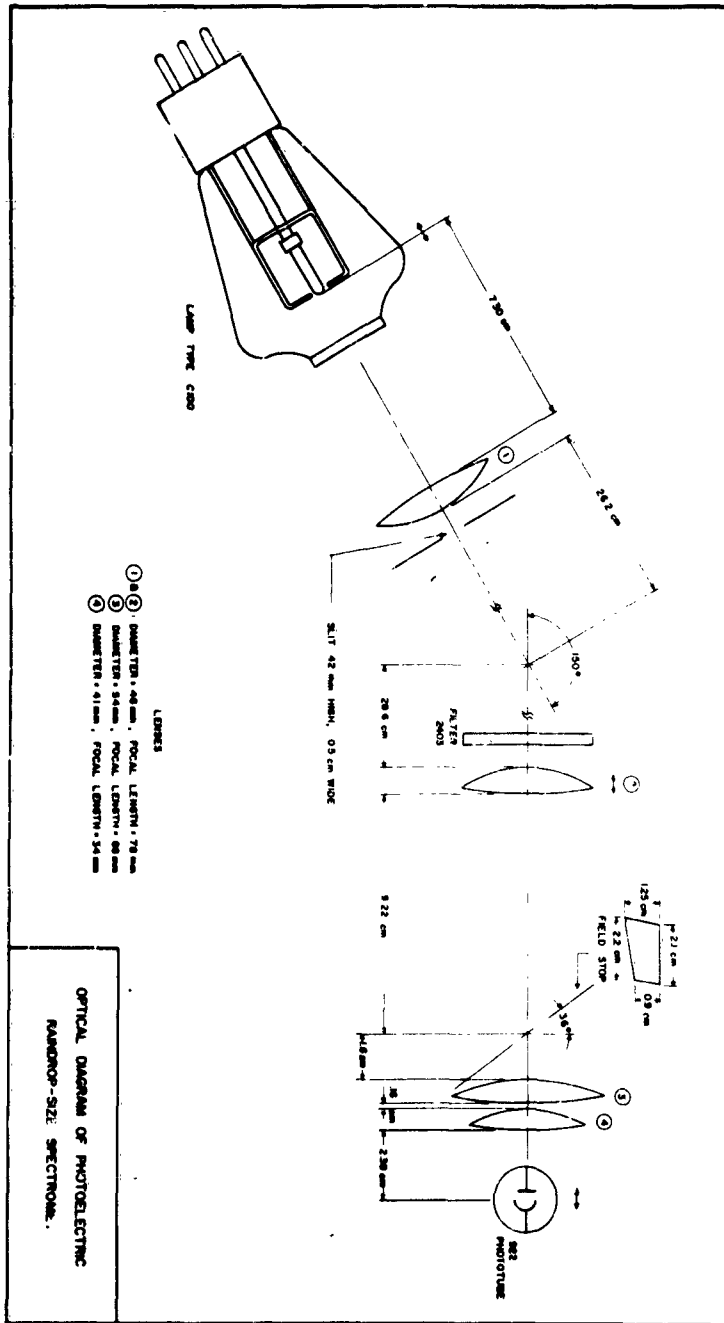
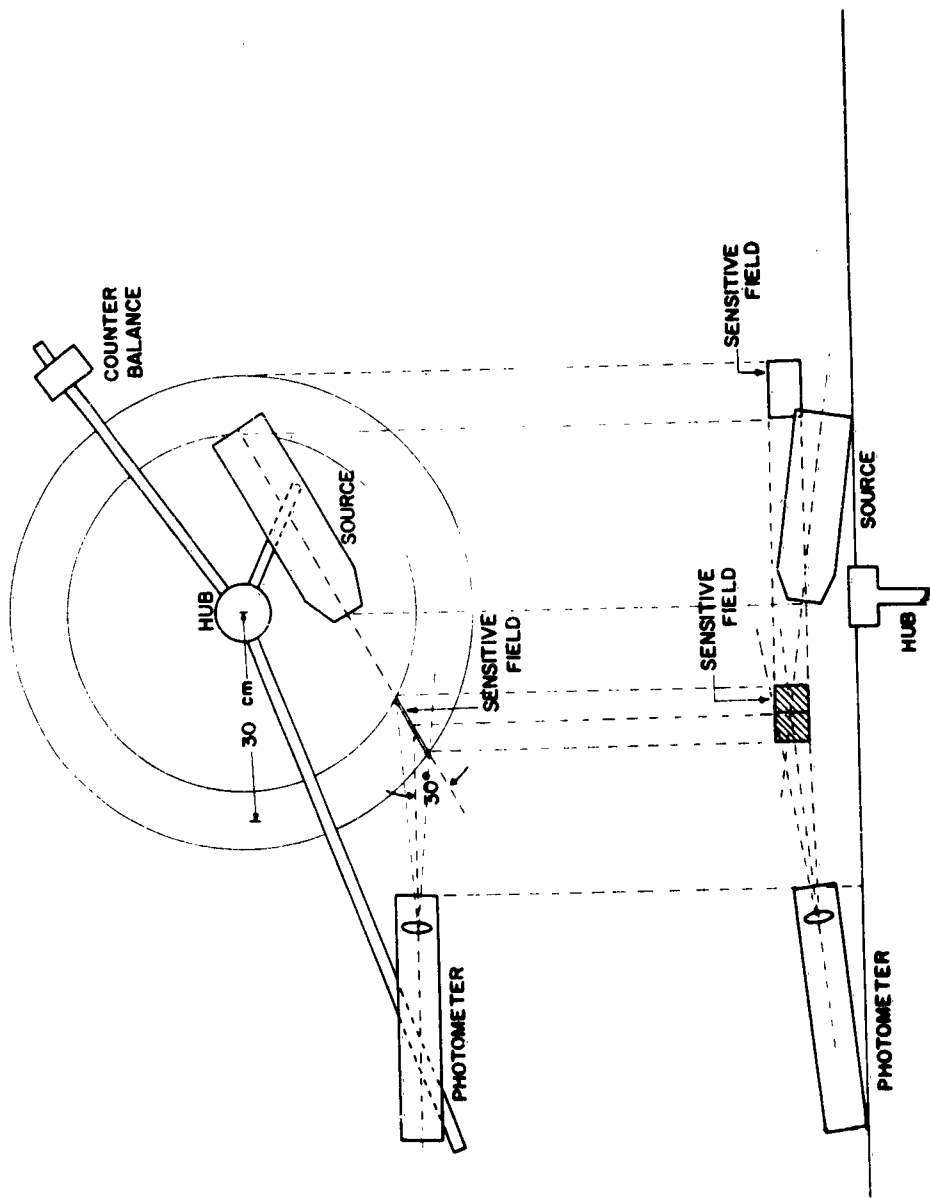


Figure 2. Selection of the angle of intersection of source and photometer optic axes.

Figure 3. Optical diagram of the raindrop-size spectrometer





RELATIONSHIP OF SPECTROMETER COMPONENTS

Figure 4. Physical relationship of the spectrometer components.

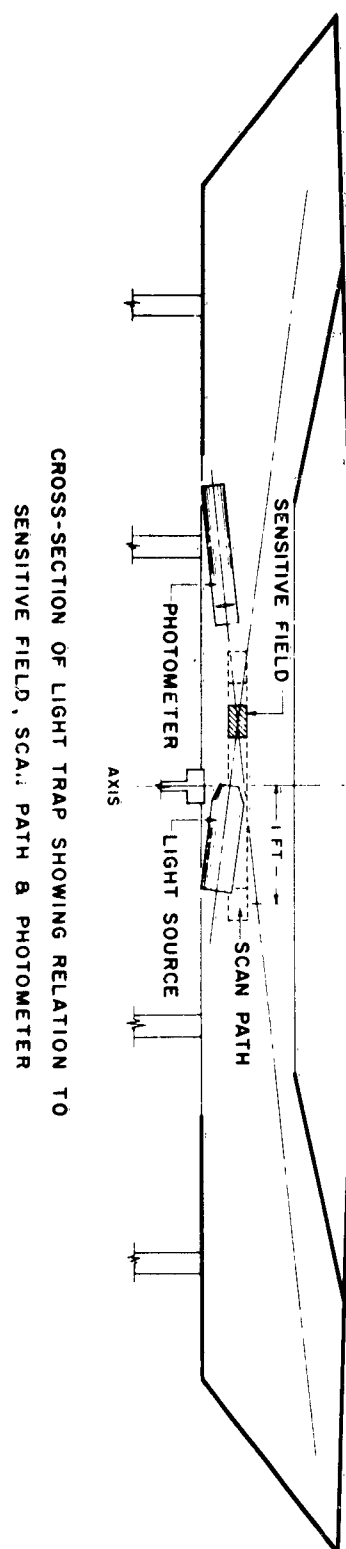


Figure 5. Cross section of the light trap showing its relationship to the sensitive field, the scan path and the photometer.

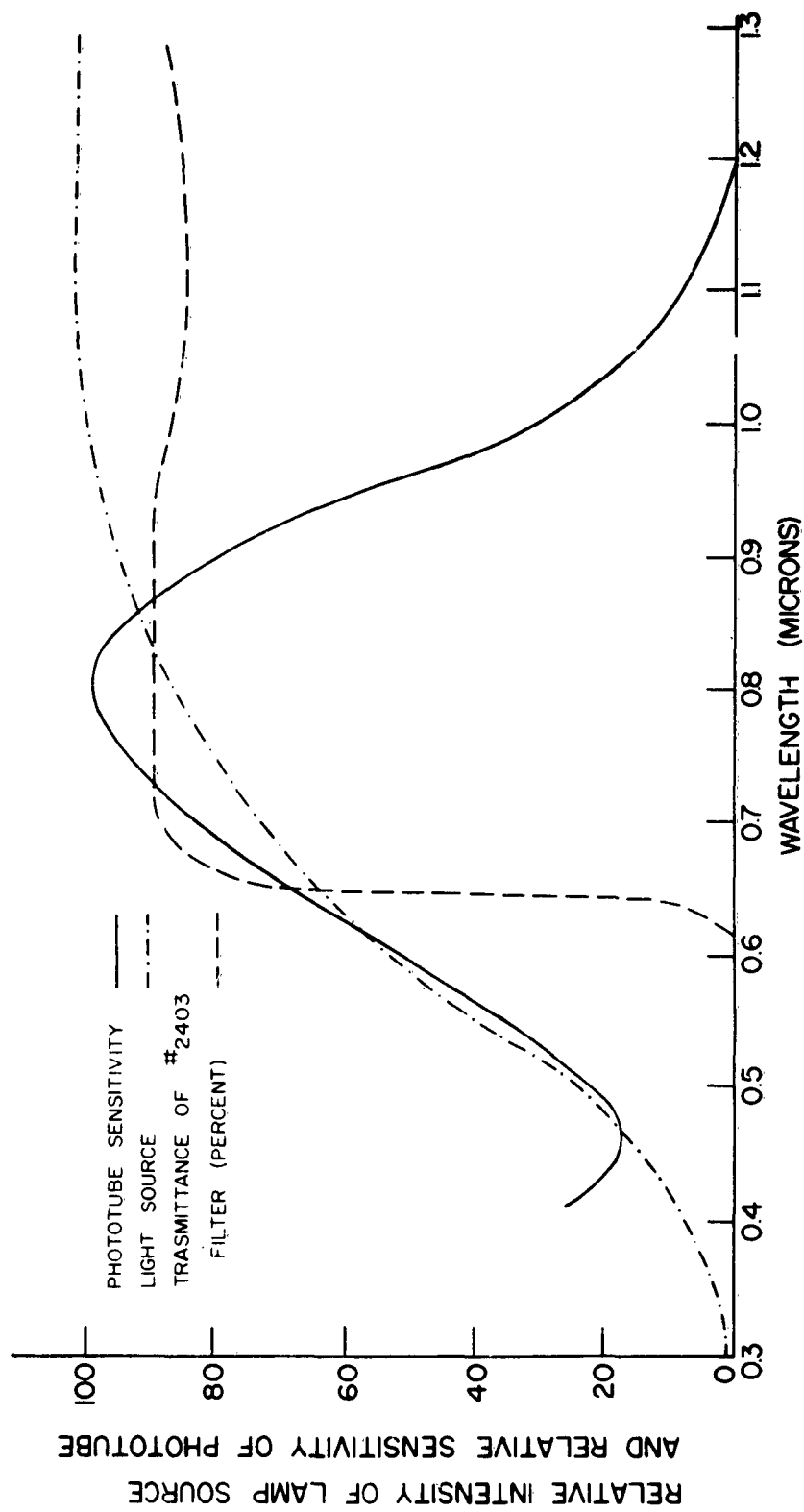


Figure 6. Spectral characteristics of the phototube, the light beam, and the photometer filter.

# PHOTOMETER SYSTEM

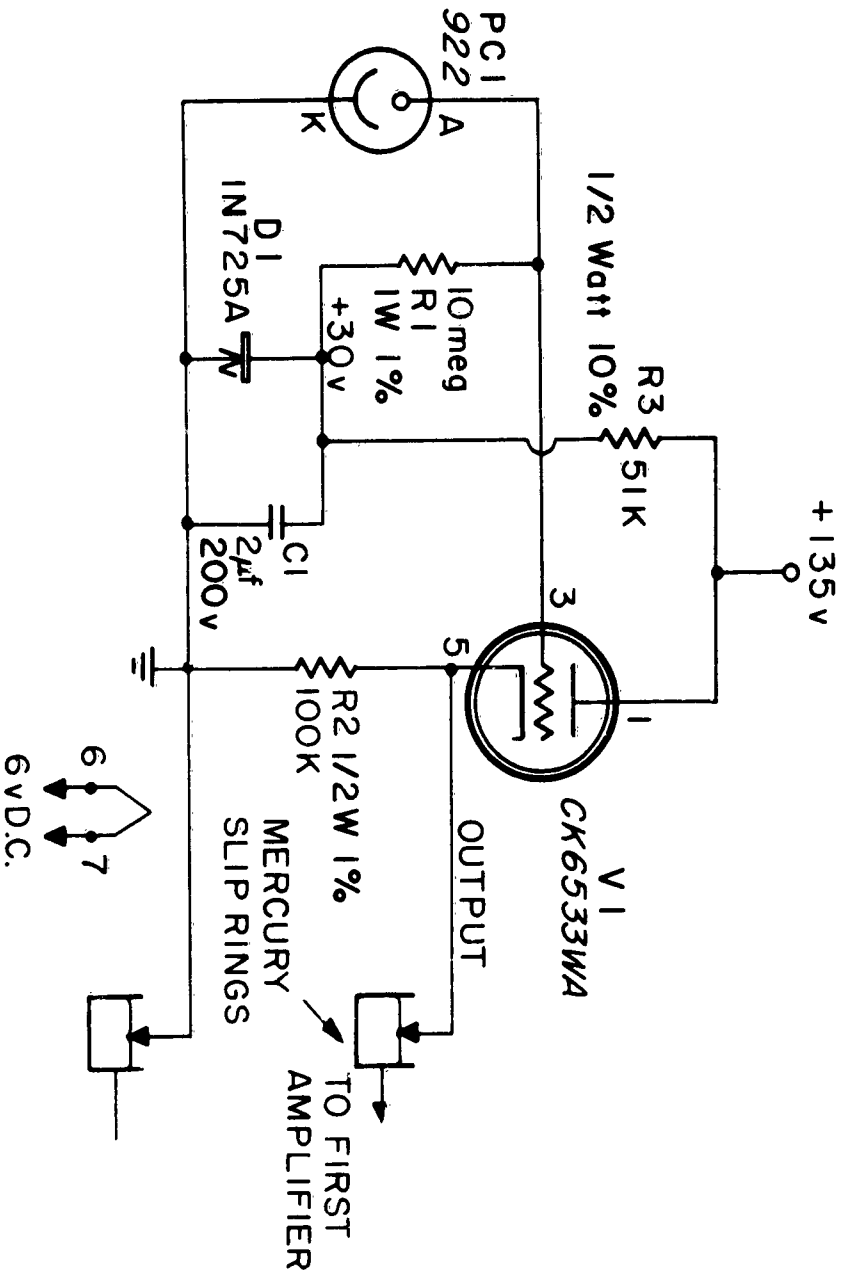
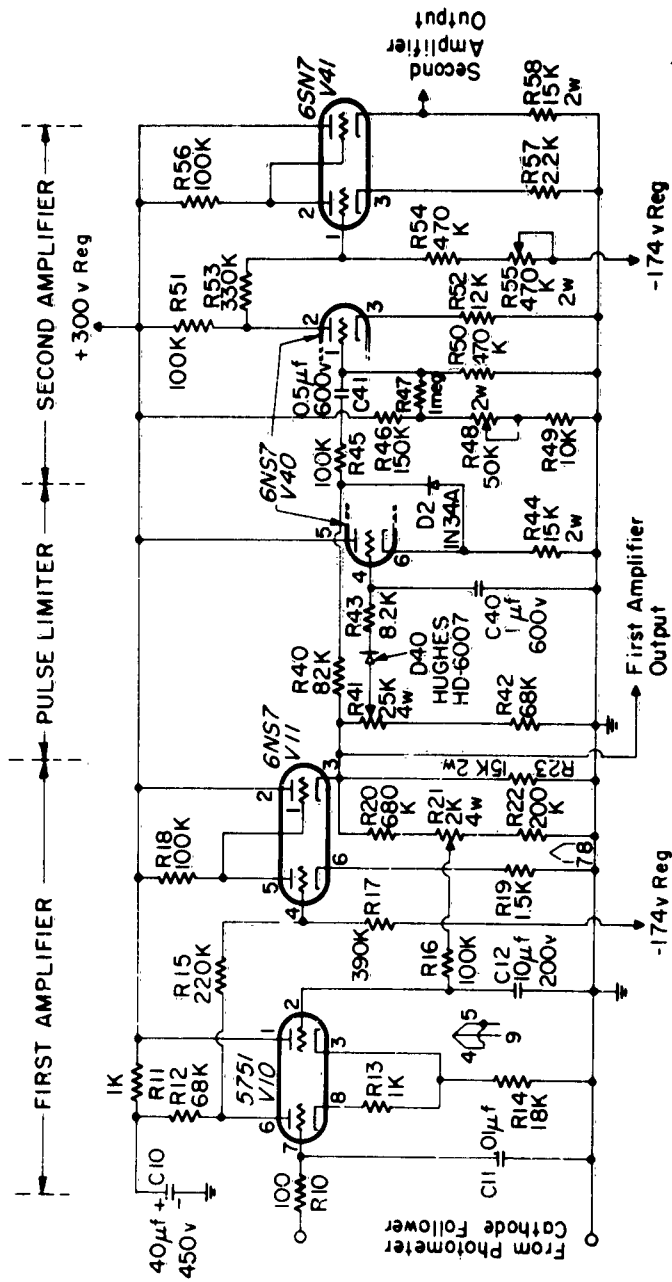


Figure 7. The photometer electronics.



All filaments to regulated DC supply  
 All capacitors ceramic disc, 1KV, 20%, unless otherwise noted  
 All resistors 1/2 watt, 10%, unless otherwise noted

Figure 8. Amplifier-Limiter circuit.

MEASURING TECHNIQUES UNDER  
WATER AND ICING CONDITIONS

BY

S. A. KOSSAYIAN

SUPERVISORY RESEARCH ENGINEER  
(Aeronautical Instrumentation)

Measurement of environmental conditions during water and icing tests at the Naval Air Turbine Test Station has been a recent requirement. Consequently, a survey was made of existing techniques and equipment, and also some new approaches were developed and tested. This paper reviews the results of these tests.

The environments under which engines were tested ranged from,

Altitude: S. L. to 35,000 ft.  
Mach No.: Static Sea Level to 0.9  
Inlet Temperature:  $-4^{\circ}\text{F}$  to  $+190^{\circ}\text{F}$   
Water Rates: 0 to 10 g/m<sup>3</sup>  
Droplet Size: 5 to 100 microns

The parameters measured were pressure, temperature, dew point, liquid water rate, and droplet size. Also, normal engine parameters were recorded to measure performance of the engine under these environmental conditions:

1. Pressure Probes:

Measurement of inlet total and static pressure are required for setting simulated flight condition and to measure airflow. During the water and icing tests two different techniques were utilized to keep probes from freezing up or blocking.

The first technique was with electrically heated probes. Figure 1 is a sample of a probe constructed at Naval Air Turbine Test Station. Nichrome ribbon was used as a heating element and insulated with sauerisen cement. Electrical power was supplied with a 20 amp powerstat. A thermocouple was attached to the probe tip to monitor tip temperature. In principle, the probe was to flash water as it impinged

on the pressure sensing hole and on the probe body. Figure 2 shows a second configuration used. In order to provide the necessary heat to flash all the water impinging on the tips, many alternate layers of resistance wire and insulation were required and the resultant probe was quite large physically. However, airflow measurements required as many as 9 penetrations in an inlet duct 32" in diameter. This made use of an electrically heated system impractical for multi-finger rakes.

A second system employed was with steam heating as shown in Figure 3. High pressure steam was supplied to the probe and channeled through the probe body. The pressure tubes are also channeled through the probe body. In principle, heat conduction to the probe tips keeps the probe de-iced. Several considerations made use of this technique ideal. They are:

1. Simplicity of construction
2. Compact size
3. Heat input using steam is very high

It must be noted that for a stationary test facility, steam heating of the probes is practical, but not so for flight work. This probe proved to be more durable than the electrically heated probes and is presently used.

Another approach under consideration, but not yet tested, is for a miniature strain gage transducer inserted in the probe tip.

Figure 4 shows two probe types that are being used to test the transducers. The probe on the left has the transducer mounted at the probe tip and the one on the right has the transducer in the body of the probe.

The probe body would be de-iced with electrical heating and temperature controlled to approximately  $+80^{\circ}\text{F}$  so as to keep the temperature effect on the transducer to a minimum.

Measurement of inlet static air pressure, prior to water and icing tests, was with a set of duct wall static taps. To prevent blockage, electrically heated wall static probes were built as shown in Figure 5 and were installed. These probes were built similarly to the total pressure probes, using

nichrome ribbon elements and variable electrical power. The probes were then installed flush to the duct wall, and the duct inside wall polished smooth. These probes were satisfactory during water ingestion tests, but ice rings formed outside the heated area during icing tests. To rectify this situation, a flight type heated pilot-static probe, (Figure 6) was modified with an extension piece and stream static obtained. This probe also includes a total pressure tap, however, our experience has been that blockage occurs at high water flow rates.

## 2. Temperature:

Normal procedure at NATTS, to measure inlet total temperature is to use thermocouples. For water and icing tests a self aspirating housing was tried. This probe is shown in Figure 7. In principle, the 180° reversal of the air separates the water from the air and a dry air temperature measured. Two factors made this probe undesirable. First, ice built up on the tip causing excessive loading and tip fracture. The teflon tip was ingested by the engine on two separate occasions, fortunately without engine failures. Also, the calibration of the recovery factor requires extensive testing throughout the operating envelope of NATTS.

A commercially available probe, the Rosemont Corporation Model 102 was then procured. This probe is shown in figure 8. In principle, the liquid water is centrifuged out of the air by a 90° change in flow direction prior to passage through a 50 ohm temperature bulb. The dry air is then discharged at the trailing edge of the probe strut. The probe body is de-iced with electrical heaters. This probe appears to be satisfactory, but complete evaluation is still pending.

Another temperature measurement of importance is that of inlet guide vanes and inlet struts of the engine during icing runs. Figure 9 shows a typical installation. On non-moving parts, thermocouple wire is spot welded to the part and covered with nichrome ribbon. On the moving inlet guide vanes, the thermocouple wire is passed through a coil made of steel tubing. The coil is mounted to the moving vane and the stationary engine case, allowing for movement between the two. This measurement is important in that it provides data showing if the engine anti-ice system is capable of keeping these parts above the freezing point.

In conclusion, the following probes, as shown in figure 10, are used at NATTS:

- No. 1 - for single finger pressure
- No. 2 - multi-finger pressure
- No. 3 - Stream static
- No. 4 - Wall static during water and cold dry runs
- No. 5 - Inlet temperature

To discuss liquid water content of the engine inlet air, a short description of the water system is first required.

Water is introduced into the air supplied by the plant blowers by a spray rig in the engine inlet duct 26' forward of the engine. The dew point of the air supplied by the blowers is measured with a cold mirror device and a commercial Foxboro Dewcel. Knowing the conditions of this air at the engine, the amount of water required to saturate the air is then calculated. This amount of water is then added to the test liquid water rate and set into the spray rig using rotometers and turbine type flowmeters for measurement. It is then assumed that the extra water added to the test water rate vaporizes and the test conditions met.

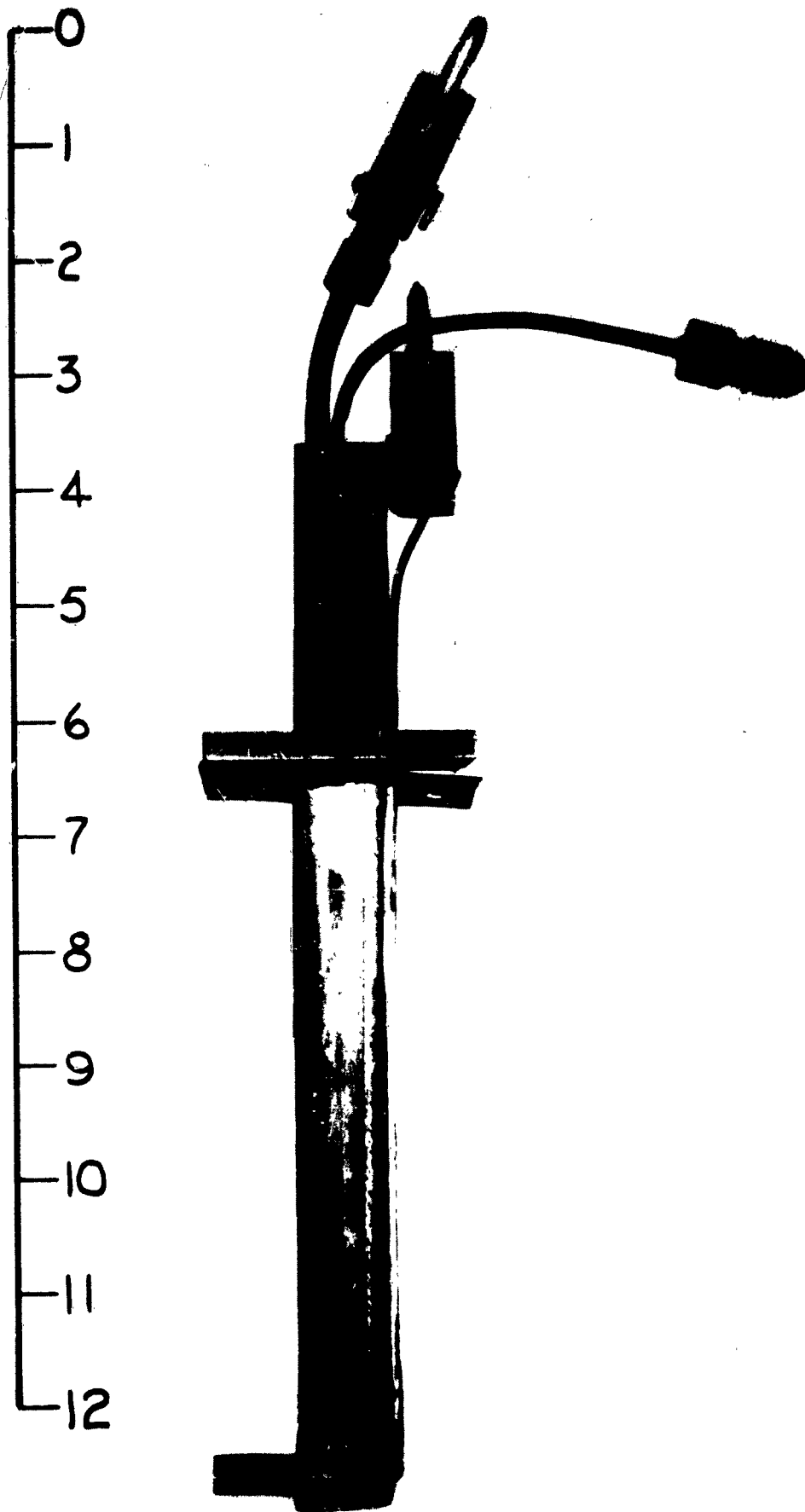


FIG. I-HEATED TOTAL PRESS. PROBE

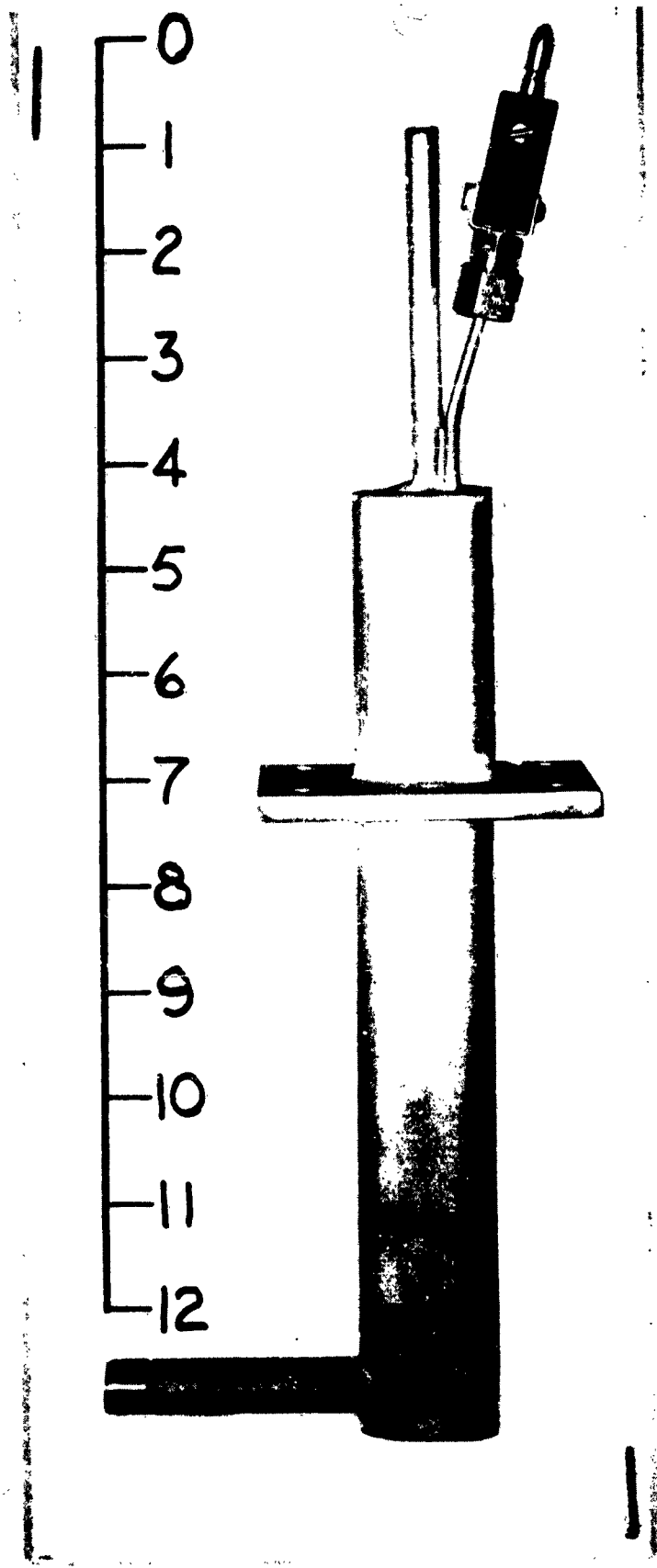
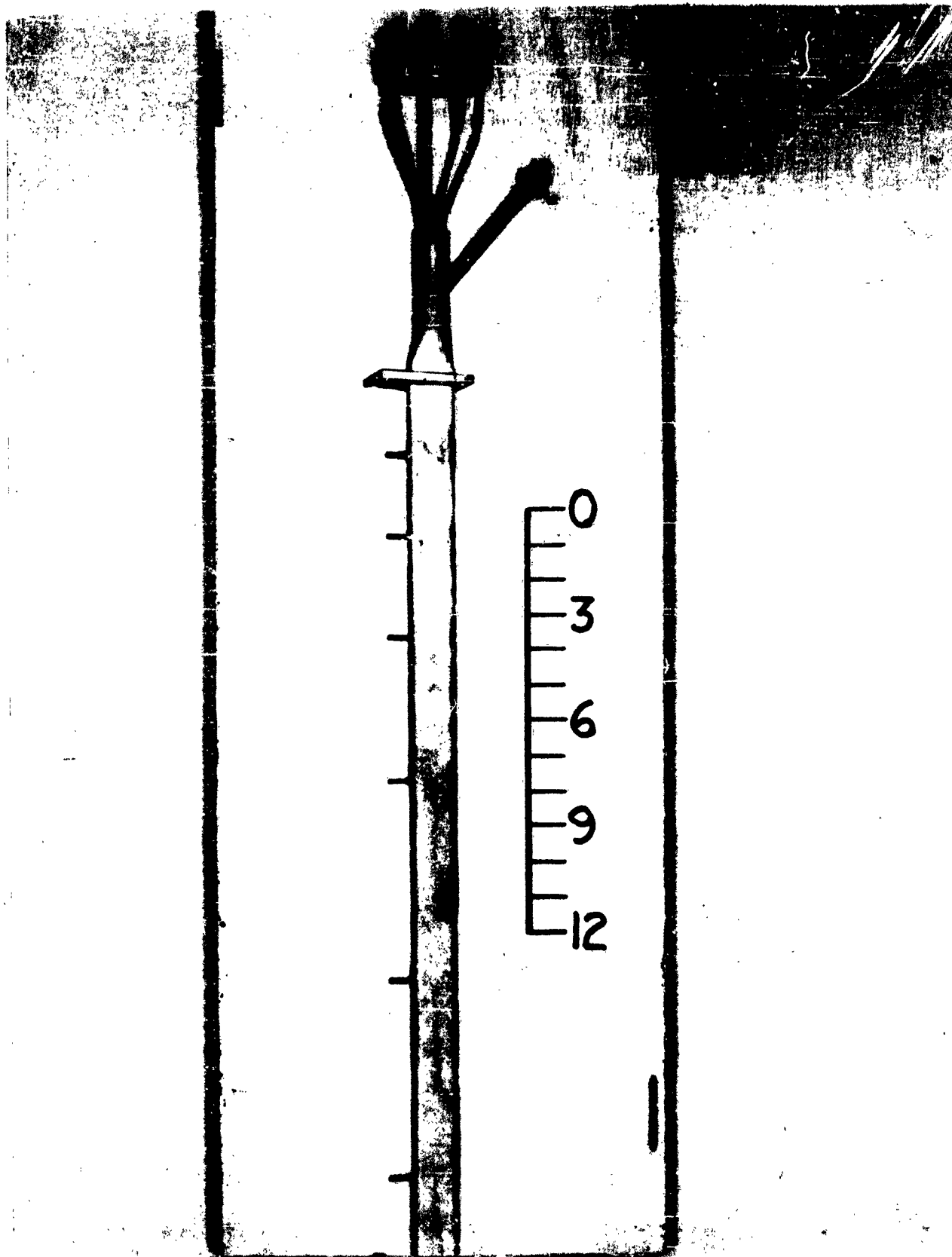


FIG. 2- HEATED TOTAL PRESS. PROBE



**FIG. 3-STEAM HEATED MULTI-FINGER  
PRESS. RAKE**

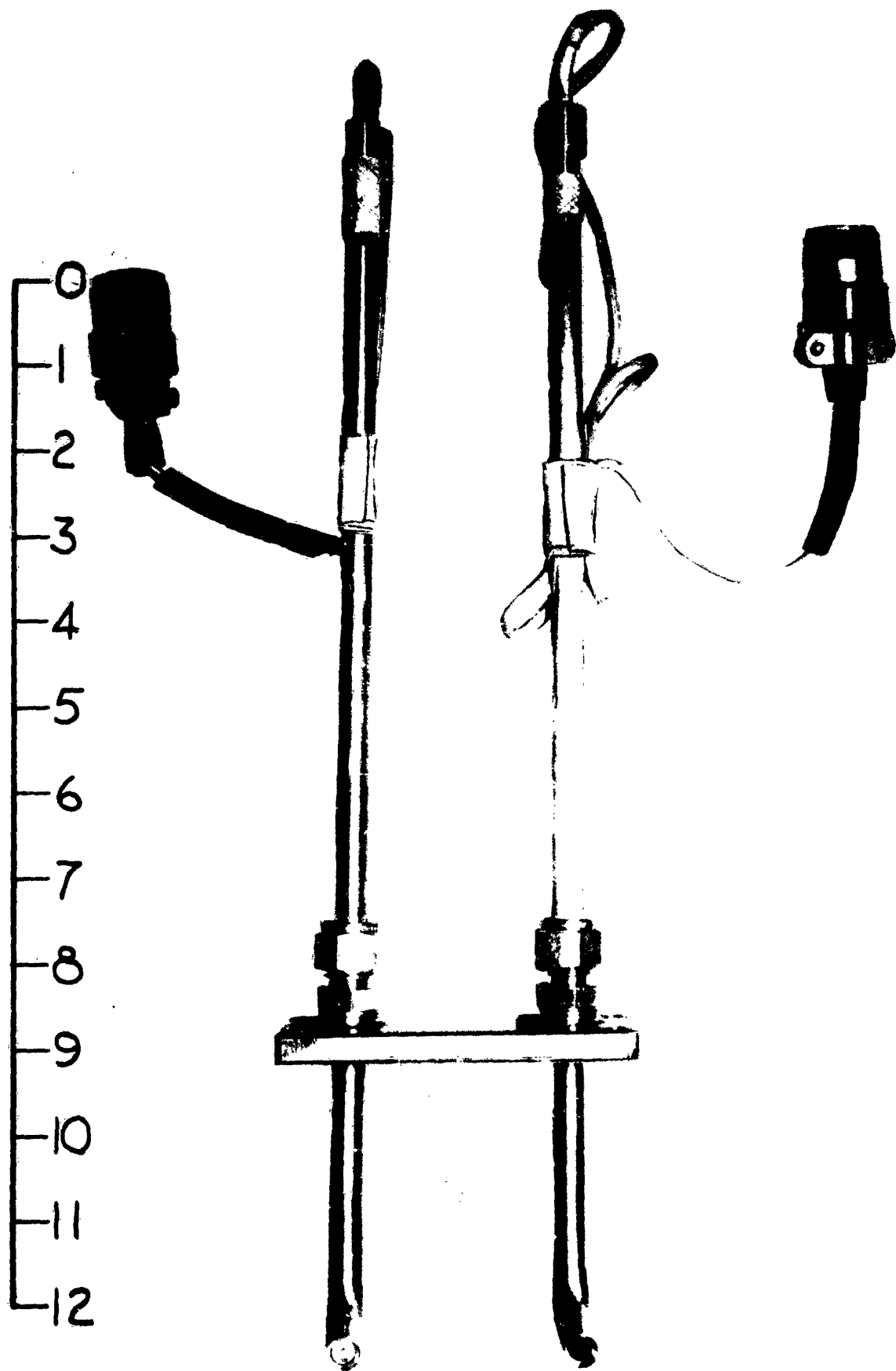


FIG. 4- TRANSDUCER TYPE PRESS. PROBE

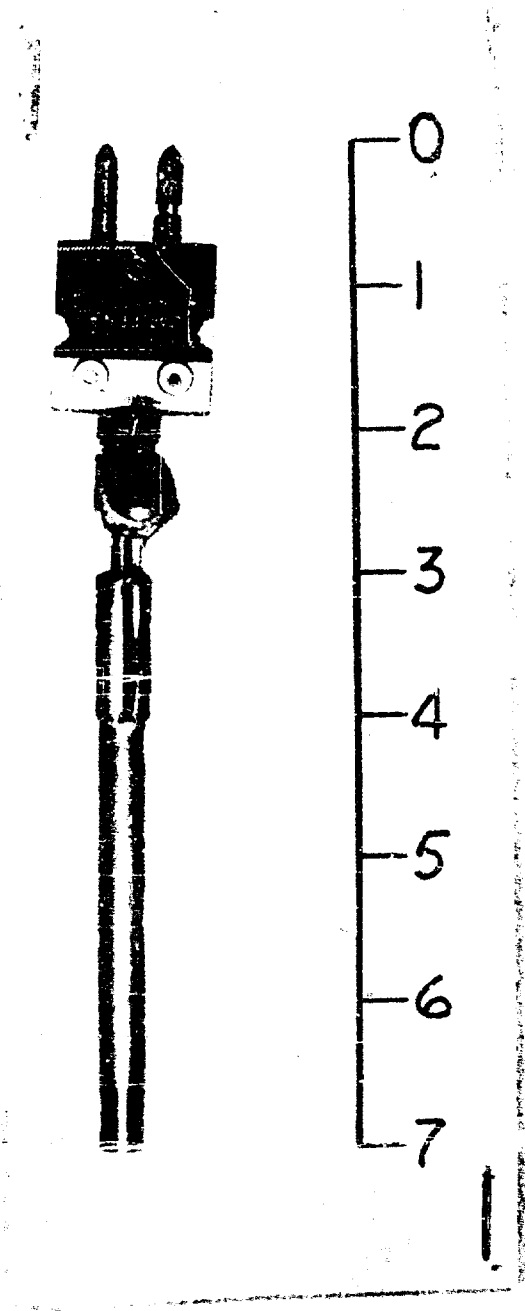


FIG.5-HEATED WALL STATIC PRESS.PROBE

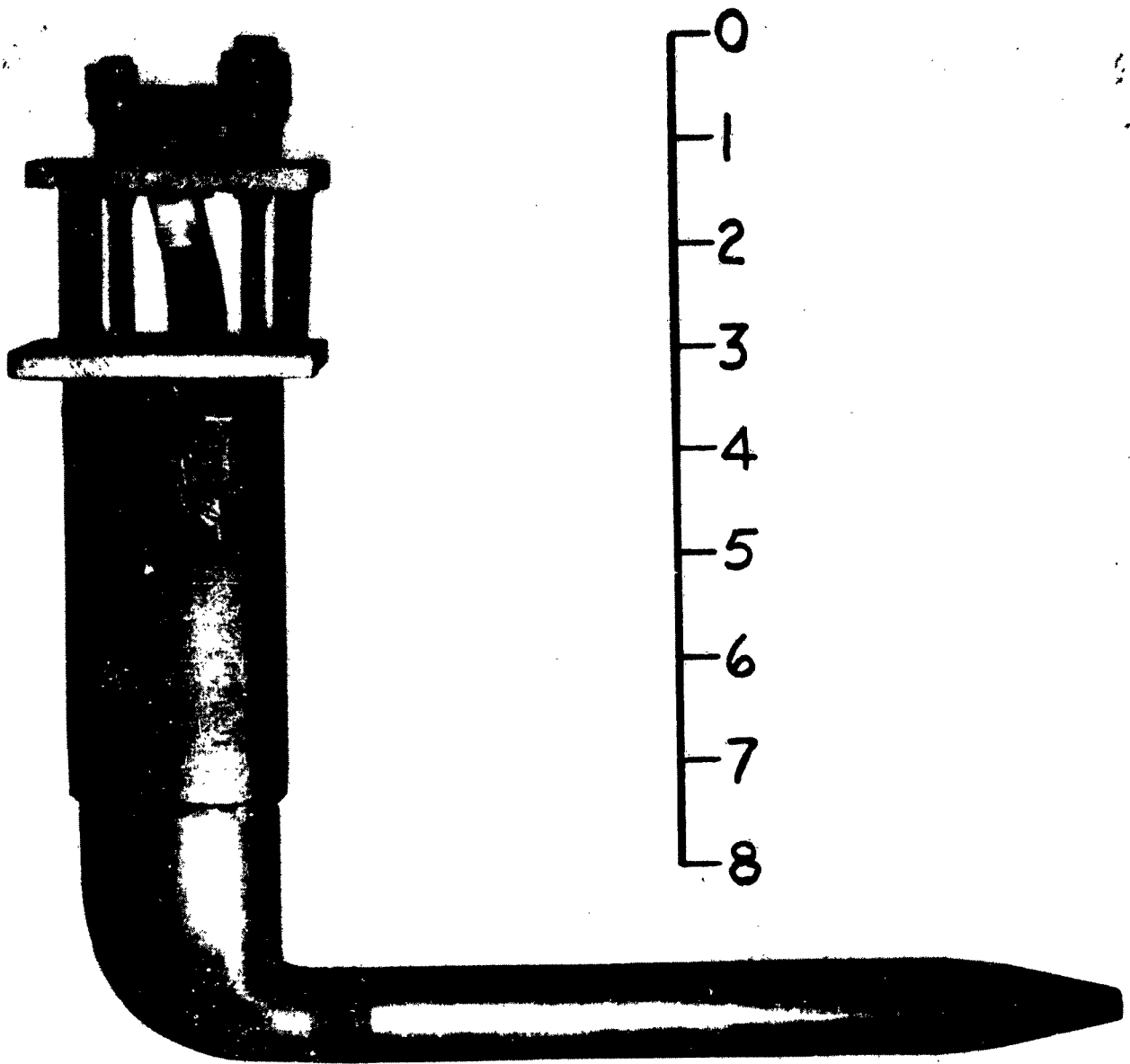


FIG.6-AIRCRAFT TYPE PITOT-STATIC PROBE

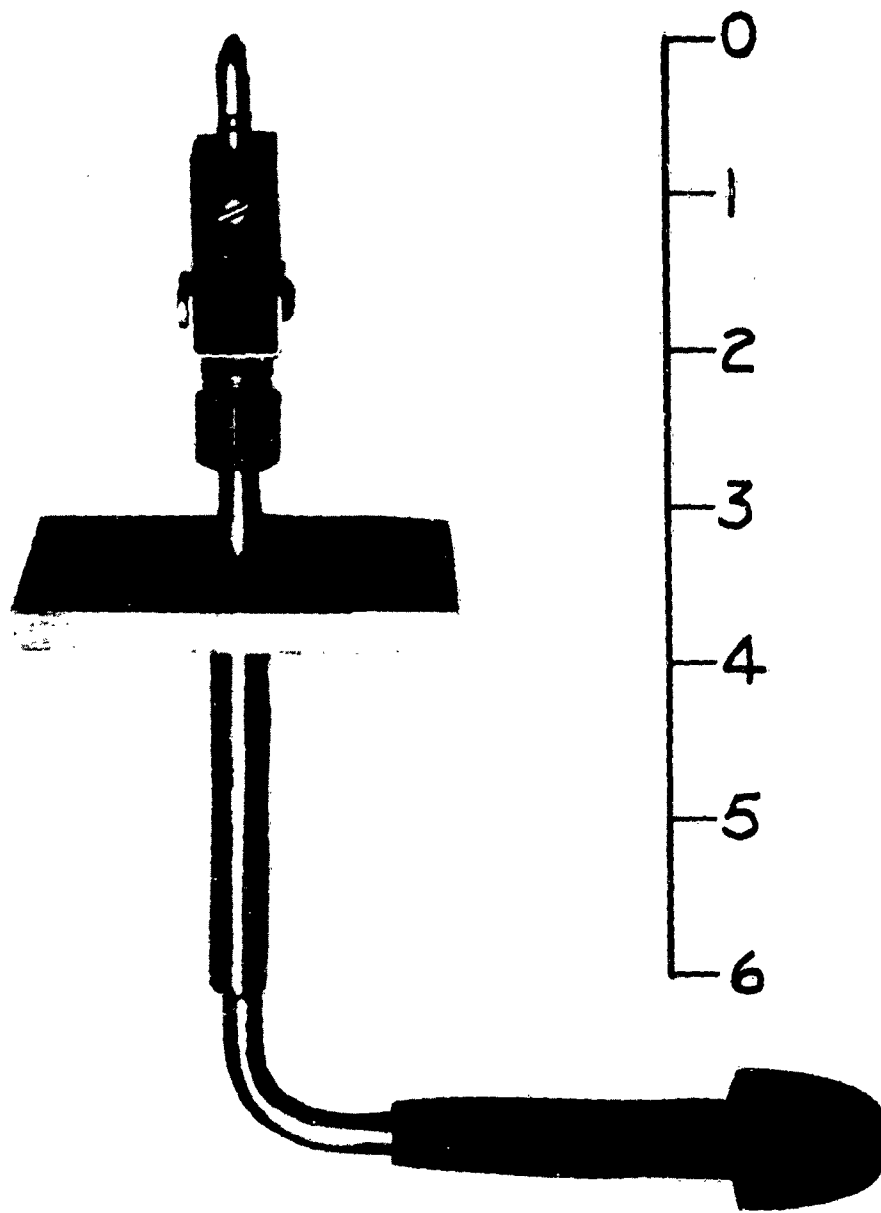


FIG. 7- SELF-ASPIRATING TEMP. PROBE

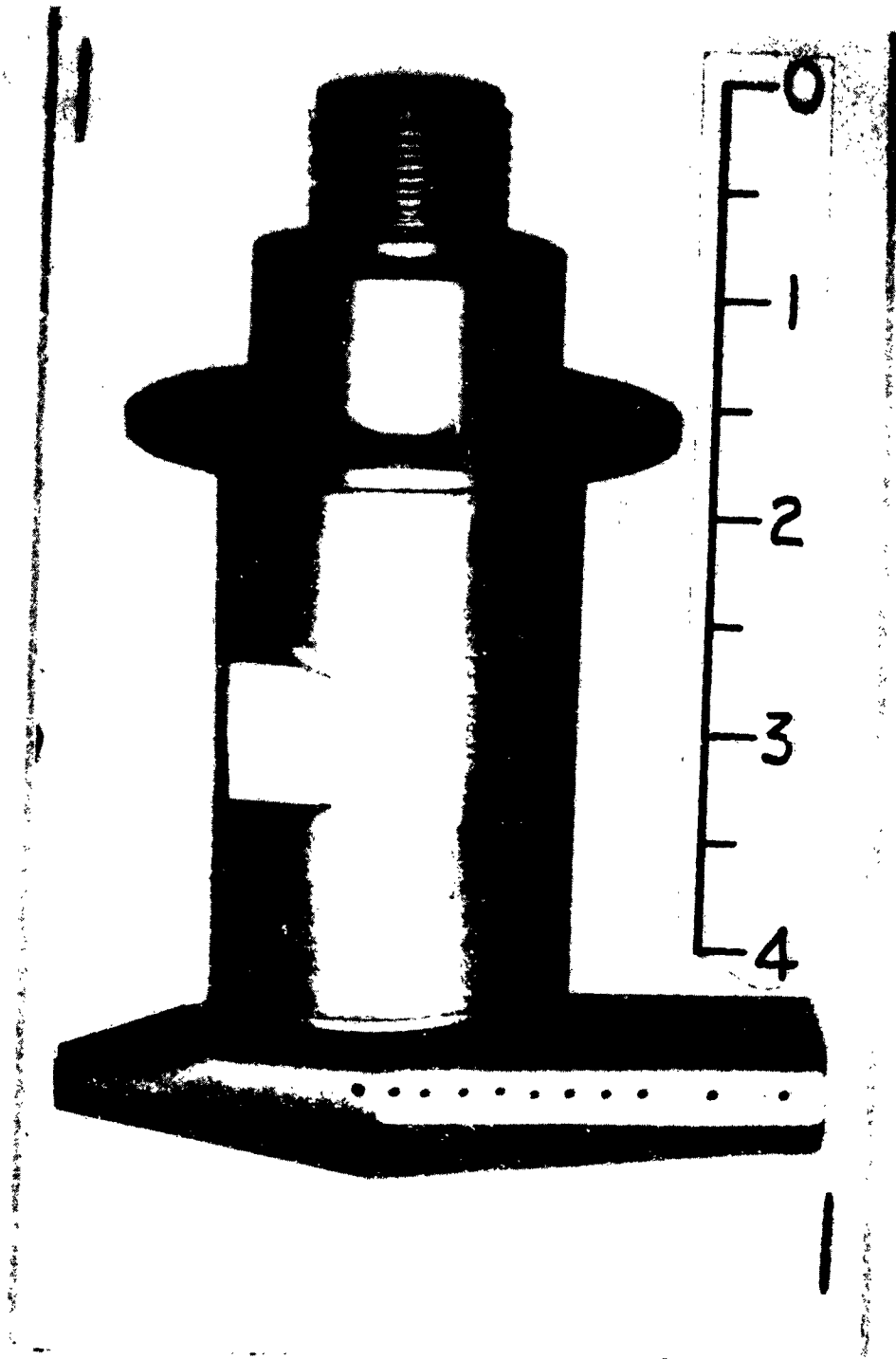


FIG. 8-ROSEMONT CORP. TEMP. PROBE

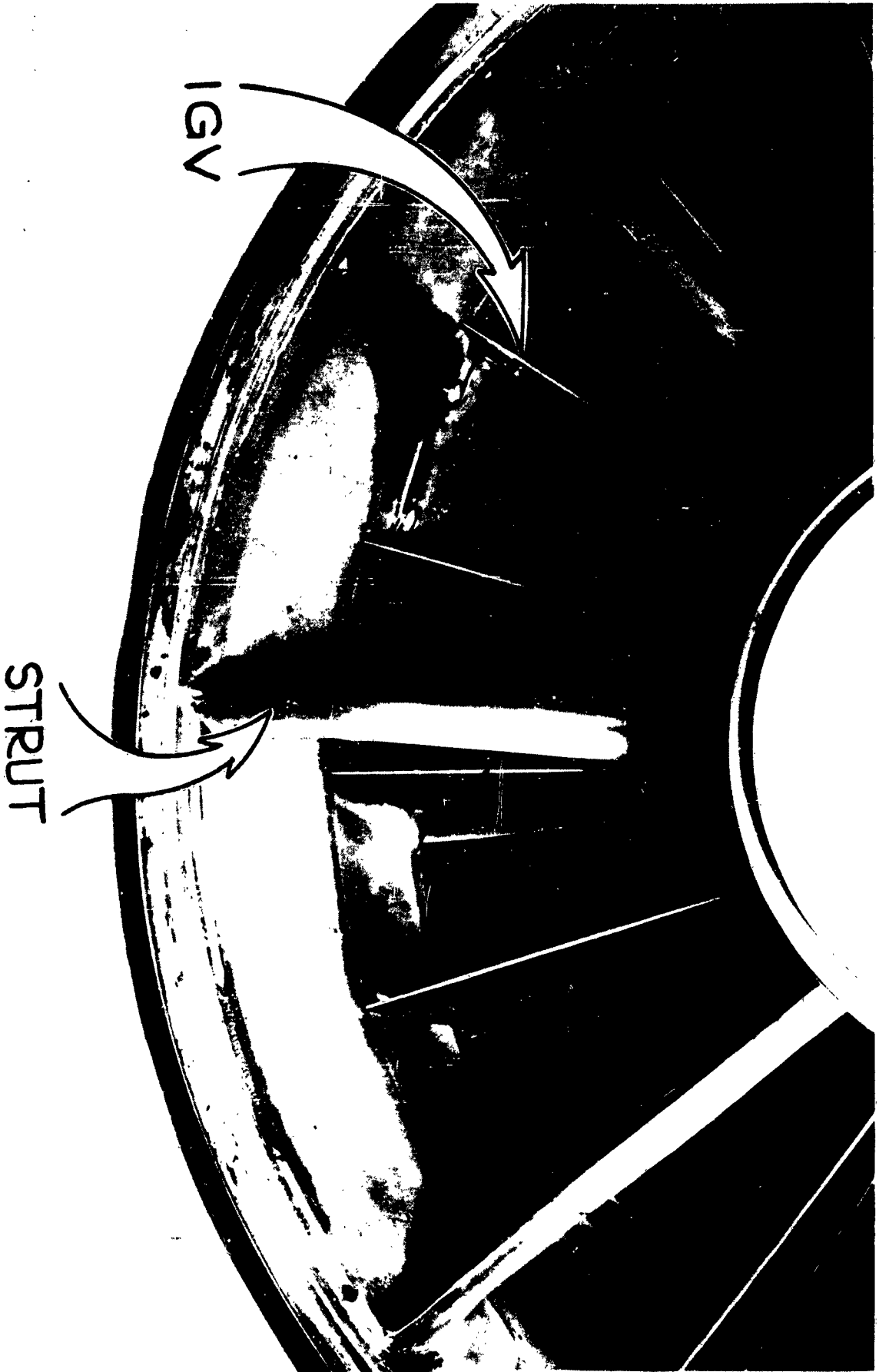


FIG. 9- INLET SKIN THERMOCOUPLES J79 ENGINE

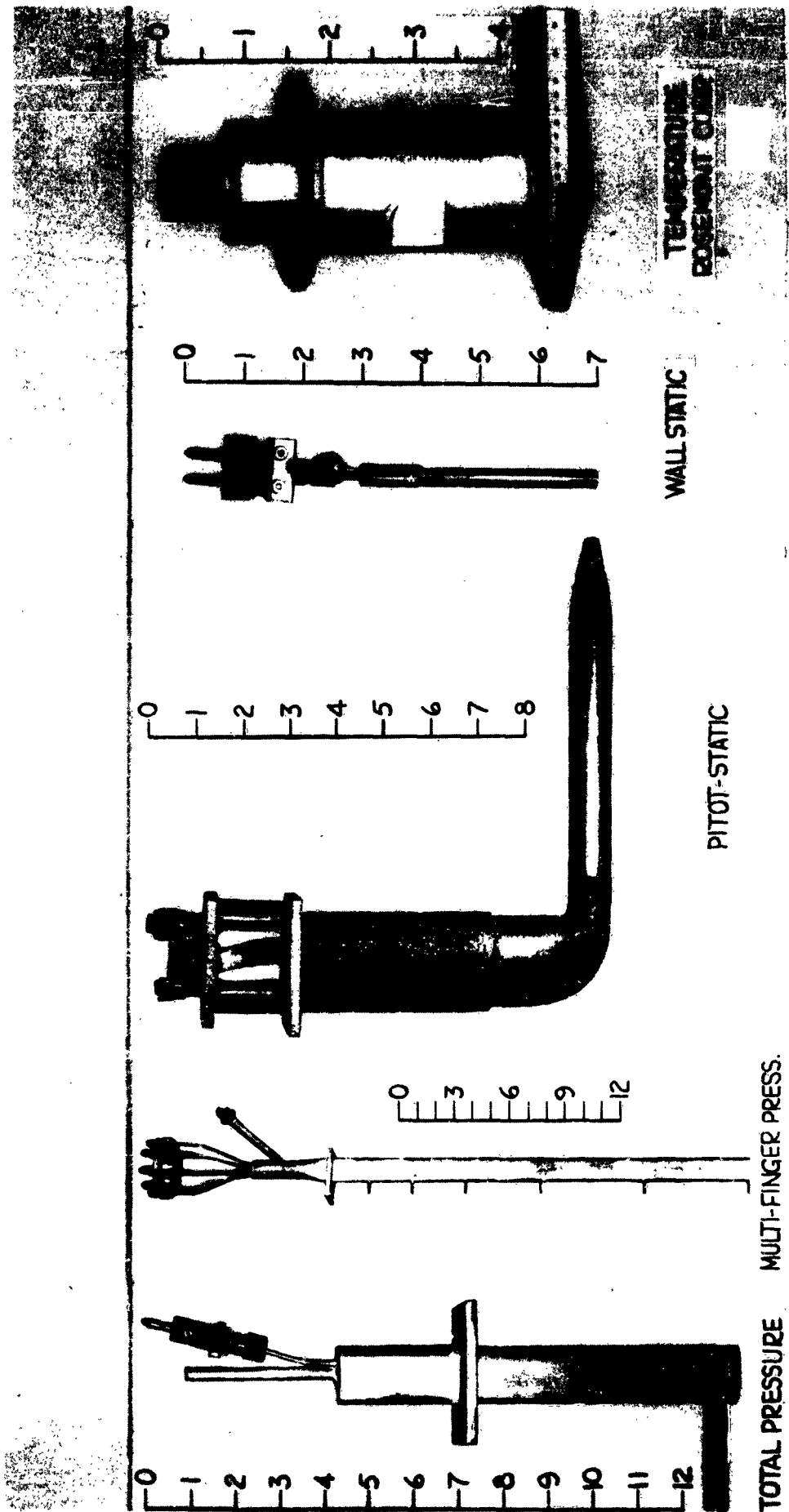


FIG. 10 - SUMMARY OF NATTS USED PROBES

A COMPARISON BETWEEN THE ROTATING MULTICYLINDER  
METHOD AND THE OIL SLIDE METHOD

by

Vincent Cirrito

Aeronautical Turbine Laboratory

U. S. Naval Air Turbine Test Station

Trenton, New Jersey

During the icing tests at the Naval Air Turbine Test Station, both the rotating multicylinder and the oil slide method for measuring water droplet sizes were used. The purpose of doing this was to determine, what, if any, relationship existed between the droplet diameters obtained from both methods. The icing tests were performed under a variety of icing conditions designed to produce a wide range of droplet sizes.

For these tests, NATTS used a water spray that was designed, constructed, and calibrated by the Allison Division of the General Motors Corporation. The spray rig contained a series of specially designed gas atomizing nozzles. These nozzles were necessary for the production of minute water particles. The number of nozzles used in the icing tests ranged from eighteen to ninety-two nozzles. The location of the spray rig was twenty-six feet upstream from the rotating multicylinder assembly.

The dew point of the air at the spray rig station was measured with a cold mirror device. Knowing the static air temperature and pressure at the rotating cylinder station, the water flow necessary to saturate the air at this station could then be calculated. The total water flow, therefore, consisted of that amount which was necessary to saturate the air and give the desired liquid water content at the rotating cylinder station. In the calculation, it was assumed that 100 percent of the water necessary to saturate the air flashed into water vapor.

Figure 1 represents the rotating cylinder assembly utilized at NATTS. The assembly consisted of five cylinders of varying diameters. These cylinders were mounted on a common shaft and inserted normally into the airstream by means of hydraulic pressure. The cylinders were rotated by an electric motor and withdrawn from the duct after a predetermined time. After the cylinders were removed from the duct, they were disassembled and weighed to determine the amount of ice collected on each cylinder. By knowing the nominal diameters of each cylinder, the amount of ice collected on each cylinder, and the ambient conditions

at the rotating cylinder station made it possible to calculate the volumetric median droplet size and liquid water content of the airstream. The volumetric median droplet size is defined to be the droplet size  $-d-$  at which half of the total volume of sample is contained in drops of diameter greater than  $-d-$  and half of the total volume of sample is contained in drops of diameter less than  $-d-$ . Figure 2 represents the oil slide assembly that was used at NATTS. The oil slide assembly consisted of an injector rod and a plastic slide. The plastic slide had three holes 0.10 inch in diameter and 0.06 inch in depth. After these holes were filled with a silicone grease, the slide was placed in the injector rod and the assembly was then inserted normally into the airstream. The cover plate, inside the injector rod, was then pulled back exposing a port in the injector rod. The slide was then pulled through the injector rod perpendicular to the airstream. A photograph of the water droplets on or in the silicone grease was then taken with a Basch and Lomb Model L Photomicrographic Camera. The droplets in the distribution photograph were then counted and categorized according to their diameters. From these data, the volumetric median droplet diameter was determined. Since no timing mechanism was attached to the oil slide assembly, it was not possible to evaluate the capability of the oil slide method to measure liquid water content.

In the spray rig calibration given to NATTS by Allison, a correlation was obtained between the rotating cylinder droplet diameter, air velocity, and the water to air mass flow ratio through the nozzles. Basically, what this correlation showed was that for a constant air velocity, the droplet size was directly proportional to the water to air mass flow ratio through the nozzles and that for a constant water to air mass flow ratio through the nozzles, the droplet size was inversely proportional to the air velocity. It was, therefore, our objective to see how our rotating cylinder and oil slide data compared, not only to each other, but also to the spray rig calibration.

In an evaluation of the drop size data taken for the same run, the rotating cylinder drop size, the oil slide drop size, and the droplet size obtained from the spray rig calibration were compared to each other. In all three comparisons, the data scatter was considerable; however, the trend of the data showed that the oil slide droplet size was greater than both the rotating cylinder droplet size obtained at NATTS and that obtained by Allison. No correlation could be obtained between the rotating cylinder and the oil slide data when related to the calibration parameters of air

velocity and the nozzle mass flow ratio. It must be remembered that, even though there is a poor correlation, the range of measurement is in the order of 5 to 100 microns.

When using either the rotating cylinder technique or the oil slide technique, certain factors have to be taken into consideration. Both methods have their advantages and disadvantages. When using the rotating cylinder analysis, there are certain features that should be kept in mind:

(1) The cylinders that are used for the rotating cylinder analysis have to be pre-chilled before they are mounted on the shaft.

(2) Since the procedure for the reduction of the rotating cylinder data is both tedious and lengthy, a considerable amount of time is required for the reduction of the data.

(3) In order to be within the limits of the rotating cylinder analysis, it is recommended that the calculated ice diameter of the smallest cylinder be 50 to 100 percent greater than the nominal diameter of the smallest cylinder. You are, therefore, limited by the fact that you must predetermine the cylinder exposure time. For the tests performed at NATTS, an arbitrary relationship was found to exist between liquid water content, cylinder exposure time, and the percentage increase in the diameter of the smallest cylinder.

(4) The rotating cylinder analysis is based upon several assumed droplet size distributions and is, therefore, limited by the fact that it cannot measure drop size distribution directly. If the assumed distribution is not the same as the actual distribution in the cloud being measured, the plots necessary for a rotating cylinder analysis may seem to contain data scatter. This data scatter would tend to indicate poor sample taking which may not be the case at all.

(5) The liquid water content obtained from the rotating cylinder analysis compared very well with the measured value. The rotating cylinder liquid water content was about 25 percent lower than the measured value.

(6) Rotating cylinder liquid water content data within the Ludlam limit compared very well with the measured liquid water content. Considering the experimental error involved in determining

the liquid water content in both methods, the relationship can be said to be essentially one to one.

When using the oil slide method, certain factors also have to be considered:

(1) It has been found at NATTS that during a run, different droplet size distributions could be obtained for a constant oil slide exposure time and also for a variable oil slide exposure time.

(2) Figure 3 represents a time study performed on an oil slide sample. Droplet distribution photographs were taken of the same oil slide sample 45, 60, 90, and 105 seconds after the sample was taken. The droplets in each of the photographs were counted and categorized according to drop diameter (Appendix I) so that a graphical picture of the evaporation effect could be shown. Figure 4 represents the graphical picture of the evaporation effect. It can be seen that the evaporation effect is more pronounced amongst the smaller droplets. It can also be seen that even though there is a pronounced evaporation effect amongst the smaller droplets, the larger droplets are essentially remaining constant in both size and number. Even though there is an evaporation and coalescence effect present in this oil slide sample, the volumetric median droplet size decreased only 9.4 percent.

(3) During the icing tests at NATTS, it was estimated that the oil slide distribution photographs were taken 45 to 90 seconds after the sample was obtained. The atmosphere in which the photographs were taken was not the same as the conditioned air in the duct.

(4) Since the oil slide sample is not subjected to the airstream for any considerable length of time, some doubt could be raised as to whether or not the drop size distribution obtained fully represents the actual drop size distribution in the airstream.

(5) The oil slide technique is very ideal for actual flight conditions since the samples can be easily obtained and, with a bit of experience, the distribution photographs can be easily reduced.

It cannot be concluded that either the rotating cylinder or the oil slide method is best for measuring droplet sizes since,

technically, there is no good reason to specify one method above the other. The poor correlation that was obtained in the comparison of the droplet sizes indicates two things. One is that when you are speaking of aircraft icing, it may not be practical to state a critical icing drop size but, rather, a critical icing range. The second is that a further study should be made of the techniques used for measuring droplet sizes.

At the present time, a report on the comparison of droplet measuring systems is being prepared at the Naval Air Turbine Test Station. This report discusses the results of the icing tests at NATTS more thoroughly than described in this paper.

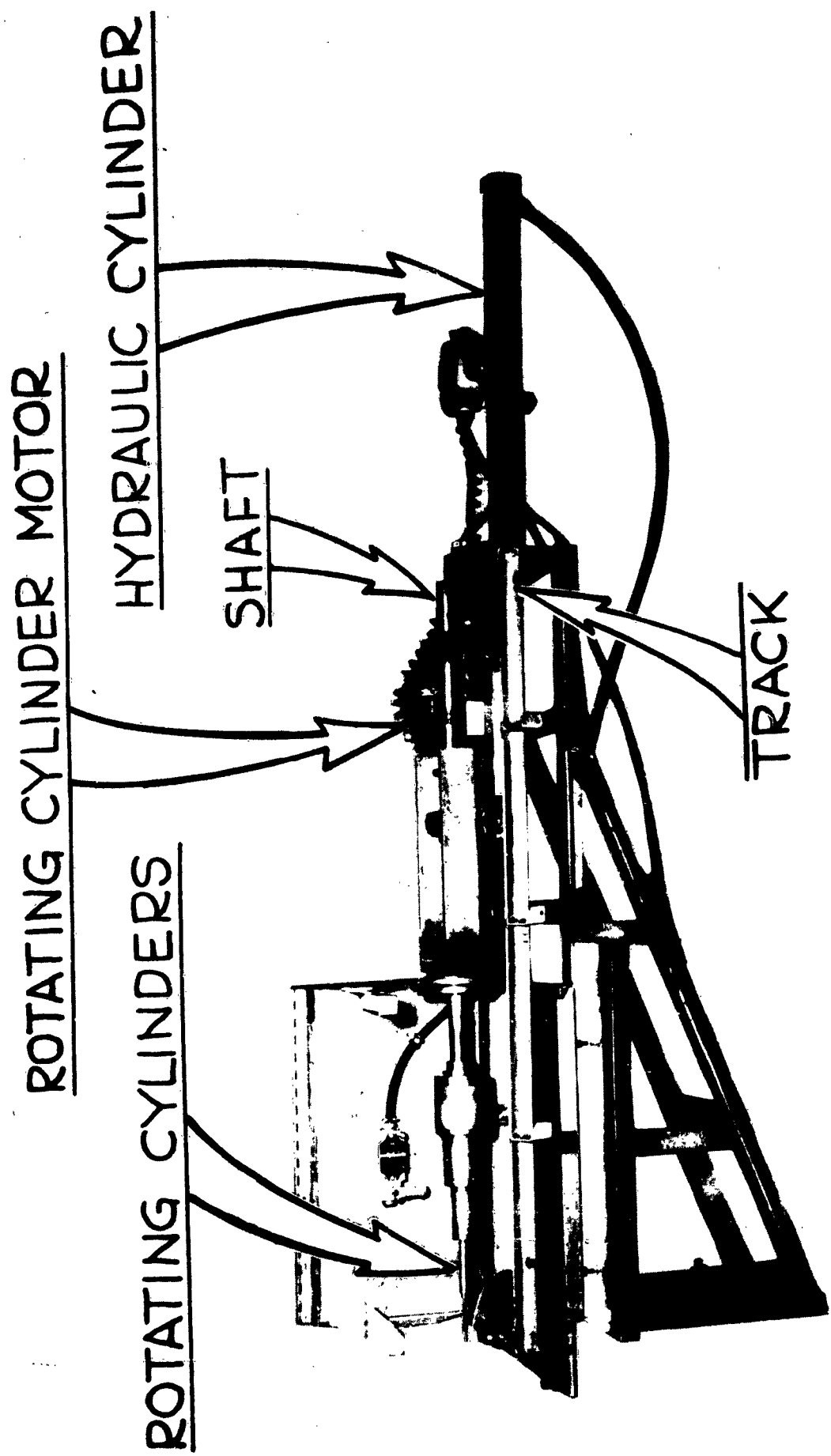


FIGURE 1 ROTATING CYLINDER ASSEMBLY

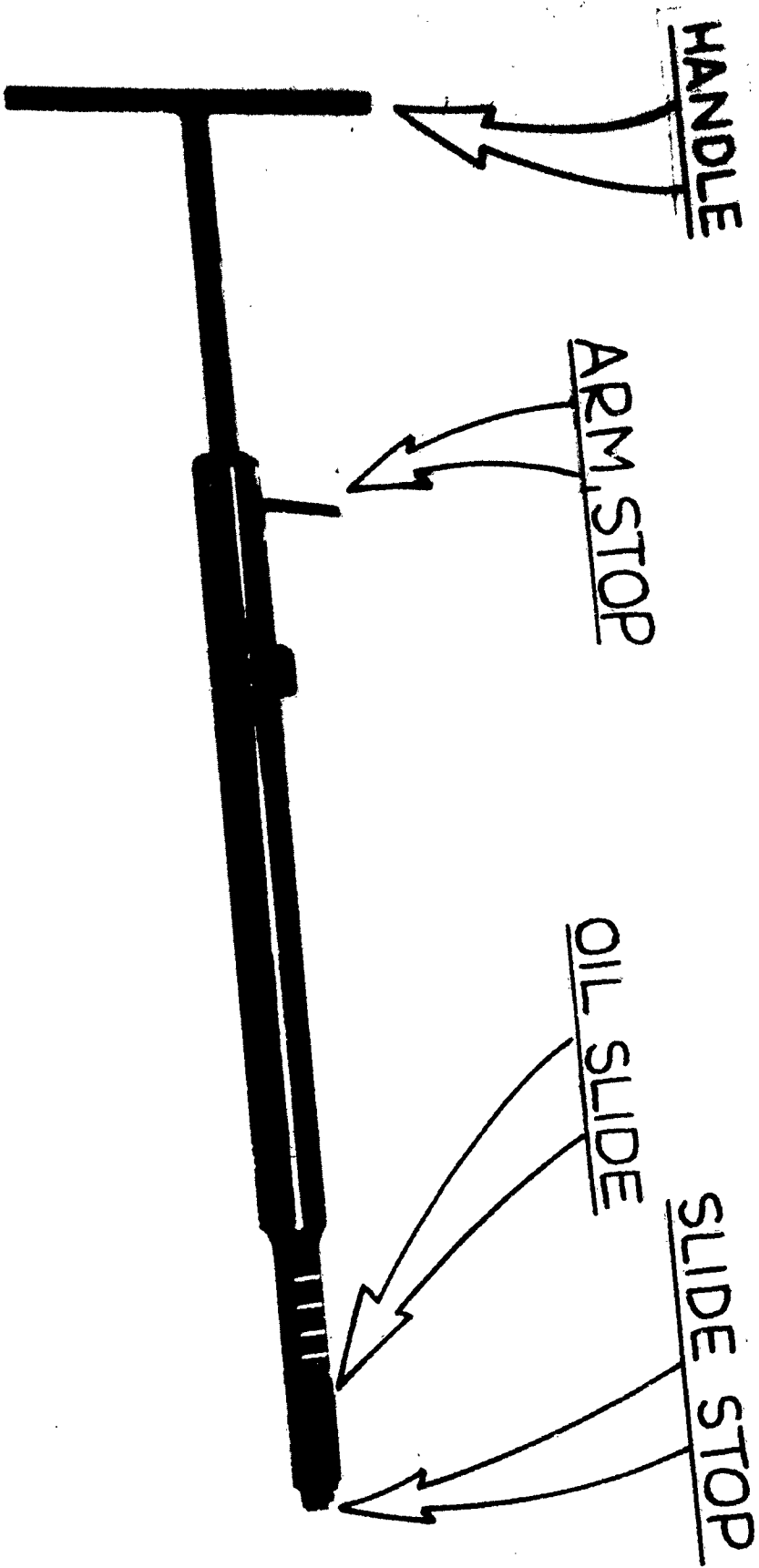


FIGURE 2

OIL SLIDE INJECTOR ROD



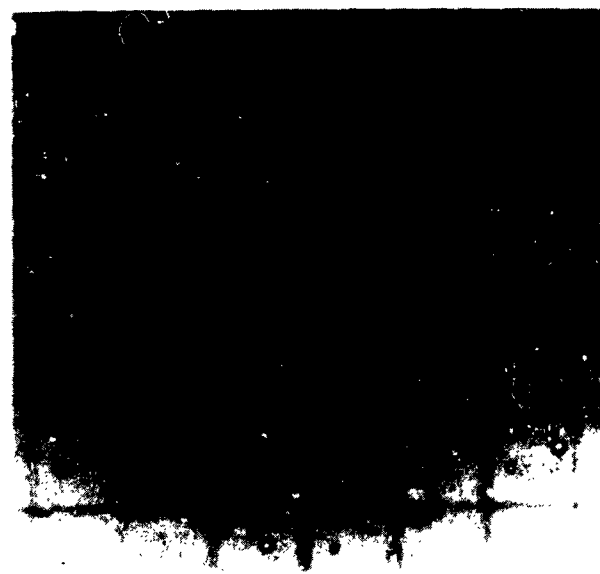
t = 45 SEC., dm = 64u



t = 60 SEC., dm = 58u



t = 90 SEC., dm = 62u



t = 105 SEC., dm = 58u

FIGURE 3 DROP SIZE DISTRIBUTION PHOTOGRAPHS  
OF AN OIL SLIDE SAMPLE AT VARIOUS TIME INTERVALS

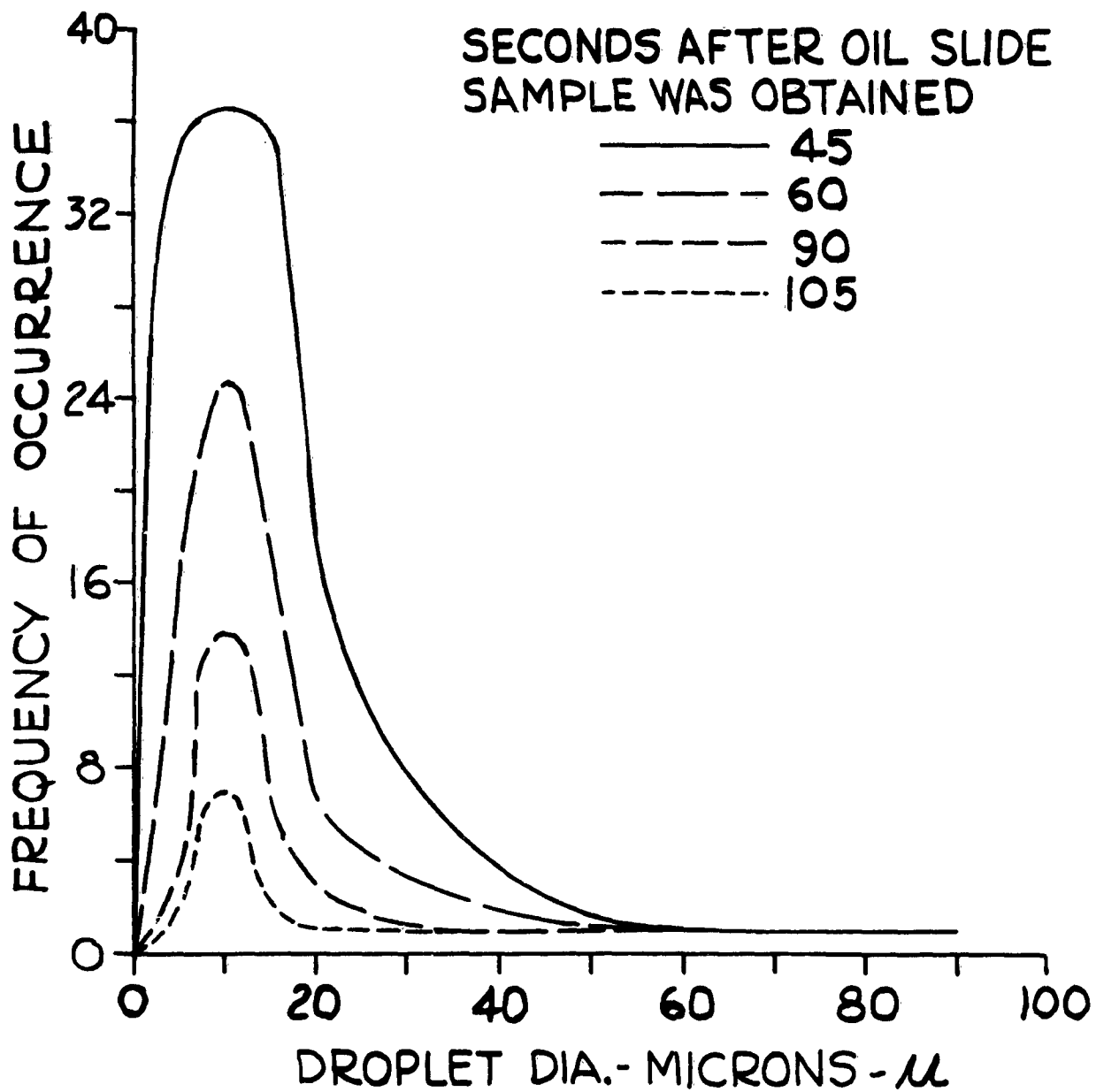


FIGURE 4 DROP-SIZE FREQUENCY FOR THE DROP-SIZE DISTRIBUTION PHOTOGRAPHS OF AN OIL SLIDE SAMPLE TAKEN AT VARIOUS TIME INTERVALS

# NATIONAL SEVERE STORMS PROJECT

## OBJECTIVES AND OPERATION

By: C. F. Van Thullenar  
U. S. Weather Bureau

### ABSTRACT

The National Severe Storms Project (NSSP) began operations in 1956 with a single airplane. It became a multiagency project in 1960 and the objectives expanded accordingly. At the time of expansion Oklahoma City was selected as the staging area. Data collection consists primarily of preactivity, activity and post-activity squall line sampling. A few examples of the data collected are given.

#### 1. INTRODUCTION

The National Severe Storms Project is new in name only. The Weather Bureau contracted for a single airplane in 1956, and each year thereafter, for the study of severe local storms. By severe local storms, so far as this project is concerned, is meant the severe thunderstorms of the Plains States and in particular, squall lines. This area of primary interest is dictated by the association of tornadoes with squall line elements.

During 1959 the Weather Bureau was instrumenting several aircraft for hurricane and other research work. In the latter half of this year it was apparent that these aircraft would be available during each spring for severe local storm study. At this same time other agencies became interested in NSSP because of problems in all-weather and high-altitude flying and air traffic control.

Beginning with the spring operations of 1960 the following agencies were represented in the NSSP:

1. U. S. Weather Bureau (USWB)
2. National Aeronautics and Space Administration (NASA)
3. Federal Aviation Agency (FAA)
4. U. S. Air Force (USAF)
  - a) Wright Air Development Division (WADD)  
(now Aeronautical Systems Division (ASD))
  - b) Air Weather Service (AWS)
  - c) Air Defense Command (ADC)

For the spring 1961 operations the same agencies participated and two more Air Force Units were added:

1. Geophysical Research Directorate (GRD), and
2. Tactical Air Command (TAC)

## 2. ORGANIZATION

With the expanded activities of 1961, NSSP became a rather large cooperative project, and it became necessary to clearly define the organization under which it could accomplish its objectives as well as show the inter-agency cooperative relationships. Fig. 1 is the currently approved organizational chart.

Because of the expanded activities the Weather Bureau felt the need for having an arrangement whereby NSSP could have the advice of others interested in severe local storms. An Advisory Panel was set up consisting of the following members:

Dr. Louis J. Battan  
Mr. Henry T. Harrison  
Dr. Glenn R. Hilst  
Dr. Joachim Kuettner  
Prof. James E. Miller  
Dr. Hans A. Panofsky  
Dr. Walter J. Saucier  
Dr. Morris Tepper

## 3. DATA COLLECTION CAPABILITY

Research aircraft available in 1961 were as follows:

USWB	GRD (USAF)	ASD (USAF)	TAC (USAF)
1 B-57	1 C-130	1 B-66	2 B-66s
2 DC-6s	1 B-47	1 F-106	
1 B-26	1 U-2	1 B-47	
		1 T-33	

The aircraft from the Aeronautical Systems Division consisted of a probe penetration aircraft (T-33), two completely instrumented penetration aircraft (F-106 and B-66) and a radar-photographic plane (B-47). The F-106 was instrumented by NASA and the B-66 by Douglas Aircraft Company, Inc. All other aircraft were instrumented for specialized or general meteorological investigations.

Recording systems were not standard; some used a digital system, some analog recorders, and some had only photo-panel.

All aircraft were not based at the staging area, Oklahoma City, at the same time. Of those aircraft listed, four were called up from Air Force bases and nine based between Will Rogers Airport and Tinker Field at Oklahoma City.

#### 4. OBJECTIVES

The general objectives of the NSSP can be quite simply stated: To study the formation, life history and decay of the squall line and related phenomena, such as tornadoes, strong winds and hail. Air Force and FAA objectives consist of a determination of the effect of turbulence on air frames and power plants and the safety of navigation through and in the vicinity of severe local storms.

To accomplish these objectives, research aircraft are dispatched in the preactivity, activity, and post-activity stages.

Generally, the efforts of NSSP have been confined to a study of a small section of the squall line consisting of only two or three cells and to individual cells. At times three or more aircraft are working in a small area. Whenever this occurs very strict ground control is maintained. FAA controllers assigned to the project work from the Weather Bureau's WSR-57 radar at Oklahoma City. Aircraft identification and a video mapper have been added to the WSR-57 output.

#### 5. DATA SAMPLES

In presenting data samples at this time it should be understood that reduction of data is not yet in final form and is subject to change. Of that which will be shown the turbulence data for 1960 will be published in an NSSP preprint series in the near future.

Fig. 2 is an example of a low level flight around a section of a squall line (upper portion) and around an individual cell (lower portion). The number in parentheses is a veeder root number. Temperature is in degrees centigrade, and water vapor content is indicated by mixing ratio in grams per kilogram. Wind is indicated in the usual manner, a long barb being equal to ten knots.

Fig. 3 represents four traverses through a dry line at different elevations. Potential temperature and mixing ratio are both graphed. Winds on both sides of the line are plotted. Note that the gradient in all four cases is given in terms of ten-second intervals. This is due to the fact that observations are read off every ten seconds. It will be necessary to return to the original records to determine maximum gradients. It will not be surprising to find gradients of moisture of the same magnitude in three to four seconds of flying time, or one-fifth to one-fourth of a mile.

Fig. 4 is a turbulence record. It was collected from run #2 on May 19, 1960, by an Air Force T-33 instrumented by NASA. The data shown is true air turbulence after subtracting out any pilot maneuvers to the aircraft. This is not a severe turbulence case but it illustrates the type and quality of data that is becoming available. More complete analyses will be published by NASA.

In reports (1,2) of the Air Force's Wright Air Development Division will be found indications that the F-106 encountered derived effective gust velocities ( $U_{de}$ ) of approximately 75 ft. sec<sup>-1</sup> subsonic and 60 ft. sec<sup>-1</sup> supersonic (mach 1.7). The F-102, with a continuous ignition system operating, and notwithstanding about 500 compressor stalls, accomplished satisfactory penetrations.

One of the most interesting results obtained during the 1960 operations, from a meteorologist's viewpoint, is found in NASA's use of a statoscope on the T-33. This instrument was used to determine incremental "D" values during the cloud penetration runs. This "D" value is the difference between pressure altitude and the double integral of the acceleration. The assumption is made that environmental pressure outside the cloud is the same in the region of entry as in the region of exit.

Both negative and positive values were recorded. The negative values appear to be recorded in the forward (downwind) portion of the cloud and the positive values deeper into the cloud mass (nearer to the center or even upwind of the center of the cloud mass). Negative values of up to 500 ft. and positive values of up to 1000 ft. were recorded. More observations of this type are required to study the dynamics of the individual thunderstorm.

Fig. 5 is a wind and temperature preliminary analysis of a B-57 flight at 35,000 ft. on a double triangle pattern. No allowances were made for motion of the systems.

## 6. RESEARCH

Since NSSP is a newly expanded project, research to date has been from data during the years when only a single airplane was available. The coming winter will be our first opportunity to work with a larger data collection.

The Weather Bureau now has on its staff in Kansas City twelve research meteorologists who will be giving full time to using the data collected. In addition some work is being done outside the Bureau by contract on grants from the Weather Bureau and/or the National Science Foundation.

NASA and ASD in order to accomplish their objectives will publish the data and conclusions from the turbulence measuring aircraft through their own channels. In addition, both organizations will prepare papers that will appear in the NSSP preprint series.

## 7. CONCLUSION

The National Severe Storms Project of the Weather Bureau is a large-scale endeavor to learn more about severe local storms. It is possible at this time only because of the excellent cooperation of the various participating agencies

## REFERENCES

Schumacher, P.W.J., Roys, G.P., Binckley, E.T., 1961: "USAF Operations in 1960 National Severe Local Storm Research Project (Rough Rider)," WADD Technical Note 60-282.

Roys, George P., 1960: "Thunderstorm Penetrations by An F-106A Aircraft at High Speed and High Altitude," WADD Technical Note 60-274.

## LEGENDS

Fig. 1 Organization Chart

Fig. 2 B-26 flight under a squall line segment (upper) and around an individual thunderstorm of a squall

line (lower). Numbers, in parentheses veeter  
root number; upper left temperature in degrees  
centigrade; lower left, mixing ratio. Wind, long  
barb 10 knots.

- Fig. 3 Traverses through a dry line showing potential  
temperature and mixing ratio.
- Fig. 4 Turbulence in the upper regions of a thunderstorm.
- Fig. 5 B-57 flight, Oklahoma City (OKC), Garden City (GCK),  
Amarillo (AMA), Oklahoma City, Abilene (ABI),  
Amarillo, Oklahoma City. Left, wind analysis-  
stream lines and isotachs; right, temperature  
analysis.

# NATIONAL SEVERE STORMS PROJECT ORGANIZATION CHART

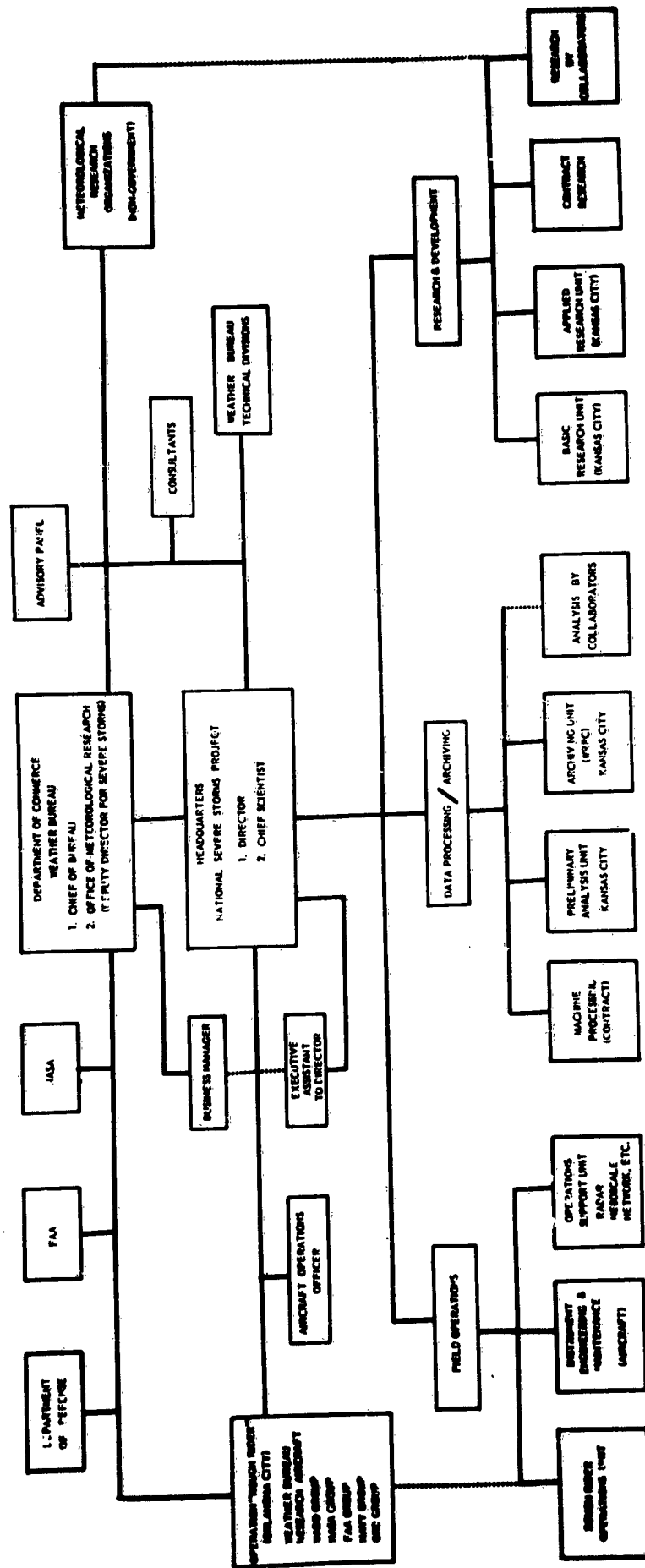
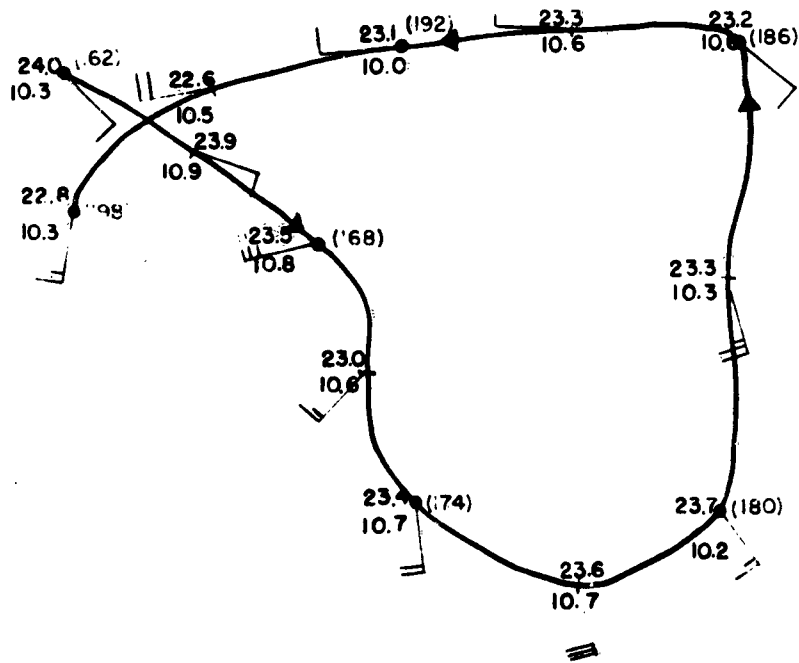
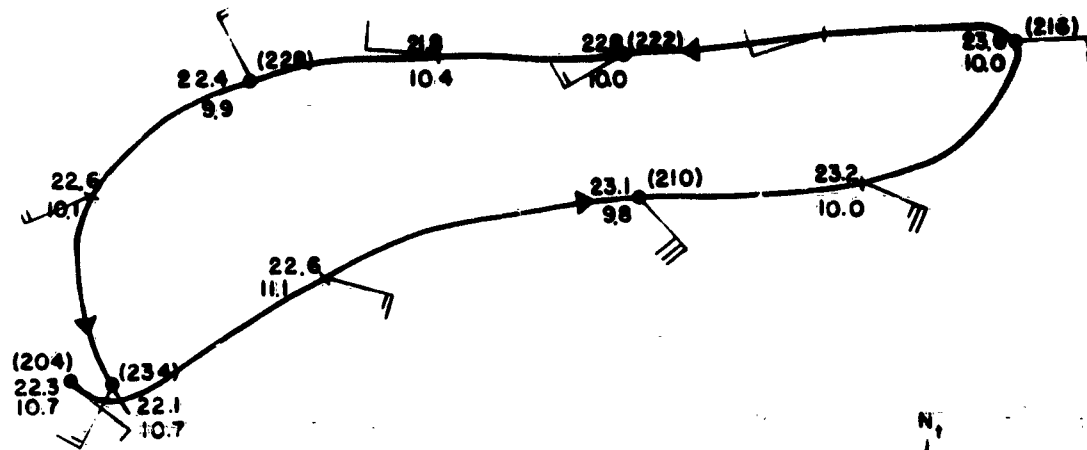


FIG. I

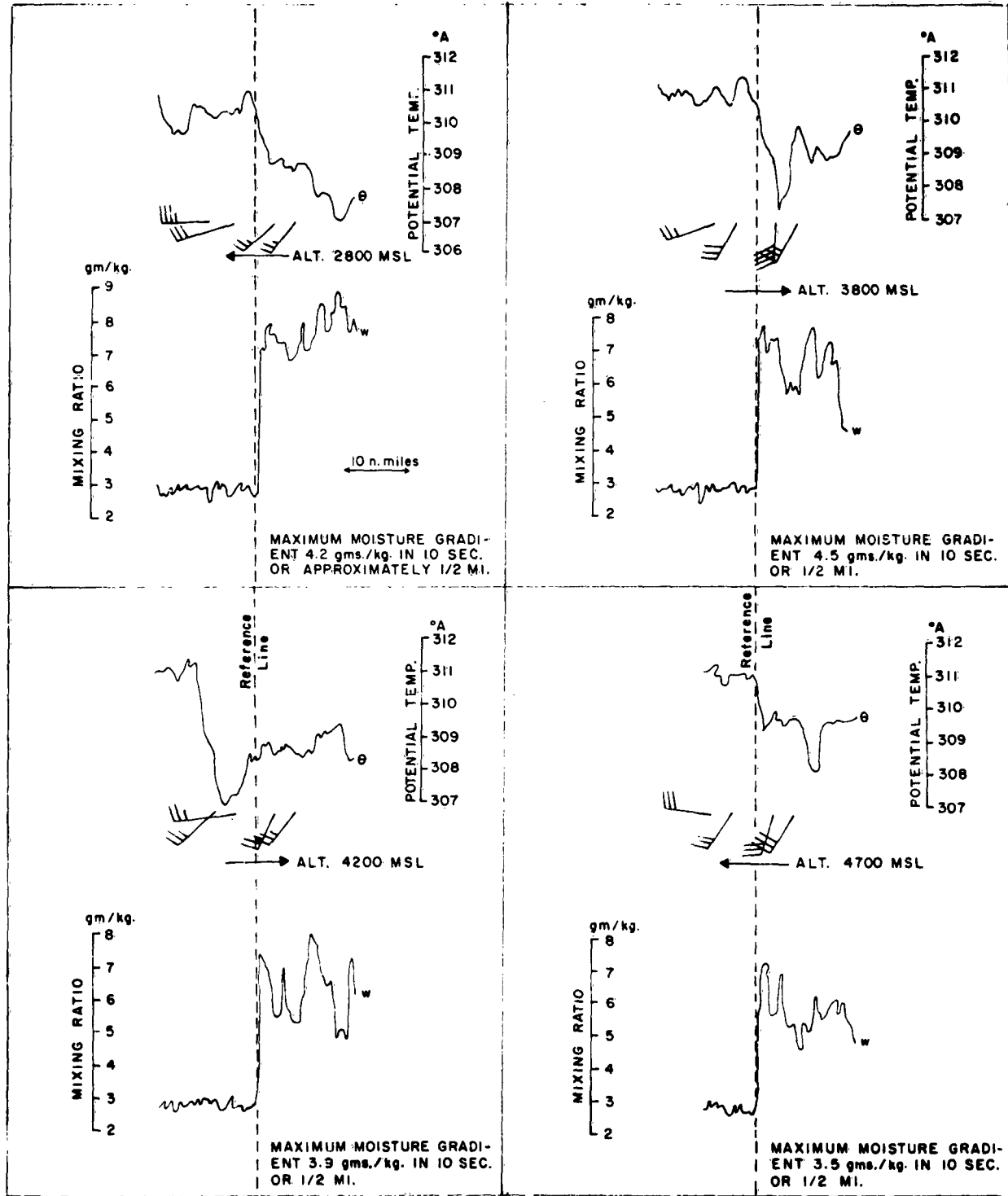


CIRCUMNAVIGATION OF SQUALL LINE SEGMENTS

FLIGHT 61-55 (17 MAY)

FIG. 2

FOUR TRAVERSES THROUGH A DRY LINE



FLIGHT #61-42  
4-19-61

FIG. 3

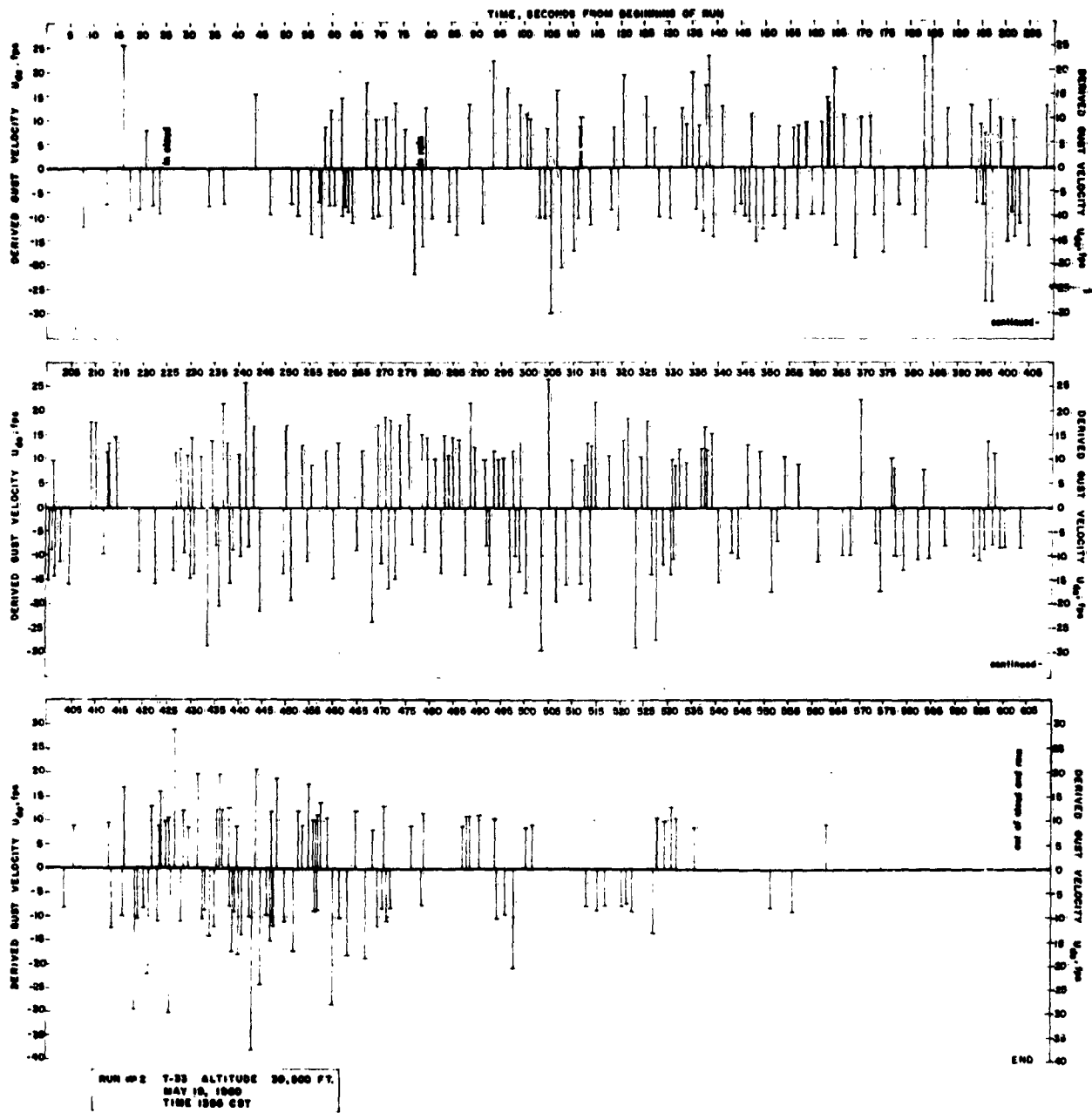


**FIG. 4**

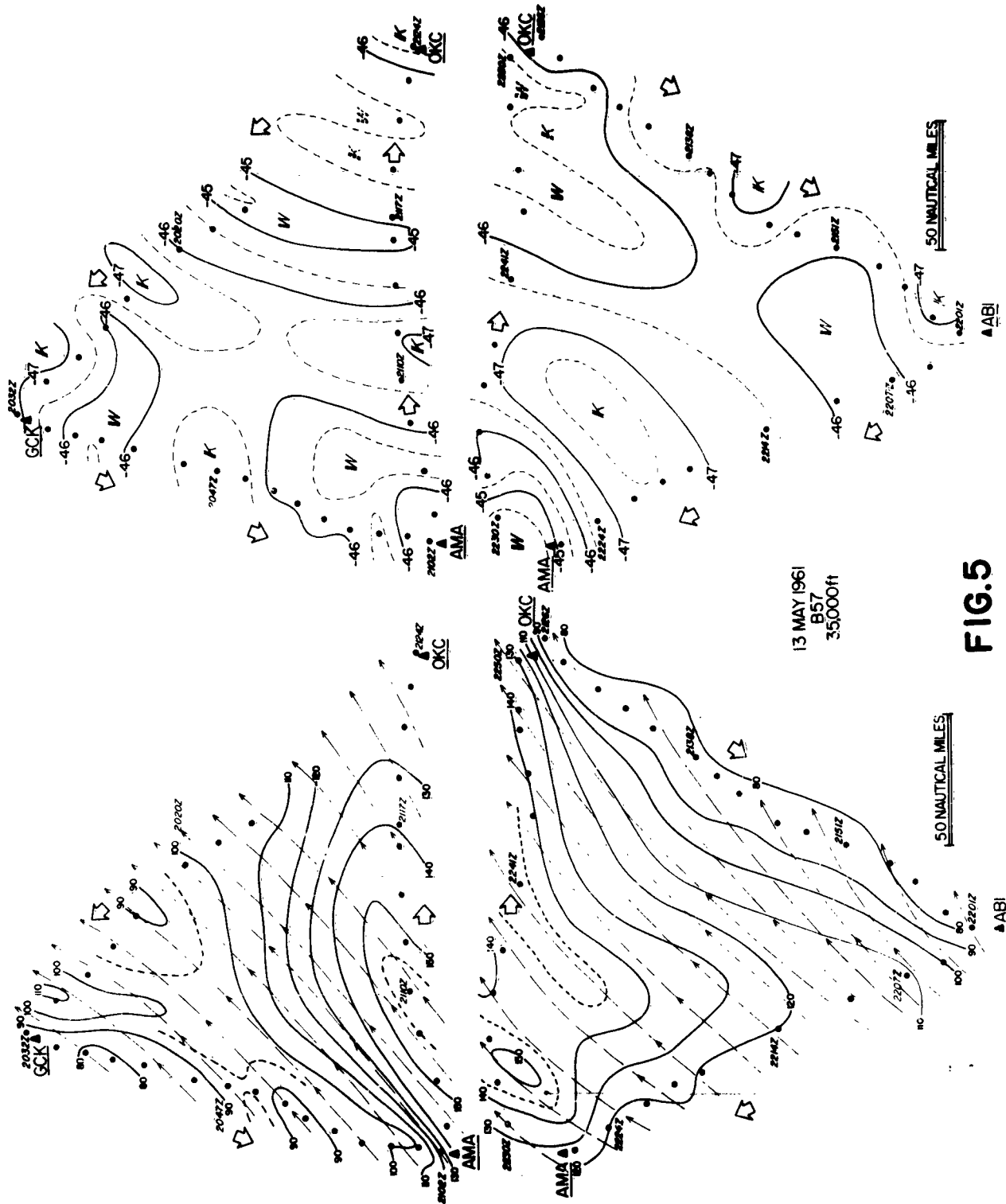


FIG.5

SEVERE WEATHER FLIGHT TESTING OF  
JET FIGHTER AIRPLANES AND ENGINES

BY

LCDR D. Z. SKALLA  
Service Test Division  
Naval Air Test Center

INTRODUCTION

1. This is to be a discussion of some of the problems and experiences encountered while flying through thunderstorms and hurricanes to evaluate the water ingestion and anti-icing capability of three fighter airplane/engine combinations: F3H/J71, F8U-2N/J57-P-20, F4H/J79-2 & -8. Water and ice ingestion test programs were initiated at NATC Patuxent River in 1958 as a result of engine failures encountered in F3H fleet airplanes, and have been included in the normal test programs for the F8U-2N and F4H due to the difficulties experienced with the F3H. Primary interest during severe weather testing is placed on evaluating the engine anti-icing capability and the ability of the engine to ingest large quantities of water and ice. Secondly, the effects of severe weather on the airplane and its components are determined.

2. The test flights are conducted by flying through thunderstorms and towering cumulus clouds, not because such practices are common in the fleet, but because it is the quickest and most convenient method of exposing airplanes and engines to the most severe natural water and ice conditions likely to be encountered during operational service.

DISCUSSION

F3H/J71 WATER INGESTION TEST PROGRAM

3. The F3H, with various modifications of the J71 engine, has undergone the most extensive severe weather evaluation of any Navy jet airplane. The test programs began in 1958 after the first failures of the J71-A-2 engines in heavy precipitation occurred. The engines were tested at Mount Washington and McDonnell began what developed into a long series of water ingestion tests. All of these tests were conducted in ar.

artificial weather environment provided by a water spray rig on the airplane or an airborne tanker.

4. Initially the failures were attributed to intake duct icing, which led to development of a duct lip anti-icing blanket. During evaluation of the duct anti-icing installation, an engine failed and the problem was first recognized as water ingestion effects. As a result, all J71-A-2 engines were modified to increased compressor clearances and redesignated J71-A-2B engines. The -2B engine successfully passed the artificial precipitation tests conducted by McDonnell by flying behind a tanker.

5. The water ingestion capability of the "B" engine proved to be unsatisfactory also, as additional engine failures were encountered in the fleet. One of the airplanes was successfully landed at Cherry Point and investigation revealed that the compressor stator seals had cut completely through spacers on the compressor rotor. McDonnell began another flight test program and developed an engine inlet duct water removal system. At this point NATC Patuxent River initiated a test program to evaluate in natural severe weather the water ingestion capability of "B" engines with the water separator installation. This project was terminated when an engine failed during a thunderstorm penetration. Excessive engine vibration developed, followed by a fire warning light. The airplane was landed with reduced power as the vibration increased with increased RPM. During the roll-out the engine seized after shut down. Inspection revealed evidence of considerable blade and stator seal rub, including a cut 8 to 10 inches long through the rotor spacer of one stage.

6. As a result of this failure, compressor clearances were again increased and the final modified engines were designated J71-A-2E. Water ingestion tests were resumed on the "E" engines by NATC (Service Test Division). In June 1959, after 10 hours in severe weather including nearly 300 thunderstorm penetrations without incident, the "E" engines were cleared for all-weather operation.

7. It appeared that the F3H/J71 water and ice ingestion problem had finally been solved. Then the bottom fell out again in October 1959 when two F3H airplanes were lost on one flight due to engine failures in heavy precipitation above the freezing level. A comprehensive water ingestion investigation was then started by McDonnell, NATTS Trenton, and NATC. Primary emphasis

was placed on evaluating the water ingestion capability in afterburner with a look at IDLE and PARTIAL power descents. Two standard "E" engines with rear of vane clearances of .150 to .160 in. and an engine modified to compressor clearances recommended by NATTS were evaluated at the Naval Air Test Center in natural severe weather. In addition, several improvements to the engine anti-icing system were evaluated. After 370 thunderstorm penetrations - including several flights in Hurricanes Donna and Ethel - without an engine failure, the project was terminated in October 1960. The water ingestion capability of both the modified and the unmodified "E" engines was satisfactory and the "E" engines were again cleared for all-weather operation. Present intentions are to increase compressor rear of vane clearances to .155 - .160 in. as an added safety precaution.

8. The only noticeable effect of water ingestion on J71-A-2E engine operation and performance throughout the last test program was a droop in RPM. Two types of droop were encountered: (1) an RPM reduction of 1 to 4-1/2% due entirely to the effects of water ingestion on the fuel required characteristics of the engine; and (2) an RPM reduction of as much as 15% - depending upon airspeed - due to complete or partial blockage of the fuel control total pressure ( $P_{t2}$ ) sensing probes by ice. The first type of droop required no recovery action by the pilot and was of little significance except possibly at idle RPM. Recovery action consisting of a throttle reduction was required when the second type of droop was encountered. It is possible that this large droop in RPM was mistaken for an engine flameout by the pilots involved in the two failures of "E" engines. Redesigned  $P_{t2}$  probes, which were evaluated satisfactorily during the project, are being installed in all engines.

9. During project flying, two mild compressor stalls were encountered while lighting the afterburner in very heavy precipitation, so it is possible that large quantities of water have an adverse effect on stall margin.

10. Failures of the longitudinal artificial feel system were encountered with great regularity during thunderstorm penetrations in the F3H as a result of the bellows ram air line being blocked by ice. Approximately 35 to 45 lb pull force was required to maintain level flight when the system failed at 350 KIAS. This force could be reduced to approximately 10 lb by applying

full nose-up stabilator trim. Once the failure occurred, the system remained blocked until a descent below the freezing level was effected. In addition, various parts of the test airplanes were repeatedly damaged by precipitation and lightning.

#### F8U-2N/J57-P-20 WATER INGESTION TEST PROGRAM

11. Water ingestion flights in the F8U-2N began in October 1960 and are expected to be completed this summer. Progress during the winter months was slow due to lack of the desired severe weather. Approximately 110 thunderstorm penetrations have been made without encountering engine operation difficulties. A slight compressor blade tip rub was evident after the last few flights through the heaviest precipitation encountered in the F8U to date. This slight blade tip rub is not uncommon in high time J57 engines and, although probably due to water ingestion, the compressor rub is not considered to be a serious problem unless the blade tips become scorched.

12. The major difficulty encountered in the F8U-2N has been blockage of the airspeed pitot tube in icing conditions. The new pitot tube is highly susceptible to failure in even very light ice. A secondary airspeed system with an old type pitot tube, which is standard on the F8U-1 and early F8U-2, was installed in the test airplane. Only one failure of this installation has been encountered to date.

13. The turbulence encountered in thunderstorms may prove to be a problem during slow speed penetrations in the Crusader. The intake duct is on the end of a  $26\frac{1}{2}$  ft lever arm from the center of gravity and pitches through some erratic arcs in violent turbulence. At excessively slow airspeeds, sufficient duct distortion may be produced to induce a compressor stall. At supersonic speeds pilot discomfort may become a limiting factor.

#### F4H/J79 WATER INGESTION TEST PROGRAM

14. The F4H/J79 program is just getting underway this summer and has not progressed beyond the build up phase. The test airplane is fitted with one J79-GE-2 engine and one J79-GE-8 engine. Initial results indicate that the F4H will provide a much more "gentle" ride for the pilot than the F8U due, primarily, to the closer proximity of the cockpit to the center of gravity in the F4H.

## DESCRIPTION OF FLIGHT CONDITIONS WITHIN THUNDERSTORMS

15. General. The majority of the water ingestion flights were conducted in Florida where thunderstorms are a common weather condition. Several flights were flown through storms in the vicinity of Patuxent, Washington, Norfolk, and Cherry Point. Aerological assistance was usually obtained prior to flight to determine the areas of greatest potential thunderstorm activity; however, many storms were located by airborne search methods. Often the most vicious looking storms proved to be much less severe than other relatively innocent appearing towering cumulus clouds. Outstanding cooperation in obtaining in-flight instrument clearances to penetrate the storms was received from the Air Route Traffic Control Centers. The majority of the storm penetrations were made at altitudes between 20,000 and 30,000 ft.

16. Turbulence. Turbulence is probably the most feared and respected characteristic of thunderstorms. Several airplanes have been structurally damaged by the vertical gust loads and some fatalities have resulted. Jet fighter airplanes are designed to withstand large acceleration loadings and are not susceptible to structural failure at normal cruise and climb airspeeds. None of the airplanes involved in the projects at NATC have ever been damaged by turbulence. The pilot gets a fairly rough ride, especially in the F8U, but control of the airplane has not been a problem. In fact, from a controllability standpoint, thunderstorm flying in fast moving jet airplanes is probably easier than in the slower moving prop airplanes, as the excursions in altitude, airspeed, and heading are not nearly as great. In the F8U, with the cockpit approximately  $21\frac{1}{2}$  ft forward of the center of gravity, the pilot feels the turbulence much more than in the F3H or F4H. Pilots were able to monitor most of the engine instruments in the F3H; however, in the F8U it has been difficult to focus on these instruments due to the bouncing of the instrument panel and the pilot - which usually are not in phase. During one penetration in the F8U the cockpit accelerometer was "pegged" in the negative g direction (in excess of -5g) and indicated a positive  $8\frac{1}{2}$  g. It should be remembered that these are jar-type accelerations near the nose of the airplane and the wing is exposed to a much lower loading.

17. Precipitation. Precipitation, which can reach gigantic intensity in a well developed thunderstorm, has the most significant effect (adverse or favorable) on engine operation. If the engine has adequate anti-icing and water ingestion capability, adverse effects will not be encountered and probably an increase in thrust will be realized. However, if either of the above items is inadequate, catastrophic failures may result, as in the F3H. To date, ice and hail impinging on the front of engines has not produced damaging dents or knicks in guide vanes or blades. However, ice and hail of the intensity encountered in thunderstorms has proven quite damaging to airplane components. Two F3H radomes were collapsed and various fiberglass parts of both the F3H and the F8U were continuously damaged by ice. Speed brakes, which were used to control airspeed, were often dented and chipped by hail and ice. Wing and fuselage light failures were also common. For project records, the intensity of precipitation was rated qualitatively according to the degree to which visibility through the windshield was obscured and by cockpit noise produced by heavy hail and ice.

18. Lightning. Although not the most destructive element encountered in thunderstorms, lightning is probably one of the most respected. Fortunately, lightning is not nearly as destructive as it might appear to be, provided adequate protective measures are taken. The airplane structure is an excellent conductor of electricity and nearly all lightning strikes will be conducted through the airframe and discharged off a trailing edge or point, such as wing tip, stabilator tip, or rudder. Lightning which strikes the forward part of the airplane tends to move aft due to the forward velocity of the airplane. When the lightning discharge reaches an aft extreme of a component on the airplane, it tends to hang on momentarily. This produces an arc welding effect if the component is metal, and a burning and explosive effect due to air ionization if the component is of fiberglass construction. A considerable amount of damage occurred to the trailing edges of the stabilator and wing of the F3H. In addition, the fiberglass wing tip fairings and the fin cap antenna housing were repeatedly damaged by lightning. The fiberglass tip section of the rudder was split and cracked once and blown completely off the airplane during another storm penetration in Hurricane Ethel. All of these lightning strikes appeared to hit the airplane initially at or near the nose. The radome of the F3H was punctured by lightning

once, which weakened the structure and rendered it unusable. Metal radomes were installed early in the project to protect against lightning and precipitation damage.

a. Protection Against Lightning Damage.

Basically, lightning protection for airplanes consists of providing an uninterrupted conduction path from or through all components of the airplane and discharge elements at the aft tips of the wings, stabilator, and rudder. The following modifications to the F8U and the F4H, which were recommended by Mr. J. D. Robb of Lightning and Transients Research Institute, have so far proven satisfactory in preventing the type of damage sustained in the F3H:

- (1) Metal radome (F8U only)
- (2) Metal strips from tip of radome to metal mount (F4H only - not proven yet).
- (3) Small triangular shaped, copper, lightning discharge plates attached to the wing tips, stabilator tips, and rudder tip (approximately 3 in. in length).
- (4) Copper wire strips across the top of the fiberglass fin caps and extending 4-6 in. beyond the trailing edge.

b. Lightning Protection for the Pilot.

Prior to 7 June 1961, lightning protection for the pilot, although recommended by Mr. Robb, was not considered necessary. On the above date, while flying the F8U through a small thunderstorm with a considerable amount of lightning, the pilot suddenly felt a sharp blow across the forehead coincident with a bright flash in the immediate vicinity of the cockpit. Undoubtedly this was not a direct lightning strike on the pilot, but the effects of "streamers" from the main bolt or an induction phenomenon. As a result, a "back to the drawing board" maneuver has been in progress for the last two weeks. Metal strips, as recommended by Mr. Robb, are to be installed across the top of each canopy prior to resumption of thunderstorm flights.

19. Airframe Icing. Ice accumulation on the airframe, although undoubtedly a problem in slower airplanes, has not been significant in the airplanes tested. Ice has often covered the windshield and

canopy, but has never appeared to build up to an appreciable thickness. Ice has not been noticed on other parts of the airplane, probably because it forms on the canopy first and obscures external vision. Also, the wings are not within the normal field of vision of the pilot.

20. Engine Icing. Engine icing problems, except for the J71 fuel control Pt<sub>2</sub> sensing probes, have not been encountered. All penetrations have been made with engine anti-ice on except for a few investigative flights in the F3H. It is highly probable that engine anti-icing may be inadequate at low power settings due to the reduced air flow and reduced temperature of the compressor bleed air. Consequently, engine icing problems are more likely to be encountered at or near idle RPM.

21. Hurricane Flights in the F3H. Four flights were conducted in Hurricane Donna and two in Hurricane Ethel during the F3H test program. In general, flight conditions within the hurricanes were not as severe as conditions encountered in large, well developed air mass thunderstorms. Severe icing, heavy precipitation, and severe turbulence were encountered during one flight near Cherry Point, which was comparable to conditions within large air mass thunderstorms. Most of the thunderstorms within the hurricane did not build up to the height common to the air mass type, consequently, the heaviest precipitation was at the lower altitudes. The eye of Hurricane Donna was penetrated during one flight while operating under the control of a ground radar site. The eye was defined by a comparatively clear area of several miles in diameter. Scattered to broken clouds prevailed in the eye at various altitudes; however, the ocean below and clear sky above were visible from 20,000 ft. This was quite a contrast to the solid cloud conditions existing for over 300 miles around the eye.

#### CONCLUSIONS

22. The following general conclusions were reached as a result of the tests conducted by the Naval Air Test Center:

a. Water and ice ingestion tests of jet aircraft engines are essential to insure all-weather reliability.

b. The test facilities at NATTS Trenton provide an excellent means of evaluating engines under simulated weather conditions to determine early deficiencies in water ingestion and/or anti-icing capability.

c. Although the tests conducted at NATTS are quite thorough, an in-flight severe weather evaluation is still required due to significant difference between natural severe weather and precipitation conditions created artificially.

d. Considerable lightning and precipitation damage to airplane components such as radomes, fin antennae, missile launchers, exterior lights, and trailing edge surfaces usually will be encountered in well developed thunderstorms; consequently, the storms should be avoided during routine flight operations.

e. Adequate lightning protection for radomes, fin antennae, and cockpits should be provided in all-weather jet airplanes.

# FOREIGN OBJECT INGESTION

## IN TURBINE ENGINES

BY

E. J. BRIGGS, JR.

FAA DESIGN EVALUATION ENGINEER

### INTRODUCTION

Experience has indicated that foreign objects are often ingested by engines, at times with adverse effects on engine structure or operating characteristics. Largely because the inlet areas used for turbine engines flow four times as much air as for comparable output piston type engines and have correspondingly larger air inlets, ingestion troubles have involved turbine engines much more often than piston type engines.

While much effort can be and is normally exerted to avoid these ingestions, such events nevertheless occur and are expected to continue to occur in the future. Fortunately, the general design of turbine engine compressors is such as to effectively resist drastic effects or to survive such ingestions in most instances without immediate or necessarily serious results on engine operation in multiengine aircraft. Surprisingly, extensive blade and vane damage has occurred in many instances with only slight effects on power and with minor instability and roughness.

While this discussion will cover several varieties of ingestion in turbine engines, bird ingestion will be emphasized.

#### Bird Ingestion Experience

During the last two years of United States commercial jet transport operation there have been 58 known reports of engines suffering ingestion of birds. This represents an ingestion rate of about .015 or  $1\frac{1}{2}$  instance per 100,000 engine hours. These instances resulted in damaging 40 engines to varying degrees. There were no accidents.

In 11 instances there were some indications of engine malfunctioning, though no engine shutdowns were required to complete the flight safely. The engine damage was confined principally to the compressor inlet guide vanes and early compressor rotor stages. The usual damage was bent first stage rotor blade forward tips, and distorted inlet guide vane (IGV) trailing edges. In a few instances, more extensive damage caused pieces of IGV to be released which resulted in considerable damage to the rest of the compressor and turbine stages.

There were six instances when more than one engine of the four engine aircraft ingested birds at the same time due to striking a flock of birds, and seven instances where only one engine was involved after encountering the bird flock.

During takeoffs and landings there were somewhat more bird ingestions than during the cruising portion of the flights. Because of incomplete details available for some bird strikes, the proportion of the takeoff and landing strikes cannot be accurately established, but it appears that possibly twice as many ingestions occurred at such times as at other times.

A number of instances reported as engine roughness or a tendency for mild stalls were caused by bird carcasses lodging at the engine face, by the foreign matter in the compressor, or by the distorted blading.

The flocks of birds encountered were sea gulls, starlings, pigeons, sandpipers, or in one instance, guinea hens. All of these encounters with flocks occurred on takeoff or landing.

There was one instance of particular interest, where three engines ingested seagulls during a takeoff, and numerous sparks issued from the three engines for about 15 minutes. Engine operation was otherwise normal, but after the flight was completed over four hours later, it was found that virtually all of the compressor blades, compressor stators, some turbine blades and some compressor cases had to be replaced.

Foreign, foreign object encounters reported on Comet and Caravelle jet aircraft indicate the greatest incidences in the Far East, about one encounter (not necessarily an ingestion however) for 686 flights. The frequency for the European area was one strike per 7,120 flights, and for the Americas, one strike per 2,858 flights. These data cover all United Kingdom jet operations through 1960.

The engine damage suffered in the certain early design jet engines was generally worse than on the later models and types of jet engines. This was due to the small axial clearance between the inlet guide vanes and the first stage rotor blades. On the later engines these clearances were increased from under one inch to around three inches.

Foreign object damage was reported also, from objects left in intakes, and from ice thrown from aircraft toilets. Here, as in the U. S. Civil experience, the engines have shown a remarkable ability to continue to operate with damaged blading.

Turboprop engines used in U. S. commercial transports have suffered approximately 13 bird ingestions in the few years they have been operating. Bird feathers and blood stains are generally the only evidence available to identify the few ingestions in the British-built turboprop engines with their centrifugal type compressors.

The turboprop engines used in the Electra aircraft have encountered more bird strikes than the Dart engines. This can be readily understood by comparing the narrow lipped annular air inlet located behind the propeller hub on the Rolls Royce Dart engine to the larger elliptical opening mounted above the propeller axis on the Allison engines.

These bird encounters have resulted in no engine damage or operational troubles for the Dart engine. While the Allison engine has indicated a high resistance to damage from bird ingestions, there have been instances demonstrating a momentary power drop characteristic, with virtually full recovery depending upon the quantity of bird material involved. The automatic quick feathering mechanism for use with this engine during takeoffs has been triggered on several bird strikes, resulting in a full engine shutdown. The power recovery is normally rapid, but with appreciable bird residue in the compressor, complete power is usually achieved only after some continued operations, or after a walnut shell cleaning operation.

There was a very recent instance with an Electra in Australia when several birds were struck during a takeoff. One engine torched, lost about 1,000 b.hp. and quickly recovered all but 250 b.hp. Upon completion of the flight a portion of a bird was removed from the inlet and the engine was found to be serviceable.

In the Boston Electra accident on November 2, 1960, bird remains were found in three of the four engines. This aircraft struck a large flock of starlings during takeoff, and subsequently crashed, although it was evident from inspection of the engines and propellers that three engines were producing substantially full takeoff power at the time of the crash. The other engine was fully feathered. No engine flame outs as such have been reported on these engines.

Worldwide operation of Dart turboprop engines is similar to the U. S. experience and eight ingestions have been reported, totaling ten in almost 13 million hours of engine operation.

Information gathered on U. S. Air Force bird ingestion experience indicates 73 engine strike incidents occurred in 1950 - 1955; 19 resulted in accidents, and about twice as many occurred in cruise (possibly in low level speed runs) than at takeoffs and landings. During 1956 - 1960, there were 87 bird ingestions with five accidents, and twice as many ingestions at takeoffs and landings as in cruise. Practically all instances of severe damage involved an early design engine whose compressor stators were susceptible to relatively easy dislodging from the housing which supported them. There were two instances reported of engine flame outs due to bird ingestion. One was a jet and the other a turboprop not used in civil aircraft.

U. S. Navy bird ingestion from July 1958 to September 1960 indicates 22 jet engine ingestions. Twice as many incidents occurred in low level speed runs as in takeoff or landing. Characteristically, only mild indications of engine malfunctioning was noted. Engines suffered damage requiring replacement in two-thirds of the instances reported.

#### Birds and Objects Ingested

Birds ingested in jet engines include sea gulls, starlings, black birds, pigeons, sandpipers, guinea hens, prairie chickens, osprey, a stork, a hawk, and a "rabbit". Other typical foreign objects which have been ingested and found responsible for engine damage either in service or on test are listed as follows with examples of the resulting damage:

3/4" by 8" Pipe	Caused nicking and bowing of stator and rotor blades.
Landing Gear Pin and Flag	Extensive blade damage.
Pressure Rake	Extensive Nicking.
Canvas	No damage, engine shutdown quickly.
Small nuts, bolts & dowel pins	Nicking, but capable of continued operation.
A 1/4 Inch Bolt	Damaged 14% of the compressor blades and vanes, but the compressor showed excellent efficiency.
Hoist Chains	Practically denuded the compressor.
Test stand inlet screen support rod	Deeply nicked the first two rotor stages and stators.

#### Hailstone Ingestion

During a recent seven year flight study of hailstorms over the United States Middle West where hail conditions predominate, 1 in 800 flights encountered one inch or larger hailstones, and 1 in 1600 flights encountered 2 inch or larger hailstones. Hailstones from a given storm tend to be approximately uniform in size.

It can be assumed that the most likely large size hail is the 2 inch stone. While 2 inch stones can badly damage a 300 m.p.h. aircraft, the more usual 3/4 inch hailstones would cause similar damage only at approximately twice this speed.

Turbine engines should be sufficiently resistant to impact damage from hail as to survive multiple hail strikes and continue producing appreciable output with one inch and two inch hailstones injected at cruising speeds, and rough air speeds respectively. This would assure the ability to continue controlled flight under all likely conditions. While the likelihood of

encountering hailstones larger than two inches is present, it is slight. Further, aircraft damage would likely be a critical factor of itself, and more prone than engine damage due to the larger exposure.

(Reference, NACA Technical Note 2734 and Am. Meteorological Society Bulletin on Hail Size and Concentration, Vol. 27, No. 2 of February 1946.)

### Bird Flocks Densities and Altitude

Bird ingestion in turbine engine has been mostly seagulls or smaller birds such as larks, starlings, and sandpipers.

Small birds such as starlings have been seen in flocks composed of as many as 10,000 birds. The flocks are highly variable in shape and density. Flocks may be a compact group up to 100 feet across, or a loose flock 600 feet long and 10 feet wide. While feeding on the ground, a flock would be compact and extend for 100 feet or more. Upon flying up suddenly, such a flock would form a thin horizontal sheet of compactly placed birds with possibly one per cubic foot. Minimum density might be 1/5th of this figure for loose flocks.

Gulls present a somewhat similar picture except there would be possibly from one to three per cubic yard of air space. The densest flock would be from startled gulls. The shape of flocks might be as much as 200 feet across and the loosest flock when traveling, spread out in long lines of several hundred yards.

Bird flocks are more apt to be encountered during takeoff when the birds are frightened while feeding, or are moving in groups to or from feeding or roosting areas on the ground. Bird encounters are most likely at altitudes below 1,000 ft. near airports, feeding or nesting places, and up to 5,000 or 6,000 ft. during migration periods.

## Ingestion Effects on Engines: (See Illustrations)

The effects of foreign matter ingestion in engines can be categorized as follows:

1. Direct impact damage on struts, compressor inlet guide vanes, or first stage compressor rotor blades.
2. Blockage of airflow by both displacement of air, and partial obstruction to flow of air. Compressor blade stall resulting from severe velocity and directional changes of the air entering and proceeding through the compressor. Compressor surge resulting from blade stall and compressor speed changes. All of these effects cause reduction of airflow through the compressor with a sudden gas temperature rise until or unless fuel flow is reduced to compensate.
3. Disruption of proper combustion and reduction of hot gas flow to the turbines and possibly even complete loss of combustion or flameout.
4. Engine rotor speed reduction due to increased mechanical loads and the reduced quantity of hot gas available from the combustion section to drive the turbines.
5. Deposition of certain adhering types of foreign matter (oil and dust or organic matter) on compressor rotor blades, vanes, housing inner passages of the engine. This causes continued disruption of air velocities and flows. Deposits such as bird tissues will tend to reduce in quantity in a short time from the action of air, mechanical forces, and heat.
5. Nicking, bowing, bending, and possibly rupture of vanes, and blades from the action of striking hard materials as they pass into and through the various stages of compressor and turbine blades and vanes and from actual interference between bent blades and adjacent vanes. Severe distortion may occur from the forces exerted on objects sufficiently large to be caught momentarily by both a rotor and stator blade. Pieces of blades or vanes released by rupturing cause further damage

down stream to other blades and vanes.

7. When minimal quantities of the softer and frangible foreign materials are ingested, engines usually digest them quickly by chopping up the material with often times only momentary reduction of output and airflow and sometimes with no engine damage. Ingested birds are typical of the softer materials, and ice characterizes frangible materials.

#### The Significance of Certain Engine Design Features:

##### 1. Impact Resistance -

Impact forces are imposed principally on the struts, the entry guide vanes and the first stage rotor blades. Any engine control sensing elements exposed to the impact of foreign objects in the airstream should be protected from impact. Inlet guide vanes should resist impact forces so as not to deflect appreciably as interference with first stage rotor blades can result. These vanes are normally hollow and somewhat thin. The elimination of inlet guide vanes from axial compressor engines would be preferable, since with foreign matter striking a rotating member, the direct force of impact is somewhat reduced. Purely centrifugal type compressors have no inlet guide vanes and therefore have an advantage in this respect as it is actually very difficult to ingest small objects into such engines unless the objects are injected at appreciable axial velocity. Good impact resistance of at least the first stage rotor blades should be assured, as the heaviest chopping action is borne by these blades. Stator vanes (and rotor blades) are obviously more resistant to being completely broken off when they are designed with support at both ends. Engines with indirect air paths to the first stage blading offer some protection from direct impact damage by foreign objects.

##### 2. Materials -

The blade and vane materials used should be adequately strong and sufficiently malleable to resist brittle failure from blows or

distortion. While aluminum is used for some axial compressor blades and vanes in some foreign engines, steel or titanium is used almost exclusively in United States designs. While aluminum offers advantages in reducing engine weight, and rotor inertia, the resistance to impact damage, distortion, and nicking is lessened. Proponents of aluminum blading have indicated that since virtually any foreign object damage to blades calls for early replacement of the part there is no advantage in using the heavier or more costly part. Titanium blading offers the attractive features of both aluminum and steel, but has the disadvantages of high cost and certain metallurgical limitations. However, blades of stiffer stronger material will minimize distortion and thus have less immediate adverse effect on power output. Since large distortions are possible at times, the material should not be so brittle as to rupture easily and free pieces to damage other blade rows.

### 3. Rotor to Stator Clearances -

Experience has indicated that generous axial clearances between the first and second stage rotor blades of axial compressors and their adjacent stator vanes minimize wedging action of objects between rotor and stator blades. Also, forward deflections occur with the added loads imposed on rotor blades by foreign objects. Clearances of one-third inch or more appear to be applicable. To a lesser degree, large axial clearances between later stages of axial compressors are needed. Centrifugal compressor turbine engines do not have stator stages to cause interference and in addition usually have the feature of centrifugal separation of heavy objects at the periphery of the rotor.

### 4. Air Passage Size -

In the smaller engines, shorter blading and narrower passages set up a scale effect which indicates greater sensitivity to a given quantity or size of foreign matter. Consequently, a given large engine may tolerate ingesting several sea gulls at one time but a much smaller engine might not tolerate one

gull. Similarly, a smaller engine may flame out with the quantity of ice or water slugs that a larger engine could tolerate. Rotor blade and stator distortion from encounters with foreign objects is somewhat proportional to the size and quantity of foreign material involved, hence the smaller engine parts will possibly be more critically distorted.

#### 5. Combustion Stability -

Combustion stability is affected by the surge and stall margin of the engine. Since normally these margins are decreased at extreme altitudes, this fact is important when evaluating possible disturbances to stable combustion. The provision of a reignition system capable of instantly reigniting engines, after flameouts, is an asset when operating conditions cause temporary flameouts due to air flow disturbances. Glow plugs or built-in glow spots in the combustor, automatic flame-out detectors to actuate reignition, or continuous ignition will all improve the adverse effects of flameouts. Combustion stability should be adequate to permit normal maneuvers, and flight in turbulence without flameout. Resistance to flameout and rapid recovery from ice, hail, or bird ingestion is important.

#### 6. Air Inlet Design -

While air inlet design is sometimes dictated by aircraft design, it is nevertheless important enough to consider when designing the engine. The arrangement of the engine inlet has significant bearing on the likelihood of airborne objects being injected or drawn into engines. Foremost among such objects are birds. Experience with turboprop engines has indicated that a narrow annular type inlet behind the propeller hub is somewhat protected against the entry of birds. The passage of propeller blades in front of an opening will also prevent some flying objects from entering, depending upon their spacing in the air. Inlets located back of the leading edge of a wing or aft of the wing on the fuselage also are somewhat protected.

The mere size effect of a narrow or small inlet will obviously preclude the entry of large birds, and should minimize the entry of all sizes of objects. Inertia separation of objects by turning the airstream may prove to be a useful trick to permit objects to bypass engines and be discharged or collected for later removal. Opinions have been advanced that air inlets in helicopters are somewhat protected by the downwash of air from the helicopter rotor blades. Flush type or side directed inlets for fixed-wing aircraft would prevent all entry of airborne foreign matter. A manually retractable air scoop could be retracted for takeoffs to preclude foreign object hazards. The airflow and pressure losses resulting with fixed indirect air intakes may preclude such devices from being adopted. Studies are being conducted by Federal Aviation Agency to evaluate turbine engine air intake design criteria with respect to the entry of airborne foreign objects.

#### How to Overcome Foreign Object Ingestion Effects

Since the problem has been presented, the procedures being followed for resolving the problem are now presented.

The FAA has always endeavored to permit a high degree of design freedom on the part of aircraft engine manufacturers as one means of discharging the responsibility of sponsoring progress in aviation. This infers that varying solutions may be accepted to cope with problems in general.

In studying ingestion hazards, evaluation of service experience must be utilized to the maximum degree. Engineering evaluation of this problem in past years made it evident that resistance to violent or disastrous engine failure was an important aspect of safety. To evaluate this aspect, high velocity ingestion of airborne objects and the normal ingestion of the usual miscellaneous objects were considered and evaluations and tests have therefore been conducted by the respective manufacturers of turbine engines for FAA certification review. It now appears that a further extension of this type of investigation is needed to evaluate bird and other airborne ingestion.

In general, the ingestion solutions separate into two basic areas, namely, (1) eliminate the probability of ingestion by appropriate air inlet design, or (2) minimize the probability of severe ingestion and minimize serious effects of the remaining ingestion probabilities.

Solution (1) may be achieved by the incorporation of (a) guarded air inlets or (b) side or backward facing inlets. Both types of inlets may have retractable features to favor use of devices in certain flight regimes only.

Certain installations, such as used in helicopters may accomplish trapping or separation of airborne foreign objects because of indirect air intakes or by virtue of the protective downwash of air from the main rotor.

The foregoing is chiefly the responsibility of the powerplant installation designer, but the engine designer can assist in catering to the need for providing an engine which can function adequately with certain air inlet configurations in mind.

Solution (2) may be attained by the partial separation of airborne objects, or by engine features which overcome the most adverse effects of ingestion. As an example, a narrow annulus inlet can be provided in lieu of a cylindrical inlet opening. This inlet presents a narrow target for any airborne object.

Partial separation of airborne objects can be achieved by inertia separation, as in a curved duct, or by turning the inlet air around a central fairing. A combination of these features with solution (1) would be the use of a guarded or retractable inlet during only the more critical flight regimes of takeoff and climb.

Engines may be designed to be more tolerant of or resist severe damage from severe ingestions in the following ways:

- (a) Better chopping characteristics of the first stages,
- (b) the provision of compressors with relatively less-critical stall characteristics,

- (c) Stronger stator and rotor blade construction,
- (d) Quick acting large capacity anti-stall bleed valves and fuel regulation.
- (e) Re-ignition devices to detect flameouts and quickly restore combustion when interrupted.

#### FAA Practices in Evaluating Engines

The foregoing suggests a number of the many considerations possible. In order to evaluate the design of aircraft engines, presented for type certification and future civil use, specific tests and engineering evaluations are specified by FAA to be conducted by the engine manufacturer.

The specific requirement contained in Civil Air Regulations, Part 13, Aircraft Engine Airworthiness which covers evaluation of ingestion hazards, follows:

"Civil Aeronautics Regulations CAR, 13.200(a). The engine shall not incorporate design features or details which experience has shown to be hazardous or unreliable. The suitability of all questionable design details or parts shall be established by tests."

The current interpretation of this requirement is as follows:

The engine should be designed to minimize the probability of catastrophic engine failures occurring from foreign object ingestion. The likelihood of flameouts, lengthy power recovery time, and severe sustained power losses resulting from ingestion of likely foreign objects should be evaluated for typical installations to establish whether the condition is hazardous. Consideration should be given to the probability of multiple bird strikes in aircraft.

## Definitions

- (a) Catastrophic failures are those which cause explosions, uncontrollable fires, engines tearing loose due to damage or otherwise cause direct hazards to the aircraft.
- (b) While flameouts are always hazardous, as are any lengthy power interruptions and large sustained power losses, these occurrences should not cause failure of other engines or loss of the aircraft and are therefore considered a lesser hazard than catastrophic failures.
- (c) Unless the engine will be restricted to installations where shielded inlets, size and shape of the inlet or other considerations render entry of certain objects unlikely, foreign objects to be considered include at least the following:

Cleaning cloth - one of typical size

Gravel - mixed, including  $\frac{1}{4}$  inch stones

Sand - all grades

Hand tools - pocket size

Bolts and screws - aircraft sizes  
(e.g.  $\frac{1}{4}$  in. X 1 in.)

Broken or loose blades - compressor and turbine (pieces and whole blades)

Water - maximum rainfall  $\frac{\text{lb. water}}{\text{lb. air}} = .0014$

Ice - typical deposits such as from inlet duct and lip.

Hail - Repeated strikes of 1 in. and 2 in. balls of approximately .7 density.

Birds - Sizes from 4 ounces up to 4 lbs.

A basic consideration used in FAA evaluations is that the engine casings should contain any likely damage

to the extent that no projectiles are created from engine parts which can cause severe secondary damage in the areas surrounding the installed engine.

While the actual effects of objects left loose in the engine inlet or the release of broken internal parts cannot always be accounted for in advance, consideration is given these possibilities in FAA evaluations. Often the extensive development testing of engines includes several unplanned and unfortunate foreign object ingestions which are useful for substantiation purposes.

Water in liquid slug form or as slush normally should not enter engine inlets in significant quantities as the inlet design and location should prevent this. Accordingly, tests of water slugs and slush need not be included unless such action is warranted from aircraft design standpoints.

Hail tests have been somewhat controversial but the following is considered to be a feasible approach:

Hail should be ingested into the engine with the engine operating at cruising outputs at hail velocities corresponding to the following values:

1. One inch hailstones at applicable maximum cruising flight speeds.
2. Two inch hailstones at applicable rough-air flight speeds.

The evaluation for hail ingestion should include the effects of single hailstones and multiple hailstones through typical inlets to determine critical conditions and quantities.

In seeking to define the standards for bird ingestion tests, actual experience, and certain recent tests, were reviewed and it was established that up to 3 or 4 gull size birds have been ingested in the large jet engines, and similar numbers or slightly greater numbers of starling size birds have been ingested in both the Allison turboprop engine and in several of the large jet engines.

Thus the following rate and manner of test ingestion is considered applicable:

Birds should be introduced into an engine operating statically at maximum output. The bird velocities used should include zero velocity at the inlet, and takeoff and maximum cruising velocities. The following rates of ingestion are suggested.

1. Small birds (4 oz.) a minimum of one, and one per 50 sq. in. of aircraft inlet entrance area up to 16.
2. Large birds (4 lbs.) a minimum of one, and a maximum of one per 400 sq. in. of aircraft inlet entrance area.

The evaluation for bird ingestions should include single ingestions, multiple ingestions and sequenced volleys to at least the maximum rates indicated to simulate strikes with bird flocks. When feasible, increased quantities should be run to determine critical conditions for each type engine.

#### CONCLUSION

It is hoped that this paper will stimulate further efforts to fully overcome the problems of foreign object ingestion in turbine engines. To this end, the FAA is sponsoring research to evaluate more fully certain aspects of foreign object ingestion and to develop more comprehensive and effective certification requirements where feasible. The FAA emphasis at present is on bird ingestion. While it would be obviously best to adapt solution (1) as discussed above, the direct flow engine air inlets of large jet engines, which contribute an important part to engine efficiency, cannot be easily protected against bird entry.

As another part of the FAA efforts, it is planned to evaluate optimized geometry of air inlets and guarding devices which will deter the entry of airborne foreign objects.

It is anticipated that the usual and continued

ingenuity of engineers of the engine and aircraft manufacturing companies will be further employed to develop more satisfactory air inlets and more damage resistant engines, as such damage presents hazards and is uneconomical.

My final observation is that it appears unlikely that birds and hail can ever be controlled to always steer clear of aircraft in flight or conversely it appears unlikely that aircraft can always be controlled to steer clear of birds and hail.

REFERENCES:

1. NACA TN 2734. "Summary of Available Hail Literature and the Effect of Hail on Aircraft in Flight"
2. American Meteorological Society Bulletin  
Vol. 27, No. 2 of February 1946
3. FAA BRD-A-90 Wildlife Leaflet 429 January 1961
4. CAR Part 13 Aircraft Engine Airworthiness  
October 1959
5. A Study of USAF Aircraft Accidents that Involved Collisions Between Jet Aircraft and Birds  
September 1955
6. U.S. Navy Study of Bird Strikes from July 1 to September 30, 1960
7. Bird Ingestion by JT3 and JT4 Engines -  
Pratt & Whitney Aircraft  
Report EM 61-80-30 of February 28, 1961

## ICING TRIALS OF THE T-38 AND T-39 AIRCRAFT

by

E. T. Binckley

Aeronautical Systems Division  
Wright Patterson Air Force Base, Ohio

For a number of years we have been working with the larger jet engines to determine their problems when operating in an icing environment. This year we have had our first experience with the smaller engines in jet aircraft, although we had previously touched on them in the helicopter field.

Our first work was done on the Northrop T-38 (Talon) and the North American T-39 (Sabreliner).

### The T-38

The T-38 is a supersonic trainer aircraft characterized by an area-ruled fuselage, short wings and a reverse curve profile. Our test vehicle was powered by two YJ-85-5 engines made by General Electric. The engine had an anti-icing system on the inlet guide vanes, struts and bullet nose, but no protection on the inlet duct lips.

Prior to the actual flying, ice ingestion tests were conducted under laboratory conditions to determine the susceptibility of the engine to ice damage. Layer ice was used to simulate the type of ice that would come off the duct lip. First tests were made with 1/8 inch thick sheet ice and no problems were encountered. The next sheet of ice was 1/4 inch thick. Ingestion of this ice caused damage to the inlet guide vanes and the first stage compressor blades. The engine did not seize or vibrate excessively, but it appeared that ingestion of 1/4 inch build-ups from the duct lip could cause flight problems. This proved to be the case in flight.

The flight trials were conducted at Edwards Air Force Base in California to take advantage of large landing areas in case of an emergency. Inflight icing conditions were created by flying the T-38 behind a KC-135 tanker spraying water from a special nozzle attached to the refueling boom. The first two runs were conducted at 18,000 feet altitude, 240 knots IAS and an ambient temperature of -15°C. The spray conditions gave about 1 gram/cubic meter liquid water content and a median volume droplet with a diameter of 60 microns. The aircraft remained in the spray on the first run until slightly less than 1/8 inch ice built up on the engine duct lip; for the second run, slightly more than 1/8 inch of ice built up.

The aircraft descended to 10,000 feet carrying the ice and at ambient temperatures of  $-4^{\circ}\text{C}$  the ice broke from the duct lips and was apparently ingested. No engine roughness or instrument fluctuations were noticed.

The third run was made with a liquid water content of 2.5 grams per cubic meter and about the same effective droplet size as stated above. The aircraft remained in the spray until  $1/4$  inch ice collected on the duct lip of the left engine. This was accomplished by immersing only the left half of the aircraft in the icing spray.

Upon descent to 8000 feet where the ambient temperature was  $-1^{\circ}\text{C}$ , the ice came off. A noise from the engine section was audible during the break off period. No engine instrument fluctuation and no vibration or engine roughness were noted. An immediate landing was made. Inspection revealed 3 bent first stage compressor blades and 3 bent inlet guide vanes on the left engine. This was the engine subjected to the icing environment. No damage occurred on the right engine which had a build up of less than  $1/4$  inch.

This substantiated the laboratory tests since the damage on the laboratory engine and the aircraft engine was identical. In view of the unprotected duct lip, no further icing tests were conducted.

The T-38 was also subjected to an ice crystal environment. These tests were developed as a result of earlier problems reported by operational organizations.

During the late spring and early summer months of 1959 a serious detriment to the mission of Air Defense Command (ADC) manifested itself in F-102 aircraft whose mission requirements included flights at high altitude in or near thunderstorms. The aircraft were experiencing a rash of compressor stalls and subsequent flameouts, as noted from incident reports received from all parts of the country and overseas. Several F-102A's were lost in thunderstorms during 1959.

In July 1959, ADC headquarters requested that ARDC initiated a program to investigate the cause of unexplained flameouts of F-102A aircraft at high altitude in or around thunderstorms, and to recommend action which would prevent such flameouts.

Testing commenced in August 1959. During the remainder of 1959 and early in 1960, an all encompassing test program was conducted in both natural and simulated thunderstorm conditions. Statistical data from ADC were carefully analyzed. As a result of this program,

a valid solution to help prevent flameouts, and pilot technique to reduce the compressor stall problem, were developed.

Test missions flown during the program were as follows:

- a. Flights in clear air in which attempts to induce compressor stalls were made by rapid throttle movements.
- b. Flights in clear turbulent air at various altitudes and airspeeds. Turbulence was created by flying in the wing-tip vortices of another aircraft.
- c. Flights in the ice-crystal spray created by a KC-135 tanker aircraft.

It was determined that the flameouts were primarily caused by ice crystals. Other aircraft were checked to determine why incidents were reported only on the F-102. Figure 1 shows that F-102 encountered compressor stalls at a greater distance behind the tanker than any similar aircraft. The concentration of ice crystals diminishes as distance behind the tanker increases. To investigate ice crystal susceptibility, the T-38 was subjected to a similar program.

In this test, a KC-135 tanker sprayed water at an altitude of 40,000 feet (ambient temperature of  $-63^{\circ}\text{C}$ ) and Mach number 0.88. The test aircraft was flown progressively closer to the tanker in the ice crystal spray, from 900 to within 175 feet behind the tanker. The engine did not stall or surge, and no adverse engine characteristics were noted. Since the ice crystal concentrations were greater than would be expected in natural conditions, no problems are anticipated with this aircraft.

#### The T-39

The T-39 Sabreliner is a lightweight, twin turbo-jet aircraft capable of fulfilling a number of transport and training missions. It was powered by two YJ-60-P1 engines installed in pods on either side of the aft portion of the fuselage. The engines had an anti-icing system which protected the engine cowl duct lip, the inlet guide vanes and the bullet nose. Although the wing and tail surfaces were not protected, the inboard portions of the wing were heated by an electric mat to preclude ice forming here and shedding into the engine area.

The T-39 was subjected to both natural icing conditions and an icing environment created with a water-spraying tanker.

The natural ice encounter occurred at 10,000 foot altitude with an indicated air temperature of 0°C. The aircraft flew in the light icing condition at 170 KIAS until about 1 1/2 inches collected on the engine cowl duct lip. The engine anti-ice system in the AUTO position did not prevent the ice from collecting. The pilots commented that they could feel the ice ingesting during flight. There was no noticeable effect on engine performance before or after the ingestions. Post flight inspection revealed damage to the first stage rotor blades. Because of the space between the first stage rotor and the inlet guide vanes, there did not appear to be any "metal contact" between these two.

The T-39 was flown behind the water spray tanker at 21,000 feet at 250 KIAS and an indicated temperature of -7°C. The icing conditions offered 1 gram per cubic meter of liquid water with about a 60 micron drop diameter for the median volume droplet. On this flight the anti-ice system was not used on AUTO but placed in the ON position. There was no ice formation on the engine cowl duct lips. The windshield accumulated considerable ice around the edges but the center portion remained sufficiently clear to provide adequate forward visibility. The wing leading edge built up about 1/2 inch of ice with ice also forming in the electric mat area. During the descent, ice shedding occurred producing numerous "thumps" in the engine area. Observation of the engines after flight revealed similar damage to that encountered in the natural ice.

The position of the aft mounted engines makes them susceptible to ice shedding from all unprotected areas forward and in line with the engines. It is not known precisely which part of the aircraft is shedding into the engines. The following unprotected positions are possible suspects: The nose area, the windshield area, the pitot mast, the wing area just inboard and outboard of the electric mat, and possibly the mat area itself. The trajectories of the shed ice vary at different airspeeds, angles of attack and ice consistencies so it is difficult to determine if the damage is being caused by one of the suspect areas or by several of them. At the time of this writing the problem is still under investigation.

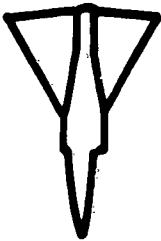
KC-135

J-57-P59W



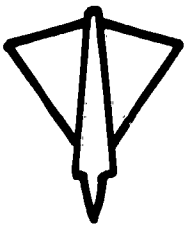
T-38

YJ-85-5

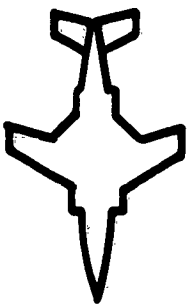


F-106

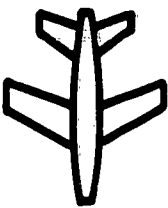
J-75-P9



F-102 J-57-P23



F-101 J-57-P13



F-100 J-57-P21

0 100 200 300 400 500 600 700 800

DISTANCE BEHIND TANKER (feet)

40,000 FT. ALTITUDE

MACH .85-.88

FIG.1 ICE CRYSTAL ENVIRONMENT CAUSING COMPRESSOR STALLS

**ICING TESTS CONDUCTED AT NATTS**  
**May 1960 through May 1961**

by  
A. Kush  
and  
E. Stawski  
Aeronautical Turbine Laboratory  
U. S. Naval Air Turbine Test Station  
Trenton, New Jersey

In the past year, icing tests have been conducted at the Naval Air Turbine Test Station (NATTS) on three turbojet engines currently used in all weather Naval aircraft. These were the J71-2E, the J79-2, and the J57-20. The icing tests consisted of simulated flight conditions through supercooled clouds. First, the effects of icing on the specific engines and their components will be discussed. Then the effects of icing on turbojet engines in general will be covered.

**J71-2E**

In icing tests conducted at Mount Washington, it was found that the anti-icing capabilities of J71 engines varied. This was due primarily to variations in leakage existing at the anti-ice air cavity or supply plenum for the inlet guide vanes.

Figure 1 is a cross section of the anti-icing cavity showing the seal configuration as proposed by the engine manufacturer to minimize the leakages. This is the configuration used in the NATTS icing tests. The cavity is located between the forward frame and the compressor case. It supplies air to the inlet guide vanes. Most of the leakage occurred in the areas between the inlet guide vane outer band and the forward frame and the band and the compressor case. The "O" ring seals were used to minimize leakages past these points. Some leakage still exists between the band and the guide vanes. No sealing was attempted there because the leakage is small and it would be extremely difficult to provide a seal there.

Figure 2 is a sketch of the J71 anti-icing system. The anti-icing airflow is controlled by an on-off butterfly valve. The airflow is then split into four lines and fed to the cavity. The cavity supplies the inlet guide vanes and two inlet pressure sensing probes with anti-icing air. In order to simulate an engine with excessive leakages, a method had to be found to reduce cavity pressure with the seals in place. One was to bleed air overboard downstream of the anti-ice valve. This provided only limited reduction in cavity pressure and, in order to obtain the desired pressure reduction, the anti-ice valve had to be modified to act as a metering valve. As an

example of anti-icing temperatures to be expected, if  $T_{T,3} = 510^{\circ}\text{F}$ ,  $T_{\text{cavity}}$  would be  $400^{\circ}\text{F}$  and  $T_{\text{IGV}} = 150^{\circ}\text{F}$ . With reduced pressure in the cavity,  $T_{\text{IGV}}$  might drop to  $110^{\circ}\text{F}$ .

Following are the results of icing tests conducted at an inlet temperature of  $+23^{\circ}\text{F}$ . The liquid water content was  $2 \text{ gm/M}^3$  (this is roughly 0.2 percent) with a mean droplet diameter of approximately  $25\mu$ . Standard engine configuration with cavity seals was used. All these runs were conducted with the anti-ice valve turned on manually before the water flow was initiated.

a. The engine operated satisfactorily under icing conditions at engine speeds of 100, 96, 91, and 86 percent with very little ice buildup on the IGV's.

b. At 81 percent engine speed, icing became severe not only on the inlet guide vanes but also on the first and second stage stators and rotors.

c. Only one ten minute icing run out of three attempted could be completed at 81 percent engine speed because of the development of severe engine vibrations. One of the major factors apparently contributing to the heavy ice buildup at lower engine speeds is the closure of the inlet guide vanes at about 83 percent engine speed.

Results of Sea Level Static Icing Tests on the J71-A-2E Engine are as follows:

Inlet Temperature =  $+5^{\circ}\text{F}$ ; Mean Droplet Diameter =  $15\mu$ ;

Standard Engine Configuration.

Anti-ice system in manual-on before water flow initiated.

a. At 86 percent engine speed, very heavy icing occurred at liquid water contents down to  $2 \text{ gm/M}^3$ .

b. At 91 percent engine speed, light icing occurred at liquid water contents up to  $3.5 \text{ gm/M}^3$ . This is probably the lowest engine speed that can be utilized at cold temperatures maintaining a relatively ice-free inlet.

c. At 95 percent engine speed, light icing occurred at liquid water contents up to  $4.5 \text{ gm/M}^3$ .

The next Figure (number 3) shows two photographs of the inlet of the J71 engine under similar engine operation but at different icing conditions. The photograph on the left was taken after an icing run at  $+23^{\circ}\text{F}$  and liquid water content of  $4.6 \text{ gm/M}^3$ . The photograph on the right was taken after an icing run at an inlet temperature

of 4°F and liquid water content of 1.1 gm/M<sup>3</sup>. Both runs were made with engine speeds around 5600 rpm. At the lower inlet temperature, the ice buildup on the IGV's is considerable. At the warmer temperatures, the ice buildup on the IGV's is slight. The ice buildup on the duct, however, is greater at the warmer temperature but the ice is mushy, whereas the ice at +4°F is the hard rime type.

At warmer temperatures, +23°F, the reduced pressure in the cavity had little effect on icing limitations. At colder temperatures, +5°F, there was a marked effect of cavity pressure on anti-icing capability as can be seen in Figure 4. The photo on the left is the inlet following an icing run with liquid weight content of 3.6 gm/M<sup>3</sup> and a tight cavity. The photo at the right shows the inlet after an icing run with liquid weight content only 1.2 gm/M<sup>3</sup> but the cavity pressure reduced to simulate minimum pressures previously encountered on J71 engines. It can be seen that even though three times as much water is being used, the ice accumulation on the inlet guide vanes is much less because of the cavity seals.

The fuel control uses the inlet pressure in programming fuel flow. If the probe becomes blocked, engine operation might be severely affected. During the engine icing tests, two inlet pressure sensing probe designs were being evaluated. Figure 5 is a cutaway view of both probes. The pressure sensing holes are here. The basic difference in design is that the pressure sensing lines were located deeper inside the probe body, resulting in better heating of these lines. At warmer temperatures, +23°F, both probes performed identically, but at cold temperatures, +5°F, the old probe blocked repeatedly during an icing run.

In summarizing the component evaluation, it was found that both the modifications proposed by the engine manufacturer, the cavity seals and the redesigned inlet pressure sensing probe, improved the anti-icing capability of the J71 engine. Both changes have been adopted by the Navy.

#### J79-2

When icing tests were first initiated on the J79-2, three difficulties were encountered almost immediately. It was found that:

- a. Ice formation on the airframe manufacturer supplied bullet-nose was excessive. Damage to the compressor blades occurred due to ice ingestion probably from the bullet nose.
- b. Certain inlet struts were iced up excessively.
- c. Engine flameout occurred during some icing runs at high liquid water contents.

Figure 6 is a photograph of the J79 inlet following an icing run at sea level static conditions with an inlet temperature of  $-4^{\circ}\text{F}$  and liquid water content of  $1 \text{ gm/M}^3$ . It can be seen that although the inlet guide vanes are free of ice, the bulletnose is severely iced.

Figure 7 is a photograph of the airframe supplied blunt bulletnose on the left and an engine manufacturer supplied streamlined bulletnose on the right. The blunt bulletnose has no provision for anti-icing air while the streamlined one does. This latter component was used for the remainder of the tests.

Figure 8 shows the J79 inlet and the streamlined bulletnose after an icing run. No heat was supplied to the bulletnose in this run so that the contribution of the shape in preventing ice formation could be determined. There is less ice buildup here than occurred with the blunt bulletnose. It was also found that the addition of heat would eliminate the bulletnose icing problem. The additional anti-icing airflow required for the bulletnose was found to be negligible.

Figure 9. Another difficulty that was encountered was icing of certain inlet struts. Figure 9 is a photograph of the inlet showing this strut icing. Some of the ice from the struts has dropped off between the time the icing run was terminated and the photograph was taken. In order to understand why only some of the struts are iced, a sketch of the J79 anti-icing system will have to be referred to.

Figure 10 is a sketch of the standard J79-2 anti-icing system which was used in these icing tests. Hot compressor discharge air is piped through four of the inlet struts into the hub of the front frame. From the hub, the hot air is fed to the remaining four struts and to the inlet guide vanes and, when modified, to the bulletnose. The air is then discharged through holes near the outer ends of the struts and trailing edge of the inlet guide vanes. These discharge struts are therefore much colder than the inlet struts because they are being heated by a smaller quantity of cooler air than the inlet struts. In order to improve the anti-icing capability of the struts, their air discharge holes were enlarged resulting in a considerable anti-ice airflow increase. The engine performance was not affected by this change.

Figure 11 is two photographs showing the inlet after an icing run before and after the strut modification was made. Both runs were under similar flight conditions. The absence of ice on the struts is evident after the fix was made.

During altitude tests, engine flameouts were encountered during icing runs. Figure 12 is a plot of corrected engine speed versus inlet temperature showing flameout limits for three conditions: 35,000 feet altitude with 0.4 percent (this is equivalent to about  $1 \text{ gm/M}^3$  at 35,000 feet) water to air ratio; 35,000 feet with 0.3 percent water to air ratio, and 15,000 feet with 0.4 percent water. These envelopes show that flameout is induced by increased engine speed, altitude, and liquid water content and reduced inlet temperature. It should be pointed out that this envelope was obtained before the strut modification was made. After the modification, the flameout region was deminished but not eliminated.

#### J57-20

In initial icing tests, the J57-20 was also found to have difficulties with the bulletnose icing. Figure 13 is a photograph of the inlet of the J57 showing typical ice buildup on the bulletnose and also on the only inlet strut. This bulletnose encloses a constant speed drive and alternator. The heat given off by the constant speed drive was to heat the bulletnose and prevent ice formation. The inlet strut was not heated. It is evident that supplementary heating should be provided for these components. Because it was felt that compressor damage and even engine failure might occur because of bulletnose icing, the maximum liquid water content this engine was tested under was only  $2 \text{ gm/M}^3$ . These icing tests were then terminated before the engine was subjected to any severe icing conditions.

#### Effects of Icing on Turbojet Engines in General

Figure 14 is a plot of various engine parameters versus liquid water content. All the parameters shown here, engine pressure ratio, compressor pressure ratio, and engine airflow all decrease with increases in liquid water content.

Figure 15 is a plot of engine flow, percent thrust loss, and percent specific fuel consumption gain versus liquid water content. The effect on thrust and specific fuel consumption are especially important because the military specification for turbojet engines (MIL-E-5007B) stipulates that the decrease in net thrust and increase in specific fuel consumption shall not exceed five percent at certain icing and operating conditions. This limitation has been sketched on the plot. It can be seen that the thrust loss on this engine exceeded the specification limit. The specific fuel consumption did not. There were data on other engines, however, where the specific fuel consumption did exceed the specification limit. The important thing on this plot is that both thrust and specific fuel consumption change by many times the five percent figure with the engine undamaged and still operating.

In addition it appears that:

a. The thrust of all turbojet engines tested decreases even though ice formation at the inlet may be negligible. Of course, blockage due to excessive icing results in very severe thrust losses.

b. As engine speed decreases, the tendency for icing at the engine inlet increases provided the inlet temperature does not increase. As engine speed decreases, the amount of anti-icing air and/or its temperature decreases.

c. Ice buildup on rotor blades is typical and probably is responsible for excessive and erratic engine vibrations.

An attempt is being made to correlate altitude with sea level icing data so as to simplify future testing. Scheduled for icing tests in the near future at NATTS are the J79-8 and J52-6 engines.

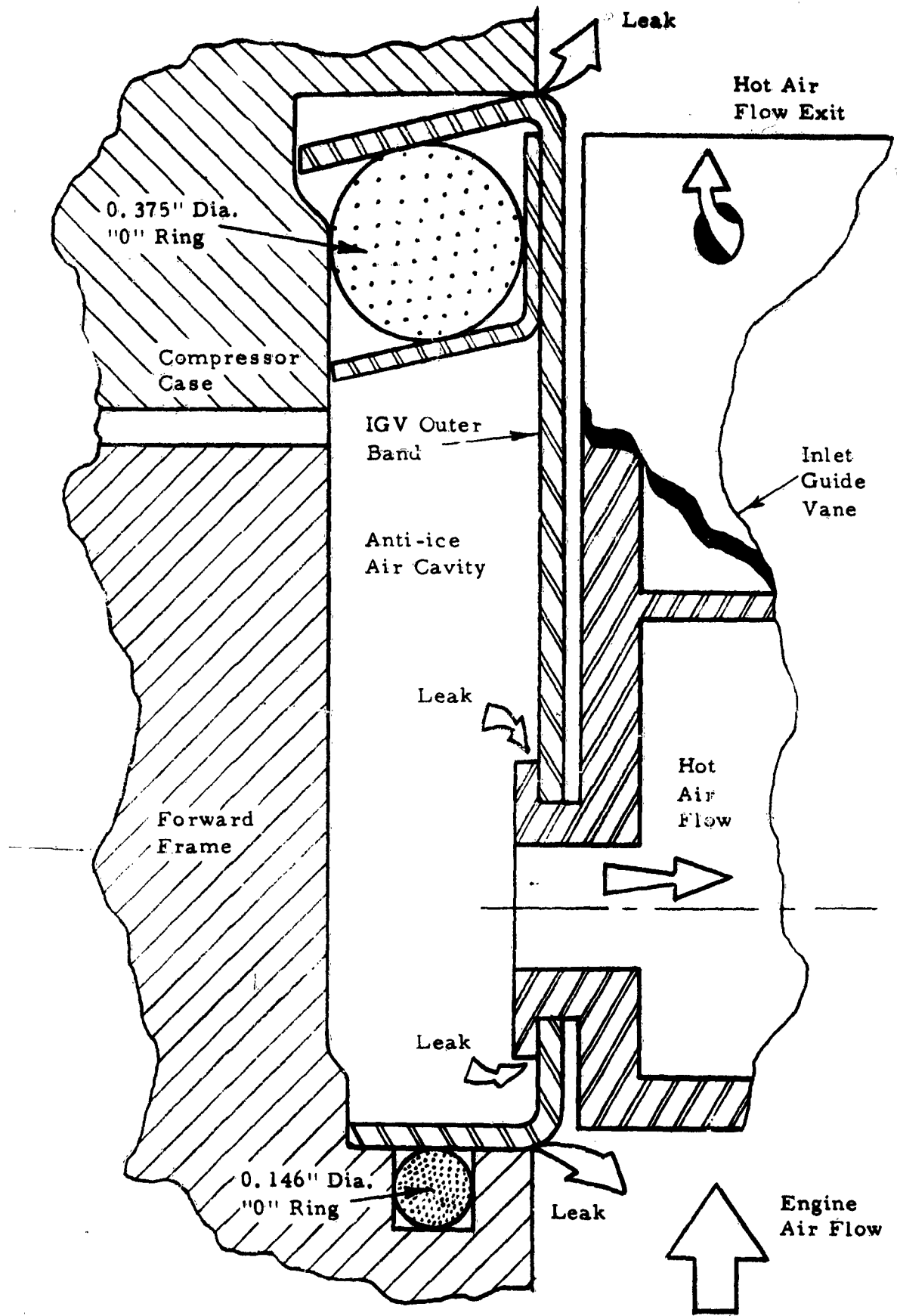
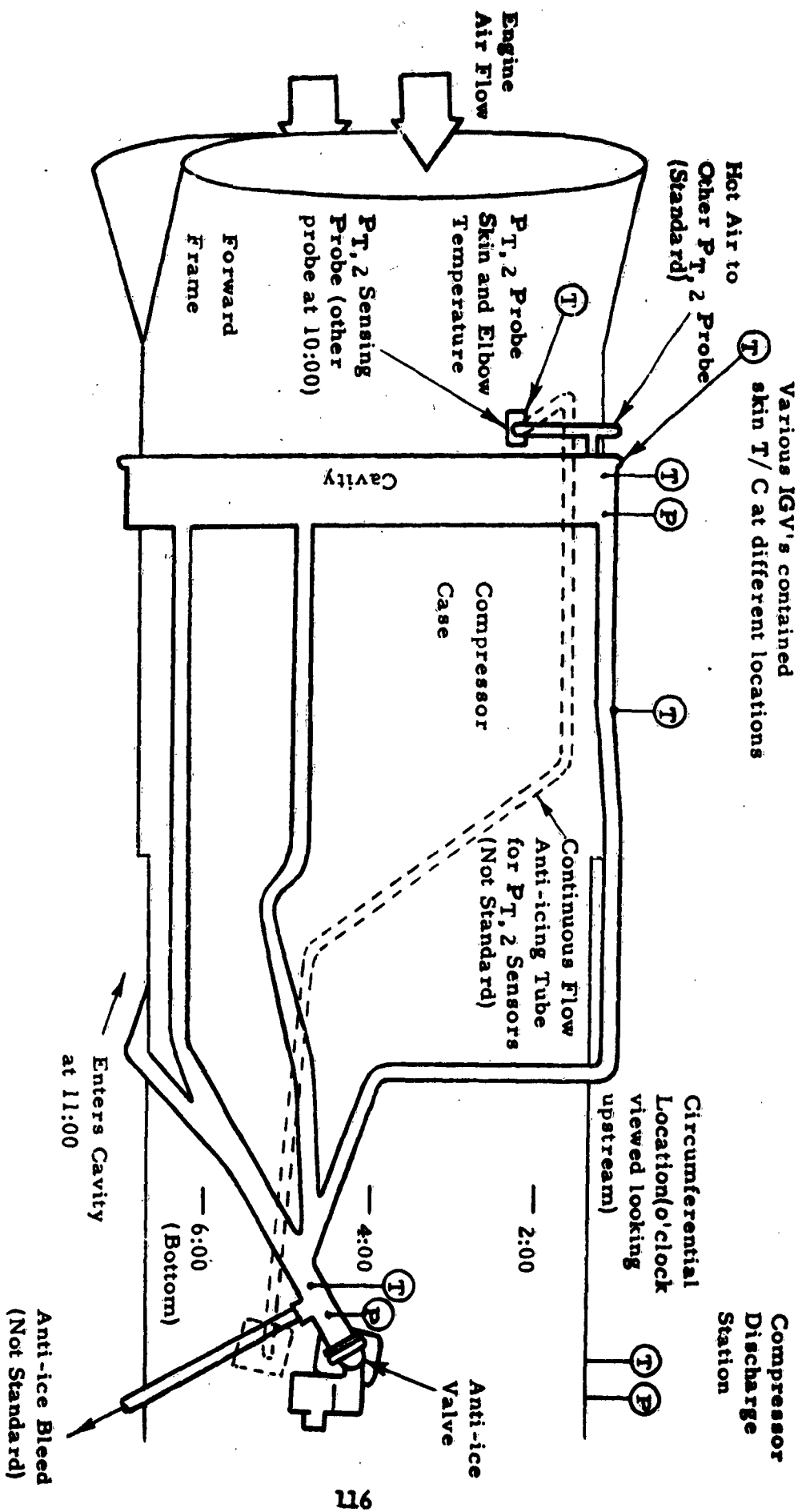


FIGURE 1 - CROSS SECTION OF J71-A-2E ANTI-ICING AIR CAVITY



116

FIGURE 2 - SKETCH OF J71-A-2E ANTI-ICING SYSTEM



Run 37:  $T_{T, 2} = 23^{\circ}\text{F}$ ;  $\text{LWC} = 4.61 \text{ gm/M}^3$   
Sea Level Static;  $N = 5591 \text{ RPM}$



Run 112:  $T_{T, 2} = 4^{\circ}\text{F}$ ;  $\text{LWC} = 1.06 \text{ gm/M}^3$   
Sea Level Static;  $N = 5600 \text{ RPM}$

FIGURE 3 - COMPARISON PHOTOGRAPHS OF J71-A-2E INLET SHOWING  
EFFECT OF INLET TEMPERATURE ON ICE FORMATION

118  
Cavity  
N = 5605 RPM  
N = 5605 RPM



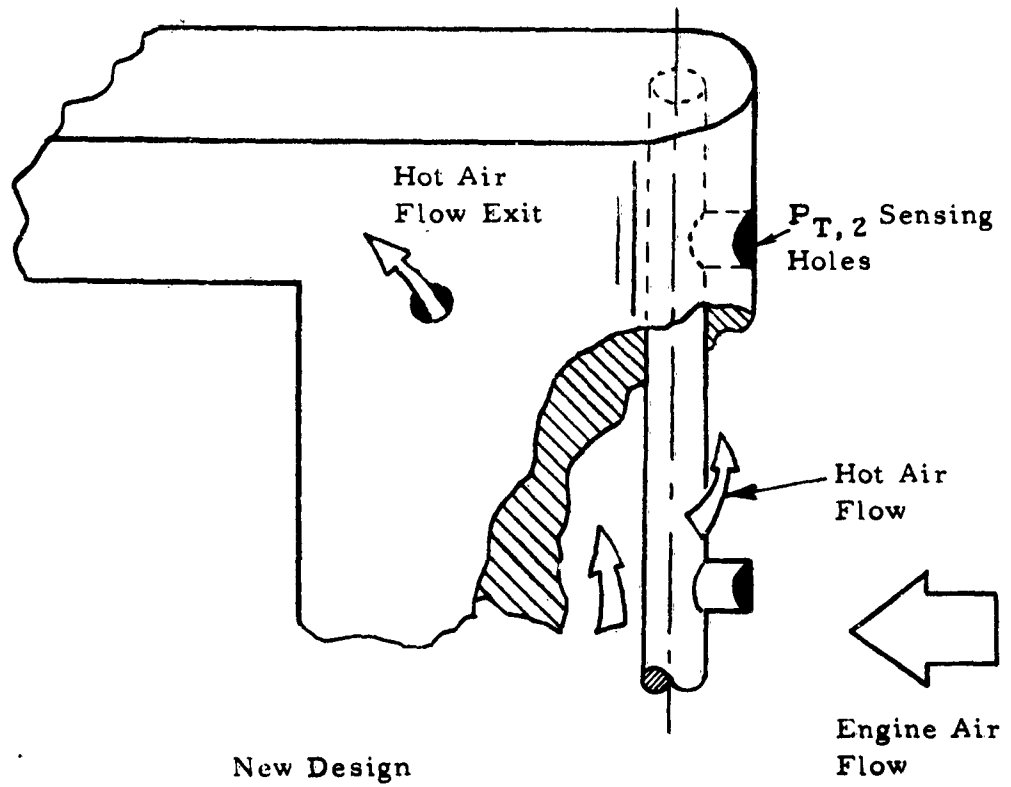
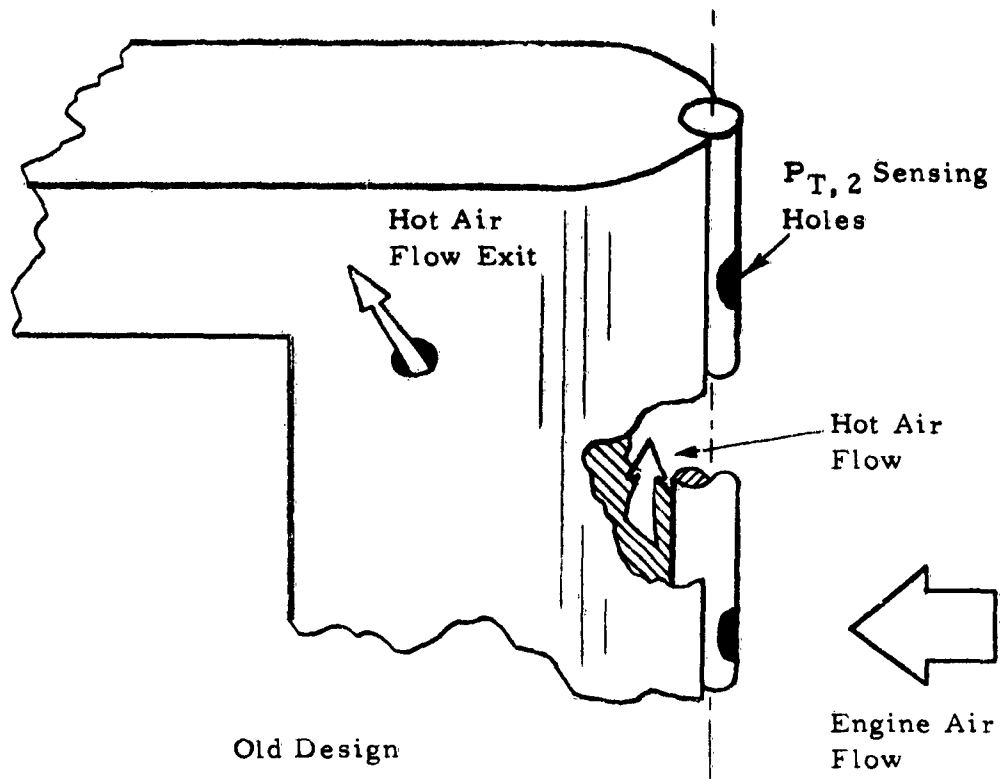


FIGURE 5 - TWO DESIGNS OF ALLISON INLET PRESSURE SENSING PROBES

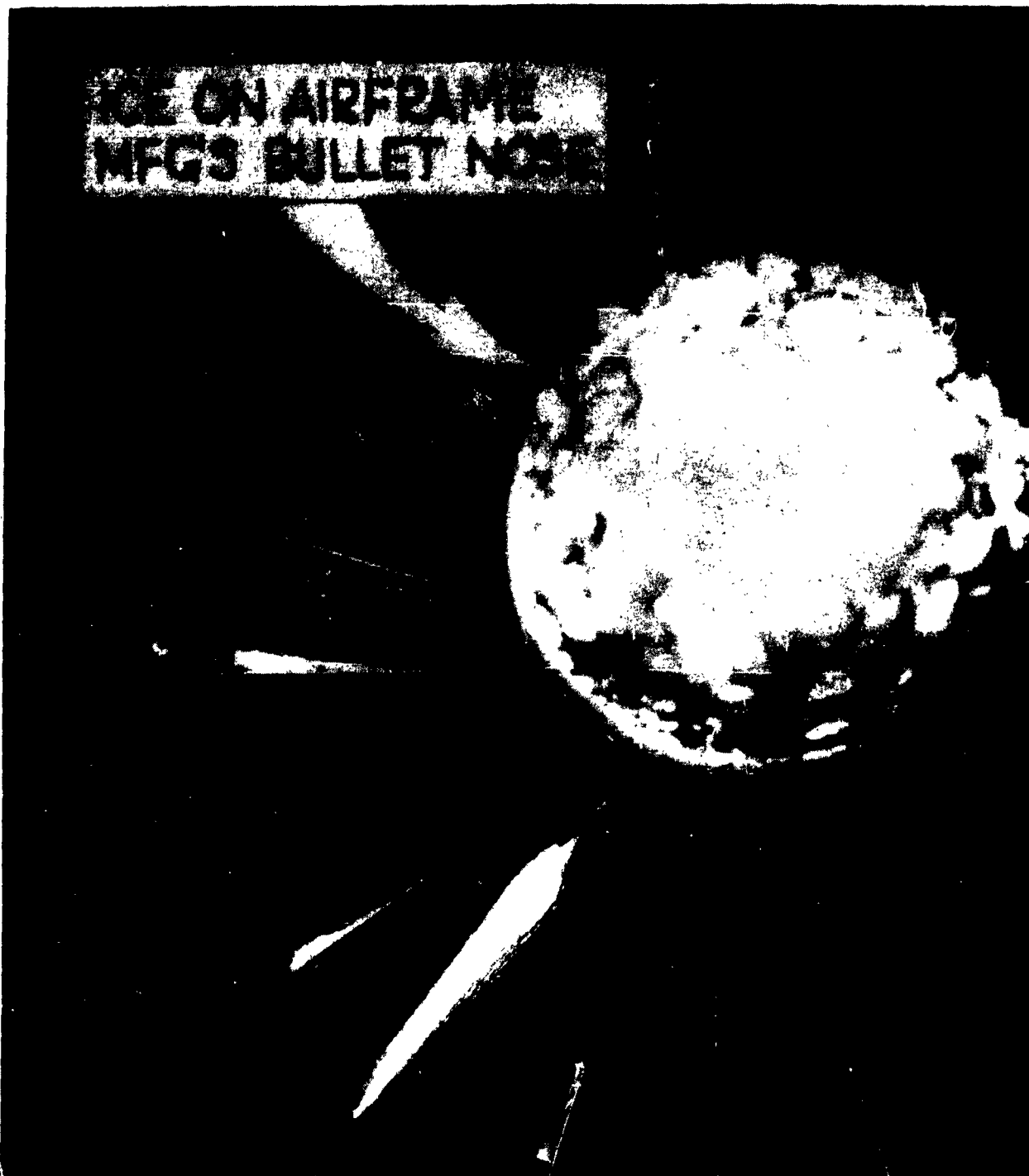


FIG.6-J79-GE-2 ENGINE INLET  
FOLLOWING AN ICING RUN AT SEA  
LEVEL STATIC CONDITIONS  
INLET TEMP.  $-4^{\circ}\text{F}$  LWC  $1\text{gm}/\text{M}^3$



SUPPLIED BY  
AIRFRAME MFG.

SUPPLIED BY  
ENGINE MFG.

**FIG.7 - COMPARISON OF TWO ENGINE  
BULLET NOSES USED FOR  
ICING TESTS**

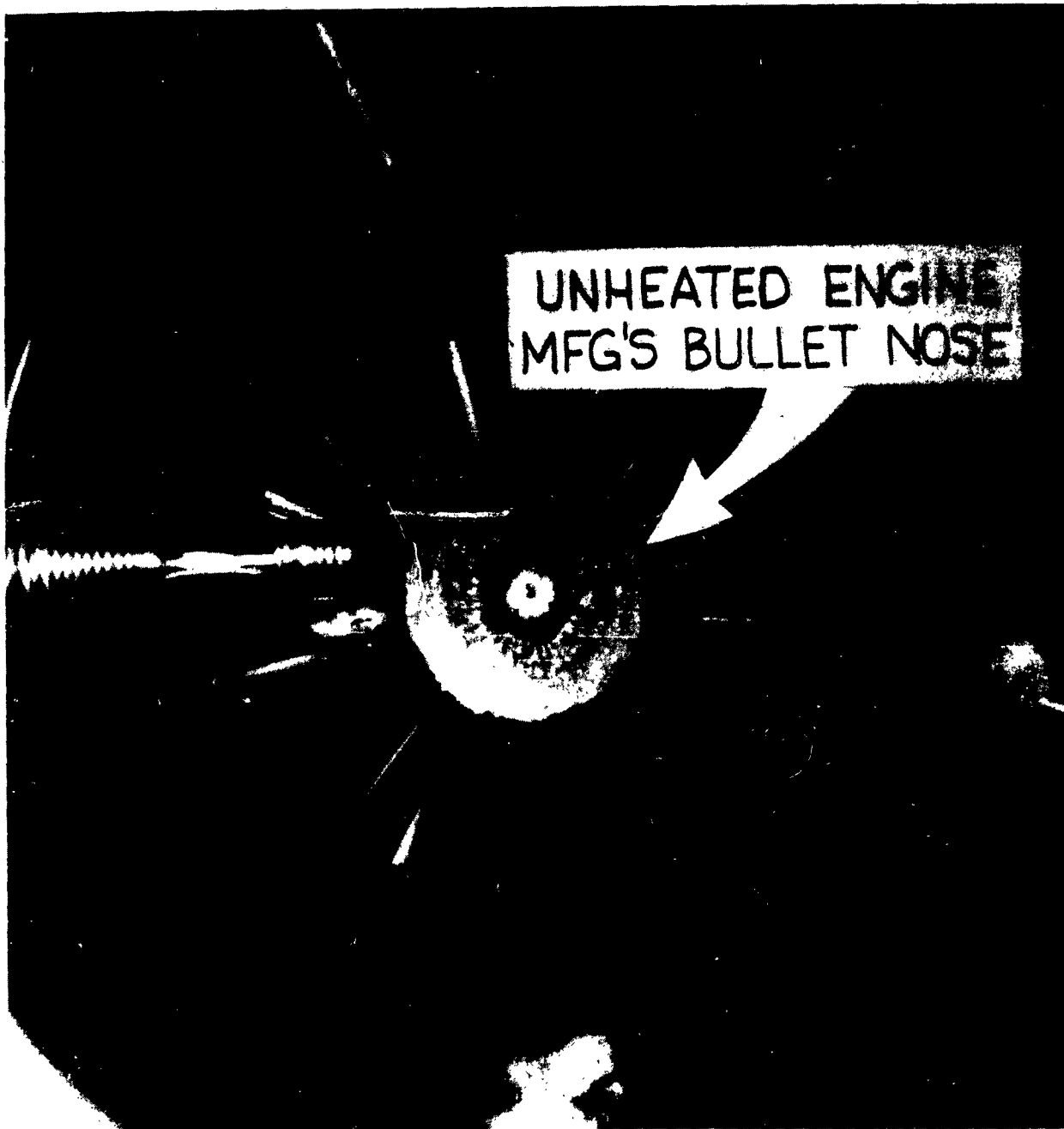


**FIG.8-J79-GE-2 ENGINE INLET  
AFTER AN ICING RUN WITH THE  
STREAMLINED UNHEATED BULLET NOSE**



**FIG.9- J79-GE-2 ENGINE INLET WITH  
ICE FORMATION ON STRUTS**

**AIR FROM  
ANTI-ICING VALVE**

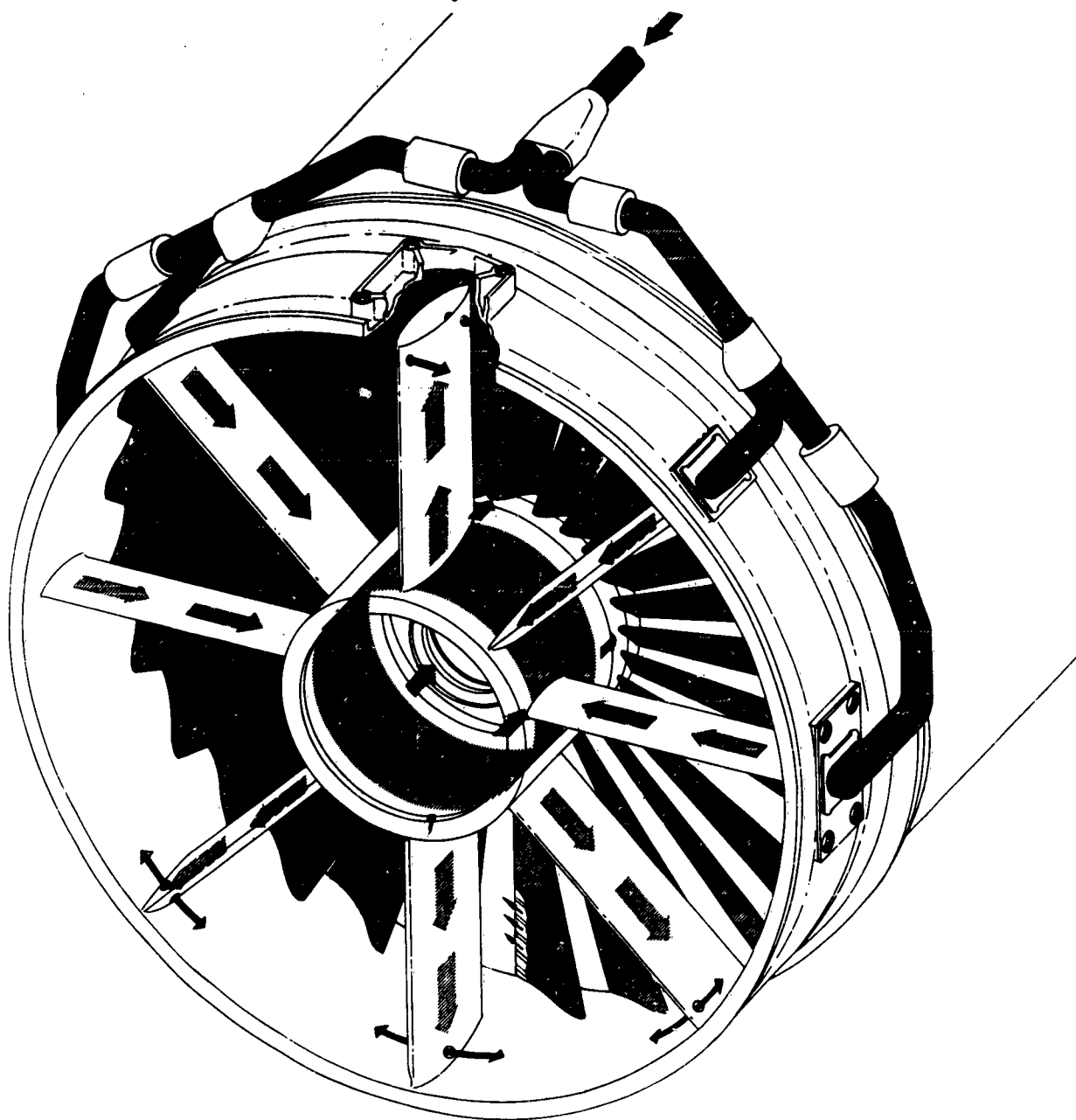


**FIG.10- STANDARD J79-GE-2  
ANTI-ICING SYSTEM**



STANDARD ENGINE CONFIGURATION



ANTI-ICE AIR TO COMPRESSOR  
STRUTS INCREASED

FIG.II- J79-GE-2 ENGINE INLET BEFORE  
AND AFTER STRUT MODIFICATION

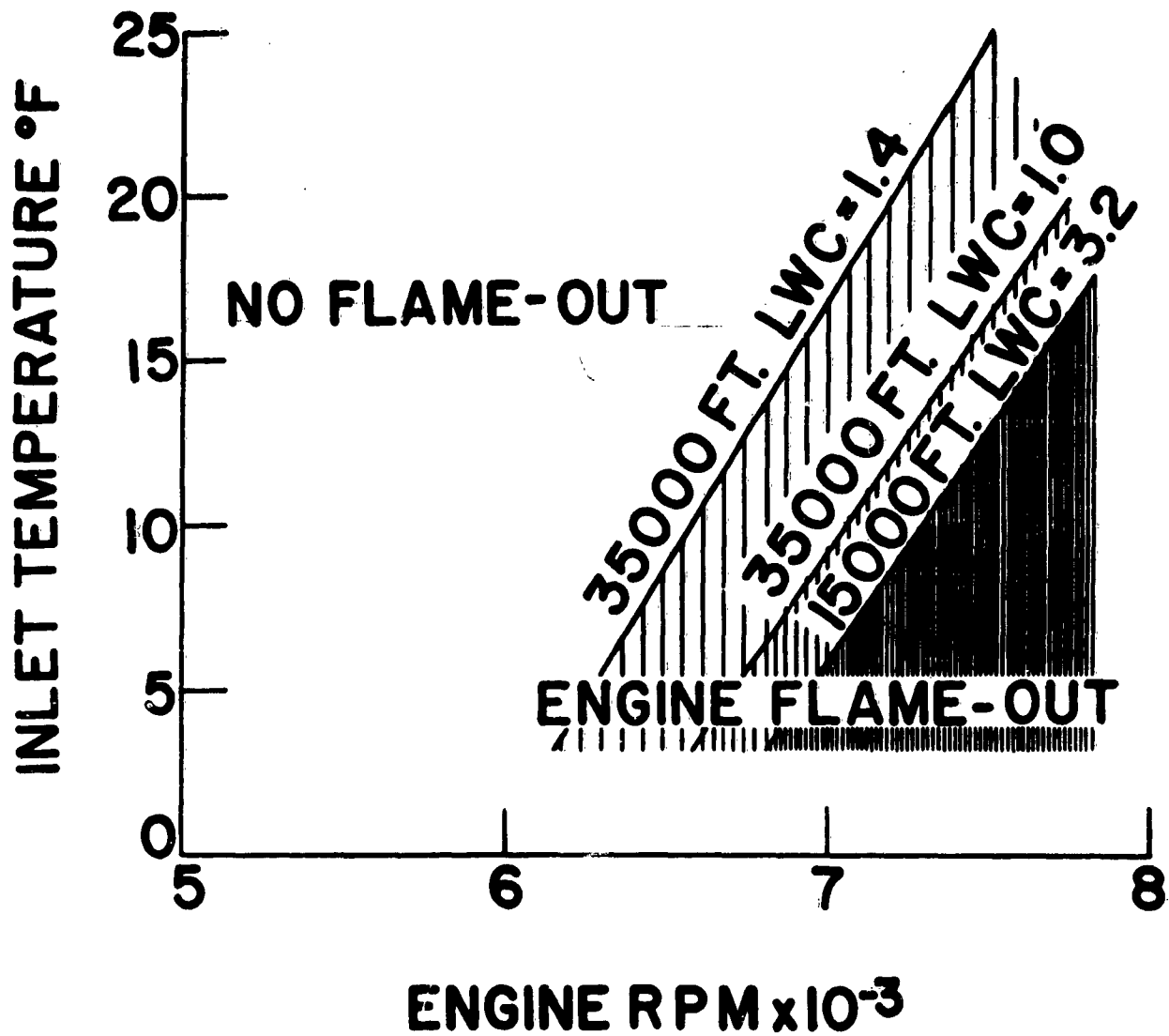
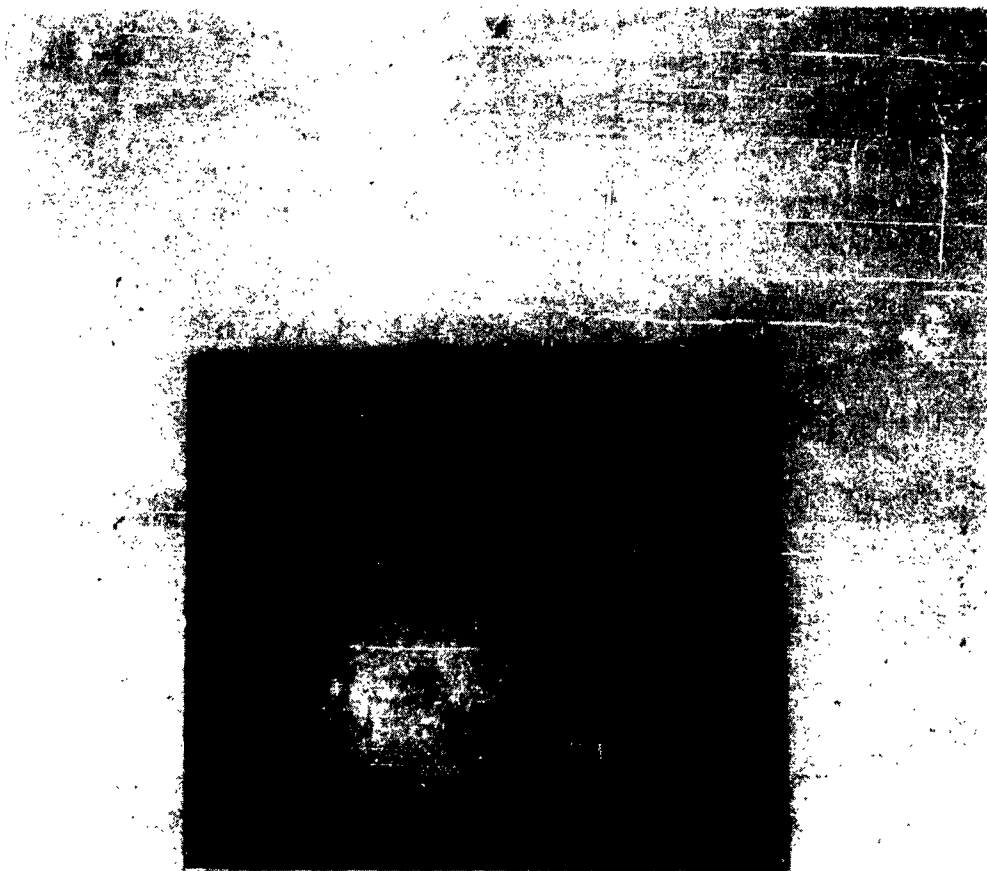
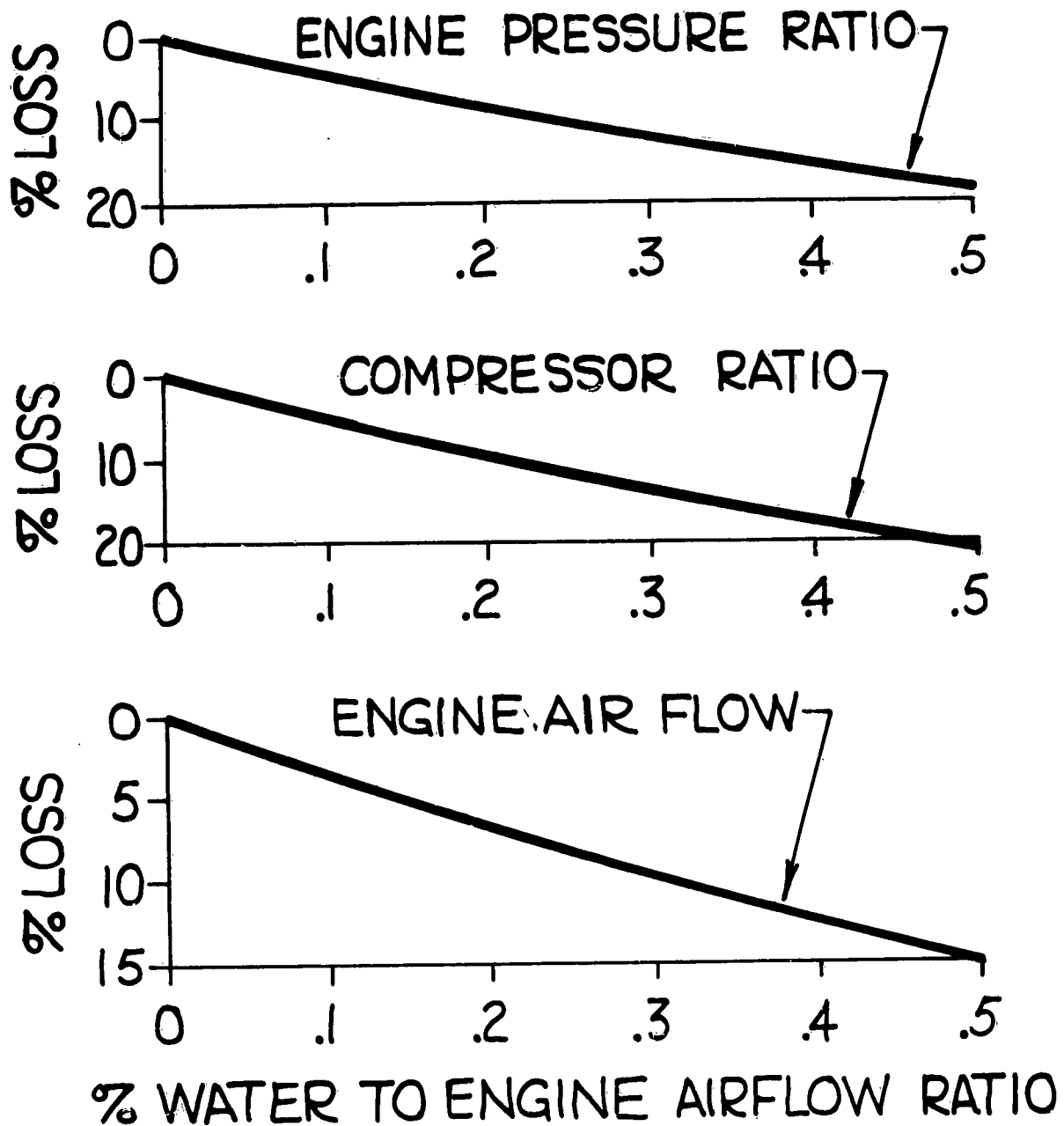


FIG.12-J79-GE-2 ENGINE FLAME-OUT ENVELOPE AS A RESULT OF ICING AT ALTITUDES OF 15000 FT. AND 35000 FT.  $M_N = 0.6$



ICE FORMATION ON  
BULLETNOSE AND STRUT

**FIG.13- TYPICAL ICE BUILD-UP ON THE  
J57 ENGINE BULLET NOSE**



**FIG.14-EFFECT OF ICING ON ENGINE PRESSURE RATIO, COMPRESSOR RATIO AND ENGINE AIRFLOW**

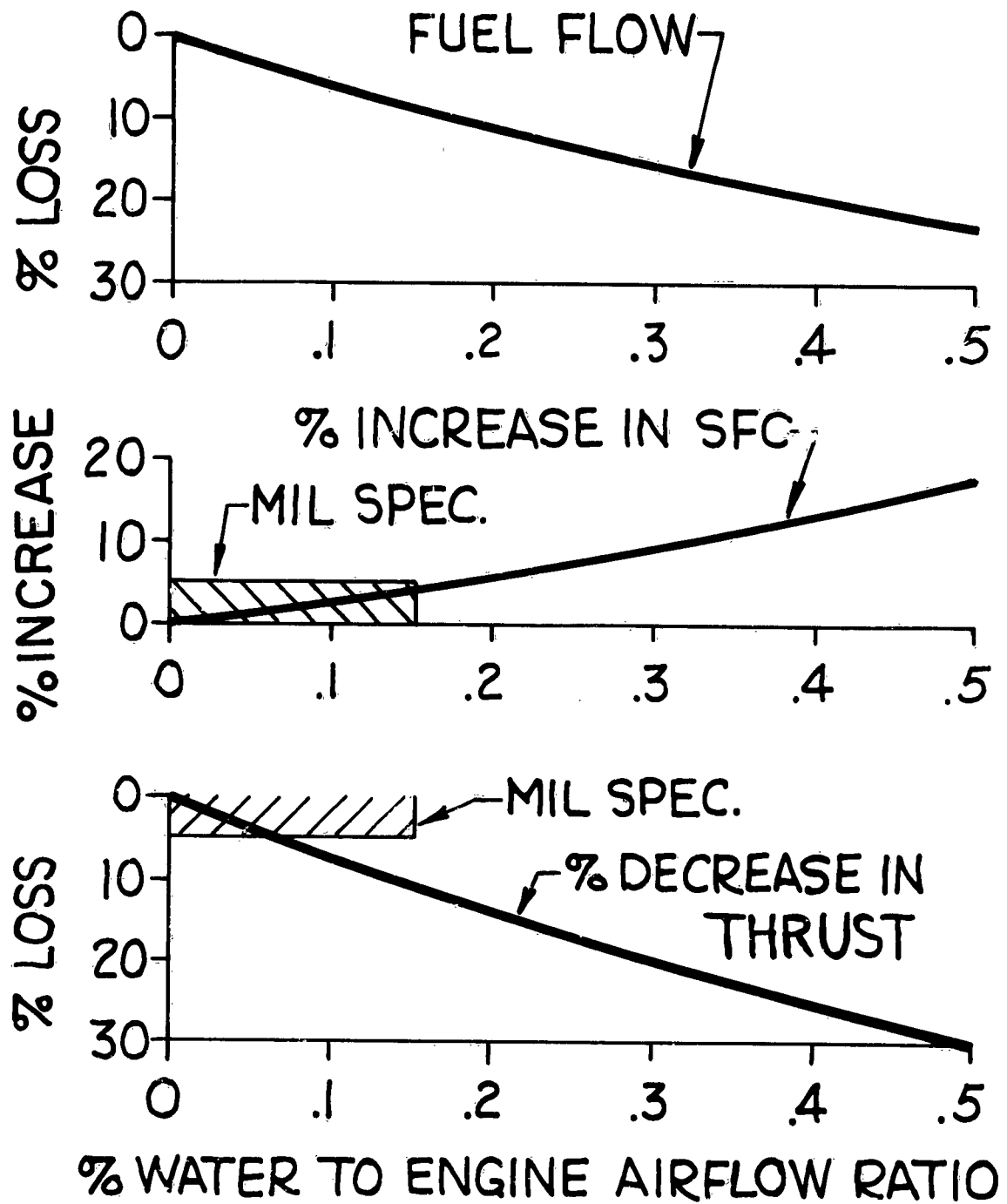


FIG.15- EFFECT OF ICING ON ENGINE FUEL FLOW, THRUST AND S F C

A RESUME OF SIMULATION TECHNIQUES AND ICING  
ACTIVITIES AT THE ENGINE LABORATORY OF  
THE NATIONAL RESEARCH COUNCIL (CANADA)

BY

M. S. CHAPPELL

Division of Mechanical Engineering

1.0 INTRODUCTION

Of the seven laboratories that form the Mechanical Engineering Division of the National Research Council, two are actively engaged in work in the aircraft icing field. These are the Engine Laboratory and the Low Temperature Laboratory. The Engine Laboratory is concerned with the anti-icing protection of the more conventional turboprop and turbojet engines as well as the newer VTOL powerplants. The Low Temperature Laboratory is concerned with fixed and rotating wing icing, basic icing phenomena, and icing instrumentation such as icing detectors, catch rate indicators, and concentration meters.

This paper will present a brief description of the facilities available for icing studies at the Engine Laboratory, together with some discussion of simulation techniques and a few of the more interesting icing phenomena observed during recent test programmes.

2.0 FACILITIES FOR ICING STUDIES AT THE ENGINE LABORATORY

Of the five test cells in the Engine Laboratory, four have been used for icing test programmes; however, the need for test cells to carry out programmes other than icing has recently restricted the icing projects to two cells, No. 4 and No. 5.

The general arrangement of No. 5 Test Cell is as follows (Fig. 1). The engine under test is secured to a rectangular structural steel frame mounted on four journal bearings. Two lay shafts, rotated by an electric motor, run through these bearings and support the engine-test-frame assembly. This arrangement permits the small amount of relatively frictionless fore and aft motion necessary to activate the hydraulic capsule thrust meter. Air enters the test cell through three

banks of sound absorbing splitters, and the engine efflux leaves the cell via an augmentor tube which forms the entry to a vertical Durastack silencer.

For icing studies the cell is equipped with a movable icing intake duct which is coupled to the engine under test. This intake duct contains a 37-nozzle spray grid (Fig. 2) designed and built by D. Napier and Son Limited. The nozzles (Fig.3) on the spray grid are of the pneumatic-atomizing type, and the system is capable of atomizing 1300 pounds of water per hour into 20-micron droplets. At an engine air mass flow of 300 lb./sec. this amount of water represents a maximum concentration at 0°C of 1.59 gm./m<sup>3</sup> (assuming 100 percent relative humidity) or a more realistic value of 1.09 gm./m<sup>3</sup> (assuming a relative humidity of 80 percent).

No. 4 Test Cell (Fig. 4) is suitable for turboprop as well as turbojet engines. The 25-ft. diameter test section allows testing of propellers up to 16 ft. in diameter. In this cell, the engine under test is secured to a flexure-pivot-mounted test frame supported by a structural steel "bridge". Both engine and propeller air enter the cell through three banks of sound absorbing splitters in the 25-ft. square intake. In the case of a turbojet installation the engine efflux is ducted through an augmentor tube into a Cullum Mk. VIII Detuner. In the case of turboprop installations (Fig 5) the engine exhaust gases are ducted into the Detuner and the propeller air is exhausted, via sound absorbing splitters, through a permanent opening in the roof at the downstream end of the cell. This cell is also equipped with a trichloroethylene-air heat exchanger for refrigerating the engine intake air should ambient temperatures turn too warm for icing tests. Temperature differentials across the heat exchanger range from approximately 20°C at 60 lb./sec. air mass flow to approximately 12°C at air mass flows of 120 lb./sec. This system utilizes the ammonia compressor facilities of the neighbouring Low Temperature Laboratory.

Equipment for producing supercooled water droplet clouds comprises a 36-nozzle spraymast (Fig.6) designed and built in the Engine Laboratory. Again, pneumatic-atomizing nozzles are used (Fig. 7) and in this cell the system is capable of atomizing 3500 pounds of water per hour to 25-micron droplets, which, at an engine air mass flow of 400 lb./sec. represents a maximum concentration at 0°C of 3.21 gm./m<sup>3</sup> (assuming

100 percent relative humidity) or 2.71 gm./m<sup>3</sup> (assuming 80 percent relative humidity).

Either of these two cells can also be fitted with equipment for simulating ice crystal or "dry-icing" clouds (Fig. 8). Artificial ice crystals are produced by feeding 11-in. x 5½-in. x 54-in. blocks of ice through two 14-in. wide banks of 10-in. diameter circular saws. Seventy-two of these saws, spaced by 1/8-in. washers, constitute one bank. Tapered washers at each end of the bank of saws "wobble" the blades so as to scan the whole ice face and thus achieve uniformity of particle size. This also ensures against long slivers of ice from between the saw blades breaking off and entering the icing duct. The ice particles cut by the saws are sucked downwards through an air ejector (Fig. 9) and are blown into the icing duct through four 6-in. square pipes (Fig. 10). These pipes discharge in the same plane as the supercooled water droplet nozzles which enables both systems to be operated simultaneously to achieve the "mush" or mixed condition environment. For pure ice crystal tests, the two banks of saws feeding through a common ejector can supply concentrations up to 8.00 gm./m<sup>3</sup> at an engine air mass flow of 250 lb./sec.

### 3.0 SIMULATION TECHNIQUES

#### 3.1 Concentration Control

In the case of No. 4 Test Cell, a pitot-static rake upstream of the spraymast measures the quantity of air being drawn into the engine intake. By atomizing a known quantity of water into this air stream any desired concentration within the limitations of the simulation system can be attained. In No. 5 Test Cell we rely on the engine manufacturer's curves of air mass flow vs. engine speed (corrected to various ambient temperatures) for our air flow measurement.

#### 3.2 Droplet Size Control

The degree of atomization from a pneumatic-atomizing nozzle of the type shown in Figure 7 is dependent primarily on the water/air mass flow ratio, being approximately inversely proportional to this parameter at atomizing air pressures above the critical. Hence, for a certain nozzle geometry, a given water flow rate can be atomized to a given droplet size by applying the specific atomizing air pressure to obtain the correct water/air mass flow ratio.

Figure 11 shows a comparison of droplet samples taken from simulated and natural icing clouds. As one can see, the range of droplet diameters is almost identical. The sample density (number of droplets in a given area) is dependent on the slide exposure time in the icing cloud and is not used as a measure of the concentration in the cloud. Figure 12 shows an analysis of the two samples plotted on the same graph. Simulation of the natural cloud is reasonably good, both as regards size and volume distribution of the droplets.

### 3.3 Evaporation Allowance

At present, allowance for evaporation from the icing cloud as it passes from the spraymast down the intake trunking to the compressor inlet is made in accordance with an empirical method proposed by the United Kingdom Ministry of Aviation. This method requires that sufficient additional water be sprayed to add 20 percent to the ambient relative humidity when the latter value is below 80 percent. For ambient relative humidities greater than 80 percent, sufficient additional water to saturate the air is sprayed.

A more sophisticated method, based on fundamental studies of evaporation from droplets conducted by J. K. Hardy, is at present being compiled in the Engine Laboratory. This revised method will take into account such relevant parameters as droplet size, dwell time, relative humidity, temperature and concentration.

### 3.4 Droplet Size Measurement

The volumetric median droplet diameter is determined as follows. An oiled plastic slide (1/2 in. x 2 in.) is passed through a section of the icing cloud causing the supercooled water droplets to impinge upon it, and a photomicrograph of the sample thus collected is taken immediately. (A special oil is used that retards evaporation of the droplets between sampling and photographing.) A Leica camera fitted to a 20-power microscope is used and the resulting 35-mm negatives are enlarged a further five times when the photographs are printed. This results in an overall magnification of 100 times. Using a plastic template with various circles corresponding to true droplet diameters of 5, 10, 15, etc., microns etched into it, the droplet diameters are measured and counted in groups, from 5 to 10 microns, 10 to 15, 15 to 20, etc. The

volumetric median droplet diameter, defined as the 50-percent volume diameter (that droplet diameter which divides the sample into two groups of equal volume), is determined using a plot similar to Figure 12.

#### 4.0 GENERAL SCOPE OF ICING STUDIES CONDUCTED AT THE ENGINE LABORATORY

Icing studies began at the Engine Laboratory during the winter of 1945-1946. Preliminary tests to establish the effects of icing conditions on the then-novel turbojet engine were carried out on surplus (and expendable) Jumo engines built in Germany during the second World War. In 1946 the United Kingdom Ministry of Aviation (then called the Ministry of Supply) became interested in our work in the icing field and in 1947 became co-sponsors of the project. Since that date over thirty-five engines have undergone icing tests at the Engine Laboratory. Among those that have been on our beds during the last few years are: the Bristol Proteus, Rolls Royce Conway, Armstrong Siddeley Double Mamba, DeHavilland Gyron Jr., Orenda 10, Orenda 14, Iroquois, various marks of the Bristol Olympus including the 100, 101, 200, and 301, Napier Gazelle, Bristol Orpheus, and the Canadian Pratt and Whitney PT-6.

In general terms, the objectives of each of these test programmes have been:

- (a) To determine the basic parameters that affect engine operation in icing conditions.
- (b) To evaluate the performance of the engine's anti-icing system with respect to its adequacy in protecting the engine from severe ice build-ups.
- (c) To evaluate the effect of icing conditions on engine performance and handling characteristics.
- (d) To perform scheduled tests as laid down in the British Ministry of Aviation Specification D. Eng.R.D. 2100 and to obtain flight clearance for the engine under icing conditions.

#### 5.0 RESULTS FROM RECENT TEST PROGRAMMES

It is not the intention of this paper to present a detailed accounting of the results of test programmes carried out on various engines during the

past few years. This type of information can be obtained from reports dealing specifically with the test results for each particular engine. It is, rather the intention of this paper to discuss some of the more interesting phenomena associated with general engine and anti-icing system configurations.

### 5.1 Various Types of Anti-Icing Systems Tested

Three major types of anti-icing systems have been tested at the Engine Laboratory during the past few seasons. These are the hot air, hot oil, and alcohol injection systems. It may be said that for conventional turbojet applications the alcohol injection anti-icing system is optimum for relatively short icing encounters of up to one half hour duration, whereas, when long endurance icing is considered, the compressor bleed hot air anti-icing system involves a lesser weight penalty. There is, of course, a certain performance penalty associated with the compressor bleed anti-icing system, but in the present state of the art this penalty is not severe, amounting to 1 to 1.5 percent of cruise thrust at the most. For turboprop engines and turbo-shaft engines used in helicopter installations, some thought should be given to the use of hot gear-box lubricating oil as an anti-icing fluid. The poor heat transfer coefficients of most oils, and their tendency to "stratify" leaving a cold more viscous layer on the walls of the anti-icing passages, are, to a great extent, offset by the quantity of hot oil available, i.e., the oil may not be a very efficient heat transfer medium but, as one is working with waste heat, one can afford a little inefficiency. One manufacturer in the United Kingdom is currently making good use of such a system in an engine intake configuration that would otherwise be very difficult to protect.

After several years of relative dormancy, the alcohol injection anti-icing system is again appearing on the scene. Recent impetus in the small turbine field (500 h.p. and less) has resulted in many of these engines appearing on the market in the last few years. Some of these powerplants are utilizing axial and combination axial-centrifugal compressors, and axial first stage blades of 1/2-in. chord and approximately 1-in. span are not uncommon. These "watch-maker" sizes imply minute clearances and hence increased susceptibility to dust and foreign object damage. Consequently intake "trash" screens are again being fitted and must be anti-iced. These screens, together with the performance penalties associated with

past few years. This type of information can be obtained from reports dealing specifically with the test results for each particular engine. It is, rather the intention of this paper to discuss some of the more interesting phenomena associated with general engine and anti-icing system configurations.

### 5.1 Various Types of Anti-Icing Systems Tested

Three major types of anti-icing systems have been tested at the Engine Laboratory during the past few seasons. These are the hot air, hot oil, and alcohol injection systems. It may be said that for conventional turbojet applications the alcohol injection anti-icing system is optimum for relatively short icing encounters of up to one half hour duration, whereas, when long endurance icing is considered, the compressor bleed hot air anti-icing system involves a lesser weight penalty. There is, of course, a certain performance penalty associated with the compressor bleed anti-icing system, but in the present state of the art this penalty is not severe, amounting to 1 to 1.5 percent of cruise thrust at the most. For turboprop engines and turbo-shaft engines used in helicopter installations, some thought should be given to the use of hot gear-box lubricating oil as an anti-icing fluid. The poor heat transfer coefficients of most oils, and their tendency to "stratify" leaving a cold more viscous layer on the walls of the anti-icing passages, are, to a great extent, offset by the quantity of hot oil available, i.e., the oil may not be a very efficient heat transfer medium but, as one is working with waste heat, one can afford a little inefficiency. One manufacturer in the United Kingdom is currently making good use of such a system in an engine intake configuration that would otherwise be very difficult to protect.

After several years of relative dormancy, the alcohol injection anti-icing system is again appearing on the scene. Recent impetus in the small turbine field (500 h.p. and less) has resulted in many of these engines appearing on the market in the last few years. Some of these powerplants are utilizing axial and combination axial-centrifugal compressors, and axial first stage blades of 1/2-in. chord and approximately 1-in. span are not uncommon. These "watch-maker" sizes imply minute clearances and hence increased susceptibility to dust and foreign object damage. Consequently intake "trash" screens are again being fitted and must be anti-iced. These screens, together with the performance penalties associated with

even relatively small amounts of bleed from the compressors of these small engines, have indicated the practicability of an alcohol injection anti-icing system as compared with the other two types of anti-icing systems mentioned above. The low air mass flows of these engines mean that relatively high alcohol/air ratios can be maintained for reasonable lengths of time without severe weight penalties. One manufacturer is currently studying a system in which the alcohol is atomized in the engine intake to the same range of droplet sizes as the supercooled water droplets in the icing cloud. The hypothesis behind this system is that the alcohol droplets will be subject to the same momentum separation characteristics as the icing droplets; thus, where the ice tends to collect so does the alcohol. Preliminary tests at the Engine Laboratory have borne out this theory and hence a basic anti-icing system can be offered that is relatively independent of the particular nacelle and intake configurations for various installations.

No mention has been made of electro-thermal (heatermat) anti-icing systems as no recent work has been done at the Engine Laboratory on this type of protection system.

## 5.2 Routing of Anti-Icing Air in Compressor Bleed Anti-Icing Systems

During the past few seasons we have had a chance to test various routing schemes for compressor bleed anti-icing systems. The major intake components that usually require anti-icing protection are the inlet guide vanes, the intake struts, and the nose bullet. Two general routings have been tried (Fig. 13): the "series" system and the "parallel" system. In the series arrangement, all the anti-icing air bled from the compressor is fed, in turn, through each of the heated intake components; usually radially inwards through the inlet guide vanes, forward inside the nose bullet and then rearward through the outer double skin passage of the nose bullet to the base of the struts, and then radially outwards through the struts exhausting either to atmosphere or into the compressor inlet near the casing. The parallel arrangement employs feeds through both the inlet guide vanes and the intake struts into a common passage in the nose bullet. The latter routing not only allows better distribution of protection to the various components, but also requires slightly less anti-icing bleed from the compressor, a feature which the performance people appreciate.

### 5.3 Effects of Variable Incidence Inlet Guide Vanes on the Normal Compressor Icing Pattern

Another interesting point observed during a test programme two years ago was the effect of variable incidence inlet guide vanes on the usual pattern of stator icing. With most compressor-bleed anti-icing systems the ice accretions on all the heated intake components become steadily more severe as engine speed and ambient temperatures decrease. Consequently, one of our primary aims in test programmes of this type is to establish, on the basis of heated component protection, the Minimum Permissible Approach Speed for descent through icing conditions. To do this, the engine is operated at various speeds, decreasing toward Flight Idle, under the coldest conditions available. As the ambient temperature drops and the anti-icing effectiveness falls owing to decreasing engine speed, the heated components go from "ice-free" through "running wet" to "iced" conditions. With fixed geometry engines the "iced" condition is the limiting factor as ice accretions on the inlet guide vanes tend to choke the compressor inlet causing engine stall. In the case of variable incidence inlet guide vanes, as the engine speed decreases, not only does the anti-icing effectiveness decrease but the vanes "close" presenting a greater frontal area and hence suffering a greater catch rate. At very low speeds and ambient temperatures (Fig. 14) the inlet guide vanes are subject to building and shedding of heavy ice accretions due to their high catch rate and decreased anti-icing protection. The pieces of ice that shed from the inlet guide vanes pass through the compressor without adhering to the succeeding stages of blading. However, at any given engine speed, as the ambient temperature rises the inlet guide vane anti-icing becomes more effective until it reaches a point where it is just able to melt the ice as it forms. The water formed by this melting ice runs back in the form of large droplets and refreezes on the first stage rotors and stators. Excessive build-ups on the rotors are prevented by the action of centrifugal force but the stators suffer very heavy ice accretions. In a relatively short period of time these stator ice formations can reach proportions sufficient to cause a running stall, as evidenced by increasing jet pipe temperature and engine speed. Inherent in this explanation is the observed phenomenon that as the ambient temperature drops the speed at which this severe stator icing occurs increases. This trend holds true until the inlet guide vanes are almost fully open at which point the increased guide vane

anti-icing and increased compressive temperature rise across the first stage combine to alleviate the situation.

Thus, one has the situation whereby the Minimum Permissible Approach Speed for descent through icing conditions is defined, not by excessive ice accretions on the inlet guide vanes themselves causing engine malfunctioning, but by excessive first stage stator icing causing engine stall. Also, if one attempts to accelerate the engine to cruise or take-off power (for instance to simulate a baulked landing) after running in these severe stator icing conditions, the inlet guide vanes swing "open" at the preset speed exposing the iced first stage stators as a secondary aerodynamic throttle and the engine goes into a severe surge. The obvious cure for this problem is to provide sufficient anti-icing to keep the inlet guide vanes clear under all conditions of ambient temperature and engine speed. This solution implies a regulating valve rather than an ON - OFF valve in the anti-icing feed pipe from the compressor in order to provide sufficient anti-icing at low engine speeds while prohibiting excessive bleed (and hence excessive power loss) at high engine speeds.

#### 5.4 Unique Icing Problems Associated with Transonic First Stage Axial Compressors

During the last season's icing tests at the Engine Laboratory we conducted our first comprehensive icing studies on an engine with a transonic first stage in the axial compressor. The significance of the transonic blading from an icing point of view is twofold. Firstly, the rotor blades generally have a large chord, and secondly, a low thickness/chord ratio with a thin almost knife-like leading edge is mandatory if reasonable aerodynamic efficiencies are to be realized.

The first point, the large chord, means large catchment areas, and because the rotors are seldom anti-iced, a high catch efficiency. As is general with all rotating blade icing, relatively little trouble is experienced at high engine speeds because, as the ice accretions build up, centrifugal force will overcome the bond between the ice and the blade and shedding will occur at regular intervals. However, as engine speed decreases, the weight of ice which must build up at any point along the blade span before shedding occurs will increase rapidly. (As centrifugal force is proportional to the mass and the angular velocity squared at any given radius one can see that rotational speed is a much stronger variable than the size of build-up.) As the

shedding frequency decreases and each individual shed becomes more severe, the chance of a shed from one blade triggering sheds from several other blades increases. Hence the likelihood of what is commonly termed a "massive" rotor shed (many rotor blades shedding at the same time) increases. These ice accretions from the first stage rotors occasionally cause damage to succeeding stages of blading, but more often pass through the compressor without incident. It is when this large slug of water and slush (the ice having been at least partly melted by the increasing air temperature through the compressor) enters the combustion chamber that malfunctioning such as large speed dips and flameouts occur (Fig. 15). As previously pointed out, these massive sheds are most likely to occur at low engine speeds where combustion tends to be a bit unstable under even the most favourable conditions. One successful cure for this problem is the use of alcohol injection in the intake at low engine speeds. On one particular engine this method succeeded in lowering the Minimum Permissible Approach Speed for descent through icing conditions from approximately 50 percent power to Flight Idle due to the elimination of this type of malfunctioning.

The second area of susceptibility of the transonic first stage is the very thin leading edges of the rotor blades. High rotational speeds increase the severity of impact on these rather tender regions. Experience gained during last winter's test programme indicates that the normal light alloys usually used for compressor blading cannot be considered as suitable materials for transonic first stages (Fig. 16). Severe damage in the form of bent and torn leading edges resulted when pieces of ice one-tenth the size of ice accretions that would be shed from the intake components during a normal 2-minute delay test, entered the engine. There is, of course, no way of protecting the engine from these very minor ice ingestions and one would suspect difficulties arising from other types of foreign body ingestion as well. It is our contention at the moment, therefore, that transonic first stage rotor blading must be made of steel or some other high strength material, preferably with a very low notch sensitivity.

#### 5.5 Total Ram Head Pitot Icing

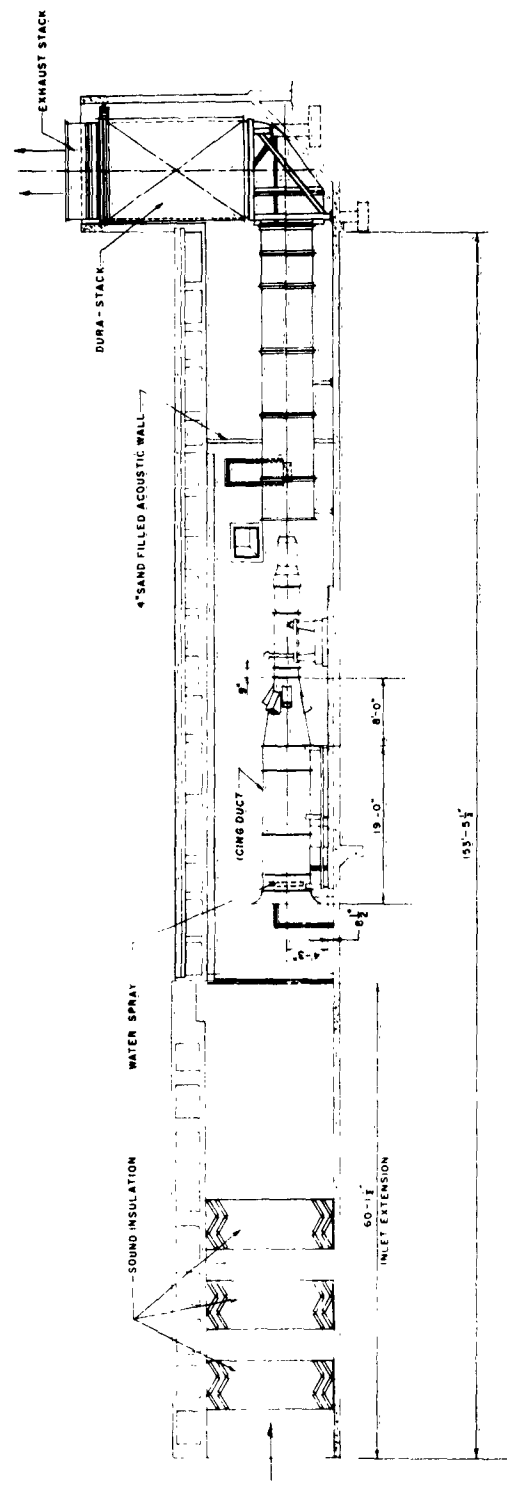
Total ram head pitot probes have also caused some difficulties under icing conditions. The two most common types of anti-iced pitot probes are shown in Figure 17. Type I usually suffers from a "cold nose" as at low engine speeds and low ambient temperatures the

anti-icing air bleed from the engine compressor is neither hot enough nor at a high enough pressure to keep the pitot tip above the freezing temperature. Type II, although rather clumsy in appearance due to the large sensing orifice required to minimize the effect of the anti-icing exhaust, functions well down to a certain severity. However, once engine speed and ambient temperature have decreased sufficiently to permit the first trace of ice to form on the pitot tip, a very slight increase in icing severity will cause the anti-icing exhaust annulus to ice over and, as no anti-icing air can then pass through the probe, the sensing orifice very quickly ices over also. Higher anti-icing temperatures, pressures and flow rates will of course cure the problem with both these types. One manufacturer, however, evolved another answer to the problem. He buried the probe, behind a shield, in a hole in the nose bullet, as shown in the third sketch in Figure 17. Needless to say, no pitot anti-icing was necessary owing to the probe's location within the anti-iced nose bullet.

#### 6.0 REFERENCES

1. Golitzine, N.            Spray Nozzles for the Simulation  
   Sharp, C. R.            of Cloud Conditions in Icing Tests  
   Badham, L. G.           of Jet Engines.  
                             National Research Council of  
                             Canada.  
                             National Aeronautical Establishment,  
                             Report 14, 1951.
2. Golitzine, N.            Method for Measuring the Size of  
                             Water Droplets in Clouds, Fogs,  
                             and Sprays.  
                             National Research Council of Canada.  
                             National Aeronautical Establishment,  
                             Note 6 (ME-177), 1951.

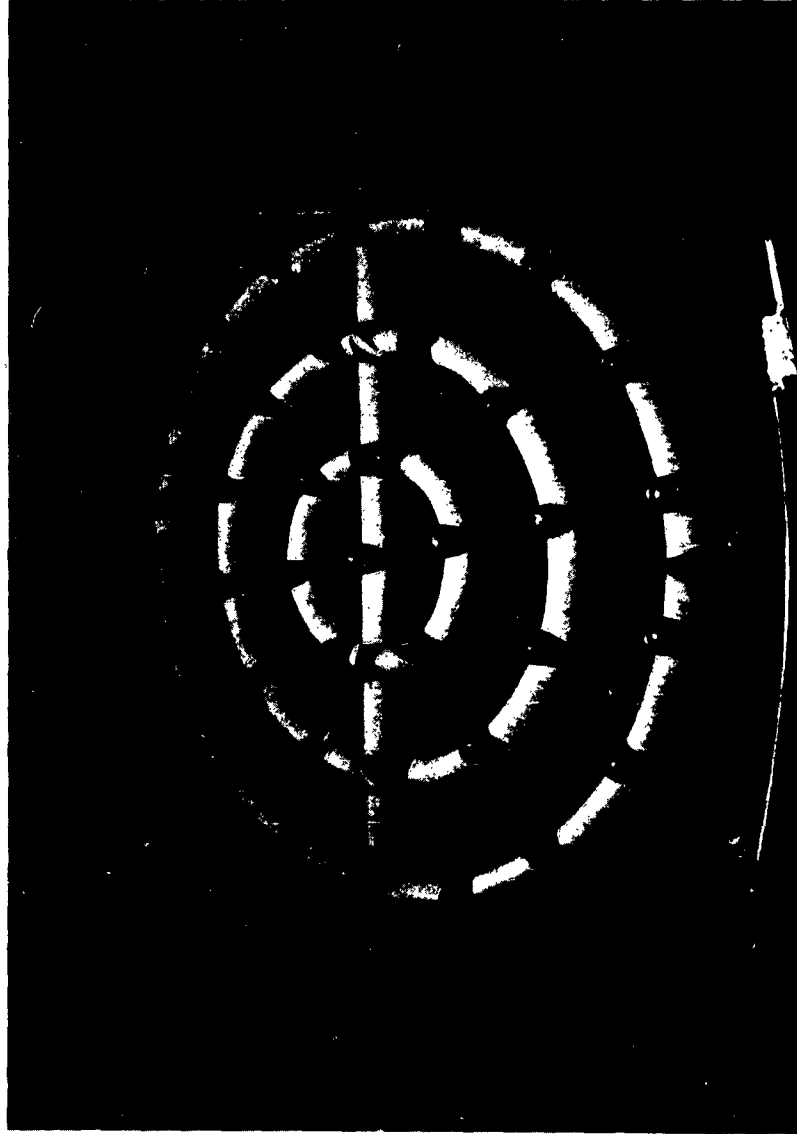
FIG. 1  
LR-305



TURBOJET ENGINE INSTALLED IN NO. 5 TEST CELL FOR ICING TESTS

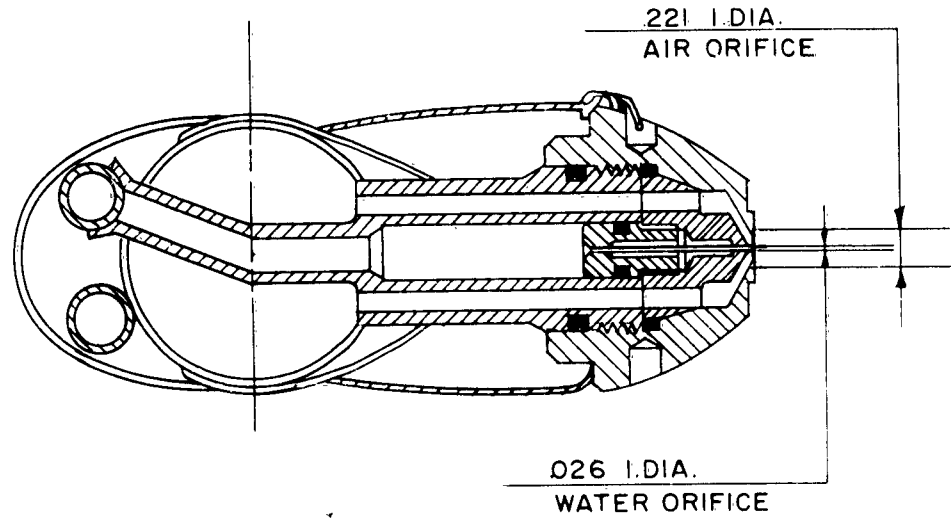
ENGINE LABORATORY  
NATIONAL RESEARCH COUNCIL  
1958 - 1959 ICING SEASON

FIG. 2  
LR-305



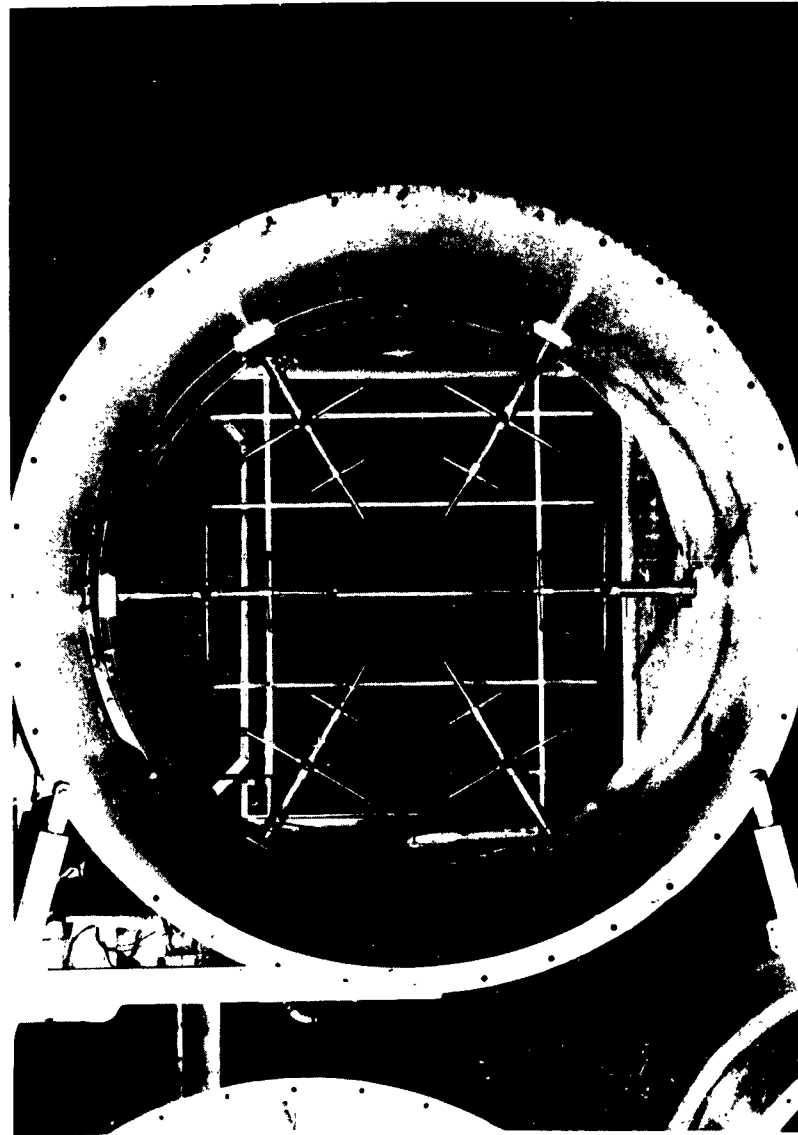
37-NOZZLE NAPIER SPRAYMAST IN NO. 5 TEST CELL

FIG. 3  
LR-305



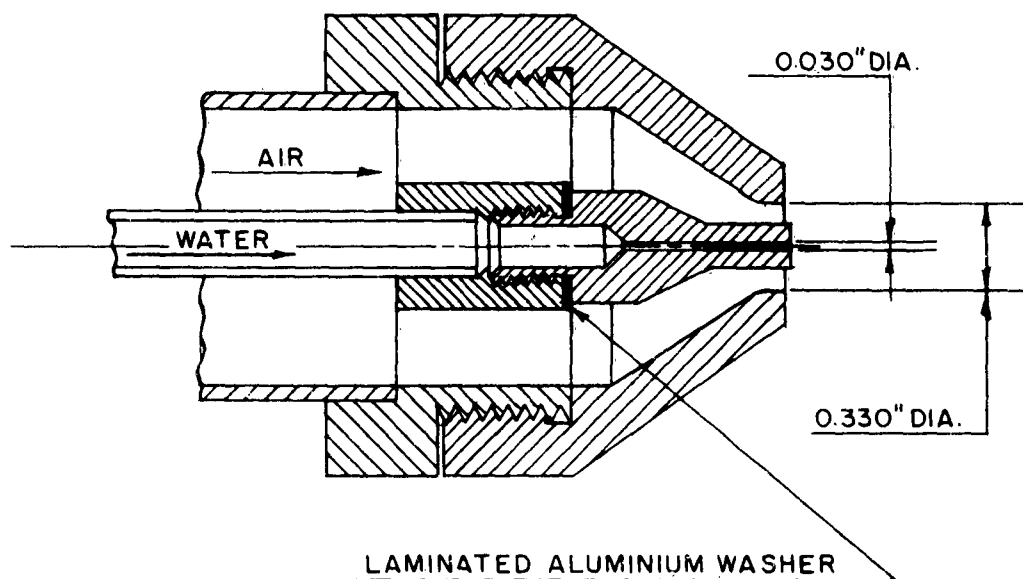
ATOMIZING NOZZLE USED ON NAPIER SPRAYMAST





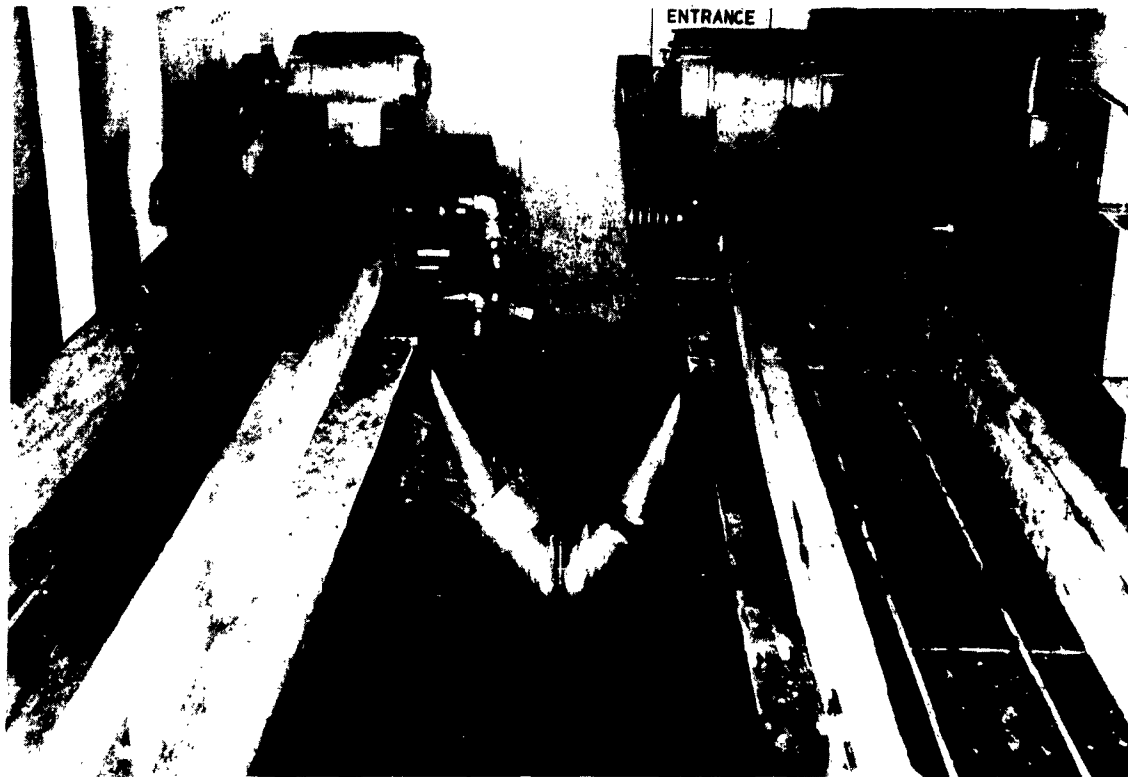
36-NOZZLE N.R.C. SPRAYMAST IN NO. 4 TEST CELL

FIG. 7  
LR-305



ATOMIZING NOZZLE USED ON N.R.C. SPRAYMAST

FIG. 8  
LR-305



ICE CRYSTAL SIMULATION EQUIPMENT: FEED TROUGHS  
AND SAW BANKS

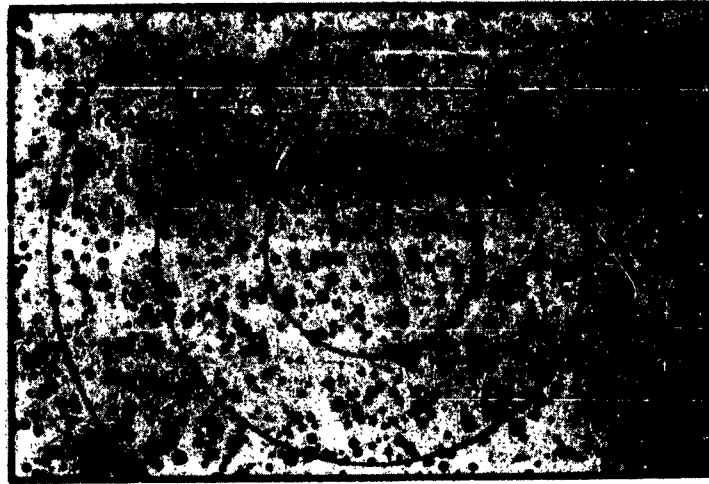
FIG. 9  
LR-305



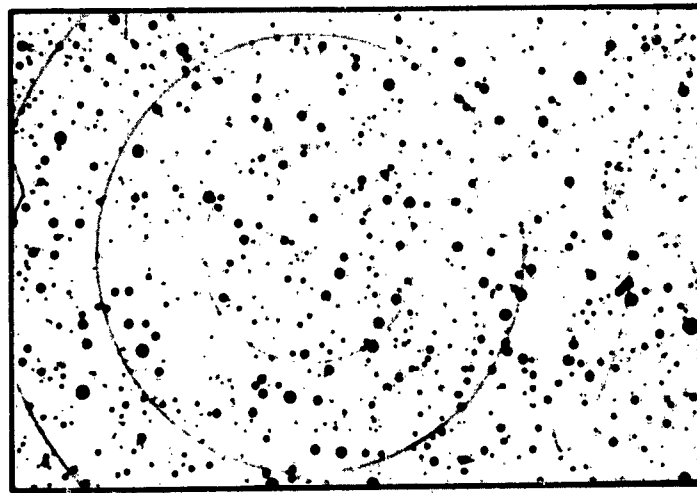
ICE CRYSTAL SIMULATION EQUIPMENT: AIR EJECTOR PUMP



ICE CRYSTAL SIMULATION EQUIPMENT: DISCHARGE PIPES  
IN INTAKE TRUNKING

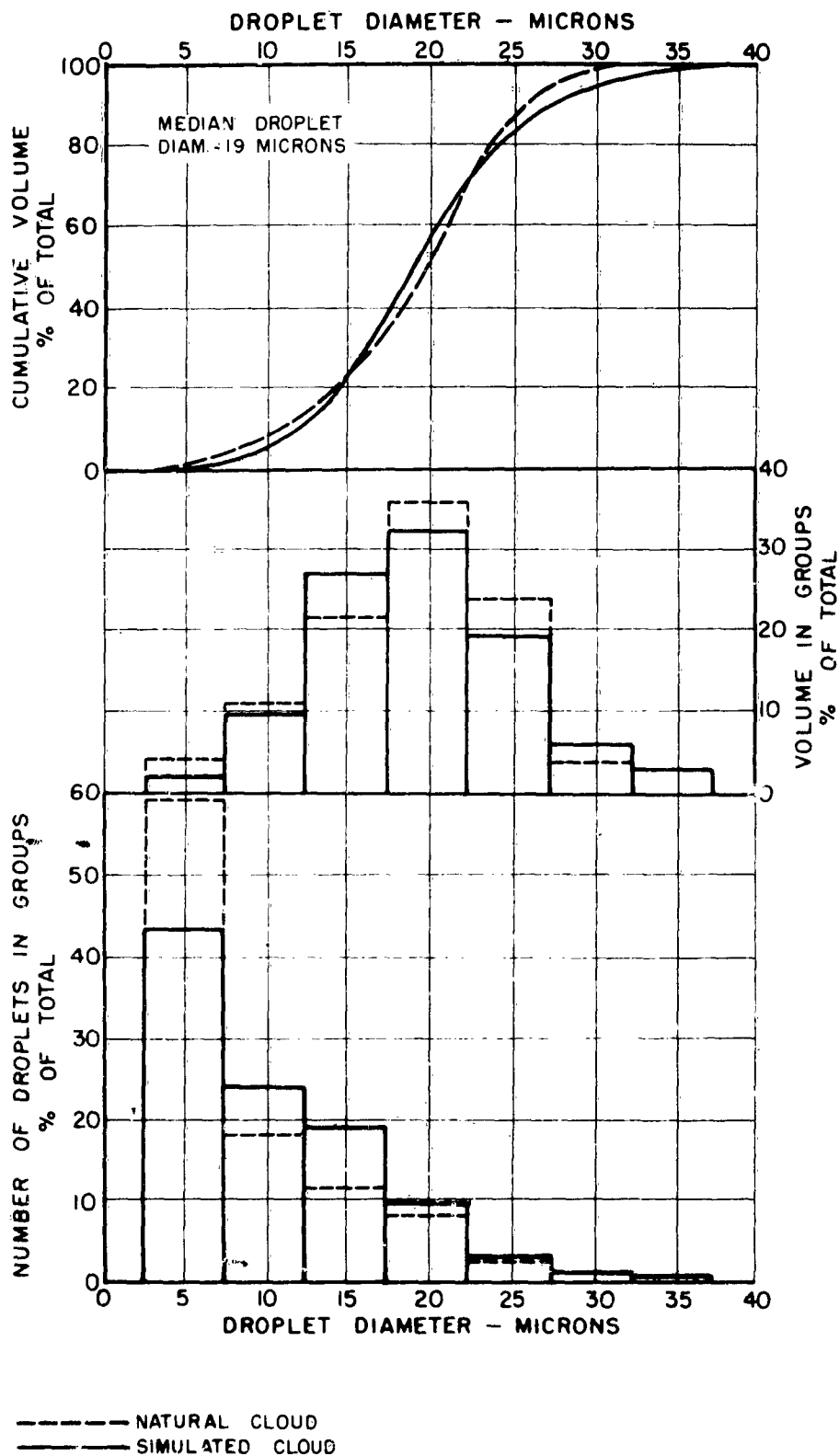


**DROPLET SAMPLE FROM NATURAL ICING CLOUD**  
(VOLUMETRIC MEDIAN DROPLET DIAMETER = 19 MICRONS)



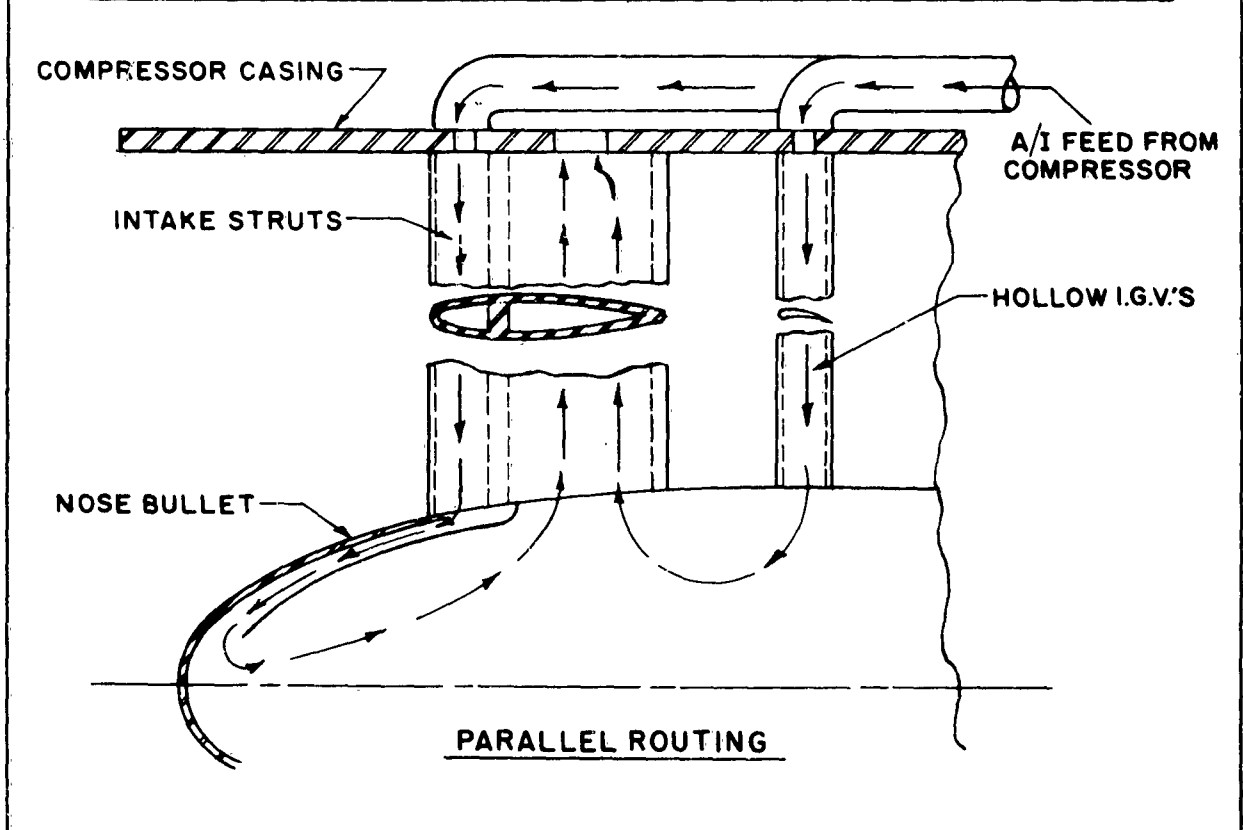
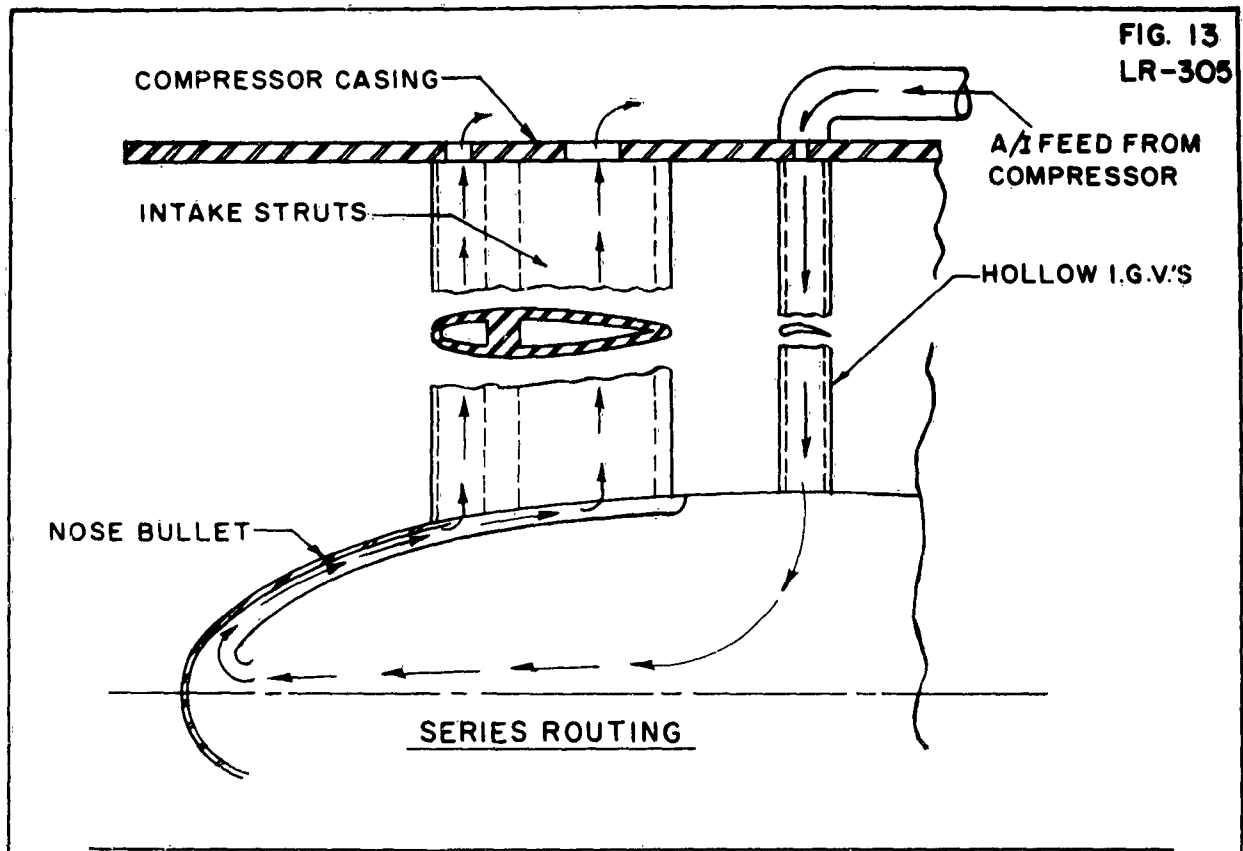
**DROPLET SAMPLE FROM SIMULATED ICING CLOUD**  
(VOLUMETRIC MEDIAN DROPLET DIAMETER = 19 MICRONS)

FIG. 12  
LR - 305



COMPARISON OF DROPLET SAMPLES FROM  
NATURAL AND SIMULATED ICING CLOUDS

FIG. 13  
LR-305



SERIES AND PARALLEL ANTI-ICING AIR ROUTINGS

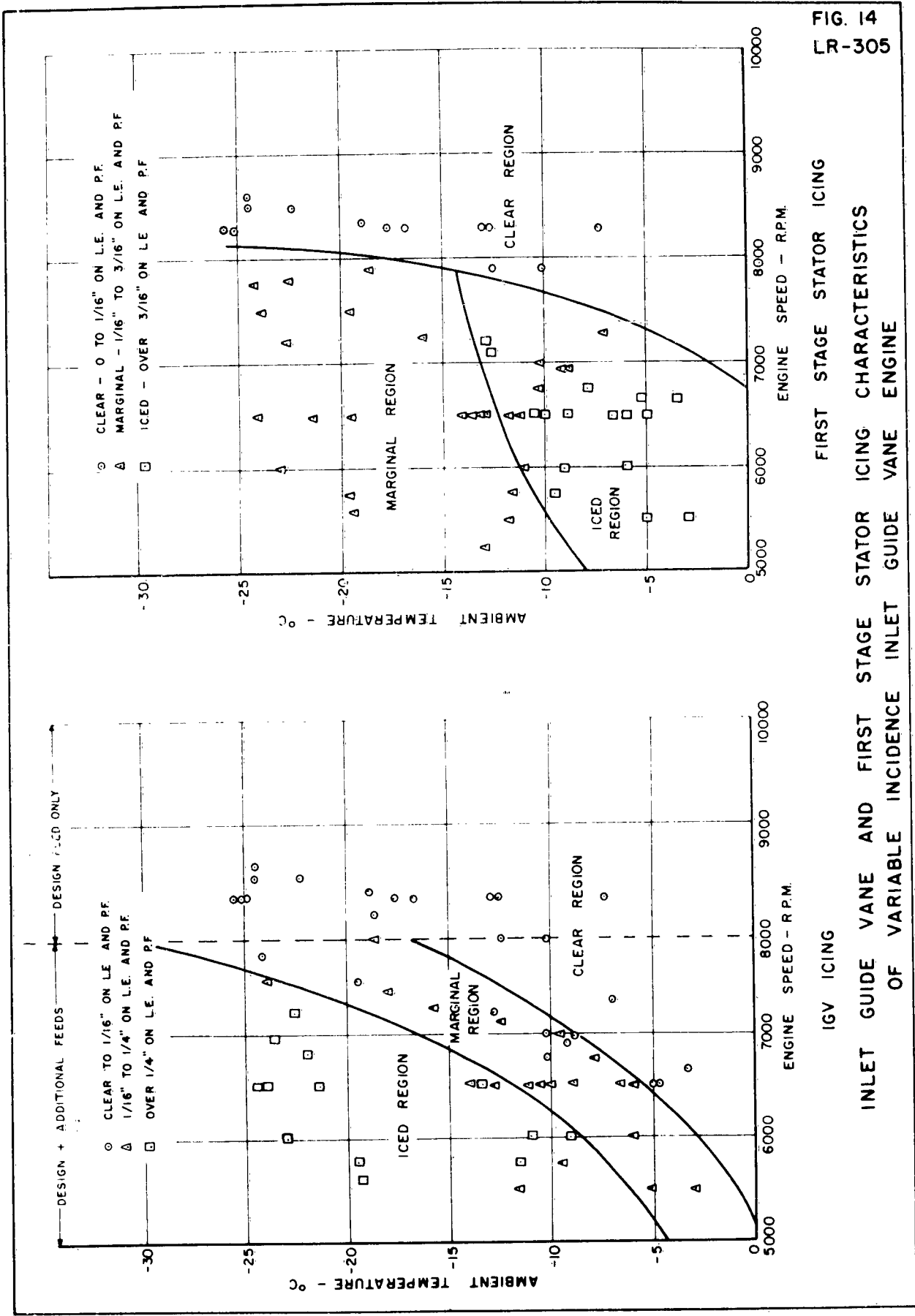
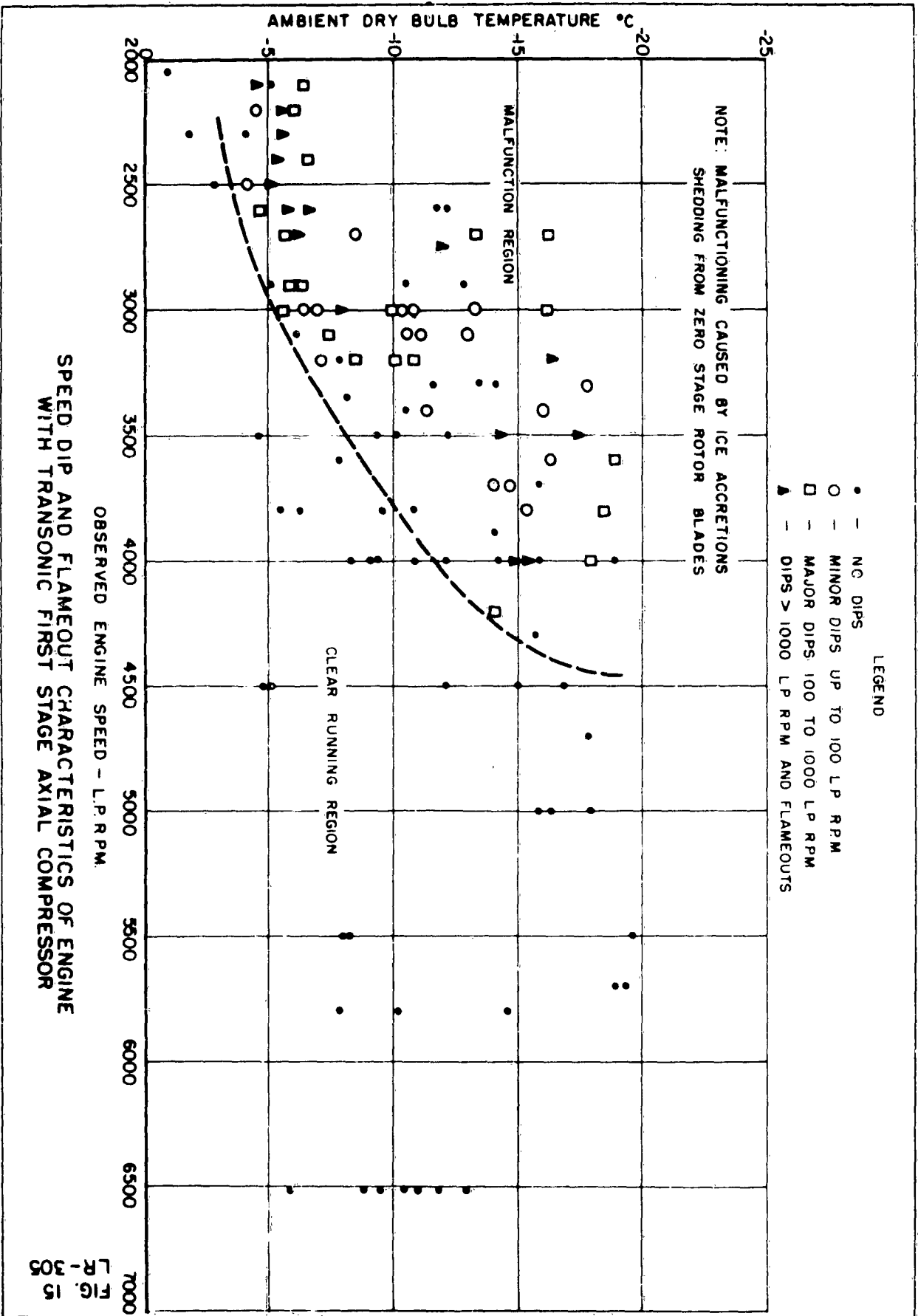


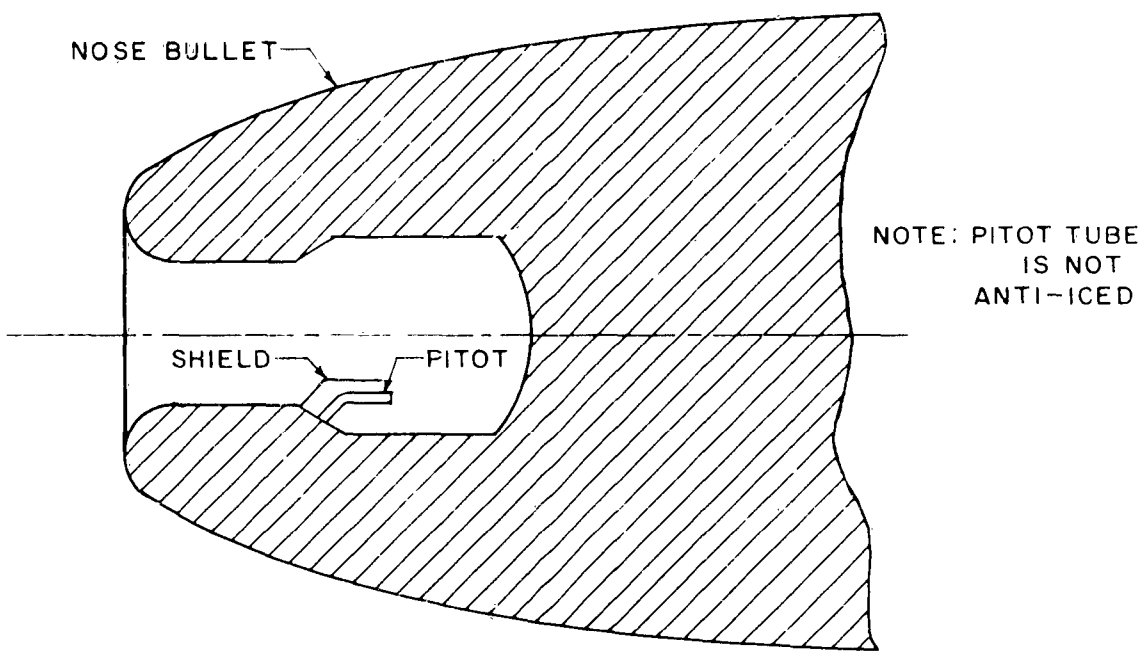
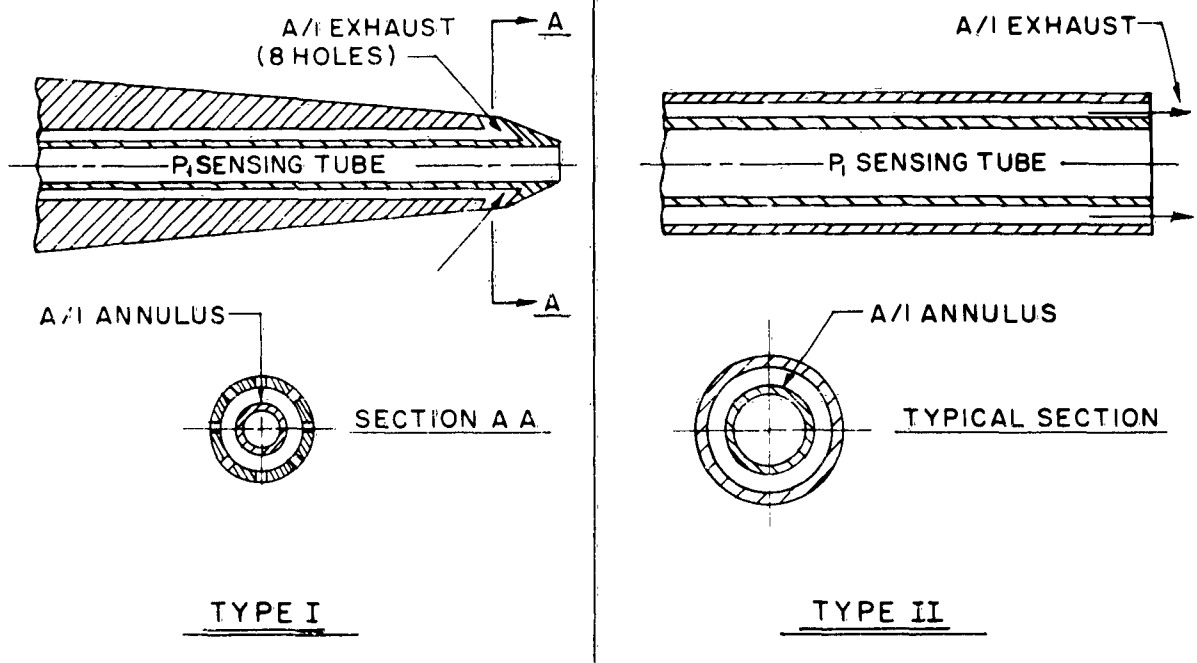
FIG. 14  
LR-305

INLET GUIDE VANE AND FIRST STAGE STATOR ICING CHARACTERISTICS  
OF VARIABLE INCIDENCE INLET GUIDE VANE ENGINE





DAMAGE TO LIGHT ALLOY TRANSONIC COMPRESSOR BLADE  
CAUSED BY INGESTION OF SMALL PIECES OF ICE



SHIELDED PITOT LOCATION

**RAM HEAD PITOT TUBE PROTECTION**

# THE EFFECTS OF BIRD INGESTION ON GAS TURBINE ENGINES

By: G. V. Bianchini  
Test Projects and Operations Department  
Experimental Test Section

## SUMMARY

This report generally discusses the potential hazard of bird strikes on gas turbine powered aircraft and specifically covers the evaluation of the structural integrity and operating characteristics of a current turbo-propeller engine during bird strikes. A resumé of bird strike experience with the cited engine in over 3.5 million hours of operation in multiple engine aircraft is also included.

## INTRODUCTION

During the development and certification of the 501 engine in 1955 and 1956 a number of studies and test programs were initiated to insure that the powerplant was capable of coping with the natural phenomena which present hazards to modern day all-weather flight operations. Among these are severe icing, hail, torrential rains, sand and dust storms, and bird strikes.

A search of available literature on bird strikes at that time indicated that C. A. A. Technical Development Report 62, entitled "Collision of Birds with Aircraft in Scheduled Commercial Operations in the Continental United States", was the most complete study and analysis on the subject. A study of this report revealed that 473 bird strikes were recorded by commercial air carriers for a period previous to 1942 through 1946. The report indicated that a bird collision occurred on scheduled aircraft each 759,000 miles of operation, which in 1946 corresponded to an average period of 0.89 days. The majority of these collisions occurred at relatively low elevations above the local ground level which would be in the take-off and landing regime of aircraft operation.

A study of the location, frequency and severity of the bird strikes on airplanes involved, indicated that only 9 percent (approximately 43) of the strikes occurred on the engines and propellers and that bird impacts in this location resulted in severe structural damage in 28 percent of the cases (approximately 12). Moderate structural damage occurred in 26 percent of the cases (approximately 11).

Although the statistics indicated that the frequency of bird strikes in the powerplant area of an aircraft was low, all of the available data concerned aircraft powered by conventional engines of the reciprocating type and few statistics were available for aircraft powered by gas turbine engines. Because of the limited bird strike data available on gas turbine engines, Allison initiated a program and assisted the C. A. A. (now the F. A. A. ) in conducting a series of bird strike tests at the C. A. A. Technical Development Center, Indianapolis, Indiana, for the purpose of evaluating the structural integrity of the Allison 501 series engine. These tests were conducted in September and October 1956, and consisted primarily of shooting freshly-killed, four pound chicken carcasses into an engine inlet at velocities ranging up to 380 miles per hour. To accomplish this test a gun, designed and developed by the C. A. A. for conducting tests on aircraft windshields, was used to project the chicken carcasses at the desired velocities. The projectile consisted of the chicken carcass backed by a styrofoam sabot 6 inches in diameter and 4 inches in length wrapped in a heavy paper bag. The entire package was 6 inches in diameter and 12 inches in length.

In the first phase of this program a "dummy" engine was used and chickens were propelled directly onto the inlet guide vanes to evaluate their structural integrity. In the second phase of the test the chickens were propelled into the inlet duct of an engine operating at its rated speed of 13,820 RPM but without its automatic control systems or propeller.

The results of the tests, as presented in C. A. A. Technical Development Report 312 entitled "Bird Ingestion Tests on an Allison T-56 Turbine Engine (Civil Model 501-D13)" written by John Sommers, Jr. and Roger C. Pate and published in May 1957, indicated that:

1. The inlet guide vanes could withstand the direct impact of this four pound chicken carcass package at speeds ranging up to 320 MPH without appreciable deformation.
2. The engine, as originally tested, could ingest these chicken carcass packages at speeds ranging up to 200 MPH without excessive structural damage.
3. The engine, as modified by the installation of strengthened inlet guide vanes and compressor stator vanes, ingested these chicken carcass packages at speeds ranging up to 290 MPH without excessive structural damage.

As indicated in the initial study on bird collisions with aircraft, bird ingestion is most likely to occur during landing and take-off which are the most critical periods of flight. The maximum bird velocity of 290 MPH which the engine withstood during these tests was well above the landing and take-off velocity of aircraft which would use this powerplant.

The completion of these tests in 1956 coincided with the early service of the C-130 airplane (powered by Allison T56-A-1 engines) in military operations and was well in advance of the Electra (powered by Allison 501-D13 engines) aircraft's introduction into service. Field surveillance of engine operation in the C-130, as well as in the Electra after it came into service, substantiated the conclusions of our experimental tests concerned with natural hazards. However, in October 1960 an aircraft accident involving a flock of birds created renewed interest and concern in the bird hazard.

As a result of this accident Allison conducted a series of tests to evaluate the 501 engine's characteristics during multiple strikes of small birds. The results of this program are the prime subject of this presentation.

A. Test Stand Evaluation of Allison Model 501-D13 Engine Characteristics During Multiple Strikes of Small Birds

1. Test Equipment, Set Up, and Technique  
(chart 1 and photograph 171416)

This program was conducted at Allison facilities, Indianapolis, Indiana, in November and December 1960, utilizing starlings, black birds and grackles. The weights of these birds ranged from 2 to 4 ounces.

A number of birds were captured alive and were put to death with use of CO<sub>2</sub> gas immediately before use in an experiment. A number of birds were also procured with use of shot guns and were quick-frozen for short time preservation. These birds, of course, were thawed prior to use in the program.

To accomplish the test, a 501-D13 engine was installed on a test stand with an Aeroproducts 606 propeller (without cuffs) and an Electra type air inlet duct and provisions were made

to introduce birds into the inlet air stream through four 2 1/2 inch diameter tubes located at the mouth of the air inlet duct just aft of the propeller. By manipulation of gates in these tubes, birds could be introduced either simultaneously or in sequence in quantities ranging up to eight birds. Although no attempt was made to give the birds an initial velocity in the aft direction to simulate a bird's entry into the duct during aircraft flight, it is felt that the tests were equal to and in some respects more severe than are strikes of this size bird in actual service.

The average drag force of the birds was experimentally determined in a wind tunnel by exposing a number of bird carcasses to the air stream at various attitudes. From these data a carcass drag coefficient was determined and it was calculated that the birds attained a final velocity of approximately 85 feet per second in the engine tests. If the birds had been ingested by an engine during aircraft take-off at 120 MPH, and did not strike the propeller or the duct before reaching the compressor inlet, the carcasses would theoretically attain a final velocity of 185 feet per second. However, under flight conditions the birds would first have a good chance of being struck by the propeller and secondly, would most definitely strike the aft portion of the inlet duct thus reducing the carcass velocity well below the calculated value of 185 feet per second to one closer to the calculated velocities in the ingestion tests. The impact with the aft portion of the duct is significant in that it breaks up the bird and the engine needs only ingest bird fragments as they disperse over the face of the compressor. Since the birds did not strike the inlet duct in the engine tests and were intact when they reached the compressor inlet, the tests were considered to be quite realistic from an impact standpoint and more severe from a blockage or ingestion standpoint than strikes in service.

Basic engine parameters were recorded by fast response electronic recorders and motion pictures were taken of the engine inlet and exhaust as well as of Electra aircraft instruments. The instruments displayed engine speed, power, turbine inlet temperature and fuel flow. It should be noted here that the signal from the thrust sensitive system switch was not permitted to auto-feather the engine but was one of the parameters recorded.

To accomplish the inlet photography, lights were installed on the test cell structure forward of the propeller and were targeted on the inlet. A high speed motion picture camera mounted on the air inlet duct viewed the compressor inlet via a 2 1/2 inch diameter mirror and exposed film at the rate of 3000 frames per second. The exhaust section and instruments were photographed by standard motion picture cameras mounted on the test stand and in the control room, respectively. The exhaust section was photographed at 64 frames per second (slow motion) and the instruments were photographed at 24 frames per second.

In an attempt to simulate propeller operating conditions in flight, the propeller flight low pitch stop setting at a 90° coordinator setting (take-off power) was reduced from the standard value of 31.5° to 18.5° propeller blade angle. Since the engine is equipped with features to prevent excessive drag, very little energy can be transmitted from the air stream to the engine to aid its recovery and this adjustment resulted in a propeller characteristic that closely approximated the flight condition. Therefore, major differences would not be expected between the results of this test program and the results of a bird strike in flight or the results of a test program conducted with simulation of engine forward velocity. It would be expected, however, that the engine could ingest more birds and recover somewhat more rapidly with the forward or simulated forward velocity due to the slight differences in propeller performance characteristics.

The effects of the low pitch stop adjustment may be better visualized and the differences between the Allison tests and actual flight or wind tunnel tests may be better explained by a plot of engine speed vs propeller shaft horsepower (chart 2). This plot presents specification engine power available at constant turbine inlet temperatures and the propeller load curves at 0 and 120 KIAS. It is readily apparent from this plot that the 31.5° blade angle is unrealistic for bird strike tests under static conditions whereas the 18.5° blade angle provides a very satisfactory compromise for static testing. Specifically, a comparison of the propeller horsepower requirements at three engine speeds is as follows:

	<u>31.5° at 120 KIAS</u>	<u>18.5° at 0 KIAS</u>
13,880 RPM	690	490
12,800 RPM	400	400
12,000 RPM	160	300

Basically, the comparison indicates that the air speed would aid engine recovery below 12,800 RPM and would hinder recovery to a small extent above 12,800 RPM.

An engine performance calibration was made prior to starting the test program and a calibration was completed after each experiment to determine the performance depreciation created by the contamination of the compressor etc. An inspection of the engine, which consisted of viewing the compressor inlet, turbine outlet, compressor bleed valves and turbine inlet thermocouples, was also completed after each experiment. After completing the calibration and inspection the engine was normally cleaned with use of four gallons of walnut shells per the standard field cleaning procedure after which another calibration was completed to verify the original performance baseline.

A total of sixteen experiments using forty-five birds was completed during the tests and the majority of the experiments were conducted at take-off power which under the prevailing test stand conditions was usually 3200 to 3500 HP.

## 2. Test Results and Conclusions

The results of this program were as follows:

- (a.) Engine flame-out was not encountered at any time during the test.
- (b.) The ingestion of one bird had practically no effect on the power and speed of the engine.
- (c.) The simultaneous or closely sequenced ingestion of two or three birds caused a loss of power and speed for 2 1/2 to 3 1/2 seconds. The minimum horsepower reached was 1000 and the performance depreciation after recovery was 450 HP.
- (d.) Four birds were ingested during each of five experiments. In two of these experiments the engine recovered and in the other three it had to be shut down by the operator to prevent overtemperature and burning of the turbine.

- In one of the two four-bird strikes from which the engine recovered there was no momentary drop in speed or power but the performance depreciation was 400 HP. In the other instance there was a drop in speed and power for 4 1/2 seconds. The minimum horsepower reached was 750 and the performance depreciation was 400 HP after recovery.
- (e.) Eight birds were ingested on two occasions. On the first occasion the momentary speed and power loss lasted 4 1/2 seconds. The minimum power was 600 HP and the performance depreciation was 1100 HP immediately after recovery and 900 HP thirty seconds following the bird ingestion. The engine did not recover from the second test involving the eight birds. It was shut down within six seconds from the strike because of excessive turbine inlet temperatures. Within this six second interval the outer half of the first stage turbine blades had been burned off.
  - (f.) The thrust sensitive system switch (auto-feather) was actuated within 0.5 to 1.1 seconds after all but two of the multiple bird strikes. The moment of impact was considered to be the instant at which a decrease in speed was evident.
  - (g.) Performance depreciation attributed to contamination of the engine from the ingestion of birds was always satisfactorily recovered by cleaning with walnut shells per the standard field cleaning procedure.
  - (h.) No compressor damage was sustained from the ingestion of birds.
  - (i.) With the exception of the last experiment involving eight birds, no turbine damage was sustained although there was slight deformation of several turbine inlet thermocouples during the test.

### 3. Discussion

As can be seen in a comparison of electronic recordings of basic engine parameters on two typical experiments during the program, (Chart 3), the engine either recovered quickly or remained in a condition that would burn the turbine blades. There was never a prolonged loss of power followed by recovery.

The momentary loss of power and speed can be attributed to both the partial blockage of the inlet air as the carcass enters the engine and the major alterations of the flow path in the compressor which are due to blockage created by the bulk of the carcass as it passes through the engine. As this occurs a secondary effect of a nebulous nature is the release of steam in the compressor from the body fluids of the birds. The blockage and contamination of the compressor result in a reduction in air flow and efficiency. Without a change in turbine operating temperatures this reduction in air flow and efficiency must result in a loss of power. Even though the turbine inlet temperature rose, at least momentarily, during the ingestion tests, power decreased because of the magnitude and predominance of the compressor losses. In extreme conditions, the blockage and contamination of the compressor can be sufficient to cause compressor stall and a resultant power loss until the compressor recovers, if recovery is possible.

In twelve of the sixteen experiments, flashes of flame were emitted from the tailpipe. These flashes are associated with the tendency for the compressor to stall aerodynamically, as previously mentioned, with a resultant decrease in airflow delivery to the combustion section. With this momentary interruption in airflow the fuel-air mixture becomes rich and the flame front moves aft through the turbine making the flame visible.

In no instance was flame ever emitted from the inlet duct or bleed manifold. In regard to the flashes from the tailpipe, it can be generally stated that the number and intensity of the flashes increased with the number of birds ingested.

The performance depreciation observed following a bird strike can be attributed to the fouling of the aerodynamic surfaces of the compressor blades and vanes by deposits of the fibrous remains of the bird carcasses with a resultant reduction in their efficiency. This depreciation was as high as 1100 HP from the ingestion of eight birds and as low as 400 HP from the ingestion of three or four birds. This performance was always recovered by the recommended field cleaning procedure which is the injection of four gallons of crushed walnut shells into the compressor inlet.

Following these tests, the field service reports concerning bird strikes were further scrutinized to correlate their information with the results of this test program.

B. 501 Series Engine Bird Strike Experience in Service

Through January 1, 1961 there have been only nine (9) bird strikes reported as occurring during some phase of flight on the 501 series engine in over 3.5 million hours of operation in multi-engine aircraft in both military and commercial service. There have also been a small number of other reports of "evidence of bird ingestion." These reports resulted when minor damage was found on the air inlet ducting or feathers, blood smears and small portions of bird carcasses were found in the engine air intake area during routine inspection etc. This does not imply, however, that other strikes have not occurred but instead have gone unreported because they were not actually observed and had no effect on the engine.

Through 1 January 1961, the 501 engine has a record of never requiring premature removal as the result of a bird strike and it is known that the engine has taken on birds ranging to four pound gulls. One engine was temporarily removed from service, at the discretion of the operator, as a precautionary measure but our records indicate that the engine was not disassembled but was immediately returned to service after simply completing an inspection, cleaning and check run.

Many of you, especially those of you who have recently been active on the bird strike problem and its effects on gas turbine engines, may be asking yourselves two questions at this moment. Namely: (1) Why so few reported bird strikes or incidents of bird ingestion on this engine in 3.5 million hours of operation and (2) why has the engine escaped mechanical damage due to bird strikes

In regard to these questions it is known that the engine is basically rugged and it is felt that the use of an 'S' shaped air inlet duct, as is dictated by the mechanical layout of the engine, is a "built in" bird strike protective measure. That is, the duct must take the initial impact of the bird. The majority of the energy then is dissipated in this initial impact with a

resultant breakup of the carcass as well as a reduction in carcass velocity. The breakup allows the birds to enter the rotating blades to be consumed with less effective inlet blockage and, with the drastic reduction in energy level, the mechanical force of the impact on the guide vanes is low. All of this minimizes the effects of the strike on the engine and it is presumed that some strikes go unnoticed.

The propeller is another possible consideration for the low number of reported strikes on the engine. Although an exhaustive study of the probabilities of birds passing through the plane of the rotating propeller and into the air inlet has not been made, hail impact tests, where ice balls were fired at the cuffs of a rotating 606 propeller, indicated that only 40% passed through the propeller undamaged. The remainder struck the propeller and were broken up or were thrown clear of the air inlet duct.

Based on a cross-check of records and an analysis of these nine reported strikes on the engine, it was determined that four of these strikes resulted in an in-flight feather shutdown, two of which were reported to have auto-feathered. The other two were reported to have been manually shutdown but based on the time element involved it is possible that the emergency shutdown handles may have been pulled after the auto-feather had actuated.

Of the five remaining strikes three resulted in fluctuations of engine parameters with almost immediate recovery. There were no discrepancies reported on the other two strikes.

After several of the strikes, a check of engine performance indicated a performance depreciation ranging from 100 to 500 HP. However, because the gas turbine engine is somewhat of a self-cleaning machine, the performance was regained with continued operation. Usually this occurred before completion of the flight on which the strike occurred - 2 to 3 hours.

It may be noted that the indications of bird strikes in service agree well with the results of our bird strike test program:

1. No flame-out encountered
2. No mechanical damage encountered

3. Fluctuations of turbine inlet temperature, power and speed with almost immediate recovery
4. Performance depreciation following a strike
5. Auto-feathering

C. Generalized Comparison of Bird Strikes on Gas Turbine Engines

Based on the analysis of our test results, the information we presently have on bird strikes on gas turbine engines in service, and a general consideration of gas turbine engine characteristics, the following generalized statements can be made concerning bird strikes on turbo-propeller and turbo-jet engines:

- (1) With the exception of the effect a propeller has on birds passing through its plane of rotation, the number of bird strikes on turbo-propeller or turbo-jet aircraft engines are proportional to their air inlet area assuming identical exposure rates.
- (2) Slightly different aerodynamic and mechanical effects can be expected between strikes, and were noted during the tests, because of the variation in the mechanics of the bird carcass entry into the compressor. The variations in the mechanics of entry can be observed in the high speed motion picture film of the tests.
- (3) The strike of a given size bird tends to have greater aerodynamic effect on a small engine than on a large engine because of the greater bird mass to inlet area ratio. Also, during the ingestion process, the bulk of the carcass and to some extent the body fluids of the bird passing through the compressor will alter the air flow to a greater degree.
- (4) The strike of a given size bird tends to cause greater mechanical damage on a large engine because of the greater leverage involved with the longer blade and vane spans as the bird strikes and the ingestion process takes place. The deflection of blades etc. tends to create interference between rotating and stationary parts.

D. Motion Picture Film - Test Stand Evaluation of Allison Model 501-D13 Engine Characteristics During Multiple Bird Strikes

E. Electra Accident

With the testing that has been completed and the experience that has been gained with the engine in service, one could conclude that the possibilities of bird strikes on the powerplants creating a major problem are extremely remote. However, there is the case of the recent accident in which birds are involved. Although this presentation makes no attempt to solve the so-called "Case of the Boston Electra", an attempt will be made to relate the Allison test results to the accident and the findings concerning the engines of that aircraft.

As can be noted from this presentation thus far, there are three major points of significance: (1) flame-out was never encountered, (2) the engine either recovered quickly or remained in a condition that would burn the turbine blades in a few seconds. There was never a prolonged loss of power followed by recovery and (3) the auto-feather system can be actuated by bird strikes. In the Electra, this could occur only on one engine because the thrust sensitive system is blocked out electrically after one engine has been feathered.

During the investigation of the subject accident the general agreement of the engine instruments, the appearance of the engines after recovery, and the propeller blade angles left no doubt that at the time of impact number 2, 3 and 4 engines were delivering substantially take-off power and that the number one engine had been feathered. (Reference Chart 4).

The engines were disassembled for inspection and an analysis of foreign materials found within the engines indicated that engines 1, 2 and 4 had ingested birds. There was no evidence of bird remains in engine number 3, however. A comparison of the three engines that had ingested birds with the appearance of our test engine at various intervals during our test program indicated that they had not ingested more than two or three birds. This observation was confirmed by the engine performance at impact since the greatest depreciation was on number 2 and was only 315 HP below specification. Ingestion of two or three birds during our tests resulted in a performance depreciation of approximately 450 HP.

Because the number 2 and 4 engines ingested birds, it is concluded that they had a temporary power loss but based

3. Fluctuations of turbine inlet temperature, power and speed with almost immediate recovery
4. Performance depreciation following a strike
5. Auto-feathering

C. Generalized Comparison of Bird Strikes on Gas Turbine Engines

Based on the analysis of our test results, the information we presently have on bird strikes on gas turbine engines in service, and a general consideration of gas turbine engine characteristics, the following generalized statements can be made concerning bird strikes on turbo-propeller and turbo-jet engines:

- (1) With the exception of the effect a propeller has on birds passing through its plane of rotation, the number of bird strikes on turbo-propeller or turbo-jet aircraft engines are proportional to their air inlet area assuming identical exposure rates.
- (2) Slightly different aerodynamic and mechanical effects can be expected between strikes, and were noted during the tests, because of the variation in the mechanics of the bird carcass entry into the compressor. The variations in the mechanics of entry can be observed in the high speed motion picture film of the tests.
- (3) The strike of a given size bird tends to have greater aerodynamic effect on a small engine than on a large engine because of the greater bird mass to inlet area ratio. Also, during the ingestion process, the bulk of the carcass and to some extent the body fluids of the bird passing through the compressor will alter the air flow to a greater degree.
- (4) The strike of a given size bird tends to cause greater mechanical damage on a large engine because of the greater leverage involved with the longer blade and vane spans as the bird strikes and the ingestion process takes place. The deflection of blades etc. tends to create interference between rotating and stationary parts.

D. Motion Picture Film - Test Stand Evaluation of Allison Model 501-D13 Engine Characteristics During Multiple Bird Strikes

E. Electra Accident

With the testing that has been completed and the experience that has been gained with the engine in service, one could conclude that the possibilities of bird strikes on the power-plants creating a major problem are extremely remote. However, there is the case of the recent accident in which birds are involved. Although this presentation makes no attempt to solve the so-called "Case of the Boston Electra", an attempt will be made to relate the Allison test results to the accident and the findings concerning the engines of that aircraft.

As can be noted from this presentation thus far, there are three major points of significance: (1) flame-out was never encountered, (2) the engine either recovered quickly or remained in a condition that would burn the turbine blades in a few seconds. There was never a prolonged loss of power followed by recovery and (3) the auto-feather system can be actuated by bird strikes. In the Electra, this could occur only on one engine because the thrust sensitive system is blocked out electrically after one engine has been feathered.

During the investigation of the subject accident the general agreement of the engine instruments, the appearance of the engines after recovery, and the propeller blade angles left no doubt that at the time of impact number 2, 3 and 4 engines were delivering substantially take-off power and that the number one engine had been feathered. (Reference Chart 4).

The engines were disassembled for inspection and an analysis of foreign materials found within the engines indicated that engines 1, 2 and 4 had ingested birds. There was no evidence of bird remains in engine number 3, however. A comparison of the three engines that had ingested birds with the appearance of our test engine at various intervals during our test program indicated that they had not ingested more than two or three birds. This observation was confirmed by the engine performance at impact since the greatest depreciation was on number 2 and was only 315 HP below specification. Ingestion of two or three birds during our tests resulted in a performance depreciation of approximately 450 HP.

Because the number 2 and 4 engines ingested birds, it is concluded that they had a temporary power loss but based

on the quantity of bird remains and performance upon crash impact as previously discussed, it is also concluded that recovery occurred in less than 3 1/2 seconds. The rapid recovery is substantiated by the lack of evidence of over-temperature in any of the parts of the accident engines and that the condition of the parts was representative of normal operating units. In the test engine the first stage turbine blades were burned off within six seconds on one experiment where rapid recovery was not accomplished.

The collision with the flock of birds occurred approximately six seconds after the aircraft became airborne and although there was a loss of one engine, presumably due to autofeather, and a momentary decrease in power on two engines, the recovery of the latter within 3 1/2 seconds made more than 10,000 horsepower available to the airplane for the remaining portion of the flight. Based on Civil Aeronautics Board data the aircraft was airborne for a total of approximately 27 1/2 seconds.

As of this date the investigation of this accident is still open.

F. F. A. A. Bird Control and Engine Bird Strike Programs

It is understood that plans are presently being completed to conduct wind tunnel tests of all commercial gas turbine engines to evaluate their tolerance to bird strikes and bird ingestion. This program is to include study and evaluation of methods to increase the tolerance of gas turbine engines to such occurrences and, if feasible, methods of preventing birds from entering engines.

It is also understood that considerable effort is presently being expended in reducing the bird population in the vicinity of airports. It would presently appear that this may be the most effective effort, from the overall standpoint of flight safety, in combating the bird hazard in that the majority of bird strikes occur during take-off and landing and that areas of the aircraft, other than the powerplant, such as windshield visibility, instrument pressure sensing points etc. can be affected.

MODEL 501-D13 ENGINE  
AND  
AEROPRODUCTS A644IF-606 PROPELLER  
INSTALLATION  
ELECTRA QEC

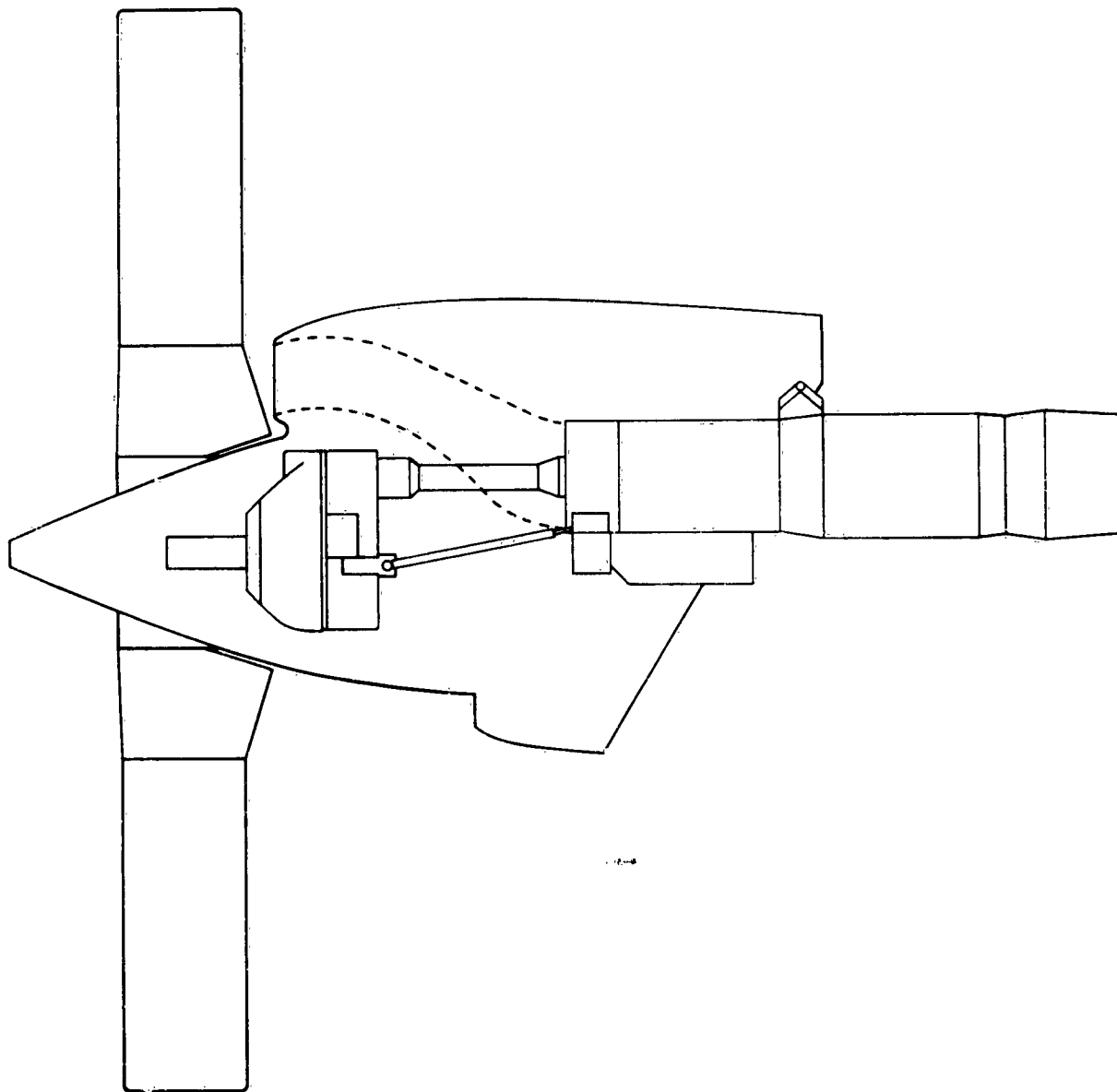


**CHART I**

MODEL 501-D13 ENGINE  
 AND  
 AEROPRODUCTS A6441FN-606 PROPELLER  
 PERFORMANCE AT STANDARD SEA LEVEL CONDITIONS

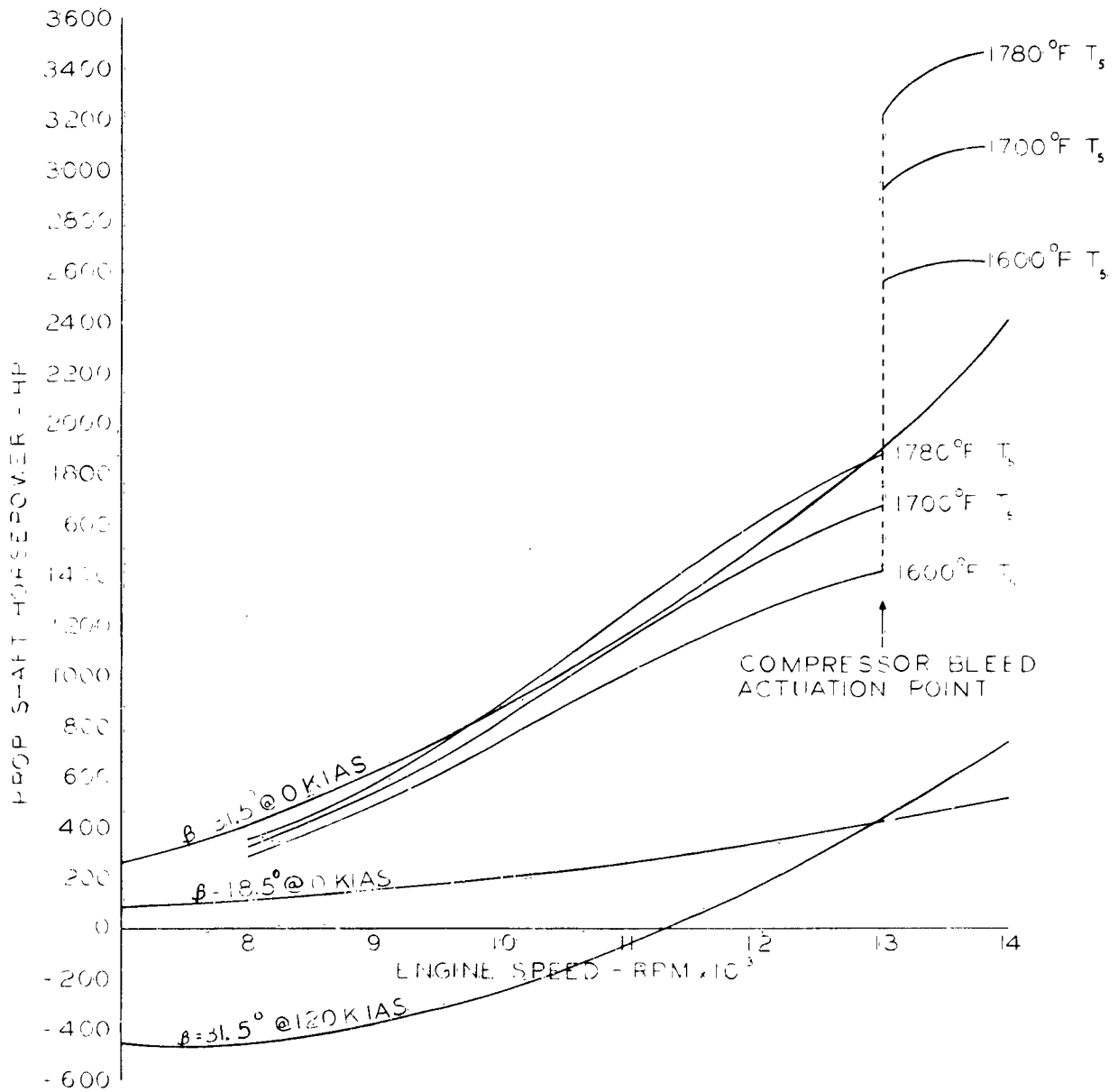
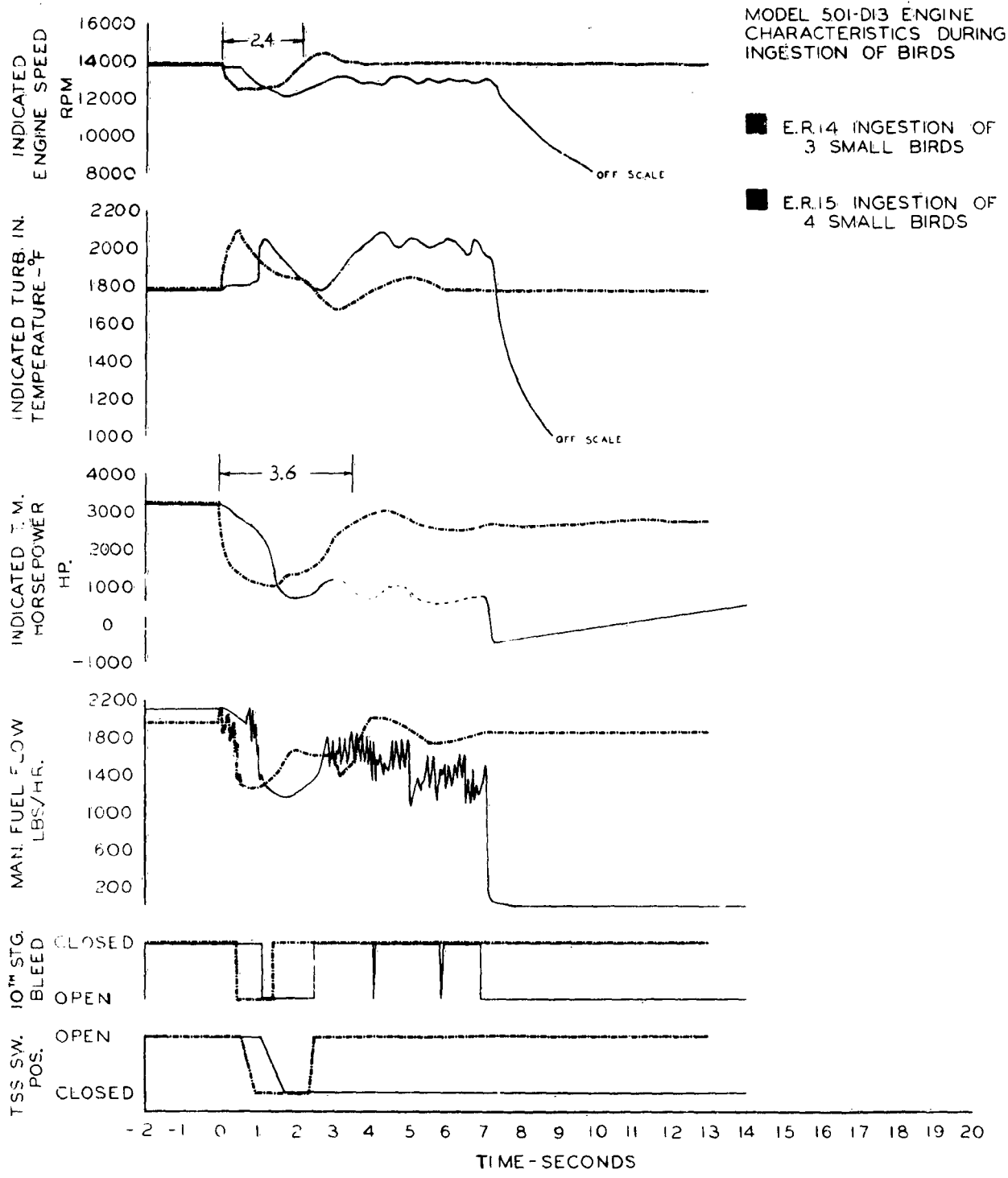


CHART 2

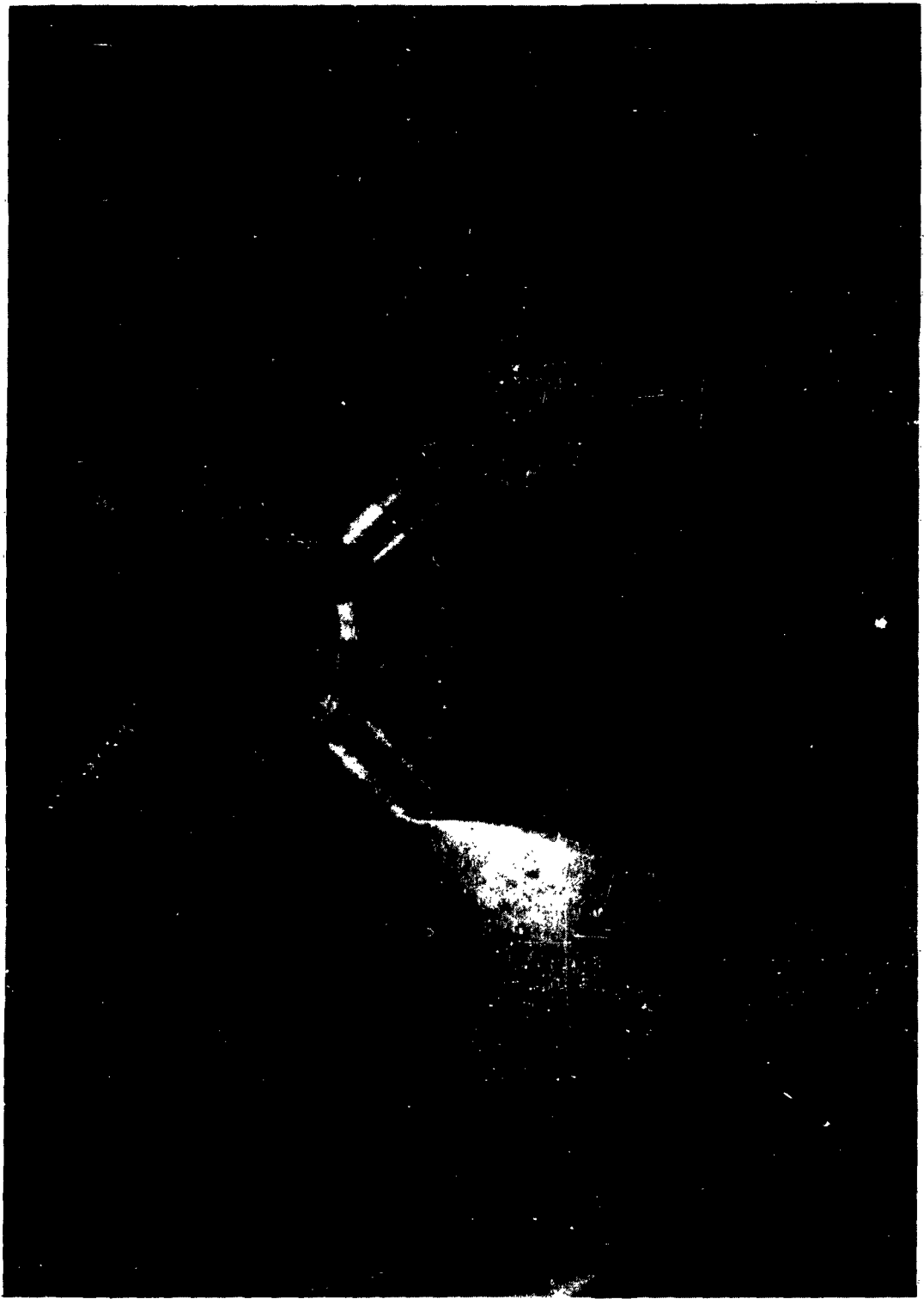


**CHART 3**

EASTERN LI88 ELECTRA N5533  
 FLIGHT 375-4  
 POWER PLANT DATA

ENGINE POSITION	1	2	3	4
HORSEPOWER				
T.M. INDICATOR	-850	3350	3360	3550
PHASE DETECTOR	-875	3315	3310	3555
TURBINE IN. TEMP.				
°C	400	978	950	960
°F	752	1793	1742	1759
PROPELLER BLADE ANGLE, °	FEATHERED	39.9	40.9	41.1 (43.0)
FUEL FLOW, LBS./HR.	UNKNOWN	1785	2050	1950

**CHART 4**



INGESTION TEST INSTALLATION ENGINE A-200138 B. U. 24 RIGID STAND NO. 3

PHOTO 171416

EFFECTS OF WATER INGESTION ON TURBOJET  
ENGINE OPERATION

by

Irving Davids

Robert S. Babington

and

William R. Warwick

Aeronautical Turbine Laboratory

U. S. Naval Air Turbine Test Station

Trenton, New Jersey

The problem involving the ingestion of water into a turbojet engine had become of increasing importance with the advent of the all-weather fighter aircraft. Water ingestion tests have been conducted at the Aeronautical Turbine Laboratory on the J71-A-2 engine used in the F3H aircraft, the J79-GE-2 engine used in the F4H, and the J57-P-20 engine used in the F8U-2N aircraft. The purpose of this paper is to discuss the effects the ingestion of water has on these engines tested at the Aeronautical Turbine Laboratory.

Method of Test

Water was introduced into the engine by means of a circular spray bar mounted in the center of the inlet duct to the engine and a ring of orifice type nozzles mounted in the duct wall injecting water perpendicular to the airstream. This is shown on Fig. Number 1. The circular spray bar was used at all times while the nozzles were used only at the high water rates required during sea level operation.

During the tests, no effort was made to control droplet size. It has been found by the Royal Aircraft Establishment in TN ME 239 that a change in air velocity will shatter large droplets of water. Since under actual flight conditions the inlet duct Mach number will differ from the flight Mach number, large raindrops should be shattered before they reach the engine inlet.

There were two procedures used in injecting the water into the engine:

(1) First procedure was to introduce the water gradually until the required water rate was obtained and then stabilize for approximately five minutes of engine operation.

(2) The second procedure was to introduce the required water rate instantaneously.

### Quantity of Water Ingested

The amount of water which an engine will ingest at a particular atmospheric water content depends on the geometry of the engine-airframe installation. Fig. Number 2 shows the total effective ingestion area of the three engines tested at the Aeronautical Turbine Laboratory. It is noted from this figure that in the case of the F3H aircraft using the J71 engine, although the jet intake area of 4.1 ft<sup>2</sup> was approximately the same as that of the J57 in the F8U-2N and actually smaller than the J79 used in the F4H, the total effective ingestion area was appreciably greater than the other aircraft. This was due to the large projected run-off area. During aircraft flight, the quantity of water ingested is directly proportional to the water concentration in the air and the volume swept out by the ingestion area. The result of this engine-airframe geometry on the quantity of water which would be ingested can be seen from the table on Fig. Number 3. This table shows the maximum amount of water which the engines would ingest at a meteorological water content of 10 gm/ M<sup>3</sup> at an altitude of 35,000 feet and a flight Mach number of 0.9. This water content of 10 gm/ M<sup>3</sup> was selected as the maximum which an engine would have to be capable of ingesting. It must be noted however, that due to a limited amount of information available as to the probability and extent of liquid water in the atmosphere, this maximum rate used during the tests could be either conservative or radical.

It is seen from this table that at 10 gm/ M<sup>3</sup>, due to the large ingestion area of the F3H installation, the J71 engine would ingest water up to a water to air ratio of 9.9 percent whereas the J79 in the F4H would ingest 4.5 percent and the J57 in the F8U-2N would only ingest water to air ratios as high as 3.6 percent. It is apparent therefore that the installation of an engine in the airframe has a marked effect on the amount of water the engine must ingest in flight.

### Results and Discussion

The major effects water ingestion has on the turbojet engine can be classified into three general problem areas:

(1) The possibility of obtaining a mechanical failure such as a compressor rub.

(2) The aerodynamic effects of water ingestion on the gas generator.

(3) The effect of water ingestion on the engine windmill starting characteristics.

#### A. Mechanical Effects of Water Ingestion.

The mechanical effects resulting from the ingestion of water are primarily those caused by the distortion of the compressor case.

In order to determine the effect water had on compressor clearances, special instrumentation was provided on the J71 and J79 engines. The instrumentation consisted of brass rub pins which were cut back by the rotating compressor when there was a decrease in clearances. By means of measuring these pins, the decrease in clearances was obtained. It was not possible to install instrumentation on the J57 engine and, therefore, the possibility of a rub was monitored by the vibration level of the engine.

##### 1. J71 engine tests.

Tests were conducted on the J71 engine over a range of altitudes from sea level to 20,000 feet. It was found that for a fixed water/air ratio changing altitude did not have any effect on compressor clearances. Changing altitude from sea level to 20,000 feet for a constant water to air ratio represents a range of liquid water content and since there was no change in clearances, this indicated that the effect of water on compressor clearances is primarily a function of water to air ratio. This is significant since it shows that the results of tests obtained at a single altitude over a range of water to air ratios would be indicative of results at other altitudes.

As mentioned previously, compressor rub is caused primarily by case distortion. Fig. Number 4 shows the circumferential variation on compressor case temperatures obtained on the J71 engine at water to air ratios of 2.5 percent and 7.6 percent. It is shown on this figure that at a water to air ratio of 2.5 percent, there was a large temperature gradient ranging from 310°F to as low as 60°F. As a result of this temperature gradient, the compressor case distorted in the shape of an ellipse with the major axis passing through the 3:00 o'clock and 9:00 o'clock positions.

This distortion resulted in an interstage seal rub which was severe enough to cut through the rotor at the eleventh stage of the compressor. This resulted in a major engine failure. Having increased the interstage radial seal clearances, it was then possible to increase the water to air ratio up to 3 percent at which time there was an axial seal rub. This was caused by the compressor rotor shifting forward an additional .075 to .085 inch. The rotor was repositioned and tests were continued at water to air ratios above 3 percent.

It is important to note from Fig. Number 4 that as the water rate was increased, the temperature gradient became uniform around the compressor case. This was caused by the water remaining in a liquid state at the higher water to air ratios. This uniform profile results in no further distortion of the case and, therefore, no further changes in compressor clearances. This can be seen from Fig. Number 5 which shows the maximum change in compressor tip clearances as a function of water to air ratio. At a water to air ratio of approximately 4 percent, there were no additional changes in these clearances. This is a definite indication that the maximum amount of case distortion was reached at a water to air ratio of approximately 4 percent. I would like to summarize that by increasing the radial seal clearances and changing the axial position of the rotor to the clearances established at the Aeronautical Turbine Laboratory, the J71 engine is capable of ingesting water up to a water to air ratio of 9.6 percent. The limit at 9.6 percent was an engine flameout.

## 2. J79 engine tests.

A minimum compressor tip rub was obtained on the J79 engine. Fig. Number 6 shows the circumferential case temperature gradient which was obtained on the J79 engine at water to air ratios of 2.1 percent and 4.7 percent. It is seen from this figure that a temperature variation of as much as 220° F was obtained at a water to air ratio of 2.1 percent. It is important to note that at a water to air ratio of 4.7 percent, a uniform temperature profile was obtained. This effect was similar to that obtained on the J71 engine. It is therefore apparent that the major problem with respect to a compressor rub for both the J71 and J79 engines occurred at low water to air ratios up to 4 percent. No problems occurred at higher water to air ratios. This is significant since it clearly indicates that any compressor rub problem would probably occur at low water to air ratios.

The rub which occurred on the J79 engine was not severe and no changes in clearances were recommended.

### 3. J57 engine tests

There was no compressor instrumentation installed on the J57-P-20 engine as mentioned previously. However, no major mechanical problems occurred based on the vibration level of the engine.

#### B. Aerodynamic Effects of Water Ingestion.

As a result of water ingestion, a turbojet engine may encounter compressor surge or an engine flameout.

When water is ingested into the inlet of a jet engine, an evaporative cooling process occurs. This process extracts heat from the air passing through the compressor and increases the corrected rotor speed of the compressor. With the increase in corrected rotor speed, the compressor operates at a higher corrected airflow and higher compressor pressure ratios. This is illustrated in Fig. Number 7. Point 1 on this figure shows the operating point for an engine with no water ingestion. As water is ingested into the engine, this operating point moves to point 2 on the curve. The corrected airflow and pressure ratio at point 2 is greater than that at point 1 because of the increase in corrected rotor speed resulting from the evaporative cooling process. At point 2, no further evaporation occurs in the compressor because the air is saturated at the compressor discharge. As the water rate is increased above that at point 2, liquid water enters the combustion chamber. Upon entering the combustion chamber, the water flashes into steam and displaces some of the compressor discharge air. This results in a decrease in airflow and a simultaneous increase in compressor pressure ratio. This process is shown on the figure as 2-3. The surge margin is decreased when liquid water enters the combustion chamber as seen on this figure. It is conceivable that an engine with a small surge margin could encounter surge during a heavy rainstorm especially if the aircraft were performing a maneuver which produced inlet distortion and a further reduction in surge margin.

Of the three engines tested at the Aeronautical Turbine Laboratory for water ingestion capabilities, the J71 engine and the J79 engine (both single spool engines) experienced a shift in the operating line as shown on this figure, process 1-2-3. With

the J57 engine (which is a twin spool engine), only a process similar to 1-2 occurred. Process 2-3 did not occur on the J57 engine since liquid water did not enter the combustion chamber.

No surge was encountered on either the J71 or J79 engines. A chug condition was encountered on the J57 engine at a water to air ratio of 3.6 percent. It was possible to prevent chug on the J57 engine by reducing engine speed slightly.

In all the engines tested, as the water to air ratio was increased there was an increase in corrected net thrust and an increase in thrust specific fuel consumption. There was approximately a 10 percent increase in thrust specific fuel consumption for the J79 engine and one-half percent increase in thrust specific fuel consumption for the J57 engine. It is felt, however, that since the time in flight through severe weather conditions is small, the increase in specific fuel consumption is not a major problem.

#### C. Engine Windmill Starting Characteristics.

Third general problem area is the effect of water ingestion on the windmill starting characteristics. Windmill starting tests with water ingestion were conducted at the Aeronautical Turbine Laboratory on the J71-A-2 engine. The effect of water ingestion on the starting envelope is shown on Fig. Number 8. It is noted from this figure that as the water ingestion rate was increased, there was a reduction in the windmill starting envelope. At the higher water to air ratios, the maximum starting altitudes occurred at 230 KIAS, the recommended glide speed of the F3H-2N aircraft. Water seemed to have little effect on the starting characteristics in the low speed-high altitude region. At the high speed-high altitude portion of the envelope, low water to air ratios (.01 or lower) had a marked effect on the engine's starting characteristics. At a flight Mach number of 0.80 for example, a water to air ratio of .01 caused approximately a 7000 feet reduction in maximum light-off altitude. This area is normally a region of very lean starting fuel-air ratios. With the addition of water, the compressor discharge temperature is lowered, causing less fuel vaporization and even leaner fuel-air ratios so that a non-combustible mixture results. Another factor is that at windmill speeds, liquid water is carried into the combustor where it absorbs some of the heat energy of the igniter plugs which further decreases the starting ability of the engine. With the J71 engine during the windmill starts, the compressor

bleed valve was normally open. This resulted in some water being discharged through the bleed port. It is possible that for an engine which does not utilize open compressor bleeds during windmill starts, there would be a greater detrimental effect of water ingestion on the windmill starting characteristics. Water tests are continuing at the Aeronautical Turbine Laboratory on other engines. All engines received at the Naval Air Turbine Test Station will be checked with regard to water ingestion capabilities.



↑  
WATER IN

**FIG. I-WATER SPRAY MANIFOLD**

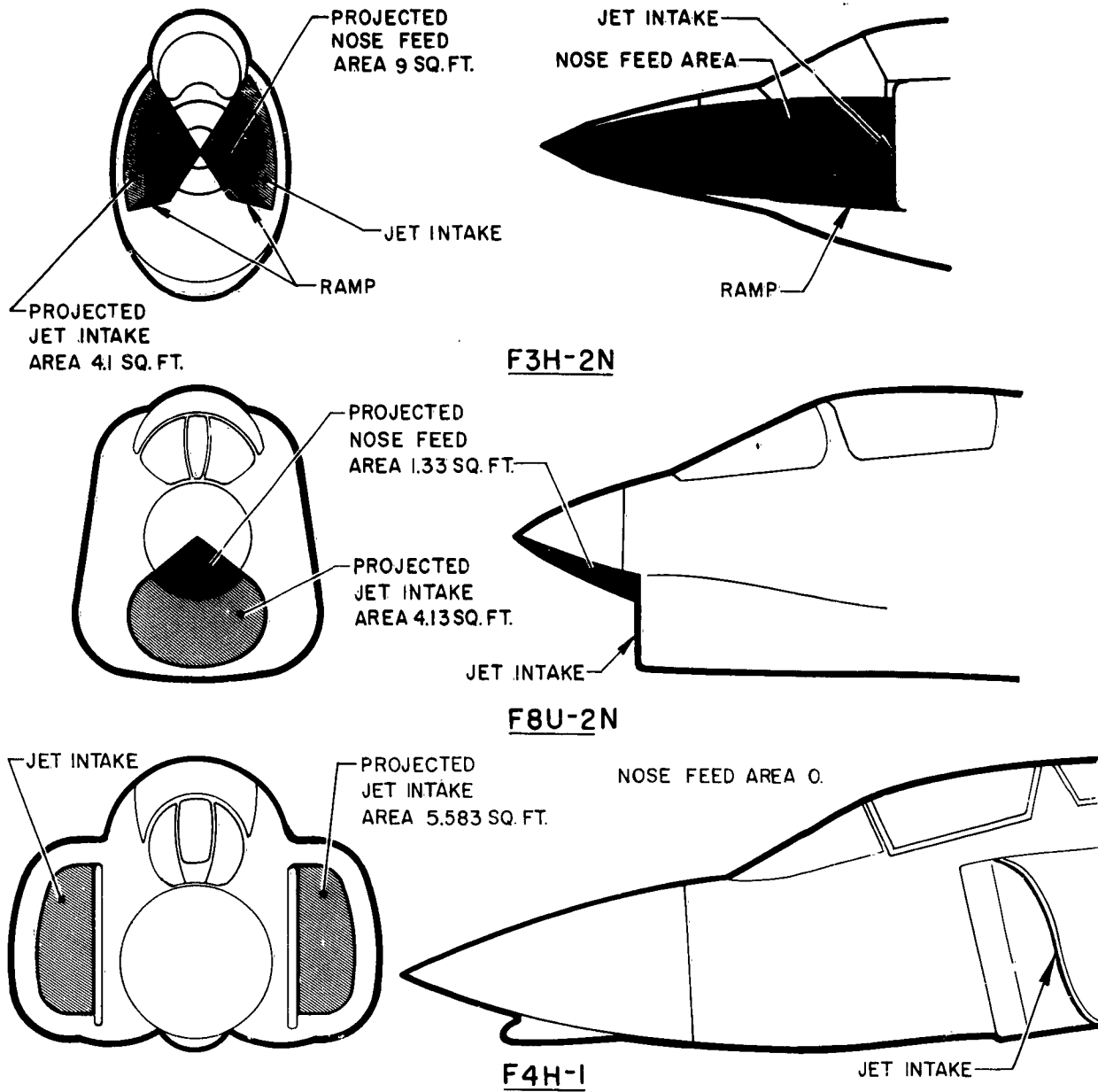


FIG. 2-EFFECTIVE INGESTION AREAS OF F8U-2N, F3H-2N AND F4H-1 AIRCRAFT

	J71-A-2 F3H	J79-GE-2 F4H	J57-P-20 F8U-2N
FLIGHT MACH NO.	0.9	0.9	0.9
LWC GM/M <sup>3</sup>	10	10	10
ALTITUDE	35000	35000	35000
AIRFLOW #/SEC.	72.0	69.0	82.0
JET INTAKE AREA(FT <sup>2</sup> )	4.1	5.58	4.13
PROJECTED RUN OFF AREA	9.0	0	1.33
TOTAL EFFECTIVE INGESTION AREA	13.1	5.6	5.46
% Ww/WA	9.9	4.45	3.6

FIG. 3 - EFFECT OF ENGINE AIRFRAME  
INSTALLATION ON WATER  
INGESTED DURING FLIGHT

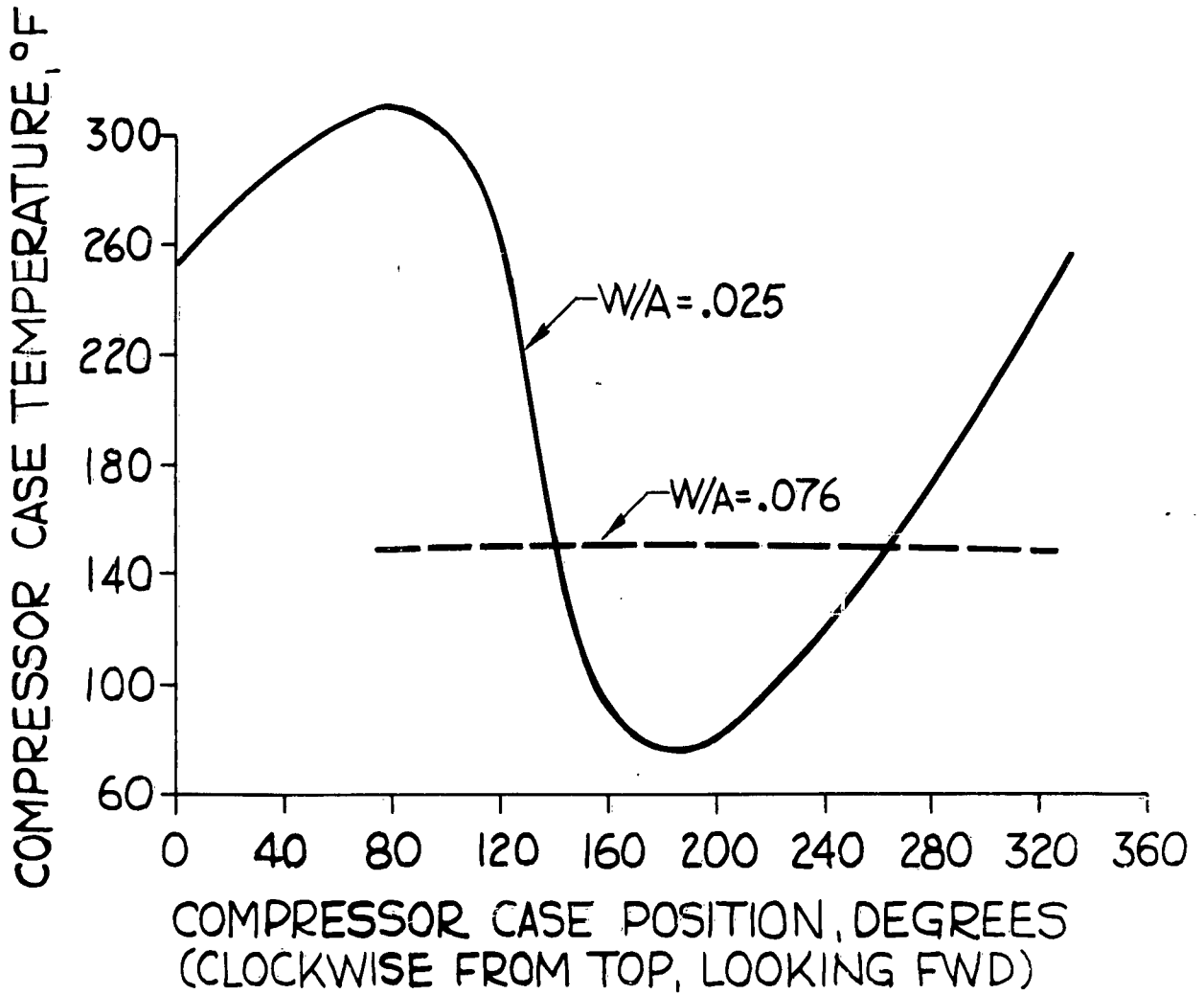


FIG. 4 - EFFECTS OF WATER INGESTION ON  
COMPRESSOR CASE TEMP GRADIENTS  
ON J71 ENGINE

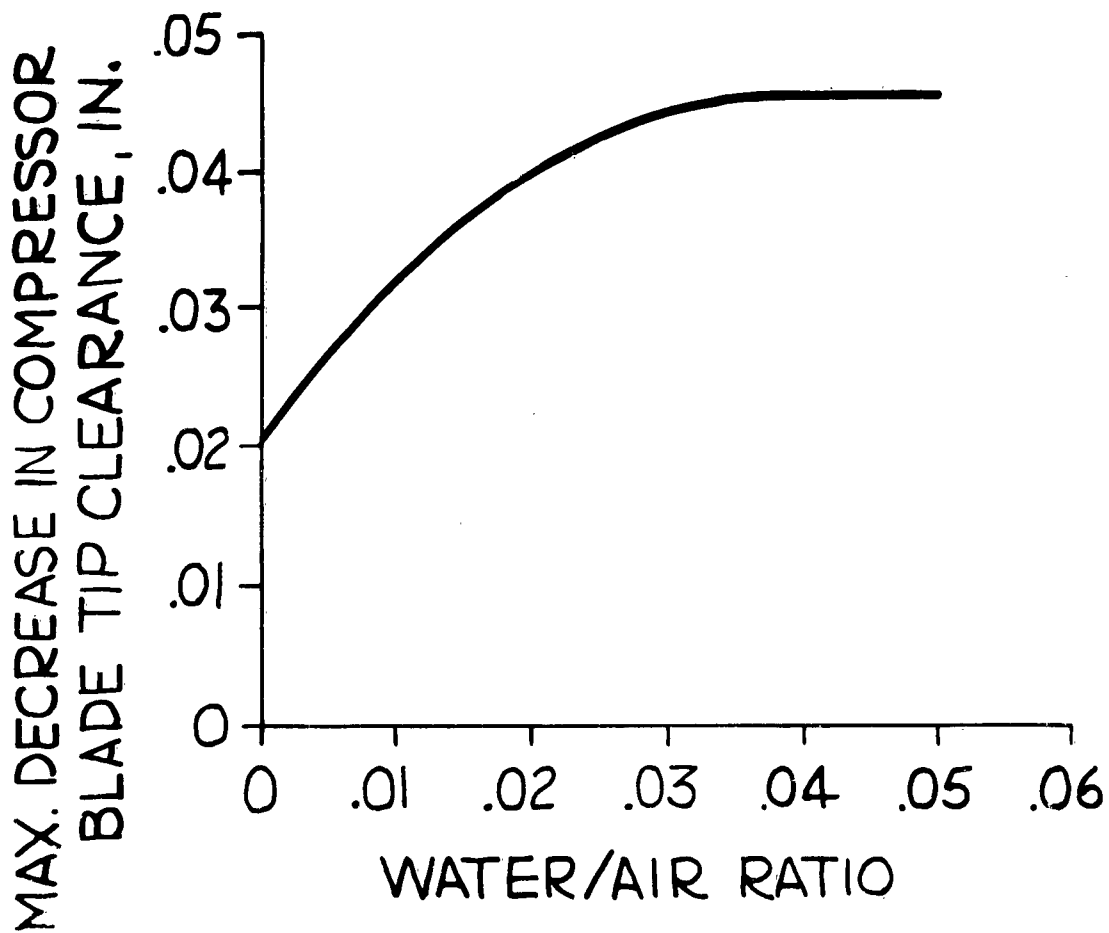
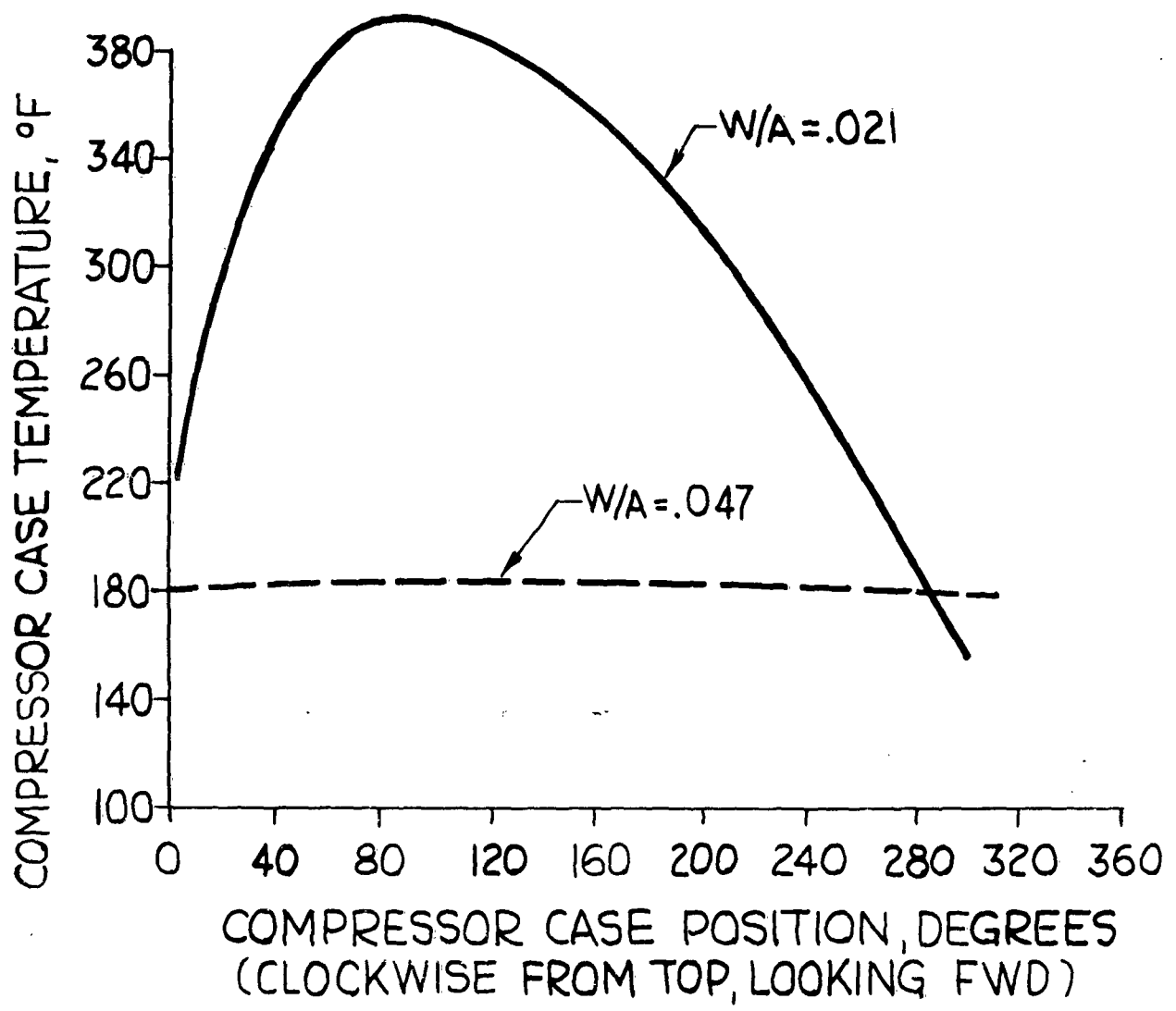


FIG. 5-TYPICAL EFFECT OF WATER  
INGESTION ON COMPRESSOR  
BLADE TIP CLEARANCE



**FIG. 6 - EFFECT OF WATER INGESTION ON COMPRESSOR CASE TEMPERATURE GRADIENTS ON J79 ENGINE**

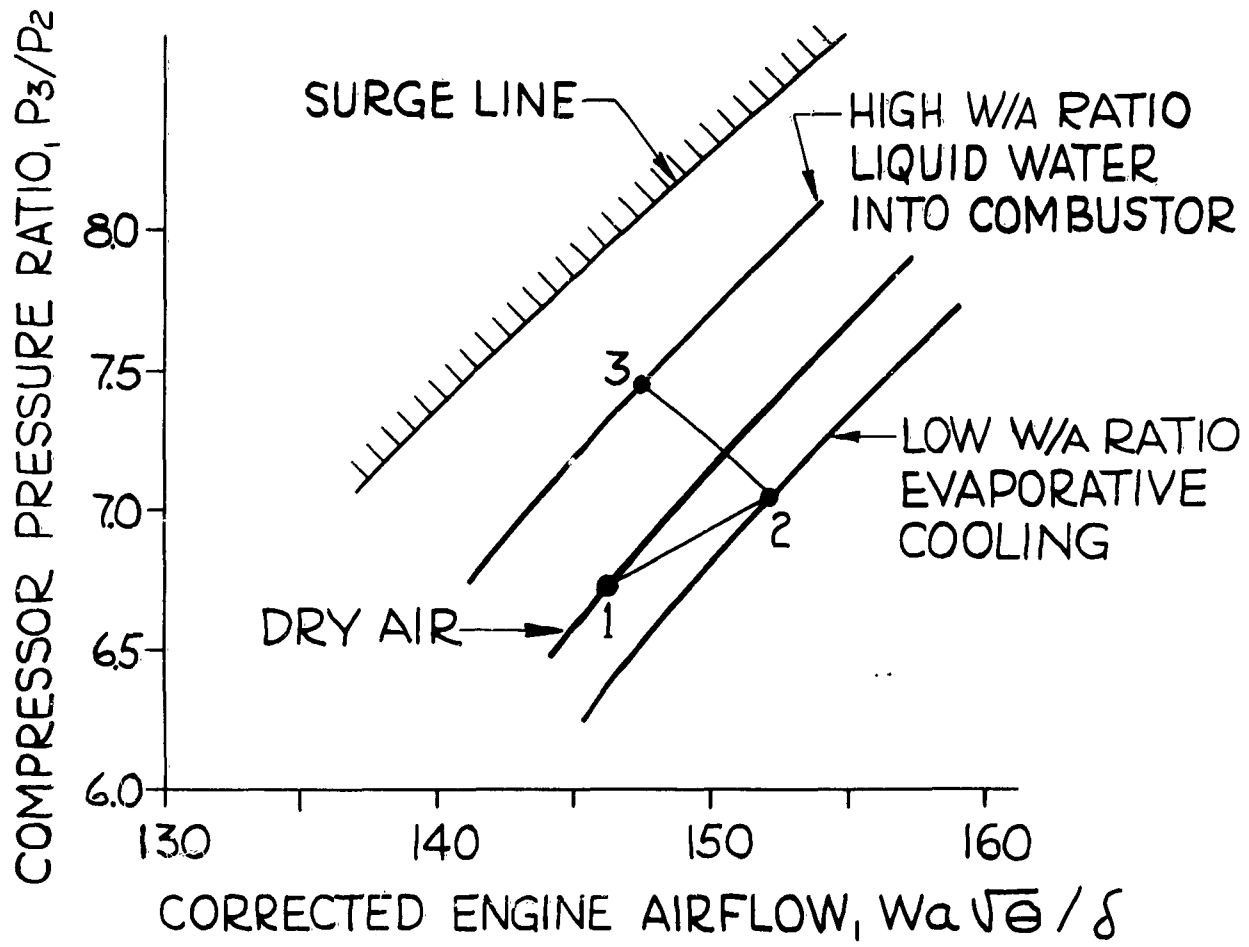
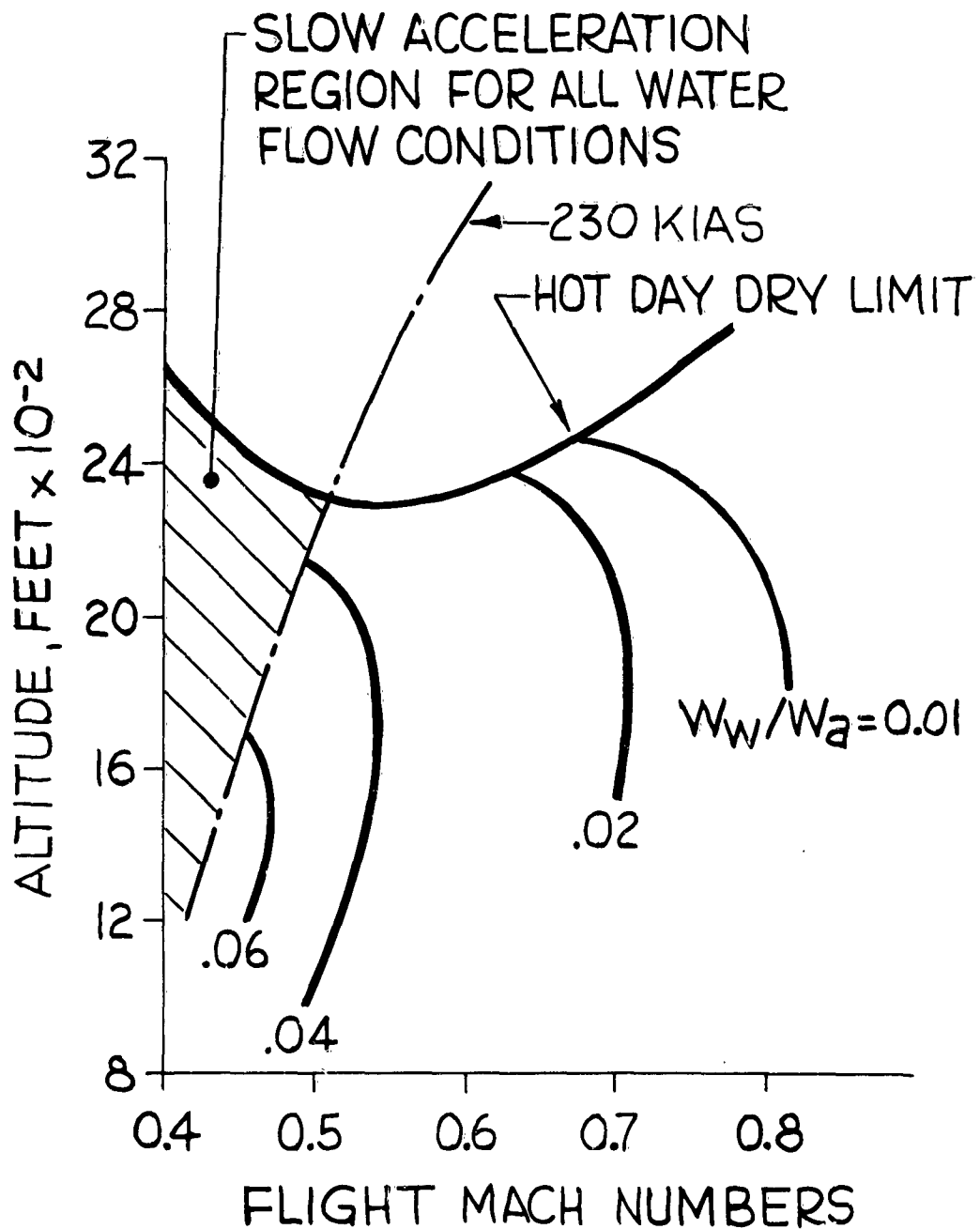


FIG.7- TYPICAL EFFECT OF WATER INGESTION ON COMPRESSOR OPERATING LINE



**FIG.8-EFFECT OF WATER INGESTION ON THE ENGINE STARTING CHARACTERISTICS OF THE J71 ENGINE**

## SALT WATER INGESTION BY GAS TURBINE ENGINES

by

Ted F. Stirgwolt

Manager - Installation and Configuration Design Operation

Small Aircraft Engine Department

General Electric Company

1000 Western Ave., W. Lynn 3, Massachusetts

### Summary

Experience with the HSS-2 helicopter operating in the Anti Submarine Warfare mission has provided a wealth of knowledge and understanding in the field of salt water ingestion by gas turbine engines. As a part of the development flights in these missions, many long hours of hovering operation have been performed during which the United States Navy and the General Electric Company have had the opportunity to gain new perspective in the operating conditions which prevail at hover over salt water.

Methods have been developed during this flight program to control salt deposition and corrosion, the two major gas turbine engine operational environment considerations. These methods have improved the overall weapon system effectiveness by virtue of providing better engine operation. Additional data obtained in the program will provide the basis for further improvements in the suitability of the turbine to operate in a salt spray atmosphere.

The interest of the Bureau of Naval Weapons of the United States Navy and their co-operative support in this program has made possible the information contained in this paper.

### Formation of Salt Water Droplets

It is fortunate that salt deposits can be readily removed from gas turbine engines because they have a rather dramatic effect on performance. Accelerated factory engine tests and helicopter flights have shown that salt water ingestion under severe conditions can cause engine power to be reduced below the hover requirement.

To understand the problem better, let's take a look at a qualitative picture of the generation of the salt spray in the helicopter atmosphere. Observation of the helicopter hovering over salt water shows that the aircraft is surrounded by a large torus of salt spray. Under the proper lighting conditions with the sun low and at one's back, the entire spray-filled volume is visible as sketched in slide No. 2. Immediately below the aircraft there appears a large blue circular spot about the diameter of the rotor. This seems to be the low radial velocity region where the downwash is turned to form the

out-flow profile. Radiating out from the helicopter in all directions is a very frothy white ring of agitated water resulting from the high velocity out-flow air in contact with the ocean surface. It is here that the water droplets seem to be formed and carried into the helicopter rotor flow system.

Note that the shape of the white ring around the helicopter is distorted by the wind velocity. In this sketch a wind velocity of approximately nine knots distorts the ring to about one rotor diameter in front of the aircraft, approximately two diameters on the side, and 3 - 4 diameters astern.

Once the droplets have been created and enter the flow system, the path traveled depends upon other operating conditions. Three different modes of operation are considered as typical. The basis for these comes from observing scale model movies<sup>1</sup> showing smoke streams passing through a helicopter rotor in ground effect with differing wind conditions.

First in Figure 3A,<sup>2</sup> at 8 knots, the helicopter rotor is tilted forward slightly to hover in a fixed ocean position. In this operating condition the slow motion movies showed a clear tendency for the rotor tip vortices to sweep to the water surface and curl back upward to the rotor inlet. This appears to be the situation in which the maximum number of droplets are carried up to the rotor plane because the tip vortices in contact with the ocean surface generate the water drops by their own scrubbing action. The drops are then in a stream which shows the clearest tendency to make a direct recirculation upward to the rotor plane. The engine operation under these wind conditions confirms that the heaviest salt deposits form in such wind conditions.

In Figure 3B, the helicopter is shown at a hover condition simulating 20 knot winds and above. Here the wind conditions are such that the combination of the rotor plane tilt and the crossflow distortion blowing the salt water droplet spray pattern aft, result in no significant quantity of salt spray blowing up in front of the helicopter. As a consequence, the hovering operation is not so seriously influenced by salt water deposition under such wind conditions.

These two operating conditions are fairly well documented with test data under actual full-scale operation. The third situation shown in Figure 3C is somewhat speculative although at least one day's operation seems to support the case. The regime of operation at zero crossflow wind conditions shows a separation layer of out-flow air immediately at the ocean surface. This layer scrubs the ocean and generates the water particles. It tends to radiate out to a large radius without a strong tendency to rise back into the rotor plane.

Under this condition, the rotor tip vortices do not penetrate through this surface layer and do not pick up as large a quantity of water for transport back up to the rotor plane.

Figure 4 is a sketch of the HSS-2 helicopter profile showing the location of the T58 engine inlets relative to the rotor. Note that inlets are above and a little behind the pilot's windshield. This indicates where the salt water particles must be transported to enter the engine.

#### Measuring Salt Water Content

During the helicopter operation flights in Key West this winter, a few observations were made to get some quantitative data about the amount of salt water and size distribution of drops in the atmosphere immediately in front of the engine inlets. The data are presented to give an indication of the concentration and size particles found.

The equipment used is shown in Figure 5,<sup>2</sup> a cutaway section of the HSS-2 cabin. The enlarged inset shows two of the devices used. At the end of the arm is mounted an isokinetic sampling collector probe and a collector ribbon type impingement sampler. These two instruments measure the quantity of salt present but do not indicate drop size.

The isokinetic sampler draws in an air sample by means of a vacuum pump in the aircraft. Air alignment tuft is used to aim the sampler into the air stream. The flow rate is regulated to keep static pressure inside the tube equal to free stream static. This method allows droplets to enter the probe with a minimum disturbance to their natural paths. The salt water droplets are drawn through a filter which traps all of the water and salt crystals.

The collector ribbon impingement method of drop sampling involves aligning the collector plate normal to the stream flow direction. Drops are separated from the air as it turns and flows past the collector plate. The particle inertia carries the drops to the plate since their mass prevents them from negotiating the flow turn around the edge of the collector plate. Of course, some of the drops are small enough to be lost in collection. However, parametric curves are available in the literature <sup>3</sup> and <sup>4</sup> relating the collection efficiency to operating conditions and drop sizes.

A plot of salt water content vs. altitude is shown in Figure 6. The data taken aboard the helicopter indicate that approximately 3 cubic centimeters of salt water per minute are ingested into each T58 engine while hovering at 30 ft. altitude.

A few other points of interest are also included on this curve — At 20 ft. hovering altitude, the data showed from 3 - 8 cubic centimeters per minute salt water ingestion. As a matter of interest, one of our test cell ingestion rates is also plotted on the curve. This ingestion was controlled at 20 cubic centimeters per minute. It is plotted at zero altitude, although we have no correlating data indicating that this represents the ingestion rate experience of a helicopter at take-off from the ocean. In the test cell, of course, we have ample data showing the rate of performance deterioration as the salt water is ingested. These data show definitely a more rapid performance deterioration rate than experienced at the 20 - 30 ft. hover altitudes. This data showed that at approximately 35 ft. altitude, the helicopter rose out of the spray atmosphere.

Under more normal wind conditions, there is a natural salt content in the atmosphere over the ocean from 1 - 10 micrograms per cubic meter. This salt content is in the crystal form rather than droplets and does not cause a deposition problem but it does cause corrosion of the engine parts.

#### Measuring Drop Size

Drop sizes were obtained by a visual method. On the Table in Figure 5 is a pistol grip drop snatcher. This instrument consists of an oil coated slide at the end of an extension. The slide is exposed to the atmosphere and the salt water droplets are captured in a layer of silicone oil which maintains the droplet identity for a short period of time. The sample is quickly withdrawn and examined under a size calibrated microscope to record drop diameters and quantities.

Data recorded from the visual observation of drop sizes are shown in Table I. General conclusions from these data indicate that the large 500 micron sized drops present at 10 ft. do not get up to the higher hover altitudes, the largest observed at 30 ft. being 150 micron. Also, as would be expected due to the longer path traveled, more evaporation takes place at the 30 ft. altitude than at 10 ft. as indicated by the increase in observed salt crystals in the drops. The aircraft climbs out of the water laden atmosphere at 35 ft. hover altitude.

Investigation of inlet separators to remove salt water droplets from the air before entering the compressor will be based upon such data. This information becomes particularly significant when considering inertial separation techniques.

#### Salt Crystallizes on the Airfoils

As the salt water laden air enters the engine, the air is continuously accelerated in its path through the compressor. Since the salt water droplet velocities are lower than air velocity, the droplets tend

to impinge the surfaces of the airfoils. The larger the particles, the better the chance of collection on the blade surfaces.

As the droplets wet the blade surface, they spread out, come into intimate contact with the surface, and begin to evaporate. During the evaporation, the ionized solution tends to crystalize out on the metal and attach to the surface through Van der Waal's forces. These forces of attraction are extremely strong and the bond between the salt and steel are impractical to separate mechanically.

Engine performance charges are chiefly caused by salt deposits in the compressor. Figure 7 is a photograph of a section of compressor stator vanes shortly after a factory test of accelerated salt water ingestion. These tests were run to examine the nature of salt attachment in the engine. Note the large projections of salt buildup along the leading edge of the airfoil. The entire airfoil surface is made very irregular by the large protruding salt deposits.

#### Performance Maintained by Deposit Removal

The obvious result of such changes in airfoils is twofold. First, the compressor efficiency is reduced by the rough surfaces. Secondly, air flow of the compressor is also reduced. Both of these changes reduce horsepower capabilities of a gas turbine engine. All of the significant salt deposits occur on the first five stages of the compressor. The early stages act as a high efficiency collection device and the rear end of the compressor remains quite free from gross buildups.

It was found that these salt deposits can be removed from all the engine flowpath surfaces. When washed, the engine power is returned to that of the clean engine. Of several alternate cleaning methods performed, a successful solution was developed based upon a generous fresh water flushing. This recovery was demonstrated over several missions in one of two engines of the HSS-2. The other engine was left unwashed for several successive missions to investigate the long-term salt buildup effects. Figure 8 shows the horsepower loss of the unwashed engines at 30 and 15 ft. hover altitude. The effects of the higher ingestion rate at 15 ft. altitude show a much more rapid initial performance deterioration rate than the 30 ft. data.

Also indicated is an interesting minimum power. After an initial rapid loss of power, the curves tend to level off during the next several hours of hover flight. It appears that at some level of salt buildup, the salt tends to break off as fast as new salt is deposited so a condition of equilibrium is approached.

The broad band of horsepower shown on the curve results from variations in salt buildup in the engines from one set of equilibrium operating conditions to the next. These are caused by such variables as wind conditions.

Some other interesting effects of salt deposits on engine performance are indicated by a curve showing horsepower vs. time on a given mission. Figure 9 shows a given horsepower output at the beginning of a mission with 8 to 10 knots of wind. The performance reduces during four hours of hover to some lower value. After a twenty-minute flight back to the base, there is indication of a recovery of some of the lost performance. After a night of storage, the initial operation of the engines the next day shows a further recovery of performance.

The performance recovery can perhaps be explained by break-off of salt buildup during the flight back. The overnight recovery can possibly be explained by the salt crystal structure growing wet and mushy over night and being partially blown off at start up the next day.

The power curve for the higher wind conditions is shown to give a qualitative picture of less power decay at higher wind conditions. Operation at a higher wind condition also indicates a tendency to recover power on the return flight and after the overnight period.

#### Wash Procedure Also Controls Corrosion

Engine airfoil life has been extended over 10:1 by expanding the use of the wash procedure developed to restore engine power. A procedure for removal of salt deposits harmful to engine performance is naturally an important basis for engine corrosion protection.

Early attempts to reduce corrosion employed passing a cleaning agent through the engine operating at idle conditions. One such cleaner was AD-9 walnut shells. This proved ineffective because the shells seemed to leave the inner radii of the flowpath dirty and corrosion would appear to be very heavy near the hub of the airfoils and fairly clean at the tips.

Washing the engine while operating at idle, either with fresh water or with a solvent such as Aerosol, had another effect, particularly when the compressor was heavily salted. The introduction of water at the front end washed the salt off the front of the compressor and redeposited it in the rear stages and on the combustion and turbine surfaces. Our final maintenance wash procedure is shown in Table II.

The most effective way found to flush the T56 is to rotate the engine on the starter while generously spraying fresh water into the inlet. This way, the water has ample opportunity to thoroughly flush out the entire engine without high enough temperatures or air velocities to cause evaporation and redeposition in other parts of the engine.

After the fresh water wash, the engine is started and operated at idle conditions for a period of five minutes to allow complete drying out of all the remaining water in the engine. The anti-icing valve

is opened during dryout period to blow hot air through that system.

As the engine is shut down after the dryout run, Rust Lick 606 is sprayed into the inlet. Rust Lick is an oil with an additive to displace any remaining water from the surface of the blade. Laboratory tests have shown it to be quite effective in retarding corrosion on washed blades.

The hard caked white salt buildup on the front frame of a factory test engine is shown in Figure 10. This photo was taken after some salt ingestion testing. The nature of the deliquescent salt changes as the engine begins to cool. Soon the salt becomes mushy with the absorbed water from the surrounding atmosphere. This occurs in a matter of minutes in a humid atmosphere. At this time, the ionized salt water solution in contact with a metal conductor allows the serious corrosion to begin. For this reason, the wash procedure is applied each day after the last flight.

The value of this wash maintenance can best be illustrated by showing a photograph of an airfoil which was not maintained with this procedure.

#### Airfoil Pits Formed by Corrosion

Figure 11 shows a photograph of an airfoil which has been severely damaged by corrosion. The surface is heavily pitted. These pits are typical of the attack on 403 stainless steel which is a 12 percent chrome steel. Our laboratory testing of blades from unwashed engines operating in a highly corrosive atmosphere shows unacceptable reductions of fatigue strength. As one would expect, the location of the pits establishes the actual point of failure, the most vulnerable location being at the airfoil trailing edge near the blade mount.

Other major components subject to active corrosion are the compressor rotor, compressor casing, compressor rear frame, combustor casing, and fuel nozzles. Our experience with these components indicates a different type of problem. None has lost a significant amount of strength. The effects of corrosion here have been chiefly a combination of assembly and appearance. When these parts are allowed to corrode, the accurate close fitting joints become spoiled and sometimes jammed, making disassembly difficult.

#### Fatigue Life Extended

Blade pitting can be virtually eliminated by routine application of the wash procedure. Thus, the blade fatigue strength is maintained and the useful life is extended more than 10:1 as shown in Figure 12. In addition to the obvious values of extended useful blade life, there is another performance asset associated with elimination of blade pits.

The pits themselves cause enough surface roughness to adversely affect performance of the engine.

### Coatings Prove Effective

An intensive evaluation of a broad range of coatings has shown that blade corrosion can be effectively reduced by proper coating selection. For all engines in service with corrodable steel blades, a good coating treatment is of great value in extending the blade useful life.

In our search for coatings to reduce corrosion, many were considered and discarded from simple laboratory investigations. A remaining group was considered to have enough promise to be evaluated to a much greater extent both in laboratory samples and in a flying helicopter in the A.S.W. mission.

Table III shows the list of coatings investigated. The coatings are grouped into two columns to indicate that certain coatings are not compressor temperature limited, making them suitable for use in all stages of the compressor.

These coatings were exposed to actual operating conditions by applying each type to several blades and assembling them into engines flown in the A.S.W. mission. Samples were distributed between front end and rear stages to obtain important temperature effects. Duplicate engines were assembled to evaluate coating effectiveness with and without wash while exposed to the salt spray conditions. After removal from the engine, laboratory inspection, fatigue tests, and evaluation has been carried out to establish the strengths and weaknesses of each. It is of interest to point out that the salt deposits were found to adhere equally well to all the blade and coating surfaces. None of the investigated materials showed any tendency to gather fewer salt deposits than any other.

While coatings have value, they also have problems. Another facet of our program has been to evaluate the erosion resistance in an engine test. All of the coatings proved to be subject to erosion by Arizona Road dust. Since all coatings investigated show limited life as expected, the blades will require re-coating at overhaul periods to extend the blade protection while exposed to the adverse A.S.W. atmosphere.

### New Materials Show Promise

Looking to the future, an intensive material change program is under investigation to improve the engine even further. Each new material has its own set of problems which range from unique corrosion characteristics to unique fabrication requirements. We are making

steady advancements with these and when the problems are solved, we look forward to getting better materials into fleet use. Building upon the vast operational experiences gained in the many applications of the General Electric engines, we will be building for the tougher environmental requirements of the future.

1. A.H.S. Forum, Sept., 1958, Smoke Flow Movies, Evan A. Fradenburgh, Sikorsky Aircraft
2. Foster-Miller Associates, Inc., "A Study of the Mechanism of the Deposition of Salt on Helicopter Gas Turbine Compressor Blades When Hovering Over the Ocean," 1961
3. Watson, H., Report of Symposium on Aerosols, Chemical and Radiological Laboratories, 1953, Army Chemical Center
4. Green, H. L. and Lane, W. R., "Particulate Clouds: Duste, Smokes and Mists," 1957

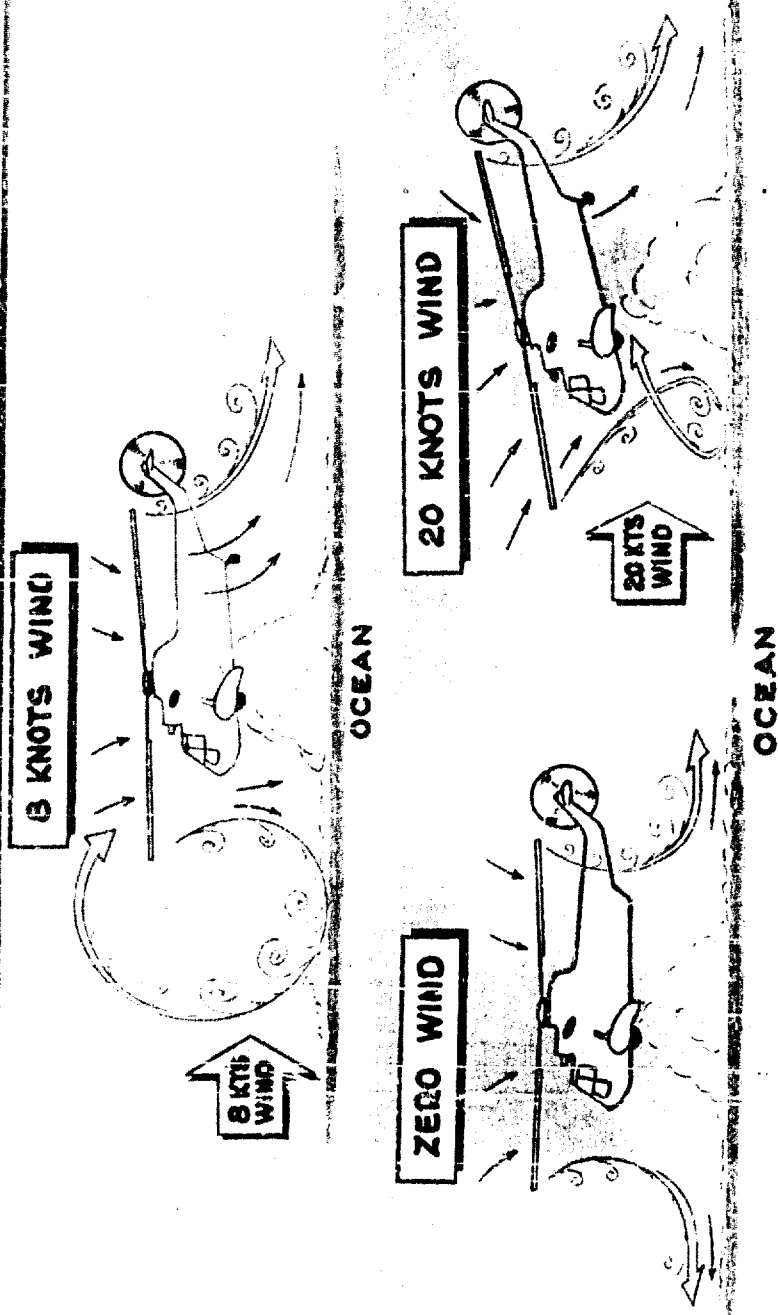


**HOVERING HO4S-2**



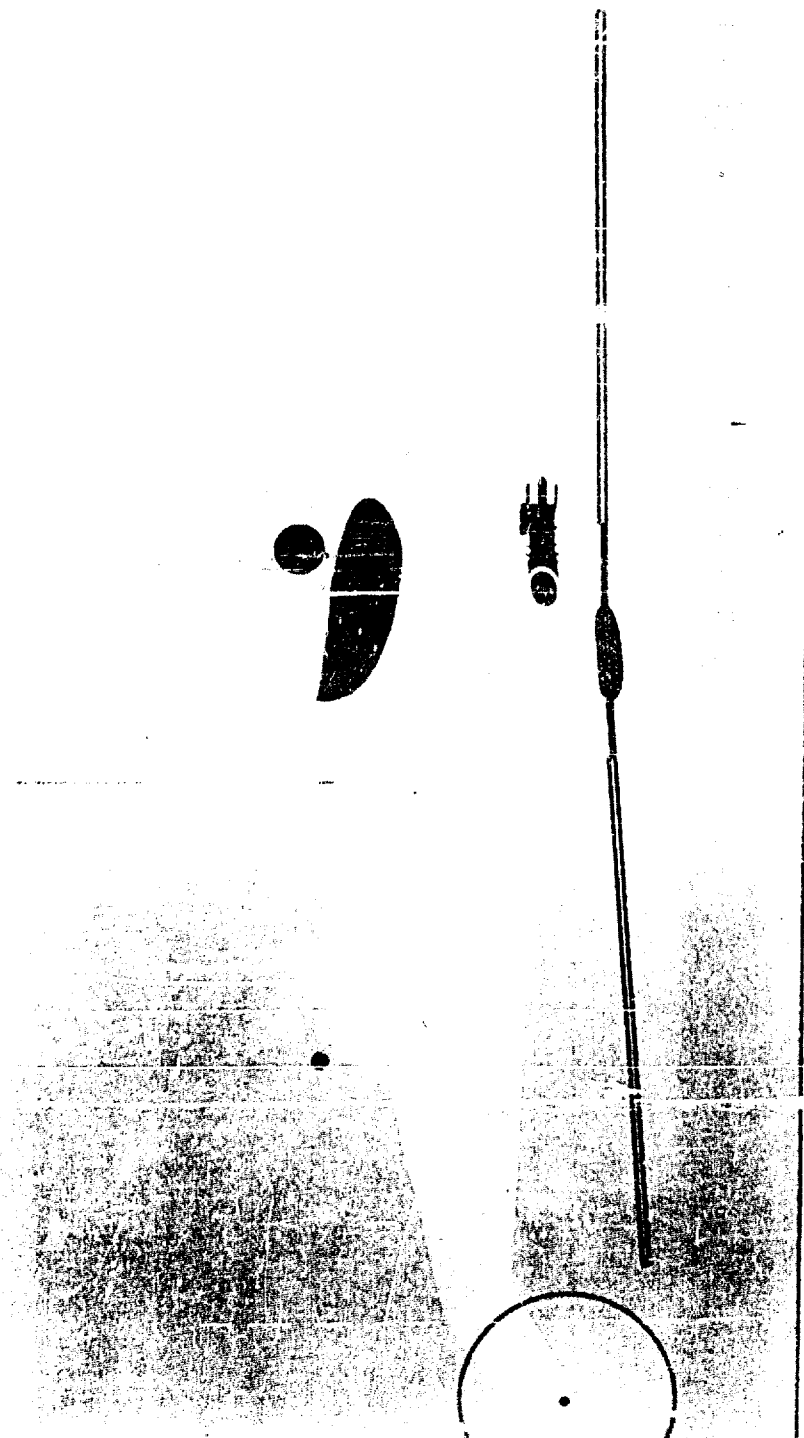
FIGURE 2

# AIRFLOW SURROUNDING A HELICOPTER

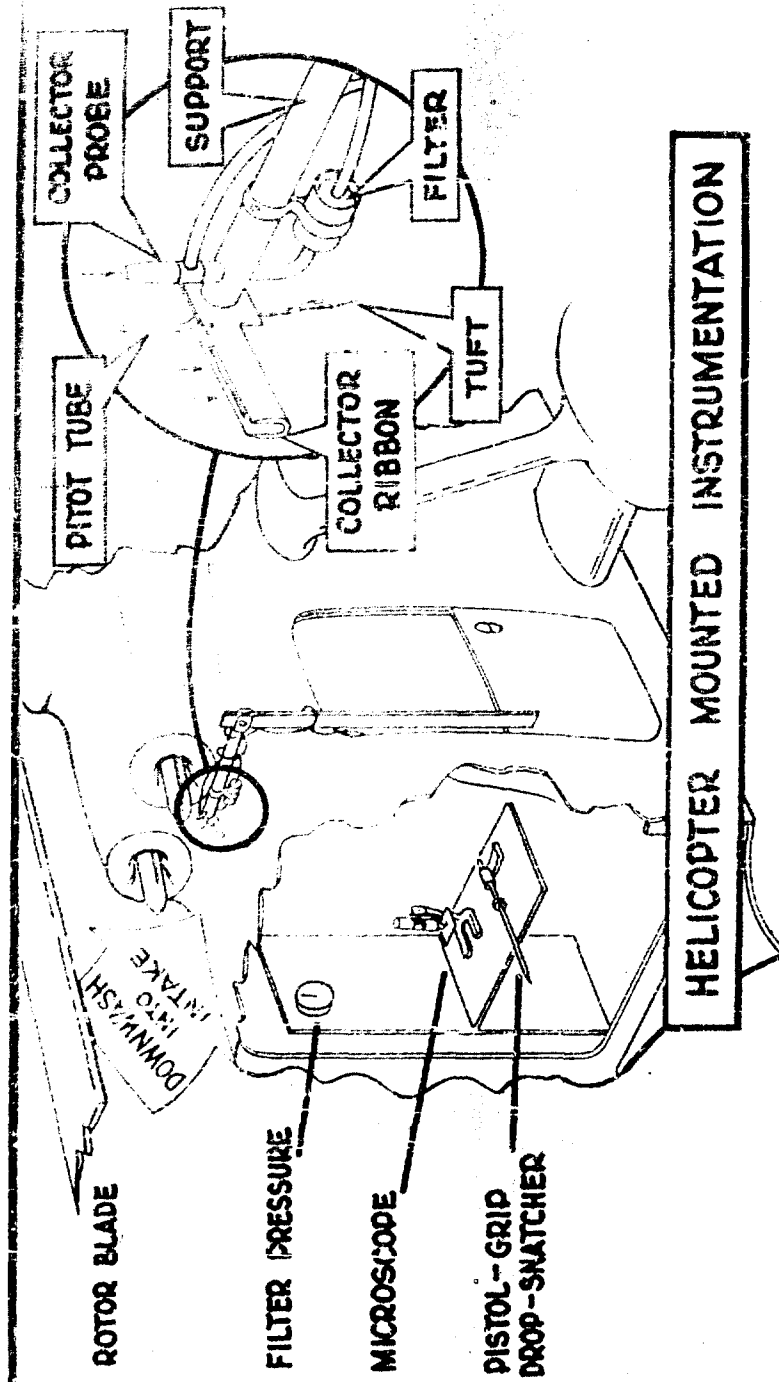


Best Available Copy

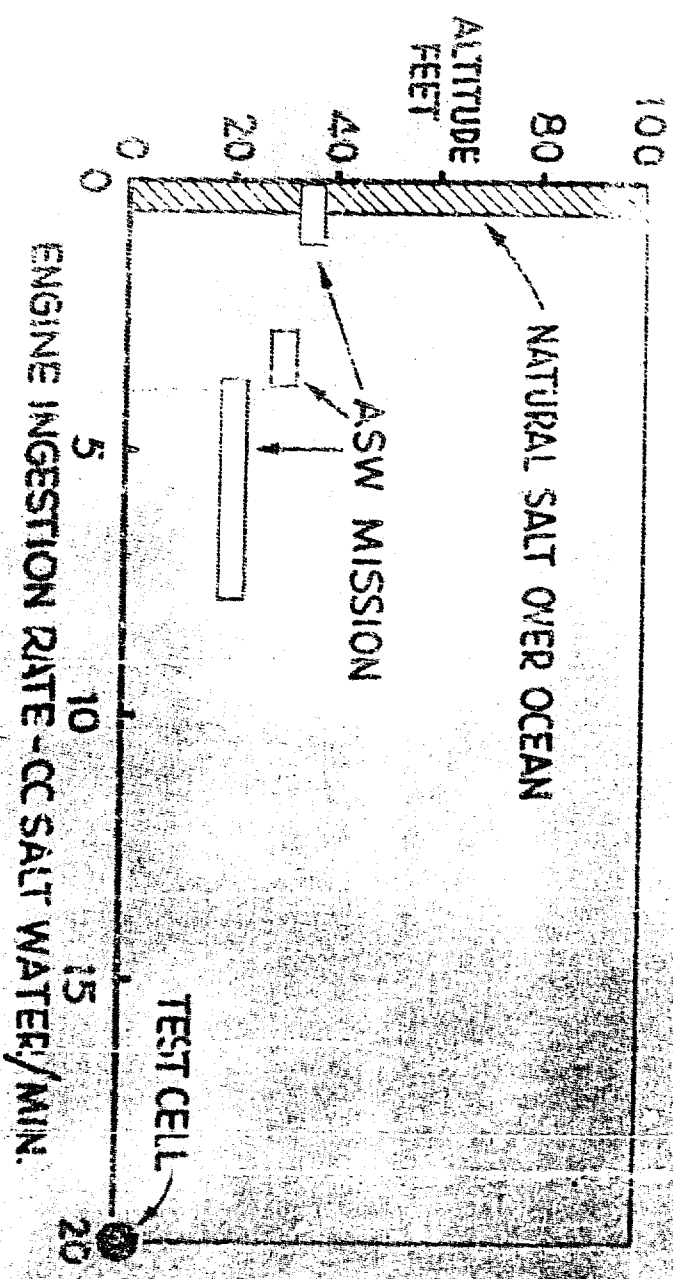
# HSS-2 ENGINE INLET / ROTOR SYSTEM



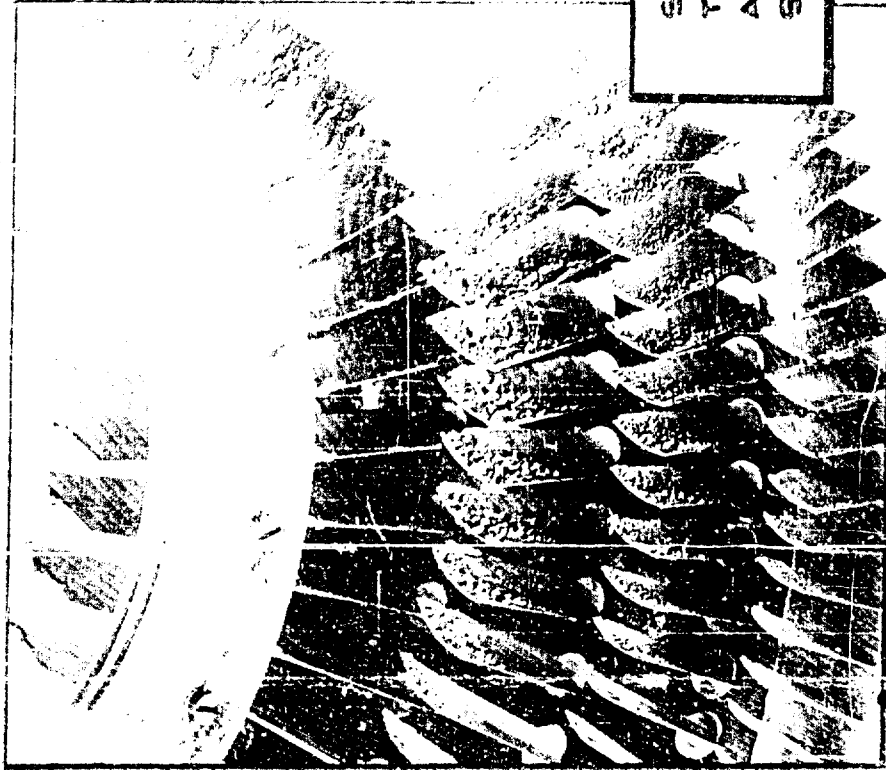
# SALT WATER DROPLET MEASUREMENT



# T58 SALT INGESTION

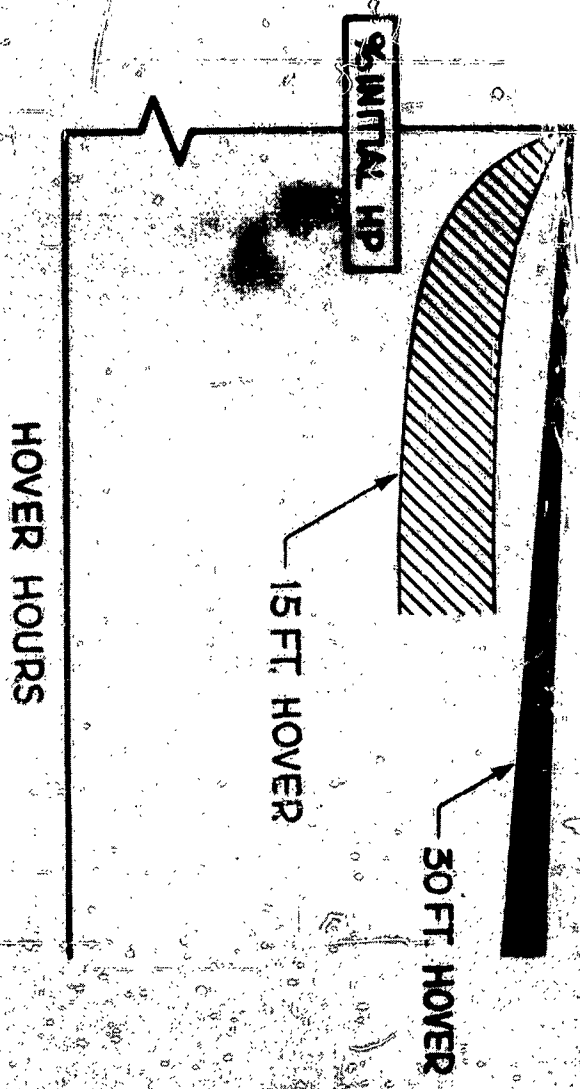


Best Available Copy

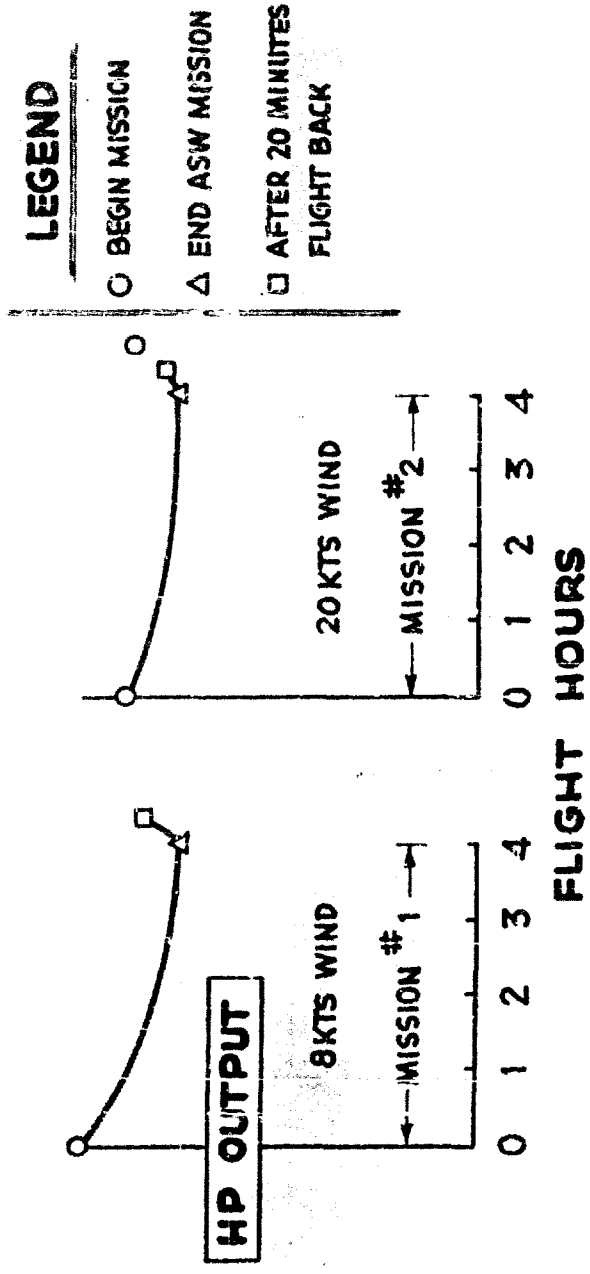


SALT DEPOSITS ON  
T58 STATOR VANES  
AFTER ACCELERATED  
SALT DEPOSITION TEST

# PERFORMANCE LOSS DUE TO SALT DEPOSITS



# ENGINE POWER DECAY VS FLIGHT TIME





**SALT BUILDUP  
ON  
T58 INLET**

**CORRODED 403  
STEEL AIRFOIL SECTION**

**NO PROTECTIVE COATING  
NO WASH PROCEDURE**



**EFFECTS OF WASH PROCEDURE ON BLADE STRENGTH**

**UNWASHED**

**WASH PROCEDURE**

**BLADE FATIGUE LIFE (BASED UPON LAB TESTS)**

## VISUAL TEST DATA

CONDITIONS	DROP DISTRIBUTION	COMMENTS
5 KNOTS WIND 10 FEET ALTITUDE	2 - 500 MICRONS 50%, 20 - 80 MICRONS	1 GROUP - 20 MICRONS 1 GROUP - 80 MICRONS FEW SALT CRYSTALS
5 KNOTS WIND 30 FT. ALTITUDE	2 - 150 MICRONS 50%, 40 - 90 MICRONS	MANY DROPS CONTAINED SALT CRYSTALS
7 KNOTS WIND VARIABLE ALT.	NO DROPS AFTER 35 FT ALTITUDE	

## **T58 ENGINE WASH PROCEDURE**

- **INGEST FRESH WATER THROUGH COMPRESSOR INLET WHILE OPERATING ON STARTER**
- **RUN ENGINE AT IDLE POWER 5 MINUTES FOR DRY OUT**
- **SPRAY RUST LICK 606 INTO COMPRESSOR INLET DURING COAST DOWN**

# COMPRESSOR COATINGS EVALUATED

COMPRESSOR TEMPERATURE LIMITED	NOT LIMITED BY COMPRESSOR TEMPERATURES
NUBELON	NICKEL CADMIUM
HINAC	NICKEL IMMERSION
TEFLON	NICKEL SULPHAMATE
HEFESITE	ALUMINUM SILICONE PAINT
	VAPOR DEPOSITED ALUMINUM
	VAPOR DEPOSITED CHROME
	VAPOR DEPOSITED NICKEL
	VAPOR DEPOSITED TITANIUM
	VAPOR DEPOSITED SAPPHIRE
	CERAMIC
	UNCOATED 403 STEEL-PLAIN & PASSIVATED

THE EFFECT OF TEMPERATURE EXTREMES UPON  
THE OPERATIONAL CHARACTERISTICS OF TURBOJET ENGINES

BY

MARTIN E. HOYER  
Supervisory Aeronautical Power Plant Research Engineer

JOHN J. MC GEE  
Aeronautical Power Plant Research Engineer

FORWARD

The treatment of the turbojet engine starting in this paper admittedly represents a simplification of the subject although the approach provides an understanding of some of the more basic problems such as the development of a satisfactory starting fuel schedule.

It is understood that many factors, which are not discussed, have an important influence, on engine starting capability, including the type and sizing of the engine starter and particularly production tolerances and the inherent accuracies of the starting system controls and fuel system controls. These latter items are generally known characteristics. The designer can successfully assemble a system if, however, a clear definition of the engine requirements are established. It appears that the engine and engine systems have not always been well enough defined for the systems designer to provide adequate starting performance. Extrapolation of available data obtained over a minimum ambient temperature range to provide estimates for operating extremes is not satisfactory.

Reference is made to the military specification without the intention of implying that these are perfect standards for design or operating objectives or to defend a somewhat arbitrary temperature extreme or other end points. However, without the specification, chaos would result. Further, the turbojet engine specification, like others, represents the coordinated efforts of industry and the military to provide continuing goals for improvement of performance and reliability. It is believed that the standards for laboratory evaluation of an engine should also be more stringent than anticipated normal service requirements to account for production variations and service depreciation.

The engines described are the Navy J79-GE-2 and GE-8 and the J57-P-16 and P-20 as A and B respectively.

## INTRODUCTION

The turbojet engine is required, as a condition of qualification, to operate successfully over the ambient temperature range of -65°F to +135°F when using fuel conforming to MIL-J-5624. This is a familiar requirement and one which all production engines have to some degree successfully demonstrated in the course of their development history. When grade JP-5 fuel is employed as with all Navy engines, the minimum fuel and ambient temperature is that corresponding to a fuel viscosity of not less than 12 centistokes. It is the use of grade JP-5 fuels on those engines primarily developed with grade JP-4, that some of the current operational problems have developed. These problems are in the areas of fuel metering, and combustor problems affecting both engine starting and accelerations and, to an unknown degree, performance. The cold JP-5 requirement has produced several problem areas in Navy engines which will be briefly discussed here. There is no intention of discouraging the use of grade JP-5 fuel; it is here to stay, but rather to stimulate some interest in further development work with this fuel to provide engine operation consistent with the high degree of excellence obtained with grade JP-4.

## ENGINE STARTING PROBLEMS

MIL-E-5007B, the turbojet engine design specification, provides a standard for engine starting time as a function of ambient temperature, as shown by Figure 1. The envelope of experience with several current Navy turbojet engines, based on NATTS testing, is also shown in Figure 1. While these engines do not meet the starting elapsed time requirements, the grade JP-4 experience from a service viewpoint is generally acceptable. It will be noted that a serious problem occurs with grade JP-5 fuel at the low ambient temperatures. One of the most significant differences between JP-5 and JP-4 is that of viscosity. Figure 2 provides a comparison. Grade JP-5 fuel employed by NATTS has consistently tested at a viscosity of 12 centistokes at -30°F. This arbitrary limit for low temperature testing has been a severe test of engine operational capability. Let us briefly examine the problems with current Navy turbojet engines with low temperature starting.

At least three current Navy turbojet engines have demonstrated service problems with JP-5 starting at fuel and ambient temperatures which are considered well within the normal operating range. Thus, Engine "A" which has successfully completed qualification testing for the Air Force at temperatures approaching  $-65^{\circ}\text{F}$  at Eglin Field, experiences field operating difficulty with fuel ignition capability at  $^{\circ}\text{F}$  20 to  $^{\circ}\text{F}$  40 with JP-5 fuel. Engine "B" has likewise successfully completed qualification testing in an Air Force installation with JP-4 fuel at the temperature extremes; but not until correction of fuel control leanout problem due to cold fuel, and to the use of revised fuel schedules. "B", however, cannot start with JP-5 fuel at temperatures below approximately  $0^{\circ}\text{F}$  during NATTS testing, and service problems are reported at higher temperatures.

To make the situation more confusing, Engine "A" when tested at NATTS, cannot duplicate the original service problem of failure to light-off at  $^{\circ}\text{F}$  20 to  $^{\circ}\text{F}$  40 fuel and ambient temperatures, and it is only at ambient and fuel temperatures of approximately  $-20$  to  $-30^{\circ}\text{F}$  that fuel ignition problems occur. At this same temperature range, however, starting acceleration problems are demonstrated with inability to accelerate to idle rpm with JP-5.

Let us look in some detail at these two engines to see the similarity of the problem, starting with Engine "A". Investigation of this problem revealed two major trends with decreasing fuel and ambient temperature: (1) As fuel temperature decreased, engine fuel requirements increased; (2) As fuel temperature decreased, the starting fuel scheduled metered by the engine fuel control leaned out. These effects are shown in Figure 3. The combined effect of these two trends was that, with decreasing temperatures, the starting schedule approached the required-to-run fuel schedule and the acceleration times to idle became progressively longer. At some minimum fuel temperature the fuel schedule had leaned out so severely that insufficient excess fuel was available for acceleration. The result was an engine speed hang-up as shown in Figure 3.

Examination of data obtained during hang-ups indicated that a combustion problem existed. Figure 4 presents time histories of two starts with identical fuel flows at speeds in the hang-up region. One start was satisfactory and acceleration to idle was accomplished in 44 seconds. The second start encountered hang-up at 35% of the idle speed and resulted in a 110

second acceleration to idle. Inlet conditions and engine fuel flows are the same, but the turbine discharge temperatures are significantly different, with the successful start being an average temperature approximately 200°F higher than the hang-up start. A comparison of the turbine discharge temperature profile for these two starts is shown in Figure 5. This comparison is made at the speed at which hang-up occurred on the second start. The curve shows a significant difference in the combustor performance for the same fuel flow and the same inlet conditions. As a result of these two factors, control lean-out and increased engine fuel requirements with cold JP-5 fuel, this engine was unable to meet its specification guarantees for starts and accelerations to idle.

In addition to the hang-up problem, a light-off problem was encountered as fuel temperatures were decreased even further. Since poor light-off characteristics can be attributed to poor ignition system or poor fuel nozzle spray characteristics, both of these items were investigated. Investigation of the standard ignition system did not reveal any significant deficiency in the system and investigation of improved ignition systems did not provide any improvement in the light-off capability of the engine. However, investigation of the fuel nozzles indicated that some of the flow characteristics of the nozzle with cold JP-5R fuel could contribute to the ignition problem and to that portion of hang-up problem due to combustion deficiencies. Both engines "A" and "B" employ pressure atomizing fuel nozzles. It can be shown that, for low volatility fuels, and JP-5 qualified for this classification, the fuel evaporated in the burner at low fuel temperatures is at a very low value. Under cold weather starting conditions, probably no evaporation occurs in the light-off region. Thus, for establishment of a combustible mixture, the degree of atomization, or fineness of drop size, is a critical item. A decrease in inlet air temperature tends to increase drop size but, more important, fuel viscosity is the dominant fuel property in the determination of the fineness of atomization. Figure 6 shows the relation between fuel flow and pressure drop across a single fuel

nozzle for ambient and cold (-30°F) JP-5R fuel. For the ambient fuel, a satisfactory spray cone angle with good atomization of the fuel was obtained with a pressure drop across the nozzle of 10 psi, but for the -30°F fuel temperature the pressure drop required for comparable spray angles and atomization was 20 psi. The fuel flow required with cold fuel for the same spray angle and atomization is approximately 17 pph, or 65% higher than that required with warm fuel. From the standpoint of the ignition problem, then, a richer fuel schedule is necessary to provide a good combustible mixture of fuel and air to the ignitor and the burner cans. The degree of atomization can affect the combustibility of the mixture, as well as flame propagation to adjacent burner cans. Therefore, the characteristics of the fuel nozzles when operating with cold high viscosity JP-5R are probably contributory to the ignition problem and to the decrease in combustion efficiency that is indicated by the increase in engine fuel requirements when operating with cold JP-5R fuel.

#### THE STARTING PROBLEM WITH ENGINE "B"

Engine "B" sea level starting characteristics, like that of Engine "A", indicates a two-fold problem as demonstrated by fuel ignition or light-off failures as well as marginal, or unsuccessful, accelerations at ambient and fuel temperatures below approximately 20°F with JP-5R fuel. However, starting performance with JP-4R fuel is satisfactory to ambient temperatures as low as -50°F. Figure 1 provides the typical results of starting tests with JP-4R and JP-5R based on NATTS test results.

The first requirement in the investigation of this problem was to establish that starting fuel schedules conformed to the manufacturer's design values by flow bench testing of the fuel control. Bench testing indicated essentially correct fuel schedules within the expected production and service tolerances. It was further confirmed that an earlier, and serious, fuel temperature sensitivity problem with the fuel control had been corrected. Fuel control lean-out over the fuel temperature range of 80 to -20°F with high viscosity JP-5R was limited to approximately 4%.

It was then desirable to establish the engine steady state operating characteristics by full-scale engine testing in the starting range below idle rpm. This was completed for JP-4R and JP-5R fuels at the ambient and

fuel temperatures of  $-30^{\circ}\text{F}$  and  $60^{\circ}\text{F}$ . Fuel temperature was controlled to simulate cold soak starts during the  $-30^{\circ}\text{F}$  operation. Figure 7 provides the results of such testing. A serious combustion problem is indicated with the JP-5R test results by comparison with the JP-4R data at  $-30^{\circ}\text{F}$  fuel and ambient temperatures. It is of interest to note that at an ambient temperature of  $60^{\circ}\text{F}$  this engine was capable of operating stably at a high pressure rotor speed as low as 12% of the military speed without excessive exhaust gas temperature rise. JP-4R operation at  $-30^{\circ}\text{F}$  was stable and controllable to approximately 14% rotor speed with fuel temperatures as low as  $-35^{\circ}\text{F}$  to the fuel nozzles. With JP-5R fuel, however, engine operation became unstable with evidence of a severe combustion problem at approximately 25% rotor speed. The exhaust exhibited heavy white smoke, and rotor speed would wander without change in fuel flow. At approximately 40% rotor speed, a significant increase in fuel flow occurred over that for JP-4R. As engine speed was further reduced, the fuel flow variation became a maximum of approximately 40% greater than JP-4R at the 25% rotor speed point.

To further substantiate the combustion problem with cold JP-5R fuel, the exhaust gas temperature plot of Figure 8 is presented. The output of 8 Siamese exhaust gas thermocouples were recorded. Eight individuals were recorded, plus the electrical average of the remaining couple for comparison. The electrical average was  $615^{\circ}\text{F}$  and  $863^{\circ}\text{F}$  for JP-4R and JP-5R, respectively, at approximately 22% of idle rotor speed. As noted from the chart, however, a relatively uniform temperature pattern exists for JP-4R compared to temperature variations of over  $1200^{\circ}\text{F}$  for the JP-5R operation. Indications were, in fact, that several burner cans had flamed out, or were burning erratically. The temperatures at approximately 2:30 and 11:00 o'clock positions were less than  $200^{\circ}\text{F}$ .

An attempt was then made to estimate the probability of successfully completing JP-5R starts at the  $-30^{\circ}\text{F}$  conditions. The previously obtained flow bench data for the fuel controls was employed to estimate the starting fuel schedules for JP-4R and JP-5R. Although this was a  $W_f / P$  type of fuel control, that is, scheduling fuel flow in proportion to compressor discharge pressure, no difficulty was experienced in employing the steady state compressor discharge pressure data obtained during the preceding engine test. This was true because of the extremely flat compressor characteristic determined from obtaining the engine operating lines with minimum exhaust nozzle area and with the maximum

exhaust nozzle area employed for A/B operation. Thus, in the absence of transient CDP data, a reasonable assumption was the use of steady state data. The  $-30^{\circ}\text{F}$  JP-4R estimate is shown in Figure 9 by superimposing the estimated starting fuel schedules on the engine equilibrium characteristic. Adequate starting acceleration seems assured by the margin over the steady state operating characteristic. The starter assistance characteristic is not known since a starter was not available during the test. Although the starter effect upon equilibrium fuel requirements is unknown, the currently employed pneumatic starter will crank to approximately 25% to 30% of the idle rotor speed without engine assistance.

The JP-5R estimate is shown in Figure 10. We note intersection of the acceleration fuel schedule and the steady running characteristic at approximately 25% of idle rotor speed. Since starter assistance is significant at this rpm, some acceleration would occur; however, between 25% and 60% of idle engine speed, the starter assistance became less significant and successful acceleration seems unlikely.

#### The Fuel Ignition Problem

Successful starting accelerations seemed unlikely at  $-30^{\circ}\text{F}$  with JP-5R fuel; however, in actual testing, the engine failed to accelerate at fuel and ambient temperatures as high as  $0^{\circ}\text{F}$ . Stagnation occurred at approximately 46% of idle rotor speed. At  $-20^{\circ}\text{F}$  and  $-30^{\circ}\text{F}$  with JP-5R fuel it was not possible to obtain fuel ignition. Starting and light-off fuel flows were equivalent to those predicted from bench testing of the fuel control.

Since this engine is equipped with an emergency, or manual, fuel control it was of interest to determine if starting could be accomplished by employing the manual system. A  $-30^{\circ}\text{F}$  start and acceleration to idle rpm was successfully completed by employing a starting fuel flow of approximately 1350 lb/hr.

No attempt will be made here to discuss corrective action for the described problems. It is demonstrated that richer starting fuel flows will overcome cold fuel light-off and acceleration problems. It may well be possible to correct the combustion problem simply by change in the fuel nozzles. Fuel control problems are correctible once they are defined. It is sufficient to state that solutions are in progress to improve JP-5 starting without compromise of JP-4 capability.

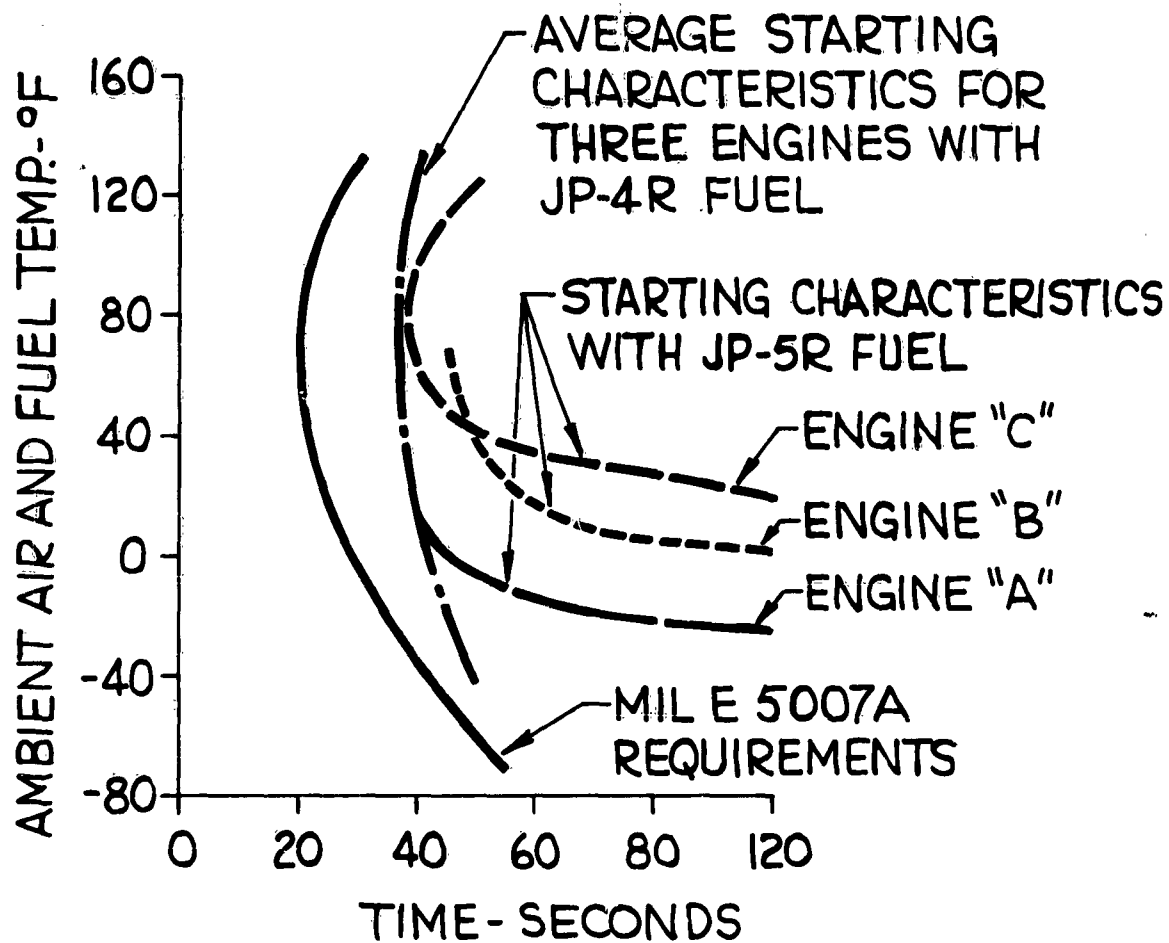


FIG. 1— EFFECT OF JP-5R FUEL ON ENGINE STARTING CHARACTERISTICS OVER COMPLETE AMBIENT TEMPERATURE RANGE

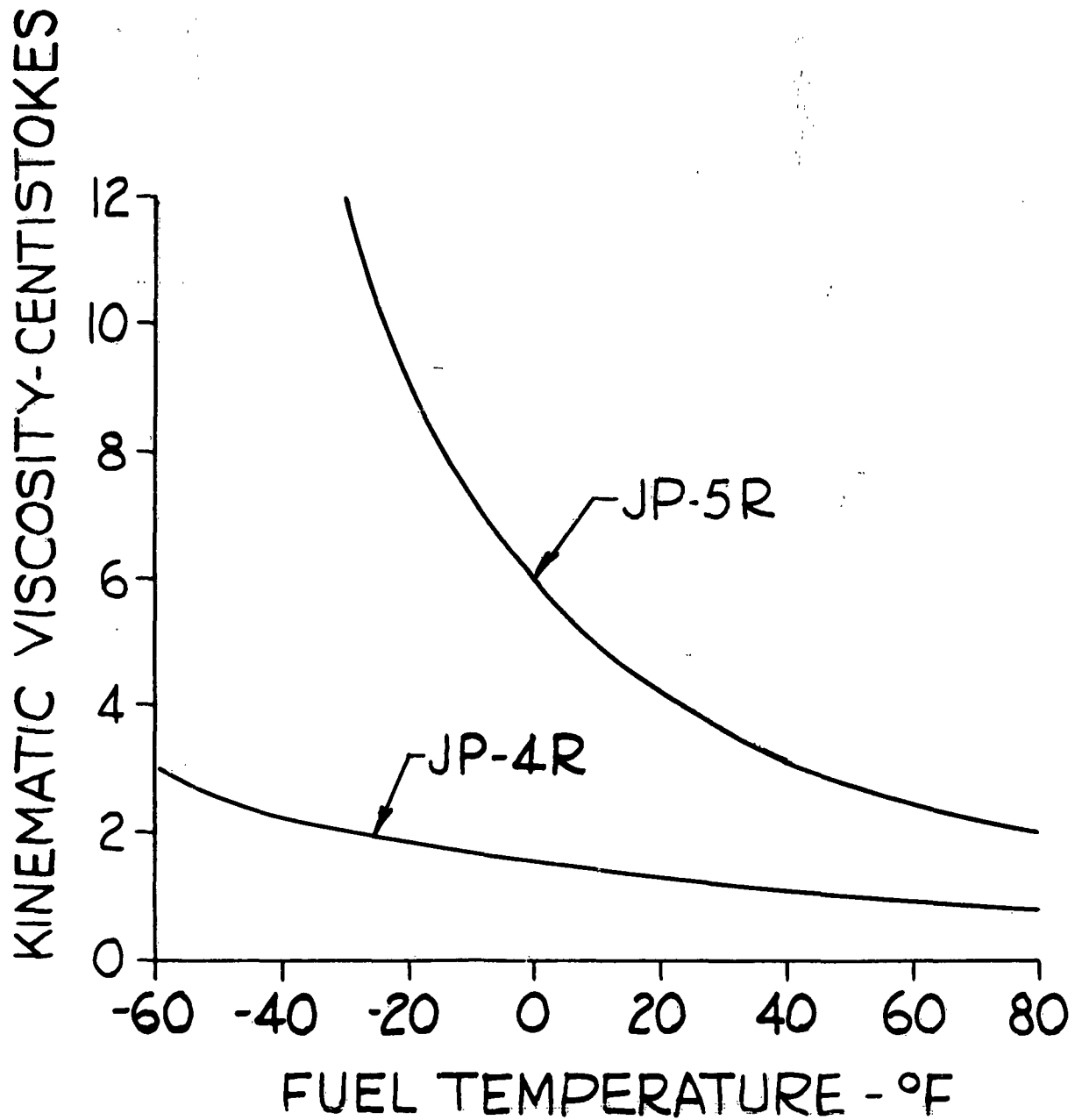


FIG.2 - KINEMATIC VISCOSITY FOR JET ENGINE REFEREE TEST FUELS

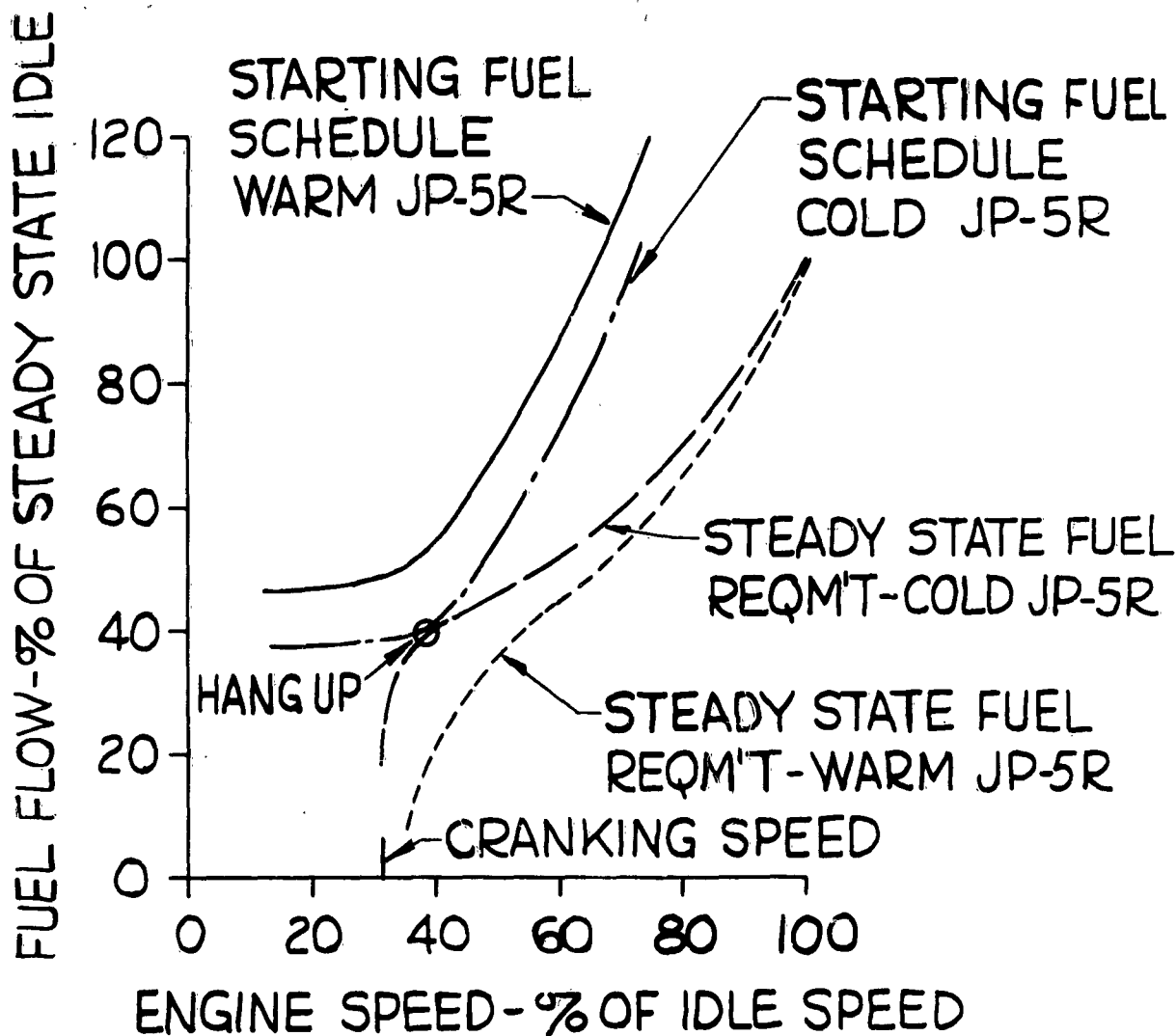
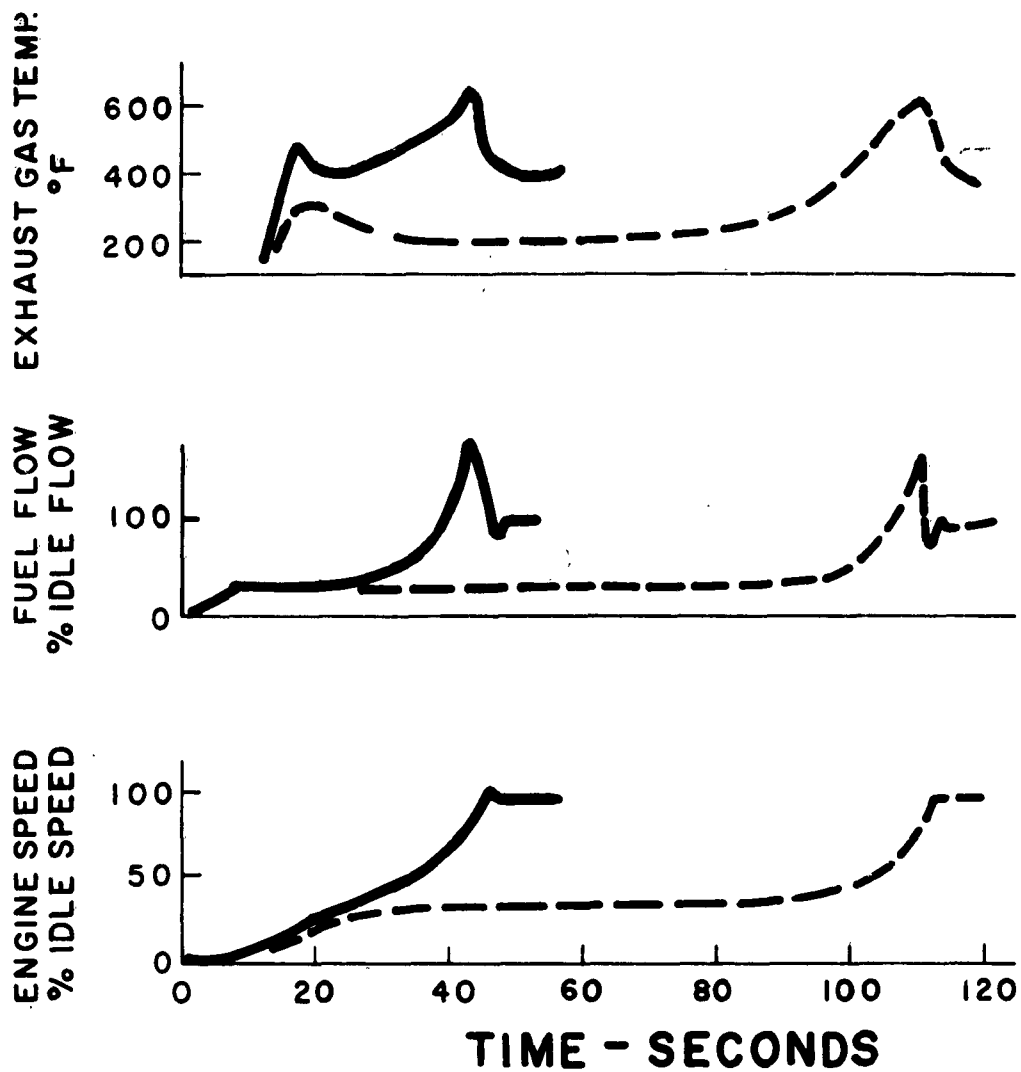
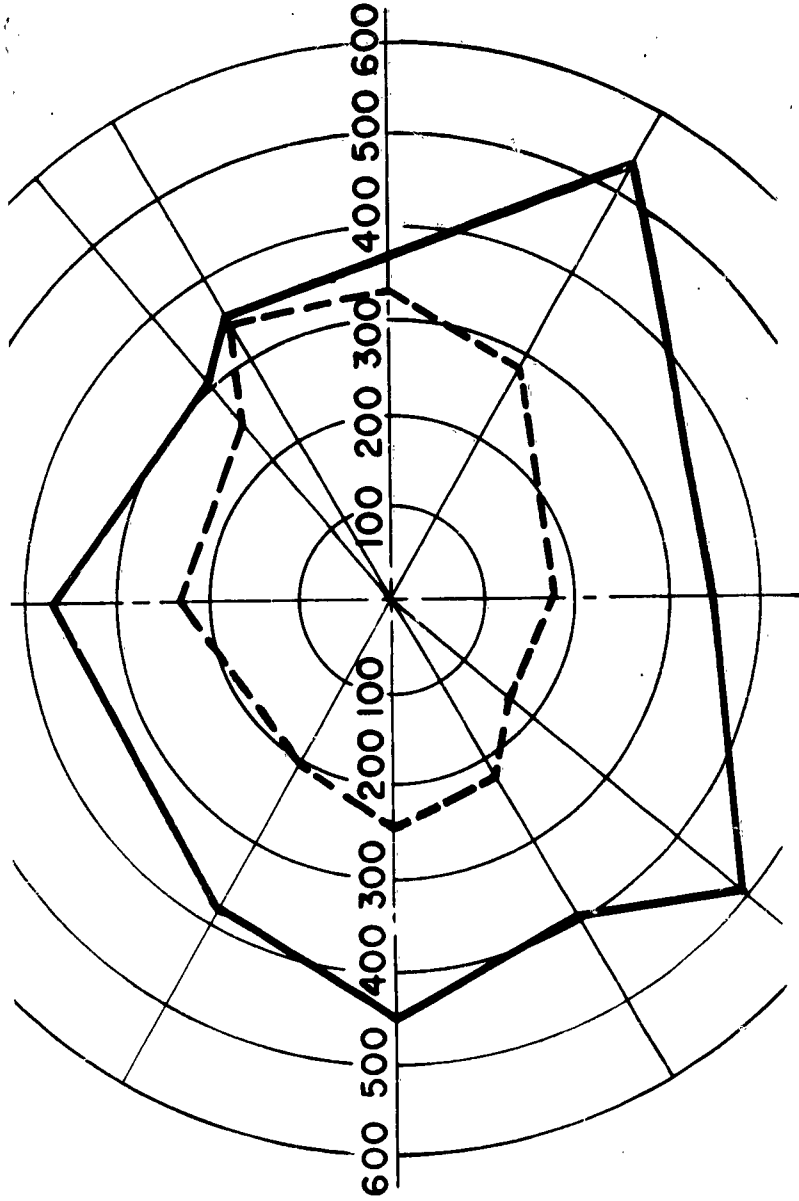


FIG. 3 — EFFECT OF JP-5R FUEL TEMPERATURE ON STARTING PERFORMANCE-ENGINE A



**FIG. 4 - COMPARISON OF A SUCCESSFUL AND A HANG-UP START WITH JP-5 FUEL FOLLOWING  $-30^{\circ}$  F COLD SOAKS.**



**FIG.5- TURBINE DISCHARGE TEMP. PROFILES**

**SUCCESSFUL & HANG-UP START**

**AFTER - 30° F COLD SOAK**

**N=35% IDLE SPEED.  $W_f=33%$  IDLE FLOW**

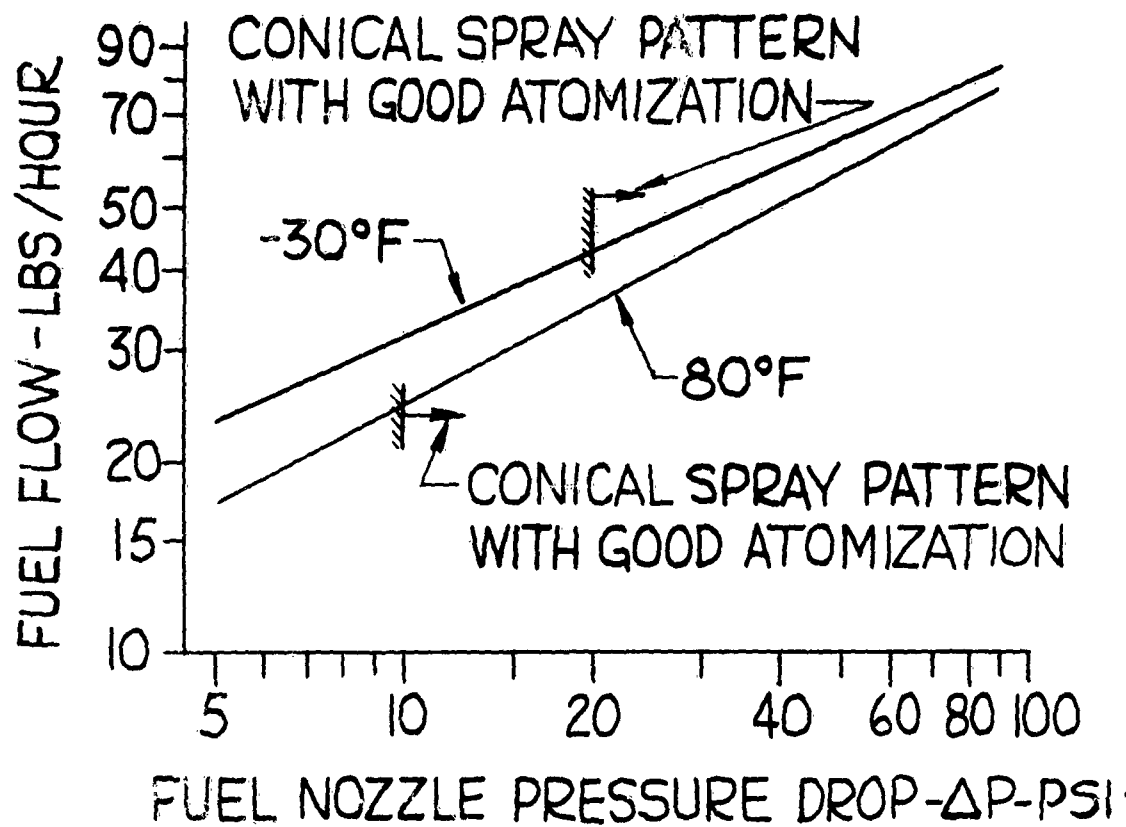


FIG.6- EFFECT OF FUEL TEMPERATURE ON FUEL NOZZLE SPRAY CHARACTERISTICS

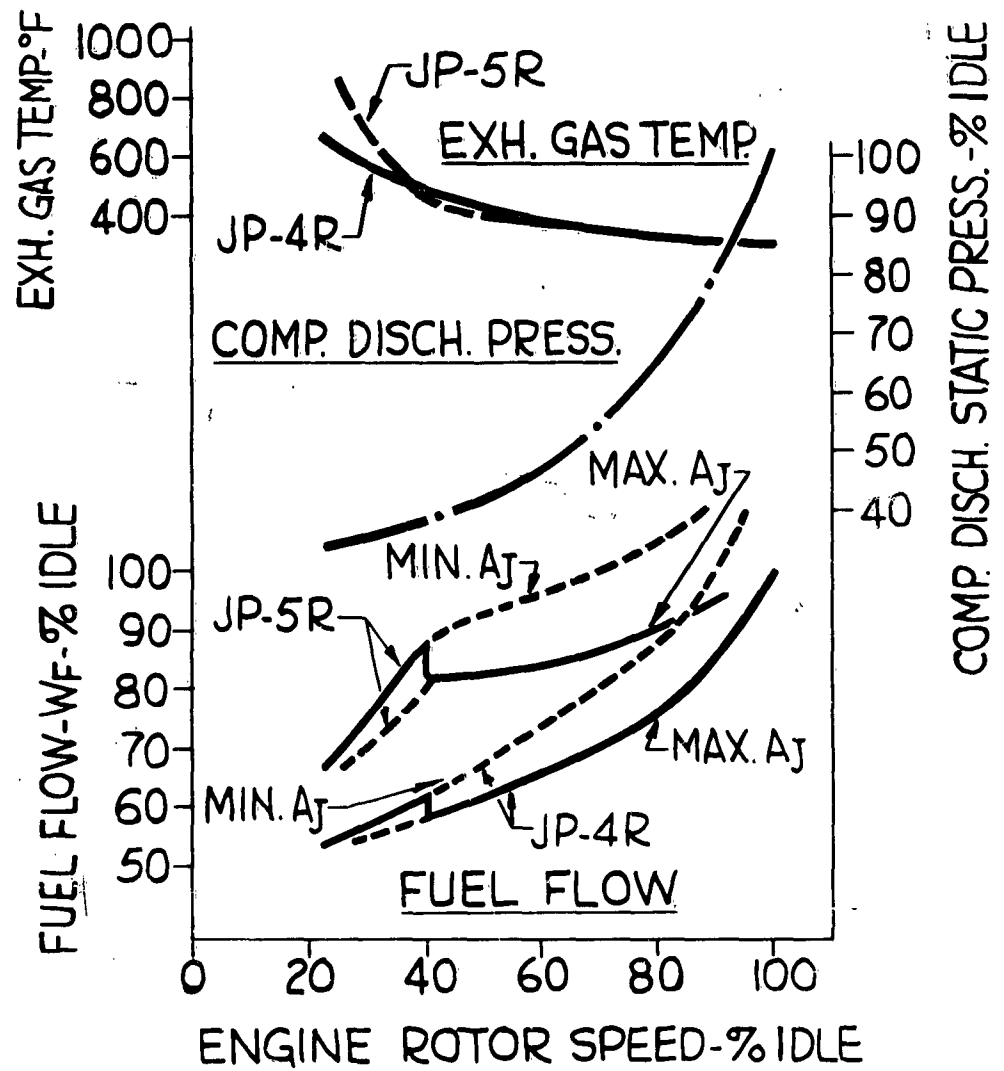


FIG.7 - TURBOJET ENGINE "B"  
 STEADY STATE OPERATION IN THE STARTING RANGE  
 SEA LEVEL I.O R P R -30°F

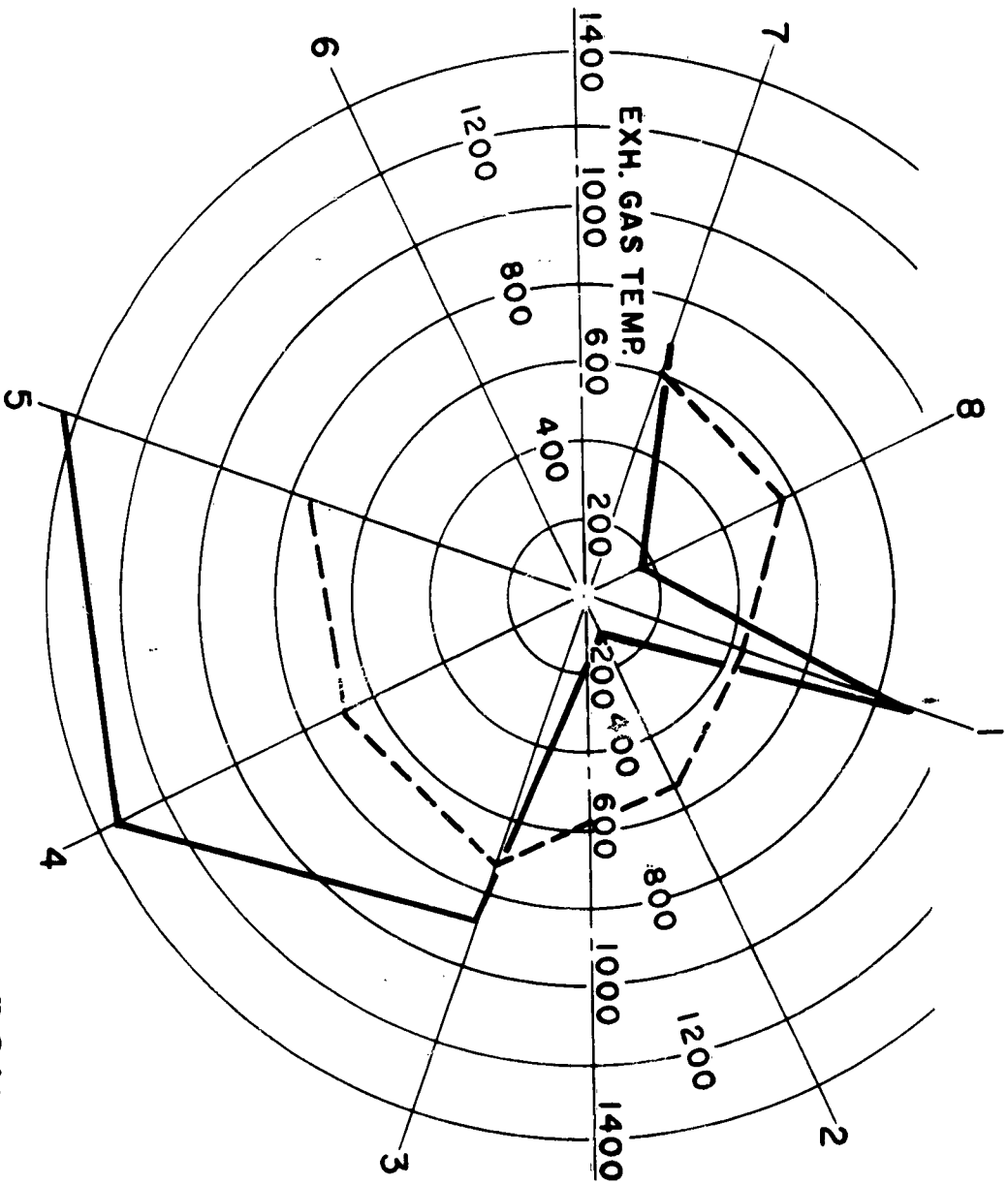


FIG.8-ENGINE "B" EFFECT OF JP-5R FUEL UPON  
 LOW TEMPERATURE OPERATION IN THE  
 ENGINE STARTING RANGE

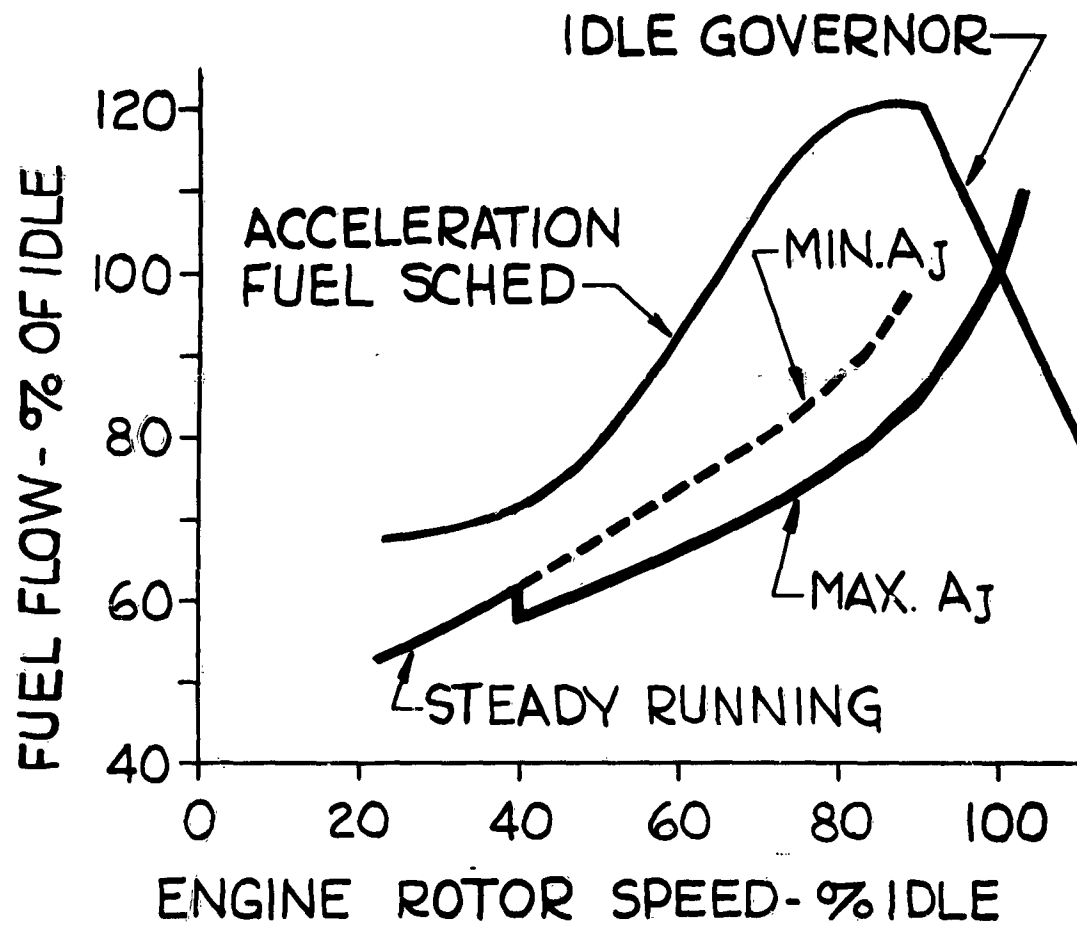


FIG. 9 - "B" ENGINE STARTING CHARACTERISTICS  
 SEA LEVEL 1.0 RPR  $T_2 = -30^\circ\text{F}$   
 JP-4R FUEL

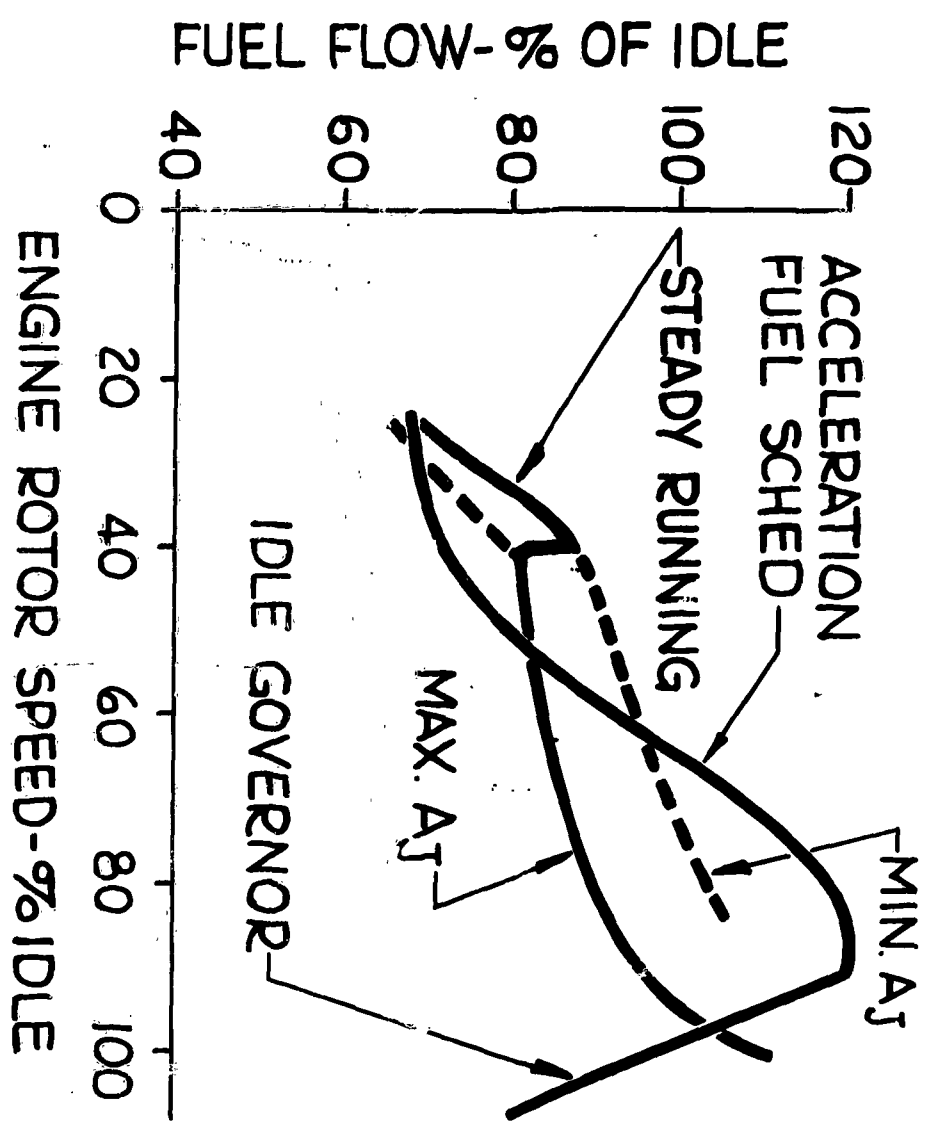


FIG.10-"B" ENGINE STARTING CHARACTERISTICS  
 SEA LEVEL 1.0 RPPR  $T_2 = -30^{\circ}F$   
 JP-5R FUEL

## NOTICE

Reproduction of this document in any form by other than naval activities is not authorized except by special approval of the Secretary of the Navy or the Chief of Naval Operations as appropriate.

The following Espionage notice can be disregarded unless this document is plainly marked CONFIDENTIAL or SECRET.

This document contains information affecting the national defense of the United States within the meaning of the Espionage Laws, Title 18, U.S.C., Sections 793 and 794. The transmission or the revelation of its contents in any manner to an unauthorized person is prohibited by law.